UNIVERSITY *of the*
WESTERN CAPE

Using stable isotopes and hydrochemistry to quantify end-member source dynamics in the Berg River of the Franschhoek and Paarl Valley.

Celine Meyer

Student Number: 3565009

A thesis submitted in the fulfilment of the requirements for the degree of Master of Science in Environmental and Water Sciences

Department of Earth Sciences, Faculty of Natural Sciences,
University of the Western Cape

Supervisor: Dr Sumaya Clarke
Co-supervisor: Prof. Jodie Miller

August 2023

Declaration

I declare that "*Using stable isotopes and hydrochemistry to quantify end-member source dynamics in the Berg River of the Franschhoek and Paarl Valley*" is my own work, that it has not been submitted for any degree or examination in any other university, and that all the sources I have used or quoted have been indicated and acknowledged by complete references.

Full name: Celine Meyer **Date:** 09 August 2023

Signature: 

Acknowledgements

I would like to thank God for blessing me with the opportunity to study further and for providing the daily strength and peace I needed to complete this thesis.

I am grateful to the National Research Foundation (NRF) for their financial assistance that enabled me to conduct my research.

I am deeply grateful to my Supervisor, Dr Sumaya Clarke, and Co-Supervisor, Prof. Jodie Miller, for their unwavering support, encouragement, and expert academic guidance throughout the entire process of my thesis.

My heartfelt appreciation goes to Dr Jared van Rooyen and Dr Andrew Watson of Stellenbosch University, for their valued support, encouragement and academic guidance during my research.

I offer my gratitude to the laboratory technicians Dr Janine Colling and Miss Volante Moonsamy at the Stellenbosch BIOGRIP Laboratory and Mr Evan Swartbooi at the UWC Environmental and Water Science Laboratory for their unceasing guidance and support during the analysis of my water samples.

My special thanks are extended to my colleagues in the UWC Environmental and Water Science Department for assisting me during my field work.

I value the support of Bellville Department of Water and Sanitation, the City of Cape Town, and the farmers and business owners in the Berg River catchment for enabling me to pursue my research on their property, and Gerhard de Kock from Hortec (iLeaf) for his assistance with the meteorological time series data at selected weather stations.

I would like to extend my immense gratitude and appreciation to my loving and supportive parents, my family, and friends who have prayed, supported, and encouraged me daily.

Abstract

The Berg River is a main source of freshwater in South Africa's Franschhoek-Paarl valley for domestic use, industry, and agriculture, but climate change or variability and poor management threaten its quality and quantity. A theoretical understanding of the basin's runoff processes, including the balance between groundwater and precipitation inputs in the river system, is crucial for meeting ecological reserve requirements and preserving ecosystems. By comprehending the dynamics and relationship between the river and its end-member sources by evaluating the contributions of groundwater and precipitation to the streamflow and the seasonal behaviour of solutes, the ecological health and functioning of the river and its associated ecosystems can successfully be managed and maintained. This study involved 25 sampling campaigns conducted between 2020 and 2021 along the Berg River in the Franschhoek and Paarl valley at 40 locations to sample precipitation (n=3), groundwater (n=15), and main river and major tributaries (n=22). The aim was to assess the temporal and spatial variations of the isotopic and hydrochemical compositions to quantify the river's end-member source dynamics. Firstly, the stable isotopic analysis suggested that movement of local precipitation patterns toward the river and subsurface was affected by seasonal changes in sub-cloud evaporation and moisture recycling from the soil and surface water. Precipitation recharging the river was isotopically modified by physical phase changes along surface and subsurface flow paths, whereas the river's isotopic composition remained homogenous due to the dams and groundwater sustaining the flow. Secondly, hydrochemical techniques were used to assess the seasonal hydrochemical behaviour and solute sources influencing the river. The results revealed that in the dry season, a Na-Cl water type was dominant in the valley due to the leaching of stored regolith salts derived from marine aerosols and irrigation runoff. During the wet season, however, the increase in fresh recharge prompted the reverse ion exchange process as a dominant mechanism across the river flow path, resulting in the increase in Ca^{2+} and HCO_3^-. The river ion concentrations were primarily regulated by a mixed mechanism of rock and precipitation dominance, with anthropogenic activities as a secondary influence. Thirdly, the two-component isotope mass balance mixing model estimated that during the dry season,

precipitation contributed to 23.0% of the runoff in the upper region, 2.0% in the middle region, and 17.0 % in the lower region. Groundwater accounted for 77.0%, 98.0%, and 83.0% of the runoff in the respective regions. In the wet season, precipitation contributed to 13.0% in the upper region, 53.0% in the middle region, and 30.0% in the lower region, while groundwater accounted for 87.0%, 47.0%, and 70.0% of the runoff in those regions. Overall, groundwater discharge was revealed as an important seasonal component maintaining the flow of the river, while meteorological and land cover parameters dampened the precipitation contribution. The recommendation of the study is to expand the monitoring network in the valley by increasing the sampling frequency and by sampling other water sources with a focus on the soil (interflow) component and runoff between rain events. This will improve the understanding of seasonal runoff responses and aid in managing and protecting of the catchment's water sources in a changing climate, particularly during transitions from a groundwater-dominated to a precipitation-dominated river system.

Keywords: Climate change, Precipitation, Isotopic analysis, Recharge, Hydrograph separation

Abbreviations and notations

BFI	Base Flow Index
BIOGRIP	The Biogeochemistry Research Infrastructure Platform
DWS	Department of Water and Sanitation
GMWL	Global Meteoric Water Line
GPS	Global Positioning System
GPRS	General Packet Radio Services
IAEA	International Atomic Energy Agency
IC	Ion Chromatography
LMWL	Local Meteoric Water Line
LDPE	Low Density Polyethylene
LIMS	Laboratory Information Management System
TDS	Total Dissolved Solids
WRC	Water Research Commission
MG	Malmesbury Group
MCM/a	Million Cubic Meters per Annum
Mm^3	Million Cubic Meters
RMA	Reduced Major Axis Regression
RWL	River Water Line
TMG	Table Mountain Group
USGS	United States Geological Survey
V-SMOW	Vienna Standard Mean Ocean Water
μS/cm	Microsiemens per centimetre
μ/m	Micrometre
$\delta^{2}H$	Delta Hydrogen
$\delta^{18}O$	Delta Oxygen-18
δ	Delta-notation
%	Percentage
‰	Parts Per Thousand
r	Correlation Coefficient
°C	Degrees Celsius
D-excess	Deuterium-excess
mm	Millimeter
mg/L	Milligrams per Litre
m^3/s	Meters Cubed per Second
meq. L^{-1}	Milliequivalents per Litre

Table of Contents

List of Figures

List of Tables

Chapter 1: General Introduction

1.1 Introduction

This research aimed to explore methods to assess water sources using their isotopic and hydrochemical compositions to understand the Berg River flow regime and associated hydrological processes in the Franschhoek-Paarl valley basin. The study considered all dominant processes that recharged the river system in both dry and wet seasons, including tributaries, groundwater, and precipitation, to understand their influences on stream water quantity and quality.

1.2 Rationale

River systems are essential components of the hydrological cycle, providing freshwater to cities and ecosystems and returning global precipitation to the oceans. The scale of discharge and flow regime of a river governs 2.5% of accessible freshwater globally (Halder et al., 2015). The flow is influenced by precipitation, subsurface sources, and dam release, affecting the rate and quantity of a river's movement (Li et al., 2014).

The river flow regime, described by its mean seasonal behaviour at which water flows in a river channel, is expressed in m^3/sec. The flow of a river is dependent on the volume of water present in the system and plays a fundamental role in the ecological processes of river habitats. It governs both physical and chemical processes, which have a significant impact on the livelihood of natural river ecosystems, while also providing a vital source of water for economic and social practices (Wang et al., 2016). Natural river flows have declined due to the impact of climate change and human activities (Saifullah et al., 2015). This has resulted in approximately 22% of the world's rivers showing significant decline in their annual runoff due to water source exploitation and diversion (Walling & Fang, 2003).

Understanding the flow regime of a river is crucial for implementing effective management strategies to ensure the sustainable use of its water. The characterization of dry and wet seasonal patterns in a catchment is determined by the timing of high and low flow patterns, which are influenced by climatic and physiographic conditions. The flow patterns, in turn, govern the ecological

processes essential for maintaining the health of the river system, making it unique from other water systems on Earth (Bunn & Arthington, 2002).

Precipitation, evaporation, infiltration, runoff, and surface water-groundwater interaction, are some of the important processes which conform to a balanced entity, of the earth's hydrological cycle (Huziy & Sushama, 2017). However, the accelerating environmental changes caused by anthropogenic and natural factors have disrupted this balance, leading to variable climatic conditions that directly impact streamflow at both global and regional scales (Cosgrove & Loucks, 2015; Bhatt & Mall, 2015).

According to the Intergovernmental Panel on Climate Change (IPCC; Trenberth 2007), climate change is characterized by long-term changes in weather patterns and average climatic conditions on Earth, where in the last century the surface air temperatures have increased by 0.75ºC globally. As a result, water is a key indicator of the impacts of climate change, with rivers globally experiencing unpredictable recharge patterns from variable precipitation events that result in fluctuating flow levels. Hence, this variability in climatic conditions has a direct impact on river flows, which, in turn, affects the quality of water in a catchment (Nilsson & Renöfält, 2008).

South Africa is a semi-arid and water-stressed country that on average experiences 450 mm of rainfall per annum (Botai et al., 2018). Between 2015 and 2018, the Western Cape Province in South Africa endured an extreme drought that coincided with the most severe El Niño events recorded in southern Africa (Dube et al., 2022). This marked the first occurrence of such intensity in the past 113 years that had significant consequences on agriculture, specifically impacting the fruit and wine industry, as well as socio-economic activities like tourism and employment. (Lakhraj-Govender & Grab, 2019; Smit et al., 2019). The Western Cape Province, which is a water-scarce region, had to resort to various water management strategies, including water restrictions, desalination plants, and water reclamation, to mitigate the effects of the drought and ensure sufficient water supply to its residents (Lakhraj-Govender & Grab, 2019). The experience highlighted the need

for proactive water management practices and the importance of climate adaptation strategies to ensure the sustainability of water resources in South Africa.

Stable isotope tracers, of δ^2H and δ^{18}O have been extensively used in hydrological research for more than 60 years. Differences in stable isotopic compositions of water bodies can reflect the meteoric processes in the hydrological cycle, which defines the formation, migration, circulation, and transformation patterns of water sources on a regional to global scale (Sun et al., 2016; Bowen et al., 2019). Similarly, the exchange of hydrochemical solutes in a water body is influenced by variations in water quantity, and it partially traces the formation, transportation, and cyclical evolution of water (Vaughn & Fountain, 2005). Hence, the analysis of both stable isotopes and hydrochemical characteristics is essential to draw conclusions on variable hydrological issues (Clark & Fritz, 1997; Chen, 2020). The correlation between isotope hydrology and hydrochemistry has contributed significantly to hydrological research by obtaining river information on the origin of water, recharge patterns, major ion sources association, and gaining insight into the geochemical evolution in river systems. This integration has value towards the management and economic value of water resources at a regional scale (Li et al., 2020; Shi et al.,2021).

The quaternary catchments G10A, G10B, and G10C of the Upper Berg River catchment are situated in the Franschhoek-Paarl valley region of the Western Cape, South Africa. It comprises of a flow regime network that is closely associated with groundwater and surface water sources, including dams, rivers, and associated tributaries. These water bodies have been important and dependable sources of fresh water, contributing significantly to environmental flows to sustain riparian development, as well as to domestic and agricultural practices within the catchment to increase the economic growth of the area (DAFF,2015; Madlala, 2015).

1.3 Description of research problem

The Berg River, which passes through the towns of Franschhoek and Paarl, faces several environmental pressures such as climate variability and various land uses. As the demand for water in the Western Cape continues to rise, it is essential to ensure the sustainable water supply to local farmers, water users, and the ecological

reserve of the Berg River. The surrounding ecosystem depends on the flow of the Berg River during dry and wet periods to support various physical, chemical, and biological interactions among riparian vegetation, animals, and microorganisms. Moreover, 65% of farms and wine estates are located in the Berg River catchment, which relies on the river's water for irrigation, livestock, and recreational purposes. During the 2018 drought outbreak in South Africa, many farmers suffered significant losses due to the water shortage from the river to irrigate their crops and maintain their land. Therefore, a comprehensive understanding of the interactions among various hydrological components and variable processes occurring at both spatial and temporal scales is necessary to ensure the sustainable use of the Berg River. However, there is limited knowledge regarding the generation of streamflow, specifically the balance between groundwater and precipitation inputs, within the Berg River system across the valley, studied over a spatiotemporal scale using isotope hydrology. Therefore, it was necessary that recent data was obtained to identify seasonal variations and threats imposed on the surface water quantity and quality.

1.4 Thesis statement

The research assumes that the application of complementary methods, specifically isotopic and hydrochemical tracers, to evaluate the seasonal variations in source water contributions and the processes that govern streamflow and hydrochemistry within the Berg River Catchment. The assumption is that distinct variations in river stable isotopic ratios and hydrochemical fingerprints will reflect the signature of dominant recharge end-member sources, such as precipitation and groundwater. By integrating these techniques, the research will provide essential information on the catchment's flow regime and mechanisms governing river quantity and quality characteristics, enabling water managers and scientists to ensure the sustainable use of the river in the context of an ever-changing climate and for the benefit of the surrounding ecosystem.

1.5 Research questions

1. What are the dominant processes controlling the rivers' stable isotopic composition in the catchment area?

2. How does hydrochemical processes control streamflow ionic compositions, during dry and wet seasons?
3. How does the seasonal contribution of groundwater and precipitation, influence the runoff, in the catchment area?

1.6 Research objectives

The aim of this study was to use a combination of isotopic and hydrochemical tracing techniques to identify the seasonal end-member sources and processes that sustain the flow regime of the Berg River in the Franschhoek-Paarl valley.

The specific objectives of the study were to:

1. To characterize the seasonal mechanisms regulating the isotopic composition of the river, groundwater and precipitation resources of the catchment area, using stable isotope techniques.
2. To characterize the seasonal hydrochemical behaviour, controlling factors and solute sources influencing the Berg River, using hydrochemical techniques.
3. To identify the proportionate contribution of the dominant end-member sources, of the Berg River, during dry and wet seasons using an isotope mass balance mixing model.

1.7 Research significance

The Berg River, a crucial source of water in the quaternary catchments G10A, B, and C, is important for agricultural, domestic, and ecological use, particularly in the lower reaches of the catchment where it contributes to small floods (Ractliffe, 2009). Given the ongoing climate variability and water crisis in the Western Cape, it is vital to assess, monitor, and protect this critical surface water resource. Effective catchment management and mitigation plans require detailed scientific knowledge of the river, including its quantity and quality, flow variability, and storage-discharge characteristics necessary to sustain the surrounding ecology. Therefore, understanding the seasonal recharge patterns and related streamflow responses through simultaneous in-situ monitoring using hydrochemical and isotopic techniques can provide additional theoretical support and knowledge on the basin's hydrological runoff processes, addressing water circulation pathways

and spatiotemporal geochemical processes in the river system. By monitoring streamflow patterns and chemical variations, stakeholders can gain new hydrological information to improve the protection, management, maintenance, structural development schemes, and optimal level of use to ensure the sustainable management of the river resource in the era of climate change.

1.8 Outline of the thesis

The present study is structured into seven chapters. Chapter 1 provides an introduction to the research problem, including the background, aim, objectives, assumptions, research questions, and the significance of the research. It also outlines a general overview of the thesis. Chapter 2 presents the literature review, which provides the necessary guidance and information on the research objectives and methodological approaches required to achieve the proposed objectives and overall aim. Chapter 3 describes the study area, including regional hydroclimate, hydrogeology, soil, land cover, and sampling sites. The methods and materials used in the research to sample, test, and generate results are also discussed. Chapters 4 to 6 comprise the results generated by the selected methods. Each chapter discusses the results relevant to a specific objective and includes figures and tables. In Chapter 7, the results and discussion of each objective are summarised, and recommendations are provided for future research in the catchment.

Chapter 2: Literature Review

2.1 Introduction

Over the years, rivers in southern Africa have been assessed due to its ongoing significant changes in water volume, quality, and flow regime attributed to reduced rainfall events and human activities (O' Keeffe, 1986; Lakhraj-Govender&Grab,2019). These river systems are essential sources of freshwater, necessary for supporting domestic and agricultural services and sustaining ecological systems along the river (Li et al., 2014). The streamflow and chemical composition of rivers in most environmental settings depend on two prominent contributing water sources: surface runoff and baseflow. The equilibrium state between these water sources is influenced by the catchment's geological characteristics and, to a marginal extent, the season of the year (Darling et al., 2003).

Low and high flows are seasonal patterns that are important components of a river's flow regime. In many cases, low flows, originate from discharged water that migrates from aquifer units below the river bed during the dry season (Smakhtin, 2001). High flows are a result of high stream discharge due to the large quantity of surface runoff flowing into these systems, which is prominent in the Berg River and its tributaries during wet seasonal conditions. The habitual flow regime of a river system can be altered either by natural climatic patterns or by human interventions, such as dam construction. Wang et al., (2016) assessed the sensitivity of streamflow in China to climate change in varying climatic zones and observed that surface runoff was highly vulnerable to variations in precipitation and temperature. A 10% change in precipitation was estimated to change runoff by 15-25%, while a projected 2 degree increase in temperature was estimated to reduce streamflow by 5-12%. (Lorena et al., 2010; Wang et al., 2016).

To determine the contribution of water to the flow regime of a river in response to rainfall events, it is essential to understand the various runoff processes in relation to the drainage basin's physical terrain, climatic parameters, and human modifications that may influence the overall source contributions to the stream (Birkel & Soulsby, 2015). In past research, stable isotopes and hydrochemical

tracers have shown valuable results on instream hydrological processes influenced by the transport of water along various flow paths, the transit time of water, and the hydrological connection between water bodies (Congjian et al., 2015; Silva et al., 2018). In the case of two diverse sub-catchments within the Jonkershoek catchment in the Western Cape, of similar rock fractured quarzitic sandstone lithology to the Berg River catchment stable isotopes of water (^{18}O, ^{2}H), EC and pH were used to analyse seasonal recharge sources and flow pathways during baseflow conditions. The findings, as illustrated in Figure 1 by Mokua et al. (2020), revealed that the isotopic compositions of the stream water closely resembled those of groundwater throughout the dry and wet seasons. This suggested that the stream received slow discharge from springs during the dry season, coinciding with reduced rainfall. In contrast, the wet season revealed interflow and the contribution of perennial and ephemeral springs to the stream's water source (Mokua et al., 2020).

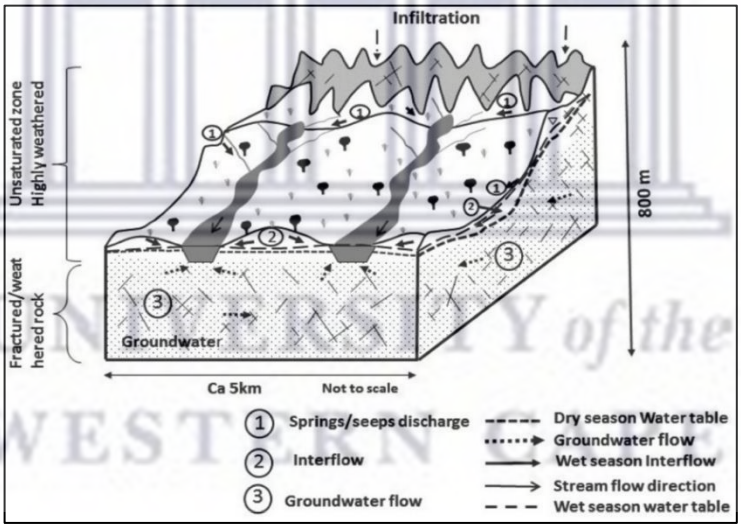

Figure 1: Seasonal streamflow generation processes in Jonkershoek catchment: A conceptual model differentiating mountainous (grey) and foothill (white) zones) Source: Mokua et al., (2020).

According to Madlala (2015), during baseflow conditions, the Berg River is highly dependent on the contribution of groundwater discharge and dam release to sustain the streamflow. However, understanding how much water is contributed by all water sources, the variation in runoff dynamics during both dry and wet seasons, and the solute exchange among the water sources is vital in water resource management.

Chapter 2 reviewed the key literature relevant to the proposed study and the methods applied to achieve each research objective. This chapter discussed the concept of applying stable isotopes in hydrological studies, the processes that modify isotopic signatures among various water sources, the processes and mechanisms governing river solute chemistry, and the methods used to partition the contribution of water to the streamflow regime.

2.2 Tracing River recharge through seasonal stable isotopic signatures

Stable isotopes of hydrogen ($^{2}H/^{1}H$) and oxygen ($^{18}O/^{16}O$) in water are natural and reliable hydrological tracers that vary spatially and temporally in arid and semi-arid regions. They can identify patterns and processes at ecological and hydrological scales, such as atmospheric processes, water recharge, river flow variations, and interactions between surface water and hydrological systems (Clark & Fritz, 1997; Congjian et al., 2015). Hence, stable isotopic tracers can delineate seasonal contributions of water origins in a river system (Liu et al., 2015).

Stable isotopes of hydrogen and oxygen are inherent to water molecules and serve as unique identifiers. Their isotopic signatures can be modified during various stages of the hydrological cycle, such as mixing with different water sources and fractionation processes (Clark & Fritz, 1997; Kendall & Caldwell, 1998; Shamsuddin et al., 2018). These modified signatures provide insights into the origin and evolution of water before it recharges the river (Huang & Wang, 2017; Kong et al., 2019). Previous studies have successfully used stable isotopic tracers in both groundwater and surface water to identify water exchange and circulation processes among varying surface and subsurface water bodies (Mokua et al., 2020; Jung et al., 2021). Their non-reactive nature increases the accuracy of hydrological analyses, and they have been effective in investigating runoff generation processes in small regional watersheds ranging from 0.01km^2 to 100km^2 (Baskaran et al., 2009; Klaus & McDonnell, 2013; Bhagat et al., 2021), evaluating a watershed's residence time (McGuire et al., 2005), and estimating contributing water sources for river flow (Chen et al., 2020; Bhagat et al., 2021).

Isotope fractionation is the separation of isotopes of different mass quantities due to hydrological processes such as evaporation and condensation, leading to varying isotopic characteristics of water bodies (Clark & Fritz, 1997; Chen et al., 2020). The spatial and temporal variation of isotopic signatures in natural water bodies provides information on water circulation and transformation processes, making it applicable in ungauged catchments (Craig, 1961; Clarke & Fritz, 1997).

Globally, physical processes like evaporation and moisture recycling can lead to isotope fractionation, altering the isotopic signature of rivers and their recharge sources (Lambs et al., 2011; Sharma et al., 2017; Gat, 1996). Catchment properties control streamflow generation, including dominant flow paths and water transit time (Ala-aho et al., 2018; Halder et al., 2015). Large rivers often show light isotope enrichment along the flow path due to elevation effect, increased evaporation (Ogrinc et al., 2018), and the input of water sources with distinct isotopic composition (Kumar et al., 2019). The isotopic variation in rivers is influenced by seasonal variation in climatic controls and catchment characteristics governing hydrological processes (Gao et al., 2021).

Daily temperatures >0ºC drive evaporation of water, leading to preferential evaporation of lighter isotopes compared to heavier isotopes. This results in residual water becoming enriched in heavier isotopes and depleted in d-excess values (Dansgaard, 1964; Haiyan et al., 2018; Shi et al., 2019). This phenomenon has been used to assess water loss downstream in arid and semi-arid environments (Gibson et al., 2002). Under low flow conditions, river water tends to be isotopically enriched due to surface water evaporation (Zhou et al., 2017).

Precipitation to river flow isotopic relation

All water sources derive from precipitation through various pathways, and the characterization of river recharge relies on comparing the distinct isotopic signatures of precipitation and rivers (Clarke & Fritz, 1997). Previous studies have emphasized the need to analyse the isotopic signature and variation of precipitation to determine the origin of water sources and understand their unique input signal (Gat et al., 2010; Harris et al., 2010; Guan et al., 2013). Therefore, characterizing how precipitation is stored and discharged as streamflow within a catchment is a

fundamental step in hydrology, as noted by Miller et al. (2021). Recharge rates, which influence the flow regime of river systems, can vary due to factors such as climate, precipitation, land cover, and topography. Given the variability in precipitation quantity, intensity, and formation resulting from global warming, understanding the Earth's water balance at regional and global scales has become crucial (Liu et al., 2013). The $\delta^{2}H$ and $\delta^{18}O$ isotopic compositions in precipitation are linked to climatic and environmental parameters, and comprehending these factors is essential for studying the isotopic variation and evolution of precipitation, as highlighted in previous hydrological studies (Machavaram et al., 2006; Tweed et al., 2020).

Stable isotopic ratios ($^{2}H/^{1}H$ and $^{18}O/^{16}O$) in precipitation can trace atmospheric water and provide insights into moisture conveyance and precipitation production processes (Adar et al., 1998). Local precipitation can show a specific isotopic signature due to varying meteorological dynamics and moisture sources (Peng et al., 2010), emphasizing the importance of understanding precipitation sources and controls when analysing streamflow processes in river systems. Seasonal isotopic variability in precipitation has played a crucial role in previous research, allowing for the identification of hydrological processes and drivers of seasonal streamflow generation at a regional scale (Kumar et al., 2019).

Over time, the assessment of isotopic compositions in precipitation has evolved to understand the controls governing isotope fractionation at a spatiotemporal scale. These controls, including the temperature, amount, continental, latitude and altitude effects, govern the enrichment and depletion of isotopic compositions in precipitation on a global scale, as described by Dansgaard (1964) and Gat et al. (2001). The Rayleigh Fractionation describes the isotopic depletion of a moisture cloud along its storm trajectory, resulting in variable meteoric isotopic signatures (Clarke & Fritz, 1997). Factors influencing cloud formation and air parcel generation can produce distinct raindrop characteristics (Aggarwal et al., 2016), while moisture recycling through evapotranspiration can modify atmospheric moisture fractions, thus altering the isotopic composition of precipitation (Peng et

al., 2011). Understanding these factors is crucial for assessing streamflow processes and seasonal streamflow generation (Kumar et al., 2019).

Dansgaard (1964) proposed the "amount effect," which shows a negative correlation between the amount of precipitation and its isotopic composition (δ^2H and $\delta^{18}O$), and the "temperature effect," which shows a positive correlation between temperature and isotopic composition. However, despite experiencing increased average rainfall amounts due to its close proximity to Table Mountain, the 12-year continuous monthly rainfall dataset collected at UCT in the Western Cape did not show a significant correlation between the δ^2H and $\delta^{18}O$ values with temperature and rainfall amount. However, it did show notable seasonal variability (Harris et al., 2010). Therefore, the absence of a strong relationship between the isotope composition of rain and temperature in the dataset collected aligns with the expected pattern for low latitude locations (Rozanski et al. 1993). As air masses rise and cool, they gradually deplete the isotopic composition of precipitation with increasing altitude, known as the "altitude effect" (Poage et al., 2001). In high-altitude terrains, the altitude effect is directly detected in river systems dominated by rainfall recharge (Jódar et al., 2016). The depletion range accounts for approximately -0.15‰ to -0.5‰ for $\delta^{18}O$, and approximately -1 and 4‰ for δ^2H per 100m (Dansgaard, 1964; Clark & Fritz, 1997). The temperature effect produces raindrops of a heavier isotopic composition during condensation at higher temperatures (Gat, 2010). The altitude effect is a temperature-associated component, and the isotopic composition of precipitation shows a linear relationship with altitude in mountainous regions (Yang et al., 2019).

The "continental effect" describes the gradual depletion of heavy isotopes in precipitation as it moves inland from a marine moisture source. This effect is most significant in larger continental regions, as the remaining moisture is depleted in heavier isotopes during a rainout event. However, smaller regions are less affected, as suggested by previous studies (Tazioli et al., 2019). The "latitude effect" is observed as a depletion of heavy isotopes with increasing latitude and decreasing temperature (Rozanski et al., 1993). While the temperature and amount effects are

primarily influenced by local geographical factors, the latitude, continental, and altitude effects are typically analysed on a larger spatial scale (Li et al., 2017).

Runoff is crucial for supplying water to rivers and can be categorized as surface or overland runoff, and sub-surface runoff, which includes interflow and baseflow. When precipitation infiltrates the subsurface, its isotopic composition may be modified. Infiltration varies in degree and can filter and dampen the seasonal precipitation signature in streams. The flow path affects the degree of groundwater and river recharge, especially in basins with preferential flow (McGuire & McDonnell, 2006). Runoff variation depends on catchment characteristics, physical processes, and mixing with other water sources. The timing and pathway of meteoric water entering a stream may significantly differ from the initial precipitation isotopic signature due to these factors (Liu et al., 2013; Gou et al., 2018). Hence, the variable isotopic composition of meteoric water in streams is affected by the circulation and redistribution of water through the catchment by surface and subsurface runoff, which eventually integrates into streams to form a cohesive isotopic signal (St. Amour et al., 2005).

Understanding the hydrological processes of a drainage basin requires quantifying how water sources like precipitation generate and sustain streamflow (Machavaram et al., 2006). Natural and human-induced factors can alter the natural flow regime of a river. The amount of water entering a river system from a rainfall event and contributing to streamflow depends on the catchment's characteristics, such as slope, elevation, land cover, land use practices, soil, and geology (Zhou et al.,2015). These factors influence the flow pathways and connectivity between hydrological sources and storage entities, creating a spatiotemporal relationship between precipitation and river flow (Chiverton et al., 2014). Therefore, precipitation falling within a catchment can follow various flow pathways and storage entities before contributing to total stream discharge. In the Berg River Catchment's sub-basins, three dominant runoff source dynamics influence the isotopic composition of streamflow: (a) channel precipitation and overland flow, (b) subsurface discharge, and (c) input from dams.

Meteoric Water Lines:

The Global Meteoric Water Line (GMWL), defined by Craig (1961), describes the relationship between hydrogen and oxygen isotopic compositions of precipitation at a global scale. Local precipitation, however, may deviate from this relationship due to control factors as proposed by Dansgaard (1964) and form the LMWL. The unique equation for the GMWL is $\delta^2H = 8*\delta^{18}O+10$, with the slope of 8 determined by isotope fractionation effects during equilibrium processes and the intercept of 10 influenced by kinetic isotopic fractionation during non-equilibrium evaporation. Evaporation tends to remove lighter isotopes, resulting in higher proportions of $\delta^{18}O$ and δ^2H in the evaporated water source than precipitation. The unique isotopic fingerprint formed by mixing water bodies with distinct isotopic signatures can identify rainfall-runoff processes (Birkel et al., 2011).

Rainfall in a region creates a unique Local Meteoric Water Line (LMWL) that can be identified by its slope and intercept (Dansgaard, 1964; Clarke & Fritz, 1997). The moisture source can be identified by the LMWL equation and precipitation's climatic and physical parameters (Guan et al., 2013). In previous research conducted in the Western Cape, South Africa, Harris et al. (2010) established a LMWL equation: $\delta^2H = 6.41* \delta^{18}O+8.66$ ($R^2=0.88$) which showed noteworthy similarity to the line of best fit derived from the Cape Town Airport dataset (IAEA/WMO, 2006): δ^2H 6.51* $\delta^{18}O$+ 8.89 (RMA) (Figure 2). Both LMWL equations showed a close correlation with the GMWL, but with an intercept of less than 10‰, suggesting relatively insignificant equilibrium conditions in relation to evaporative processes. In southern Africa the LMWL slope is generally reduced relative to the GMWL due to semi-arid climatic conditions and evaporation occurring between the source cloud and soil profile, as discussed by Abiye et al. (2021).

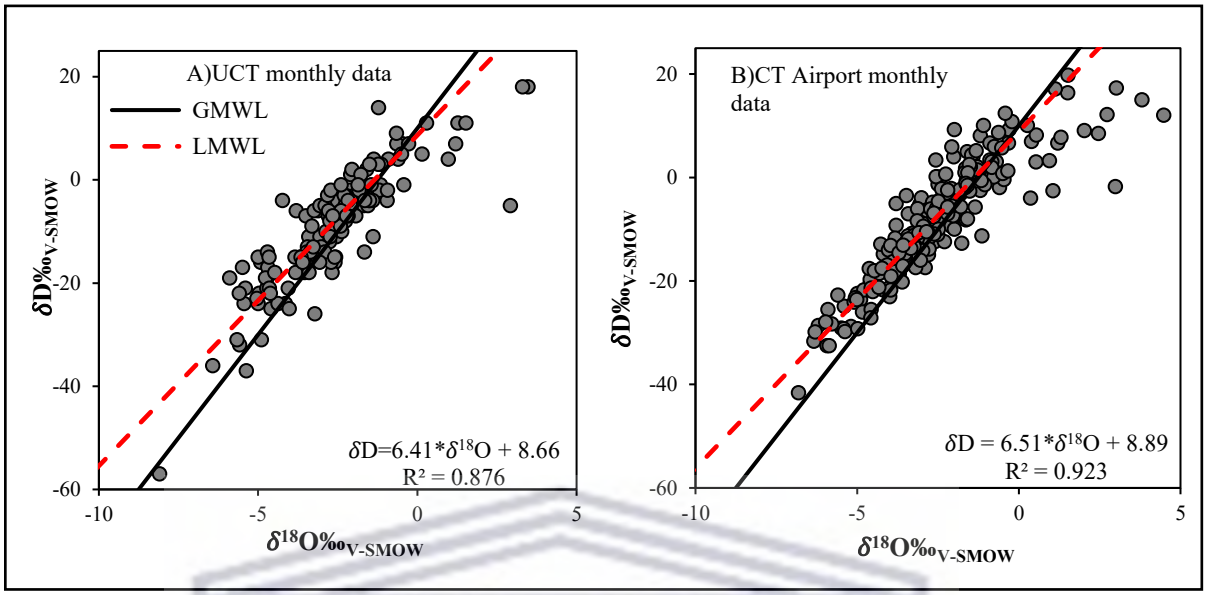

Figure 2: Dual-isotope comparison for A) UCT monthly rainfall samples (1995-2008) and B) Cape Town International Airport monthly rainfall samples (1961-2013). (Data Source: IAEA/GNIP, 2021)

Deuterium excess:

Dansgaard, (1964) developed the concept of d-excess, represented by the equation $d = \delta^2H - 8*\delta^{18}O$, which is influenced by local meteorological parameters, ambient water vapor isotopic composition, and isotopic fractionation processes like sub-cloud evaporation and moisture recycling (Fan et al., 2016; Sun et al., 2016; Shi et al., 2019).

Higher d-excess values than the global average of 10‰ indicate a higher proportion of evaporated moisture, while reduced values suggest the effect of sub-cloud secondary evaporative processes (Kendall & Coplen, 2001; Chen et al., 2021). Liu et al. (2008) observed that in northwest China, condensed raindrops experience sub-cloud evaporation during precipitation, causing moisture-generating precipitation to mix with locally recycled vapour. This process is regulated by Rayleigh and kinetic fractionation. According to Zhou, (2021), found that precipitation undergoing kinetic fractionation led to varying fractionation factors between $^2H/^1H$ and $^{18}O/^{16}O$ ratios, resulting in periodic lowering of the RWL slope value.

Surface water and groundwater d-excess values are influenced by moisture sources, climatic conditions, evaporation rates, water-rock interaction, and recharge

processes (Yang et al., 2019). Shi et al. (2019) discovered that local climatic conditions, such as evaporation rates and river recharge sources, influenced the d-excess values of surface waters in the Upper Yellow River in Northwest China. They observed that lower d-excess values correlated with higher $\delta^{18}O$ concentrations, indicating increased evaporation. In addition, the d-excess factor has been utilized by Ala-aho et al. (2018) to distinguish between evaporative and non-evaporative stream hydrological sources. This approach can be useful in identifying the isotopic evolution of source waters based on river d-excess values.

Groundwater to river flow isotopic relation

Groundwater and surface water are often connected, and groundwater seeping into a river can change its isotopic composition by isotopic exchange (Shamsuddin et al., 2018). Additionally, the isotopic composition of groundwater can differ from surface water, depending on factors such as the geology of the area and past flow paths of water in an aquifer. Hydrogeological processes have been studied for the past century, with particular focus on the contribution of groundwater sources to river flow during dry and low-flow seasons (Madlala, 2015; Bhagat et al.,2021). Understanding the isotopic composition of groundwater can therefore help to comprehend the isotopic composition of associated river water.

The interaction between groundwater and the Berg River has been extensively studied, particularly in the headwaters where baseflow maintains the river's perennial flow and effluent nature (Clark & Ractliffe, 2007; Madlala, 2015). The catchment's aquifer system is replenished by winter rainfall from April to October, with discharge rates depending on hydraulic gradients. Groundwater discharge sustains river flow during low-flow and baseflow conditions. To maintain the river's flow, it's essential to understand how sub-surface and surface water interact over time (Miller et al., 2014).

Stable isotopic ratios, such as $^{2}H/^{1}H$ and $^{18}O/^{16}O$, are ideal for assessing subsurface origin and flow processes, including evaporation, lateral flow, downward infiltration, and groundwater-surface water interactions (Levy and Xu, 2011). For example, environmental isotopes ($\delta^{18}O$,$\delta^{2}H$ and ^{3}H) combined with major ion hydrochemistry proved as a valuable approach for understanding the evolution of

groundwater salinity in the Sandspruit River catchment, a tributary of the Berg River (Naicker,2012). These ratios have been used since the 1970s to gather information that was previously difficult to assess using other tracer techniques (Adomako et al., 2011). Winter, (2007) observed that substantial groundwater contribution to streamflow of the Dismal River, Rocky Ford Creek, and Crow Wing River in America maintains permeable groundwater areas, resulting in stable river flow conditions regardless of headwaters or stream length.

Dansgaard, (1964) proposed that isotopic variations in groundwater are influenced by climate during recharge and altitude effects along the flow path. Gaining streams depend on groundwater and are susceptible to chemical changes due to inflow of water with different chemistry (Fetter, 2000). Shallow groundwater has distinct isotopic signatures compared to water in deeper aquifers that have longer residence times (Ahmed et al., 2011). Aquifer systems can also be replenished by surface water sources (Brunner et al., 2010). Groundwater and surface water interaction is critical for sustainable water management and ecological protection in Africa, particularly in regions with variable rainfall where agriculture is a vital economic activity (Siebert et al., 2010; Levy and Xu, 2011). Groundwater-surface water interaction is typically classified as connected or disconnected at the river scale. In connected systems, groundwater contributes to river flow by discharging through the streambed, while in disconnected systems, the unsaturated zone's subsurface lithology determines flow discontinuity and has no impact on streamflow (Brunner et al., 2010).

Baseflow is the delayed outflow of groundwater into stream channels between storm events (Miller et al., 2014; Price, 2011). It sustains perennial systems during dry and wet seasonal flows and riparian ecosystems (Singh et al., 2016; Madlala, 2015). Increased infiltration, recharge, and subsurface storage result in more baseflow, while increased evapotranspiration and surface runoff reduce it (Price, 2011). Groundwater feeding into streams may reveal marginal isotopic variation in regions where the streams drain large permeable subsurface reservoirs. Variability in groundwater discharge is more prominent in regions where streams drain subsurface reservoirs of reduced permeability or during increased rainfall events (Winter, 2007).

Artificial storage – river flow isotopic relation

Large water storage features relative to groundwater inflows can dampen isotopic variation in rivers (Jasechko, 2019). In some cases, dams are built to collect and store water during wet seasons, but the amount of stored water can affect discharge to rivers during dry periods (King et al., 2008). This can have significant impacts on runoff generation and regional streamflow in catchments, especially when combined with human activities such as urbanization (Woo & Thorne,2003). For example, in South Africa, the Berg River Dam is used to store approximately 130 million m^3 of water during high rainfall events, which can be released downstream during low flow periods to sustain the catchment's ecological integrity and ecological reserve requirements of the National Water Act (Act 36 of 1998). However, anthropogenic activities such as land modifications and dam embankments have changed the natural flow regime that previously existed in the Berg River Catchment (Hughes,2010). Thus, knowledge of the isotopic signature and reservoir influence on the Berg River stream network below the dam is still inadequate.

Dams can also affect the environment by changing sediment flux, water quality, timing, volume, and temperature, which in turn can have negative impacts on the biotic communities in and around the river (Milner et al., 2019). For instance, the construction of a dam in China resulted in an increase in water storage time, which led to an increase in evaporation and isotopic composition enrichment of heavy $\delta^{18}O$ and $\delta^{2}H$ isotope ratios in the stored water (Wang et al., 2019). The isotopic composition of dam water releases depends on factors such as capacity, mean depth, and retention time, with longer retention times resulting in more evaporation, heavier isotopic composition enrichment, and lower d-excess values.

2.3 Berg River Solute Evolution Processes

Land and ocean entities are linked via hydrological networks, such as rivers, which facilitate material and energy exchange along the flow path (Meybeck, 1987). The hydrochemical composition of a watershed is determined by its flow path, emphasizing the importance to assess the basin's ion composition to understand the geochemical sources and processes controlling river solutes (Lintern et al., 2017).

Ions in surface water can originate from natural sources, such as weathering of terrestrial rocks and atmospheric precipitation, as well as anthropogenic sources (Khatri & Tyagi, 2015). The origin and ion composition of rivers reflect the connectivity between precipitation, groundwater, and the river, which in turn relates to the quantity and quality of water in the catchment. Seasonal changes in streamflow source contributions result in fluctuations in the composition of solutes in stream water (Tao et al., 2021). The concentration of river solutes varies seasonally due to end-member sources and reactive processes, and the connectivity between rivers and adjacent water sources is essential for managing suitable river quality (Kondolf et al., 2006).

Rivers in arid and semi-arid environments are threatened by reduced recharge and deteriorating water quality (Xiao et al., 2016). This can indirectly reduce the quantity of available water in the river. The chemical composition of the Berg River's streamflow, groundwater, and rainfall can be influenced by natural or anthropogenic sources and can vary with changes in water discharge (Torres et al., 2015). The major ions and physiochemical parameters, including Ca^{2+}, Na^{+}, K^{+}, Mg^{2+}, SO_4^{2-}, HCO_3^{-}, Cl^{-}, SiO_2, pH, TDS, and EC, are considered natural water tracers that, along with stable isotopic tracers, can signal the hydrochemical processes that govern runoff chemistry and help identify water flow pathways contributing to streamflow (Sferratore et al., 2006).

Water chemistry in rural and urban areas can be influenced by both natural and anthropogenic factors, such as dam construction, poorly treated domestic water discharge, urbanization, and irrigation return flow (Khatri & Tyagi, 2015). According to Postel, (1998), with more than 50% of available surface water already being used for human needs and expected to increase to 70% by 2025. Hence, assessing the hydrochemistry of stream water is crucial for understanding the dynamics between evaporation, precipitation, and anthropogenic and chemical weathering influences (Gibbs, 1970; Meybeck, 1987; Mitchell et al.,2013). Understanding how land use and land cover affect streamflow and hydrochemistry is essential for river management and ecological restoration (Huang et al., 2013). Nonetheless, natural weathering processes may modify the runoff ionic composition and recharge a river system, which can significantly impact the river

quality, even without substantial anthropogenic pressure (Liu et al., 2019; Han et al., 2018).

Madlala, (2015) conducted an assessment of the Berg River and groundwater quality in the Upper Berg River catchment. However, the study did not investigate the specific mechanisms governing the ion compositions below the Berg River dam. The findings revealed that Na-Cl was the dominant water type, with minor amounts of Ca^{2+} and HCO_3^-. This was suggestive of active salinization processes, which could be attributed to water-rock interactions or human activities. Monitoring of the Berg River's salinity since the 1970s, as established by extensive research conducted by Fey and De Clercq (2004), identified dryland salinity as the primary contributor to the high salt concentration in the catchment. Dryland salinity is a major global concern, particularly in arid and semi-arid regions, where salts accumulate in the plant root zone and across the landscape due to varying water balance conditions (McFarlane et al., 2016), where rainfall percolation leads to the leaching of these ions from rock and soil into rivers (Xiao et al., 2021). In agricultural catchments, the major sources of salt accumulation are regulated by factors such as rainfall, marine aerosols, wind deposition, sea water intrusion, irrigation salinity, rock weathering, evaporation rates, and the geological soil profile (De Clercq et al., 2010). Sodium ions in stream and spring water are believed to originate from unaltered mineral grains present in the chemically inert TMG sediments. These salt mineral grains may have been deposited and accumulated within the sediments as impurities of cementing agents or through the evaporation of saline water.

Graphical methods are often used in water quality studies to represent hydrochemical data and analyse large datasets to define water chemistry and the geochemical processes affecting water quality variation (Aza-Gnandji et al., 2013). The most common graphical methods include Piper, Stiff Pattern, Gibb's, and Durov plots (Singh & Kumar, 2015). Among these, Piper diagrams (Piper, 1944) are particularly useful as they can represent multiple samples on a single plot and enable analysis of water type, mixing, and chemical processes among major dissolved constituents (Sharma et al., 2017; Singh & Kumar, 2015). Chemical weathering plays a significant role in the composition of river water constituents

and is influenced by the weathering of different rocks, climate and streamflow rates (Wu et al., 2016). The Gibbs plot, introduced by Gibbs in 1970, is a widely used tool to analyse the relationship between TDS values and the molar ratios of $Na^+/(Na^+ + Ca^{2+})$ or $Cl^-/(Cl^- + HCO_3^-)$ in surface waters. This plot helps understand the mechanisms that affect solute chemistry and the changes in river water chemistry over time. The plot identifies three main mechanisms: rock dominance, characterized by moderate TDS values and ion ratios <0.5; atmospheric precipitation, characterized by low TDS values and ratios >0.5; and evaporation dominance, characterized by high TDS values (Jiang et al., 2020).

Approximately, only 15% of the Earth's surface is currently protected from direct human impact (UNEP-WCMC & IUCN, 2018). Studies have shown that irrigation increases rock-chemical weathering (Chen, 2006), and damming operations can alter rainfall distribution through elevated evaporation and humidity levels (Degu et al., 2011), leading to an increase in Cl^-, Na^+, K^+, SO_4^{2-}, HCO_3^- concentrations in rivers (Chen et al., 2002; Milliman et al., 2011). Hydrochemical and multivariate statistical analyses have proven effective in identifying the hydrochemical processes influencing natural water sources (Wang et al., 2019; Kou et al., 2019). The ion-ratio method is a valuable approach for determining the origin of solute concentrations and understanding factors like ion-exchange that affect water composition (Wang et al. 2019; Asare-Donkor et al. 2018). By examining the linear relationship between $Na^+ + K^+ - Cl^-$ vs. $(Ca^{2+} + Mg^{2+}) - (HCO_3^- + SO_4^{2-})$ (meq. L^{-1}), a slope of -1 and the distribution of water samples on the trendline suggest ion exchange as a governing process, while samples close to the x-axis zero origin indicate no influence of ion exchange (Jankowski et al., 1998). Cluster Analysis and Factor Analysis are effective tools of multivariate statistical analysis that aid in reducing and grouping extensive hydrochemical datasets, helping to deduce the dominant processes controlling surface water quality (Modie et al., 2022; Asare-Donkor et al., 2018; Wang et al., 2019; Madlala, 2015).

Wang et al. (2021) and Madlala (2015) used Principal Component Analysis (PCA) to analyse and reduce large hydrochemical datasets and identify factors controlling river solutes. Hierarchical Cluster analysis, a type of unsupervised pattern-

recognition method, has been widely used in global water quality studies to analyse the quality of water and assess hydrological connections between different water entities. It has been recognized as an effective statistical tool in ecology and geochemistry (Madlala, 2015; Wang et al., 2019; Zhou et al., 2018; Sun et al., 2016). The "Euclidean" method is commonly used for standard distance measurement and the sum of squares of deviations, and the "Ward method" for merging clusters (Liu et al., 2019), where the loadings are defined by “strong” (>0.75), “moderate” (0.75-0.5) and “weak” (0.5-0.3) (Liu et al., 2003).

2.4 End-Member Source Separation using Mass Balance

River resource management is crucial for both ecological and human needs, but in many parts of the world, demand for freshwater exceeds supply (Fan et al., 2016). Recharge is a key process that influences the hydrological interaction between different water entities and modifies the isotopic composition of water in a hydrological system (Chen, et al., 2020). Precipitation, groundwater, and surface water are all part of the hydrological cycle and share similar hydraulic relationships. However, quantifying the seasonal contributions of precipitation and groundwater to streamflow is a challenge for resource management and the efficient use of water resources in a catchment.

A catchment's response to direct runoff and groundwater discharge can vary within a drainage basin depending on physiographic conditions (Zhou et al.,2015). Groundwater discharge may decrease during storm events, while rainfall events stimulate perennial rivers through groundwater seepage into the streambed by baseflow. The hydrogeological characteristics surrounding a stream influence its baseflow conditions, making it highly variable (Singh et al., 2016). To better understand source contributions to rivers in regions with variable water sources due to changing climatic conditions, separating river flow into dry and wet seasons to define groundwater and rainfall components can be useful.

Hydrograph separation techniques using stable isotopic hydrology or geochemical tracers have been effective since the 1970s to quantify pre-event and event runoff components during storm events, aiding in streamflow generation at a reach to catchment scale (Uhlenbrook and Hoeg, 2003; Machavaram et al., 2005; Li et al.,

2017; Gou et al., 2018, Fan et al., 2016; Dinçer et al., 1970). According to Klaus & McDonnell, (2013) and Shao et al., (2020), a hydrograph separation technique using stable isotopes requires a collective group of assumptions to quantify the contributions of varying components to streamflow.

1) Water sources contributing to a river must have distinct isotopic compositions or variations that can be accounted for.
2) The isotopic signatures of studied water sources are generally consistent but can account for any showed variation in space and time.
3) Surface water bodies have a minor contribution to streamflow generation.

Various methods have been developed to separate baseflow including graphical, hydrological simulation, tracer-based mass balance, electrical conductivity mass-balance, and automated baseflow separation using digital filters (Zhang et al., 2012). The graphical method is easy to implement but time-consuming and subjective, while the hydrological simulation method requires continuous time-series hydrological and climatic data to calibrate accurately (Smakhtin & Masse, 2000; Zahraei et al., 2021; Shao et al., 2020). Tracer-based mass balance, incorporating environmental tracers, has also been employed (Bhagat et al., 2021; Chen et al., 2020), as well as electrical conductivity mass-balance (Stewart et al., 2007), and automated baseflow separation methods using digital filters which was used by Madlala, 2015, in the Berg River headwaters.

Traditional methods such as graphical hydrograph separation and recession analysis lack objectivity and physical ground-truthing, making the accuracy of estimates questionable (Foks et al., 2019). Automated separation methods such as HYSEP and UKIH were found to underestimate baseflow in the semi-arid Hailiutu River Basin in China, while RDF-E misidentified quick flow values during dry periods. However, when used in combination with tracer-based methods, RDF-E was able to accurately identify baseflow (Shao et al., 2020).

The tracer-based mass balance model is the most objective method for separating various streamflow contributors as it relies on continuous monitoring of ion or isotopic concentrations in overland runoff, stream water, and groundwater. This

method uses steady-state mass balance equations and is capable of identifying and separating streamflow components in gauged and ungauged systems. The method has been applied in many studies to quantify the relative contributions of various water sources to streamflow using a simple batch-mixing model based on the mass conservation of stable isotopes ($^{18}O, ^{2}H$). The method assumes conservative mixing between the two sources and has been used in two or three-component mass balancing models (Klaus & McDonnell, 2013; Gibson et al., 2000; Gibson et al., 2016; Li et al., 2017; Trinh et al.,2017; Haiyan et al., 2018).

The simple mass balance approach, based on distinct isotopic compositions in varying natural water bodies, can quantitatively estimate river recharge by identifying the contribution of varying end-member sources (Bhagat et al., 2021). This approach is founded on the idea that total streamflow is generated by a mixture of water source dynamics with varying characteristics (Pinder and Jones, 1969). While this method can be laborious and time-consuming, especially in large watersheds, it has been found to be an accurate and objective technique for separating direct runoff and baseflow and delineating flood events based on water constituents (Klaus & McDonnel, 2013; Shao et al., 2020; Trinh et al., 2017).

The isotopic mass balance model is a widely used and accurate technique for identifying and separating various streamflow components based on the isotopic compositions of specific water bodies. This approach has been employed in various studies have validated the effectiveness of this approach to assess runoff processes at different scales (Fan et al., 2016; Trinh et al., 2017; Chen et al., 2020; Shao et al., 2020; Bhagat et al., 2021). For example, Li et al. (2017) used a two-component isotope mass balance model to distinguish headwater sources in China's Loess Plateau and the Berg River Catchment in a 60% agricultural watershed. The study found that precipitation isotopic composition varied while groundwater was constant, validating the mass balance approach. The contribution of each source was identified in different seasons, revealing that headwater flow responded quickly to rainfall while groundwater was significant in generating flow downstream. For example, a two-component isotope mass-balance was applied to assess the contribution of surface and subsurface sources to the Sandspruit River in the Berg River Catchment using the environmental tracer $\delta^{18}O$ and SiO_2, which revealed that

groundwater was the dominant contributor to the flow and that surface runoff contributed during the onset of the storm event (Damons et al., 2018). Despite its labour-intensive nature and the need for extensive monitoring data, the isotopic mass balance model is objective, quantifiable, and can establish trends in water constituents.

2.5 Summary

This literature review focused on stable isotopes in water as tracers for understanding ecological and hydrological processes. Isotope fractionation reveals insights into water circulation and transformation influenced by processes like evaporation. Catchment properties control streamflow, while rising temperatures enrich residual water isotopes. Stable isotopes help identify hydrological characteristics, trace water sources, and detect deviations at different scales. Understanding factors influencing river water's isotopic composition is crucial for interpreting its signature, with implications for water resource management and climate studies. The review also addressed the knowledge gap regarding the impact of climate, altitude, and lithology on isotopic variations, as well as the significance of groundwater-surface water interaction in the Berg River Catchment.

In river systems, the land-ocean connection facilitates material and energy exchange. Factors like meteorology, water source composition, flow rate, input sources, and geological characteristics determine river water quality. Arid and semi-arid rivers face challenges from reduced recharge and declining water quality, necessitating effective management. The review highlights the knowledge gap regarding solute concentrations below the Berg River Dam and emphasizes the influence of natural processes and human activities on the chemical composition of rivers, which require assessment. Quantifying the contributions of precipitation and groundwater to streamflow poses challenges for water resource management. Various methods have been developed to separate streamflow source contributions, with the tracer-based mass balance model being regarded as the most objective approach. Hence, stable isotopic tracers and the analysis of major ions using statistical and graphical methods are valuable for understanding hydrochemical processes and water flow pathways in rivers.

Chapter 3: Research study area, design and methodology

3.1 Introduction

The following chapter provides the context of the study area with reference to the regional climate, hydrogeology, dominant soil and vegetation cover. Thenceforth, the research design and methodologies are discussed regarding the collection and analysis of the data. Discussing the methodology of the research was pivotal, in achieving the study's objectives. The credibility of the report is established by incorporating quality assurance, limitations, and ethical considerations.

3.2 Description of the study area

The Franschhoek-Paarl valley is located at 33° 54' 36.3" S;19° 7' 33.07" E, and is part of the mountainous Berg River sub-catchment. It includes the quaternary catchments of G10A, G10B, and G10C, which fall under the jurisdiction of the Stellenbosch and Cape Winelands District Municipality in the Western Cape Province of South Africa. The streamflow regime within these catchments is dependent on: direct precipitation, groundwater discharge, interflow, surface runoff, and dam release (Madlala, 2015).

3.2.2 Regional hydroclimate

The study area experiences a Mediterranean climate, with warm dry summers (November to March) and cold wet winters (April to October). The catchment experienced an average monthly temperature that ranged between 13°C to 31°C during the dry season (Figure 3). In comparison, during the wet season, temperatures varied between 5°C to 28°C.

The data depicted in Figure 5 represent monthly precipitation levels sourced from La Motte, Dwars, and Vinpro Hortec Stations. These data reflect a specific time period rather than long-term averages. The observed variations in precipitation intensity throughout the hydrological year indicate seasonal fluctuations in rainfall patterns. This pattern demonstrated a distinct winter rainfall pattern with high precipitation amounts, primarily occurring between May and August. The Western

Cape is susceptible to extreme winter rainfall distribution that originates primarily from cold fronts of a low-pressure system closely related to mid-latitude cyclones moving in an eastward direction across the South Atlantic Ocean (Otto et al., 2018). However, when high-pressure systems move further south, this causes dry conditions in summer. In the Upper Berg River catchment, the mean annual precipitation (MAP) ranges from 700-800 mm/year, with approximately 80% falling between April and September (De Clercq, 2006; Belcher et al., 2015; Madlala, 2015; Fell, 2017). However, based on the 2020-2021 weather data (Figure 3), the catchment experienced a MAP of 717.32 mm. The presence of the Drakenstein and Franschhoek mountains in the catchment has an orographic influence, where mean and annual precipitation amounts can differ significantly across the catchment.

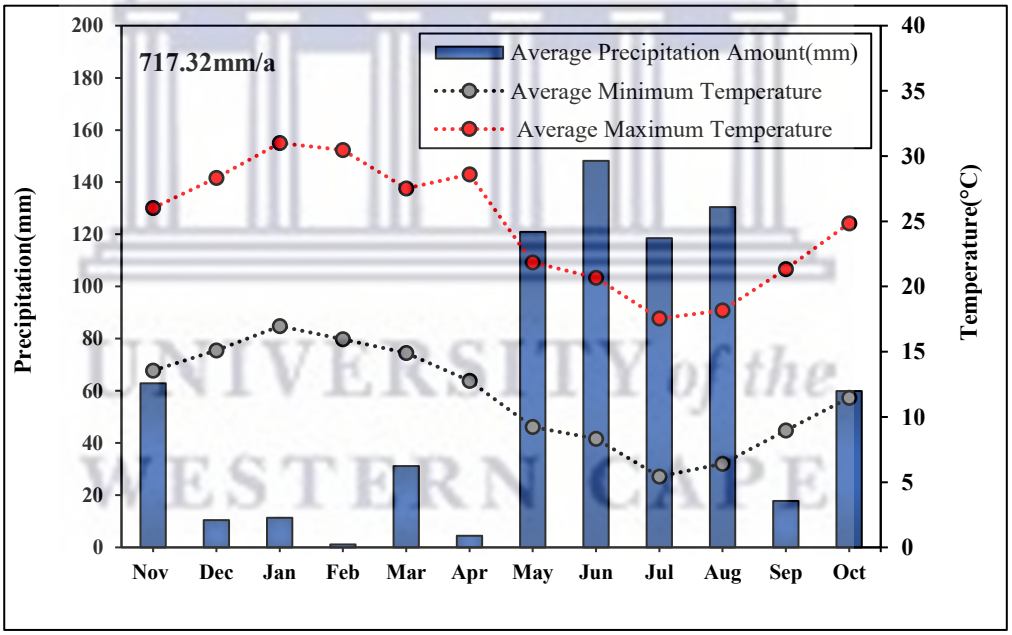

Figure 3: Average monthly precipitation and temperature in Franschhoek-Paarl Valley. Meteorological Service Provider: iLeaf (2021)

The data provided by La Motte, Dwars, and Vinpro Hortec stations in February 2021 of Figure 4, had the lowest average Relative Humidity (RH) at 55%, making it the driest month, while July 2021 had the highest average RH at 70%, making it the wettest month. RH (%) is inversely proportional to the Evapotranspiration (ETo,mm) rate, computed by the Penman-Monteith method (Allen et al., 1995). Thus, during the dry season when the temperature increased and RH (%) decreased,

the air became drier and could hold more moisture relative to colder air, leading to an increase in ETo (mm) rate. Conversely, in the wet season, as the temperature decreased and the surrounding air became moister, reaching saturation, the RH (%) increased, resulting in a decrease in the ETo (mm) rate. The annual average ETo (1196.49 mm) for the hydrological year was higher than the annual mean precipitation (716.32 mm), respectively.

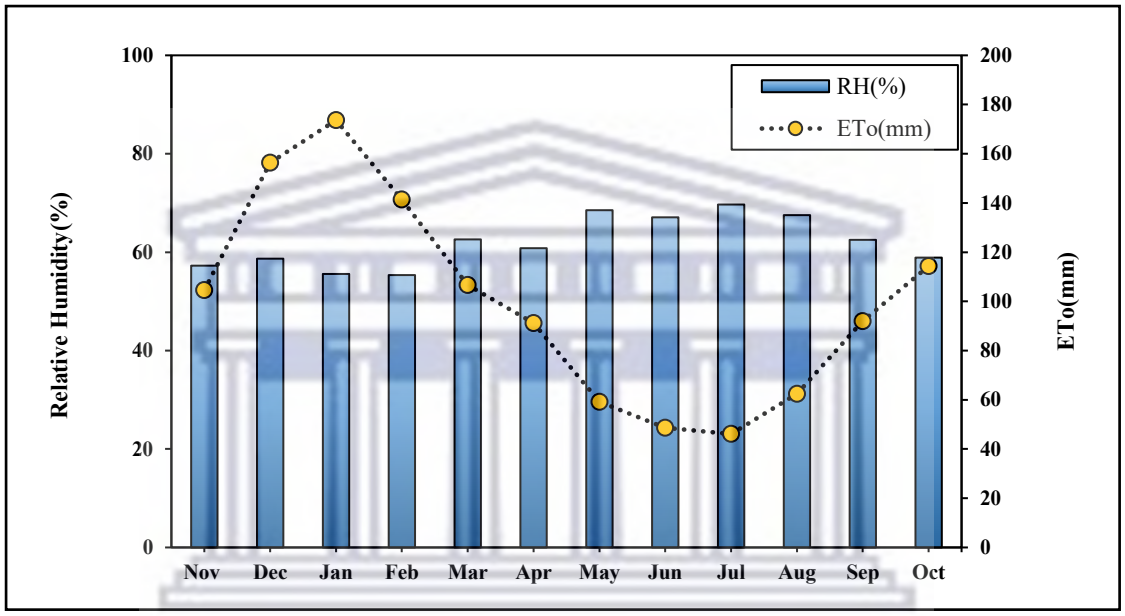

Figure 4: Average monthly Evapotranspiration (ETo, mm) and relative humidity (RH, %) for Franschhoek-Paarl valley. Meteorological Service Provider: iLeaf (2021)

3.2.3 Hydrogeology

The dominant geology underlying quaternary catchments G10 A, B, and C of the Berg River catchment, tabulated in Table 1 comprises a combination of inert sandstone from the regional fractured hard rock TMG origin, comprising the dominant water-bearing aquifer units, namely the Peninsula and moderately mineralized sand, silt and mudstone of the Nardow, and the Franschhoek basement formation. Underlying the TMG formations are softer argillaceous rocks such as shales and mudstones of the Malmesbury Group (MG). The most prominent unit of the MG is composed of grey to purple phyllitic shales and fine-grained greywackes,

which are more susceptible to weathering processes. The MG also includes the intruded granites of the Cape Granite Suite (Scheepers & Armstrong, 2002).

Figure 5 and Table 1 data from Theron (1984), Theron et al. (1992), Duah (2010), and Pietersen & Parsons (2002) reveals that the Peninsula Aquifer System has the largest hydrogeological thickness and represents the largest aquifer unit in the area. It is a prominent underground feature beneath the Berg River Dam in the Upper Berg River catchment. The aquifer system's visible layers, which are mostly unconfined or semi-confined, sustain rivers and mountainous headwater streamflow through interflow and baseflow along the northern and eastern boarders of the catchment (Colvin et al., 2009). The secondary fractured aquifer unit is associated with the dominant Peninsula formation in the continuous mountain ranges of the Western Cape. This exposes the aquifer to elevated recharge and rainfall events, while also influencing the presence of rainfall and snow in the area due to its resilient orographic effect (Colvin et al., 2009).

Table 1: Regional stratigraphy of the Franschhoek-Paarl Valley.

AGE	GROUP	SUBGROUP	FORMATION	THICKNESS (M)	LITHOLOGY
QUATERNARY (1.8-PRESENT)		Quaternary Cenozoic deposits			Scree, alluvium
ORDOVIAN-DEVONIAN (490-360 MA)	TMG	Nardouw	Rietvlei	280	Feldspathic, quartz arenite
			Skurweberg	390	Quartz arenite, Sandstone
			Goudini	230	Sandstone, Siltstone
			Cedarberg	120	Silty Shale
			Pakhuis	40	Shale, Diamicite
			Penninsula	1800	Quartz arenite, sandstone
			Graafwater	420	Shale, sandstone
			Piekenierskloof	900	Quartz arenite, conglomerate and minor shale
NAMIBIAN-CAMBRIAN (1000-545 MA)	Malmesbury	Swartland	Moorreesburg	±300m	Shales, greywacke, phyllite, limestone and quarzitic sandstone.
	Cape Granite Suite				Agglomerate and basalt; Course porphyritic granite

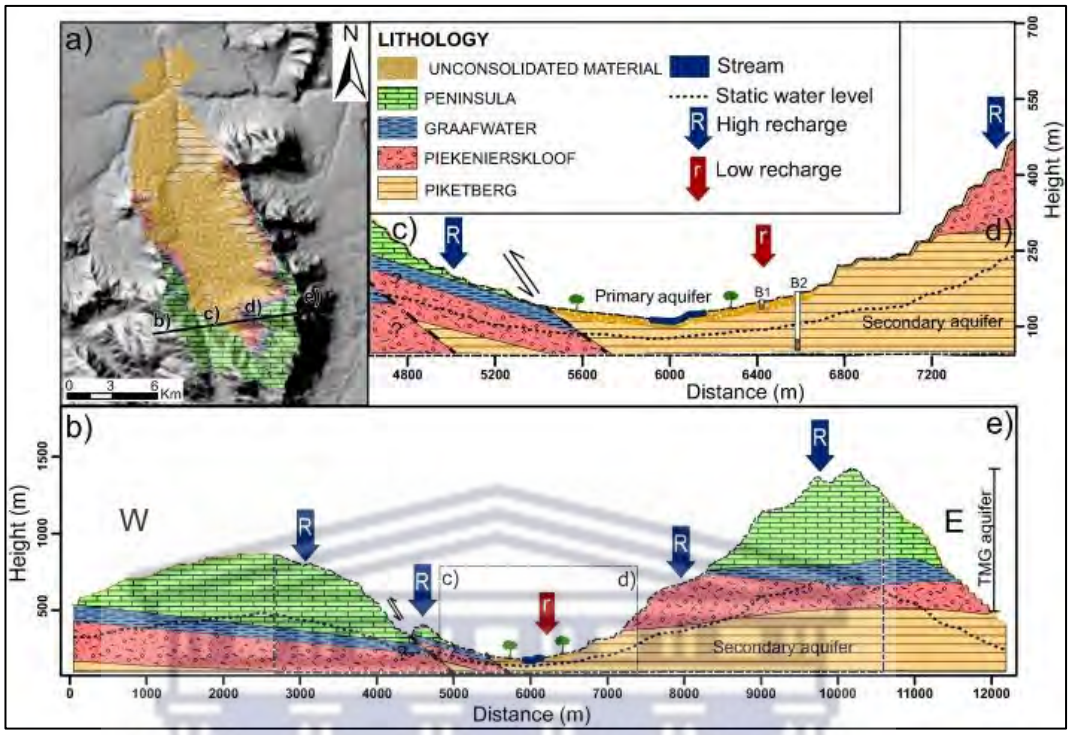

Figure 5: Interconnection of aquifers and TMG material deposition: A cross-section example from Velorenvlei Catchment, adjacent to Berg River Catchment (Source: Watson et al., 2018).

The TMG aquifer system in the upper catchment area, characterized by fractured, secondary porosity and chemically resistant quarzitic rocks, is a significant sub-surface feature in South Africa (Clark & Ractliffe, 2007). Additionally, the catchment area is marked by the presence of alluvial deposits, which contribute to the aquifer's heterogeneity deposited by streams.

Fractured rock formations of the Peninsula and Nardouw aquifer units exhibit reduced porosity and a heterogeneous flow path due to folding and faulting in the Cape granite suite and TMG Nardouw formations. The geological formations present in the catchment show a high level of fracturing, which enables water, dissolved geological constituents, and contamination to travel via fracture flow within the aquifer and interact with surface water bodies (Madlala, 2015). According to Clark & Ractliffe (2007), significant groundwater recharge in the Berg River occurs in the upper regions of the catchment near Franschhoek, driven by substantial rainfall activity and rugged topography. Alluvial deposits contribute to the recharge process by providing pathways for water infiltration into the

subsurface. Additionally, fractures within the aquifer lead to the emergence of springs and seeps, with alluvial deposits serving as important sources of groundwater discharge.

These sources contribute to the sustenance of groundwater, which in turn supports the continuous flow and effluent characteristics of the Berg River. The discharged water from the aquifer typically has low dissolved salts, with Cl^- and Na^- ions being dominant (Smart & Tredeoux, 2002). The aquifer, which is primarily composed of inert quartzite rocks, is generally characterized by reduced levels of Ca^{2+} and Mg^{2+}, as the ion salts are diluted and flushed out of the system during precipitation recharge. (Smart & Tredeoux, 2002). In elevated mountainous terrains, substantial groundwater recharge originates from the TMG, where rainfall infiltrates geological joints and fractures, percolating as interflow until it reaches the water table. This process explains the rapid flow of water from rocky plains following rainfall events, to replenish streams along the valley (Duah et al., 2010).

North of the Berg River Dam and towards the Paarl valley, the underlying geology transitions to softer clay minerals, including argillaceous rocks like shale, greywacke, and phyllite, alongside formations of quartz, schist, and limestone belonging to the Malmesbury group. The area also hosts the Paarl pluton, northwest of the Boschenmeer Gold Estate, comprising fine to medium porphyritic granite from the Cape Granite Suite (Figure 6), that intruded into the sedimentary Malmesbury Formations, with biotite elements.

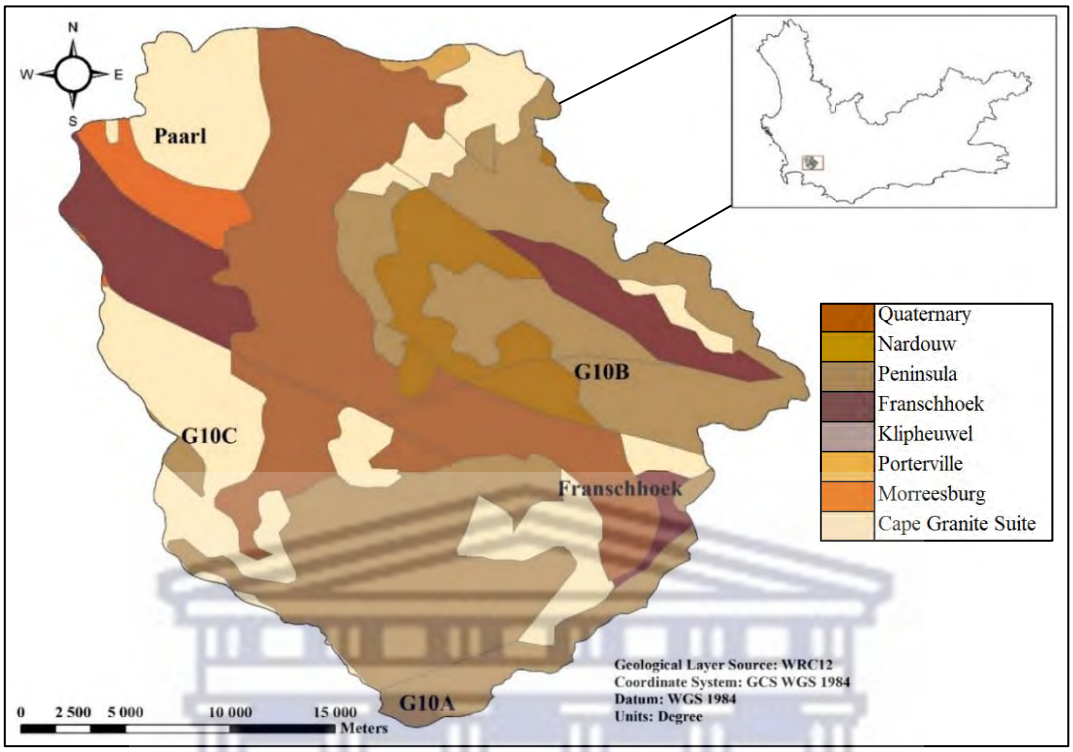

Figure 6: Geological map defining the lithological units, in the Franschhoek-Paarl valley. Source Layer Provider: Water Research Commission 2012 (WRC12).

3.2.4 Soil

The valley's soil characteristics are determined by the geological parent material. The aquifer units are concealed by small particles of silt and clay or larger particles of sand and gravel, which are abundant in the surrounding mountains. However, the catchment's flat terrain is dominated by quaternary sediment deposits such as scree, loamy/sandy soil, gravelly clay, ferricrete, and alluvium (Clark & Ractliffe, 2007).

The soil composition in the upper Berg regions, resulting from the weathering of TMG quartzites and sandstones, is typically characterized by larger particles of coarse sand and gravel of larger pore spaces and high permeability, allowing an increased infiltration rate and sandy clay texture. It is generally nutrient-poor and acidic in nature (de Villiers, 2007). On the other hand, soils derived from weathered granite and shale rocks produce soil with a higher clay content of low permeability (Mol and Campbell,1976). According to Clark and Ractliffe (2007), the primary parent material of the soil in the region plays a significant role in the distribution of poor-quality groundwater and the movement of surface runoff. Coarser soils with

larger pore spaces and steeper slopes tend to facilitate faster surface runoff, potentially leading to erosion and reduced water quality.

3.2.5 Hydrology

The Berg River has its source in the headwaters located 6 km above the Berg River Dam, situated in the Jonkershoek and Franschhoek mountains, with elevations ranging from 1300 m.a.s.l to 1500 m.a.s.l. The river meanders in a north-easterly direction, crossing deeply incised valleys along a moderately steep topographic slope of 0.67%. Its bed is dominated by cobbles and boulders, closely tracing the fold axes of the synclinal basins (Clark & Ractliffe, 2007). Stretching approximately 285 km, it begins in catchment G10A and flows at its mouth in St. Helena Bay where it meets the Atlantic Ocean (Clark & Ractliffe, 2007). During the study in the Franschhoek-Paarl valley, flow rates ranged from 0.03 to 26.33 m^3/sec in the dry season and 0.04 to 341.22 m^3/sec in the wet season (Figure 7).

In 2007, Ractliffe estimated that the Berg River catchment contributed 931 MCM/a of natural runoff, with 45% originating from the three quaternary catchments, covering only 7% of the area. In the upper G10A reach, the Berg River supplies drinking water to the City of Cape Town via the Wemmershoek and Berg River dams. The Wemmershoek Dam, southeast of Paarl, spans 3 km^2 with a storage capacity of 66 Mm^3, while the Berg River Dam covers 5 km^2 and holds 130 Mm^3 (Cullis et al., 2019). The Berg River project includes the Berg River Dam, Drakenstein abstraction works, and Dasbos pump station, connected by the Dasbos tunnel about 10 km downstream from the Berg River Dam (Rossouw, 2008; Bosman et al., 2016). During high winter flows, water is diverted from the Berg River through a 1.6 m high diversion weir and into an off-channel balancing dam. Then, it is pumped back to the Berg River Dam for storage by the Drakenstein pump station (Rossouw, 2008; Madlala, 2015).

The Berg River's surface runoff (Figure 7) mainly originates from its main tributaries: the Franschhoek, Wemmershoek, and Dwars Rivers. These perennial streams flow parallel to the fracture and fault orientations and perpendicular to the fold axes of the underlying TMG lithology (Colvin et al., 2009). They display seasonal streamflow patterns, with high-flow events occurring naturally during the

wet season and low-flow events being more prevalent during the warmer months (Struyf et al., 2012). The Franschhoek River, originating from the Franschhoek mountain range, flows approximately 30 km before joining the Berg River (Adams, 2011). The Dwars River, characterized by dense riparian vegetation, originates in the Banghoek valley between Stellenbosch and Franschhoek. It flows in a north-westerly direction, passing through the towns of Johannesdal and Pniël, before joining the Berg River.

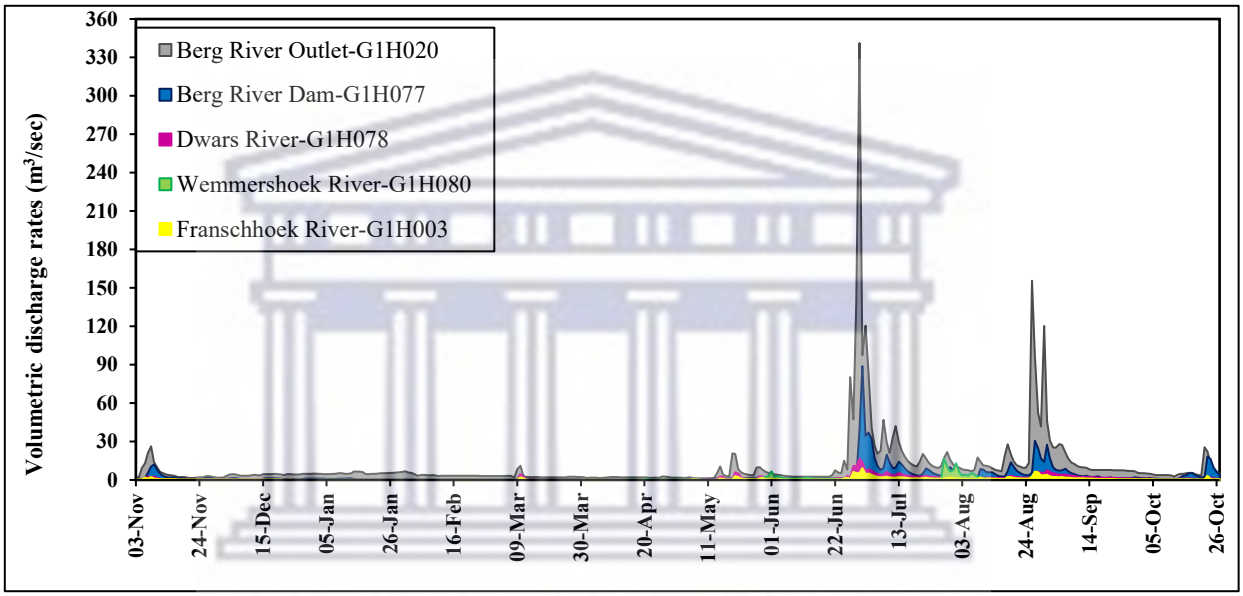

Figure 7: 2020-2021 daily average riverine volumetric discharge rates (m^3/sec) at five gauging stations in the Franschhoek-Paarl valley catchment. Data source: DWS (2021).

3.2.6 Land cover

Vegetation

The Franschhoek-Paarl valley sustains the indigenous fynbos vegetation of the Cape Floral Kingdom (Figure 8), but riparian vegetation along the Berg River is limited and localized. This has resulted in a decline in vegetation due to the rapid increase of invasive alien species, such as Eucalyptus plants (Adams, 2011; Madlala, 2015). The fynbos vegetation, particularly the Sclerophyllous bush types in the catchment area, can release organic humic acid into the river, which can lower the pH levels in the water (Struyf et al.,2012). However, humic acid can also

enhance the soil's ability to retain infiltrating rainfall by altering pore spaces and soil aeration.

Land use practices

The valley basin surrounded by the Franschhoek and Drakenstein Mountain ranges consists of 65% agricultural land cover (Figure 8), which includes irrigation, deciduous fruit, sports grounds, urban towns, and vineyard cultivation, contributing significantly to the economic growth in the catchment and dry land farming (Struyf et al., 2012). These practices rely on the river flow for irrigation, particularly during the dry summer months.

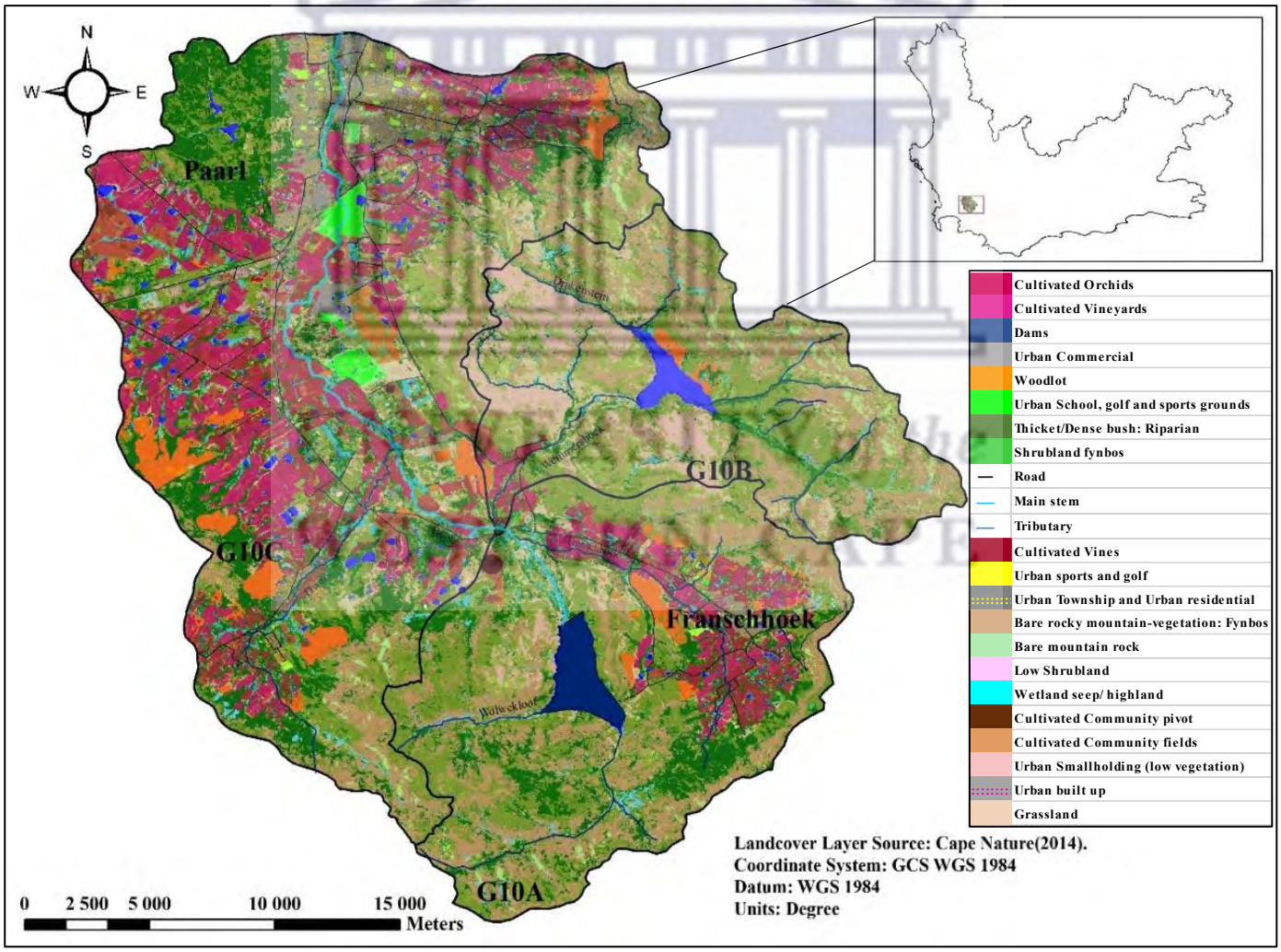

Figure 8: Landcover distribution in the Franschhoek-Paarl valley. Source Layer Provider: Cape Nature (2014).

3.3 Research design

To capture the heterogeneity and geographic source areas of the catchment, potential end-member sources of the Berg River were considered based on meteorological and environmental characteristics such as temperature, rainfall amount, geology, land cover, aquifer depth, and land-based activities. This ensured that the sampling sites capture the full range of potential influences on streamflow dynamics, from natural processes to anthropogenic impacts. To investigate the factors influencing streamflow at a seasonal scale, fieldwork and desktop-based approaches were integrated. This involved analysing baseline data, physiochemical measurements of the river, precipitation, and groundwater sources, as well as assessing secondary time series and streamflow data collected over a specific period to understand patterns, trends, and variations in streamflow characteristics During a reconnaissance visit, the locations of groundwater, surface water, and precipitation were recorded using a handheld Garmin *e*trex 30x™ GPS and corresponding coordinates provided by the Department of Water and Sanitation. This helped in evaluating the spatial trend of river water sources and the processes that influenced temporal streamflow. Surface water monitoring points were selected at various reaches (Upper, Middle, and Lower) downstream of the Berg River dam, considering tributaries, land activities in proximity, and their influence on the river. Sampling was carried out at multiple locations along the river to evaluate the magnitude and variability of flow, accounting for variations along different sections of the Berg River.

In summary, a quantitative research design was incorporated, integrating statistical, chemical, and graphical methods to establish relationships between variables. The unit of analysis for the research included the Berg River and its end-member sources, analysed within the three physiographic regions of the upper, middle, and lower valley regions on a bi-weekly basis. The study population consisted of the Berg River catchment area itself, including its various geographical features, environmental characteristics, and human activities that influence streamflow dynamics. Sampling points strategically chosen within this area investigated water quantity, quality, flow rates, and land use patterns along the river.

3.4 Data collection methods

To assess the interaction and mixing among various water sources in the catchment and the extent of water discharged into the Berg River, the sampling and collection of field-based data in the selected quaternary catchments was crucial. A total of 40 sampling locations were selected along the 30 km mainstream, including precipitation (3), groundwater (15), the main river stream, and its major tributaries (22). This allowed for investigating the spatiotemporal variations of the isotopic and hydrochemical compositions in the Franschhoek and Paarl valley area. A total of 25 sampling campaigns were conducted between 2020-2021, on a bi-weekly scale, during the dry (November to March) and wet (April to October) seasons. The water samples were filtered using a 0.45µm nylon syringe filter for major ion analysis and a 0.22µm cellulose acetate filter for isotope analysis.

To ensure the accuracy of water sampling, several steps were taken before collecting the water sample. Firstly, the bucket used for grab sampling, the polypropylene Greiner Bio-One conical tube, and the red capped cryogenic tubes were rinsed three times with the water to be sampled. This helped the equipment to acclimate to the water environment. The water was collected to the brim of the bottles, without any entrapped air, and sealed with an inner cap and tightly secure outer cap. Additional Parafilm^{TM} tape was used to prevent evaporation. Quality control measures were taken by collecting field duplicates and blanks periodically. Each sample was labelled with the time, location, and sample identification (ID). The samples were stored in the fridge at 4°C until laboratory analysis at the UWC Environmental and Water Science Department, and Stellenbosch University BIOGRIP Facility. In addition, the in-situ field parameters including temperature (˚C), pH, and EC (µS/cm) were measured once stabilised, using a digital Hach HQ40D portable multi-meter at each sampling location, and it was calibrated before every sampling event.

1) **Precipitation:** Precipitation was collected using standard conical rain gauges, following the specifications provided by IAEA (2014), at three different locations. During the hydrological year from November 2020 to October 2021, precipitation samples were collected from a collector located

near a meteorological station. A total of 41 rainfall events were recorded at RF1, 30 rainfall events at BG00047-RF, and 17 rainfall events at UWC-RF#1 (see Appendix B). The rain gauge was situated in an open area and included a container for measuring precipitation in mm, with reference to height by an automatic logger at a given time. To ensure accurate isotopic analysis, it was necessary to prevent evaporation, which could alter the water's isotopic composition. Water from the gauge was transferred into a polyethylene sample bottle for collection after each event, using a staff. To avoid fractionation, bulk rainfall was collected immediately after an event for isotopic and hydrochemical analysis. The volume-weighted mean of the seasonal rainfall isotopic composition in the catchment was used to determine the rainfall end-member component in the mass balance analysis, which was conducted to assess the seasonal response of the river water to rainfall events.

2) **Groundwater:** Before collecting groundwater samples, in-situ measurements of the depth to water table and shallow borehole depth were taken using a Solanist water level meter and tape measure to measure casing and collar height. The groundwater was then purged with a pump to obtain authentic samples that reflect the conditions of the aquifer. To do this, a low flow, WSP-12V-5 stage, submersible tornado pump was used to extract the groundwater from monitoring wells. The pump had a 26 m lift capacity-27 m cable, crocodile clips with a 50 mm diameter, and LDPE discharge tubing.
3) **Surface water:** River water was collected mid-stream to ensure that they were representative of the river's conditions and not affected by insufficient mixing or stagnant water near the river banks. Due to turbulent flow, a grab sampling method was employed using an LDPE bucket tied with nylon rope to collect the river samples. To prevent cross-contamination, the bucket, sample bottles, and sampling equipment were rinsed three times with distilled water and the sample water prior to sample collection.

3.4.1 Sampling sites

The sampling sites selected across upper, middle, and lower physiographic zones are illustrated in Figures 9-10 and summarized in Tables 2-3, including 22 river samples, three rain gauges, and fifteen boreholes. Surface water samples were gathered from the main river channel, its tributaries, and specific gauging weirs.

The upper region:

The sampling sites for river, groundwater, and rainfall were positioned downstream of the Berg River Dam, approximately 6 km west of Franschhoek. The flow of the Berg River in these regions was predominantly influenced by dam releases, with minimal impact from other human activities. Notably, the Franschhoek River (G1H003 and FRANS1) faced significant human-induced disturbances from the Langrug informal settlement and surrounding farms along its path before merging with the Berg River. Particularly, contamination of the Franschhoek River occurred at its confluence with the polluted Stiebeuel River, originating from the Hawequas mountains and passing through the Langrug informal settlement. This contamination resulted from inadequate sanitation facilities and dysfunctional toilets in the area (Winter, 2016; Fell, 2017). Moreover, at site BGR5, the Berg River received treated effluent discharged from the Wemmershoek Waste Water Treatment Works (WWTW) before converging with the Wemmershoek River at site BGR6. However, the flow of the Wemmershoek River was managed and directed towards the Wemmershoek Dam by the City of Cape Town (COCT) before its confluence with the Berg River at BGR6.

The middle region:

The middle region, situated downstream of BGR6, comprised predominantly agricultural and recreational land uses. This made the river in this area vulnerable to surface runoff carrying fertilizers and pesticides. Further downstream, the Berg River merged with the Dwars River at BGR8. Land uses in this region were primarily agricultural, with urban and recreational activities as secondary components.

The lower region:

The lower region, situated in northern Paarl, featured a semi-urban and industrial landscape. Here, the river flowed through concrete banks and encountered various anthropogenic activities such as breweries, shopping malls, vineyards, residential estates, food manufacturing, and construction sites, before ultimately reaching the G1H020 outlet. This area was heavily developed, with human activities dominating land use.

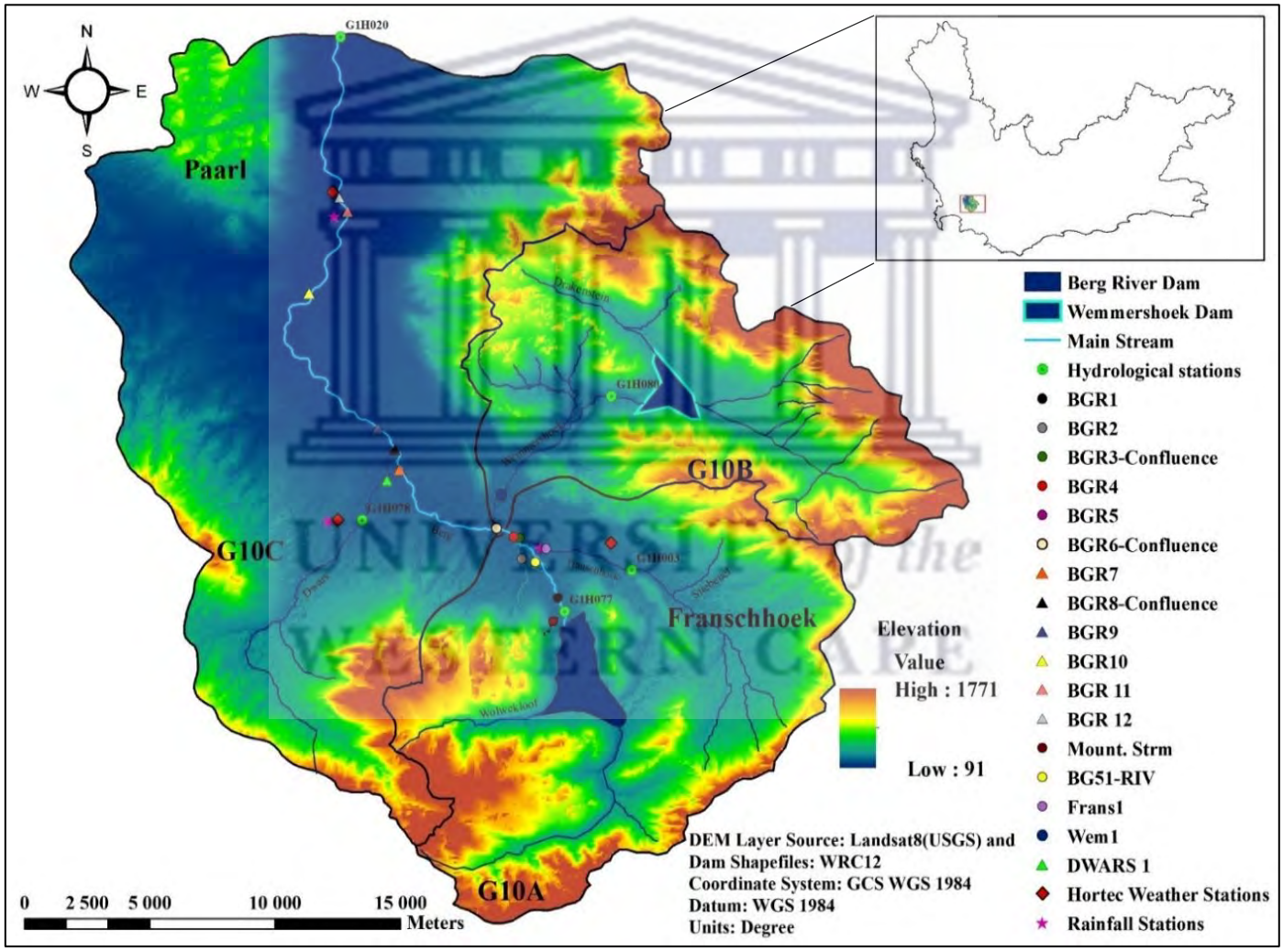

Figure 9: Surface water sample locations in relation to elevation.

Table 2: Franschhoek-Paarl valley river and precipitation sample locations.

Site	River reach location	Geographical Coordinates		Elevation (m.a.s.l)	Stream name	Note
		Latitude (S°)	Longitude (E°)			
Mount.Strm	Upper	-33.908306°	19.050778°	220	Mountainous	The sampling was limited to the wet season as it was not present during the dry flow conditions.
G1H077	Upper	-33.904944°	19.054806°	196	Berg	Berg River Dam outlet
BGR1	Upper	-33.900220°	19.052390°	189	Berg	Main stream
BGR2	Upper	-33.886875°	19.039472°	157	Berg	Main stream
BG-51	Upper	-33.887056°	19.040528°	167	Berg	The sampling was limited to the wet season as it was not present during the dry flow conditions.
G1H003	Upper	-33.890639°	19.078917°	203	Franschhoek-Tributary	Hydrological Station
FRANS1	Upper	-33.882333°	19.039472°	173	Franschhoek-Tributary	Before Berg River Confluence
BGR3	Upper	-33.879670°	19.036890°	168	Confluence	Main stream
BGR4	Upper	-33.879360°	19.036530°	165	Berg	Main stream
BGR5	Upper	-33.876390°	19.030470°	161	Berg	Main stream
G1H080	Upper	-33.852306°	19.042556°	189	Wemmershoek-Tributary	Hydrological Station at the Wemmershoek Dam
WEM1	Upper	-33.875889°	19.030167°	158	Wemmershoek-Tributary	Before Berg River Confluence
BGR6	Upper	-33.876360°	19.030390°	159	Berg	Main stream
BGR7	Middle	-33.856190°	18.995690°	147	Berg	Main stream
G1H078	Middle	-33.873583°	18.982111°	130	Dwars-Tributary	Hydrological Station
DWARS1	Middle	-33.849889°	18.993222°	135	Dwars-Tributary	Before Confluence
BGR8	Middle	-33.849360°	18.994090°	136	Confluence	Main stream
BGR9	Middle	-33.848920°	18.993830°	138	Berg	Main stream
BGR10	Middle	-33.795560°	18.963220°	121	Berg	Main stream
BGR11	Middle	-33.767444°	18.977056°	104	Berg	Main stream
BGR12	Middle	-33.762890°	18.973990°	107	Berg	Main stream
G1H020	Lower	-33.707610°	18.974500°	92	Berg	Outlet-Northern Paarl
BG47-RF		-33.883190°	19.046970°	175		Rainfall Collector
La-Motte		-33.881300	19.071480°	211		Meteorological Station
RF1		-33.875530°	18.979470°	179		Rainfall Collector
Dwars River		-33.875473°	18.979540°	179		Meteorological Station
UWC-RF#1		-33.769290°	18.976230°	113		Rainfall Collector
Vinpro Hoofkantoor		-33.760800°	18.971680°	112		Meteorological Station

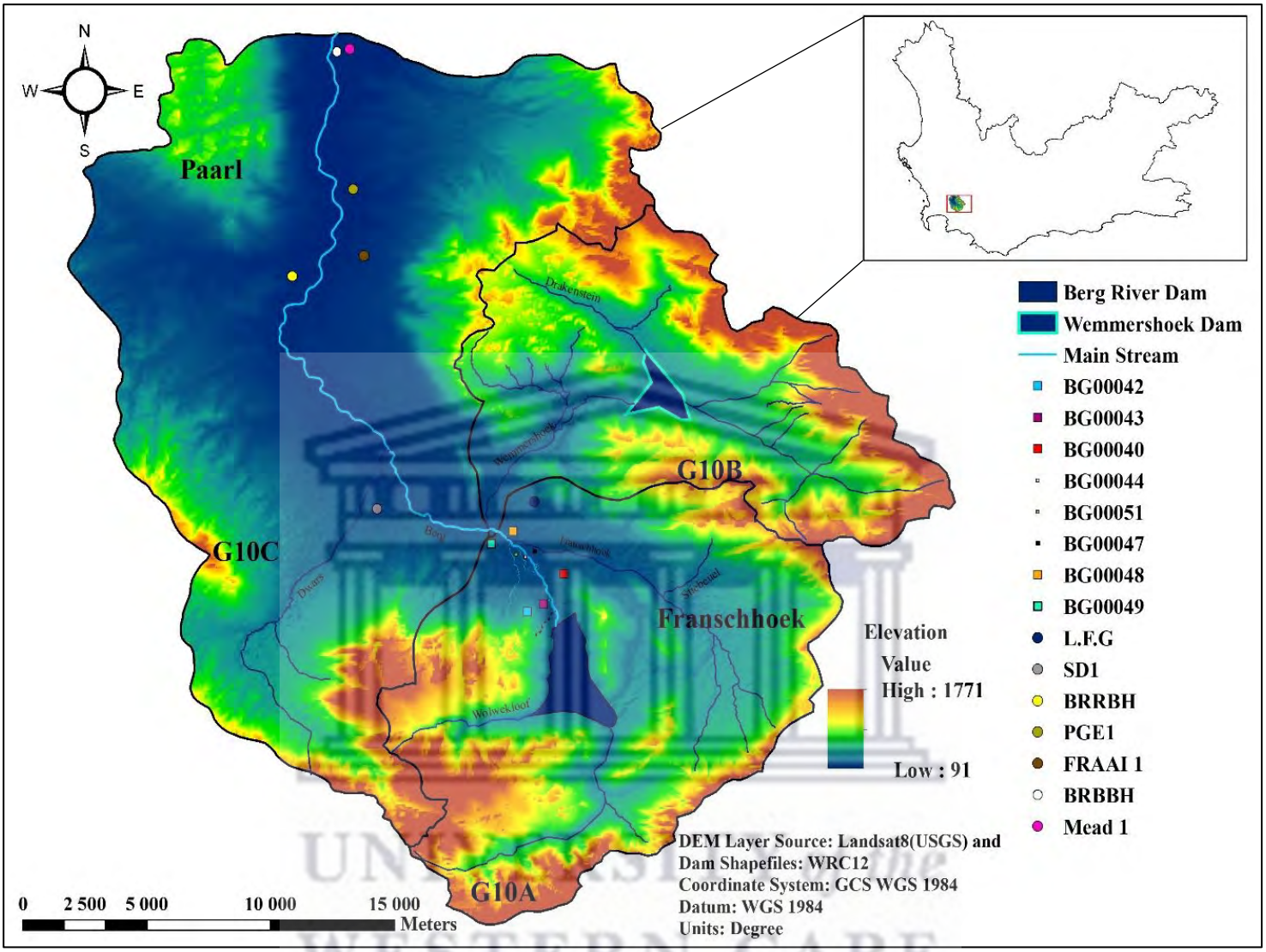

Figure 10: Borehole sample locations in relation to elevation.

Table 3: Franschhoek-Paarl valley groundwater sample locations.

Site	Physiographic location in the valley	Geographical Coordinates		Elevation (m.a.s.l)	Borehole Depth (m.b.g.l)	Borehole Type
		Latitude (S°) WGS 1984	Longitude (E°) WGS1984			
BG00042	Upper	-33.90278°	19.04751°	241	43	Monitoring
BG00043	Upper	-33.90106°	19.05033°	191	35	Monitoring
BG00044	Upper	-33.88701°	19.04091°	173	35	Monitoring
BG00051	Upper	-33.88715°	19.04014°	176	10	Monitoring
BG00040	Upper	-33.89273°	19.05359°	187	35	Monitoring
BG00047	Upper	-33.52594°	19.02495°	165	17	Monitoring
BG00048	Upper	-33.88020°	19.03927°	170	17	Monitoring
BG00049	Upper	-33.87953°	19.03126°	164	31	Monitoring
LFG	Upper	-33.86706°	19.04694°	206	120	Irrigation
SD1	Middle	-33.86958°	18.98983°	172	150	Irrigation
FRAAI 1	Middle	-33.78276°	18.98499°	128	90	Irrigation
BRRBH	Middle	-33.79569°	18.963890°	129	130	Irrigation
PGE1	Middle	-33.759941°	18.981115°	113	150	Irrigation
BRBBH	Lower	-33.709611°	18.974194°	105	8	Irrigation
Mead 1	Lower	-33.709806°	18.974806°	112	120	Irrigation

3.5 Data processing methods

3.5.1 Secondary source, extraction

To perform the climate-stable isotopic analysis, meteorological and hydrological data of daily average air temperature, humidity, and rainfall levels, were needed. The data were obtained from the nearest weather stations provided by Hortec Analytical and iLEAF automated weather station services in Southern Africa. The iLEAF platform, accompanied by Stratus 200 4G modelled weather stations, integrated GPRS technology to detect and acquire real-time raw weather data, was accessible via the iLEAF portal (**https://ileafweather.com/LogIn.aspx**) using a registered username and password. To ensure data quality, the raw weather data was checked and verified before being stored in the cloud.

The river flow data was automatically measured at the hydrological gauging stations. The stream gauge in a stilting well measured the discharge passing through the stream channel per unit time (Q, m^3/s). Streamflow measurements were automatically recorded at hourly intervals and collected a daily basis by DWS officials who verified and stored the data in their hydrological archive. The stream-

flow data was obtained electronically from the **www.dwa.gov.za/hydrology** site using the station identification number within the quaternary catchment and then sorted in Microsoft Excel™.

3.5.2 Laser Absorption Spectroscopy for Water Isotope Ratio Analysis

Sample Preparation

Water samples were analysed for stable water isotope ratios ($^{2}H/^{1}H$ and $^{18}O/^{16}O$) using the Los Gatos T-LWIA-45-, Triple Liquid Water Isotope Analyser (# GLA431-TLWIA, Canada) at the BIOGRIP Node for Soil and Water Analysis at Stellenbosch University. Samples with electrical conductivity less than 1000 µS/cm underwent filtration through a 0.22 µm FilterBio® cellulose acetate syringe filter to remove particulate matter. The filtered samples were then stored in polyethylene bottles with caps securely sealed using waterproof parafilm tape to prevent atmospheric interaction. Subsequently, 1.9 mL of pre-filtered water was dispensed into 2 mL Wheaton® MicroLiter® glass vials, each fitted with PTFE (Polytetrafluoroethylene) septum caps to prevent water evaporation. Finally, the vials were arranged in an automated sample loading tray according to the specified order for analysis.

Post processing and accuracy of data

The Los Gatos TLWIA 45-EP instrument was primed with deionized water, followed by the introduction of three standards (1E, 3E, and 5E) (Table 4) and ten unknown water samples. Each sample underwent up to four repetitions per run, with nine injections measured per repetition. The average of the last five injections for each sample was calculated to determine the ^{2}H and ^{18}O isotopic ratios.

Table 4: Los Gatos Research (LGR) working standards vs VSMOW.

Standards	$\delta^{2}H$ (‰)	$\delta^{17}O$ (‰)	$\delta^{18}O$ (‰)
1E	-165.7 ± 0.5	-11.26 ± 0.15	-21.28 ± 0.15
3E	-79.6 ± 0.5	-5.83 ± 0.15	-11.04 ± 0.15
5E	-9.9 ± 0.5	-1.52 ± 0.15	-2.99 ± 0.15

The Los Gatos TLWIA 45-EP instrument ensured precise and accurate measurements by addressing various error sources like memory effect, instrumental drift, pressure, and sample volume effects. For the conversion of isotopic ratios into delta values, all water samples were calibrated and normalized by utilizing a predefined calibration standard relative to V-SMOW. The instrument consisted of a PAL LSI liquid autosampler (model #522870, Switzerland) connected to an extended PTFE transfer line (1m), a heated injection port (~100°) covered with a PTFE septum (Trajan 6mm HT predrilled, 4mm thick, USA). The autosampler was programmed to inject 1µL of liquid using a 1.2 Hamilton microliter syringe (model: 7701.2N, Romania) into the injection port. After injection, the liquid sample was vaporized using a heater injector block (KNF Neuberger model #024675) and subjected to laser analysis in a double-mirrored cavity chamber. The interaction of vaporized water molecules with a laser resulted in the reflection of light, measured by a photodetector.

The post-processing, normalization, and organization of isotopic ratios were done using LIMS for Lasers 2015 software (Coplen and Wassenaar,2015), This software allowed for the importation, computation, and assignment of specific sample submissions to a particular project. During the post-processing process, quality assurance was maintained by validating the raw isotopic data and correcting for instrument errors. The analytical uncertainties for the analysis were determined to be ±0.15‰ for $\delta^{18}O$ and ±0.5‰ for $\delta^{2}H$. The derived isotopic ratio data were converted to the conventional δ notation, relative to the standard Vienna Standard Mean Ocean Water (VSMOW):

$$\boldsymbol{\delta}=(\mathbf{R}_{\mathbf{sample}}/\mathbf{R}_{\mathbf{VSMOW}}-1)\ \mathbf{x1000‰} \qquad [1]$$

The $\boldsymbol{\delta}$ notation refers to the isotopic ratios of $\delta^{18}O$ and $\delta^{2}H$, and $\mathbf{R}_{\mathbf{sample}}$ and $\mathbf{R}_{\mathbf{V\text{-}SMOW}}$ refer to the isotopic ratios of $^{18}O/^{16}O$ for $\delta^{18}O$ or $^{2}H/^{1}H$ for $\delta^{2}H$, respectively, in the analysed water samples and the mean seawater of the Vienna Standard Mean Ocean Water (V-SMOW).

3.5.3 Major Ion Concentration Measurement using Ion Chromatography

Major ion concentrations in mg/L, including Ca^{2+}, Mg^{2+}, Na^{+}, K^{+}, SO_4^{2-}, Cl^{-}, PO_4^{2-}, and NO_3^{-}, were determined using an IC autosampler instrument at the Stellenbosch University, BIOGRIP Central Analytical Facility. The instrument used liquid chromatography methods to separate charged particles based on their molecular properties and specific ion-exchange processes in the mobile or stationary phase. This procedure resulted in the measurement of concentrations for different cations and anions found in the water sample, reported in mg/L. The mobile phase is responsible for transporting ions through the system, either in a liquid or vaporized phase (Figure 11), while the stationary phase consists of a physical structure, such as the column.

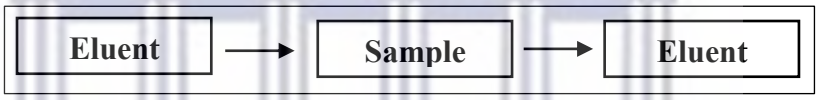

Figure 11: The sequential process of the mobile phase in the IC system.

The analysis of cation and anion concentrations were analysed in two separate systems used in each sample (Table 5).

Table 5: Cation and Anion Analytical Instruments: A Comparative Overview

CATION ANALYTICAL INSTRUMENT	ANION ANALYTICAL INSTRUMENT
• **INSTRUMENT: METROHM 930 COMPACT IC FLEX OVEN/DEGASSER** • **COMPONENTS: METROSEP C6 SEPARATION COLUMN (4.0X250MM) INTERCONNECTED TO A METROSEP C6 GUARD COLUMN, EC DETECTOR** • **APPLICATION: THE DETECTION OF CONDUCTIVITY.**	• **Instrument:** Metrohm 930 Compact IC Flex oven/SES/PP/DEG (Metrohm, Herisau, Switzerland). • **Components:** Column oven, MSC and MSM module, peristaltic pump, integrated degasser, Metrosep A Supp 5 separation column (4.0x100mm) interconnected to a Metrosep A, Supp 5 guard column, EC detector • **Application:** Sequential suppression by the MSC and MSM module and the detection of conductivity by the EC detector.

Preparation and introduction of the Cation and Anion Eluent:

The cation and anion eluents were prepared separately using high-grade salts (puriss p.a) and ultrapure (Type 1) water (resistivity >18.2 MΩ/cm or EC < 0.056µS/cm) obtained by the Milli-Q® Direct 16 System (Merck-Millipore, Molsheim, France). For the anion eluent, Na_2CO_3 and $NaHCO_3$ analytical reagent grade chemical reagents were used, along with a the MSM suppression solution comprising of phosphoric acid (85% H_3PO_4), while the cation eluent comprised of nitric acid (HNO_3). After preparation, eluents were stored in 2000 mL Duran glass bottles enclosed with a blue Polypropylene (PP) screw cap with an aspiration filter to remove impurities, and an adsorption tube consisting of $CaHNaO_2$ (Soda Lime) were added to prevent atmospheric contamination and subsequent pH adjustments in anion eluent. The prepared eluents were then pumped through the chromatography system at controlled flow rates to maintain stability. The cation eluent containing 6.5 mM HNO_3 was introduced at a flow rate of 0.9 ml per minute, while the anion eluent containing 3.0mM Na_2CO_3, 2.0mM $NaHCO_3$, flow rate was set to 0.8 ml per minute. Any air bubbles were removed using a degassing unit, and the system was protected from minute particles and pulsations using filtration units and pulsation absorbers, respectively. The MSM module was regenerated using an eluent suppression solution with a concentration of 0.2mM H_3PO_4.

Sample preparation and system introduction:

The water sample underwent filtration through a 0.45µm nylon syringe filter before being transferred to a 15 ml tube, filled to the brim, and capped to prevent atmospheric interaction. The vial caps were later removed before the analytical process. After positioning on the Metrohm 858 IC autosampler interchangeable rack determined by the sample submission list imported into the MagIC Net 3.3 software by Metrohm, sample injections were automated to minimize cross-contamination. Prior to analysis, three blank samples were analysed to ensure system accuracy and prevent contamination. The automation of the sample transfer rack helped reduce potential cross-over contamination, and the injection was rinsed between sample preparations. The sample list was determined based on in-situ pH and EC measurements to calculate the dilution factor. All analysed samples had EC values below 1000 µS/cm, and no dilution was necessary. Filtration was crucial to

prevent instrument damage and blockages, with an additional filtration step using a 0.22 µm inline cellulose autofiltration cell. During sample preparation, 7.5 ml of the sample was extracted for cations and anions analysis using a PEEK material autosampler injector needle. For anion analysis, only 20 µl of the sample was introduced, while 10 µl was used for cation analysis. The sample was merged directly into the eluent stream in the sample loop, facilitating transportation to the guard and analytical columns of the stationary phase in the cation and anion system.

The stationary phase column was kept in an oven chamber, maintaining the anionic column at 30°C and the cationic column at 55°C. As the sample passed through the guard column, it shielded the analytical ion exchange column where ion separation occurred. The anion guard column merged anions using quaternary ammonium groups, while the cation column merged cations using sulfonate groups. Then, the sample moved to the main analytical column, where ion separation based on charge-to-size ratio resulted in unique retention times for each ion. Weak ionic bonds aided in distributing ions throughout the stationary phase.

Metrohm Suppressor Unit (MSM):

The Metrohm Suppressor Unit (MSM) was used to improve the detection of anions by reducing the conductivity of the anion eluent while increasing the conductivity of the ions of interest. It consisted of a Suppression module and a CO_2 suppression unit. The Suppression Module reduced the background conductivity caused by the anion eluent by exchanging Na^+ ions for H^+, resulting in lower conductivity (<20 µS/cm). This process also increased the conductivity of the sample's anions of interest. The cartridge contained cation-exchanging resin that replaced cations with H^+ during suppression. This reduced the background signal of the eluent and increased the detection of anionic signals. The CO_2 Suppressor Module further decreased background conductivity by converting H_2CO_3 formed during ion exchange to CO_2 and H_2O. This minimized the presence of CO_2 in the sample matrix, with over 98% eliminated in the continuously flushed degassing chamber with CO_2-free air.

Ion concentration detection and quantification:

After ion separation on the column, an Electrical Conductivity (EC) detector individually detected anionic and cationic ions. This detector measures a solution's ability to conduct electrical charge in µS/cm using two energized electrodes. Factors like temperature, ionic concentration, and electrical charge influence the sample's conductivity, with higher concentrations resulting in greater EC values. By analysing a standard of known concentration, the chromatogram (Figure 12) produced by MagIC Net 3.3 software records the retention time (RT) for each ion's travel through the column to the detection point on the x-axis. The y-axis records the response and measured electrical conductivity for each ion, and the peak response area on the chromatogram (Figure 12) shows the volume of ions in the analysed water sample detected by the EC detector unit. The peak response area on the chromatogram reflects the volume of ions detected by the EC detector in the water sample. Additionally, a calibration curve, developed using known ion concentrations, correlates the EC response area with specific ion concentrations, enabling accurate quantification of ion concentrations in the sample.

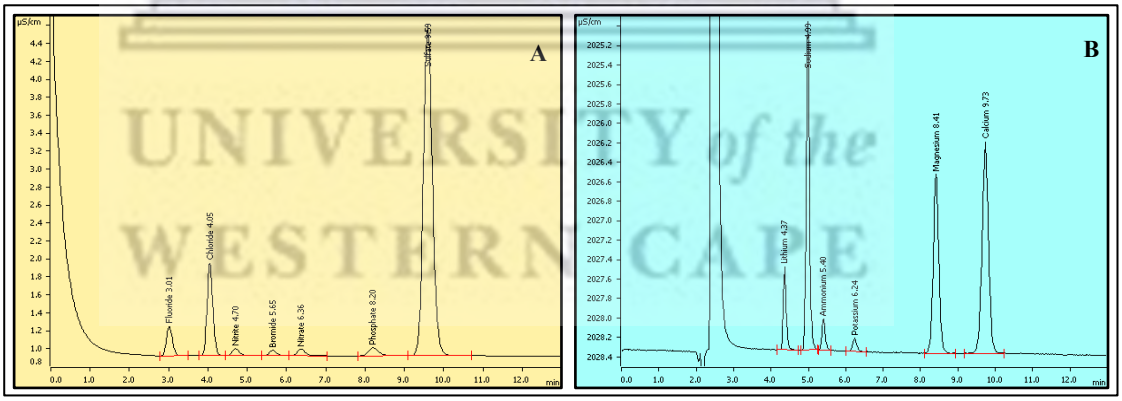

Figure 12: A chromatogram example detecting individual A) Anion and B) Cation concentrations (Source: Stellenbosch University BIOGRIP Central Analytical Facility, 2021).

Alkalinity

To determine the concentration of alkalinity in the sample collected, the Hach digital titrator method (8203) was used, with a concentration range of 10 to 4000 mg/L as $CaCO_3$ for accuracy. The sample was allowed to reach room temperature

before analysis, and a sample volume of 50ml was used, along with a titration cartridge containing 1.600 N H_2SO_4, as defined by the range in Table 6.

Table 6: Sample volumes and associated digit multipliers (Hach Company)

Range (mg/L as CaCO3)	Sample Volume (m*l*)	Titration Cartridge	Digit Multiplier
10-40	100	0.1600 N H_2SO_4	0.1
40-160	25	0.1600 N H_2SO_4	0.4
100-400	100	1.600 N H_2SO_4	1
200-800	50	1.600 N H_2SO_4	2
500-2000	20	1.600 N H_2SO_4	5
1000-4000	10	1.600 N H_2SO_4	10

The digital titrator was prepared by inserting the 1.600 N H2SO4 cartridge and ensuring the delivery tube was free of air. Air within the delivery tube was removed by rotating the conveyance node and releasing a few droplets of the titrant. The digital counter was reset to zero, and the delivery tip was cleaned before inserting it into the sample for analysis. A 50 ml sample was mixed with Phenolphthalein Indicator Powder Pillow, resulting in a colourless solution confirming a pH less than 8.3. Bromcresol Green-Methyl Red Indicator Powder Pillow was then added, and titration occurred until a light pink colour appeared, indicating the endpoint. The number of digits on the counter was recorded for concentration calculation using Equation 2 with the digit multiplier from Table 6.

mg/L as $CaCO_3$, total alkalinity= Total digits recorded x digit multiplier [2]

To determine total alkalinity, titration was performed with a 1.600 N H2SO4 solution until an endpoint pH of 4.5 was reached. Phenolphthalein indicator was used to detect the presence of CO_3^{2-}, but no colour change was observed in any of the samples, indicating that none of the samples had a pH greater than 8.3. Bromcresol green indicator revealed bicarbonate (HCO_3^-) alkalinity, titrated until a green-to-pink change at pH 4.5, determining the acid (NH_2SO_4) required. Total alkalinity and bicarbonate concentration were calculated based on the acid and sample volume used.

Dissolved silica concentration and TDS

(SiO_2, mg/L) ranging from 0.010 to 1.600 mg/L SiO_2 was analysed as close to the collection date to obtain the most accurate results using the Hach DR 6000 spectrophotometer in the UWC water quality lab following the Hach (2015), Heteropoly Blue Method:8186. The spectrophotometer was warmed up by switching it on and initiating the 651 Silica LR program. Calibration with the low-range Silica standard solution (1.00 mg/L SiO_2) was conducted before each analysis to validate the test procedure, reagents, and machine. Each analysis required a blank sample and an analytical sample. The blank sample was prepared by filling a sample vial with 10ml of the specific water sample. For the analytical sample, 10ml of the same sample was mixed with 14 drops of Molybdate 3 reagent solution, followed by a 4-minute reaction time. Citric acid reagent powder pillow was added and swirled for each cell, followed by a 1-minute reaction time. Then, Amino Acid F Reagent powder pillow was added and swirled only in the analytical sample. After a 2-minute reaction time, a blue discoloration indicated the presence of silica. The blank sample vial was cleaned with a microfiber cloth and inserted into the spectrophotometer for zeroing. The prepared sample was then placed into the spectrophotometer for reading the results in mg/L SiO_2.

TDS is a measure of the volume of various inorganic salts present in water, a relative measure of the salinity of water, and a determinant of the salt dispersal within a soil profile. The conversion factor(*f*) of 6.5, was adopted and recommended by the South African Water Quality Guidelines (DWAF,1996), enabling estimated TDS (mg/L) from a precisely measured EC (mS/cm) by direct linear correlation by the conversion Equation 3. TDS (mg/L) is the measure defining the concentration of main ions dissolved in the river and a pivotal component in assessing the hydrochemistry in any given water resource.

$$\textbf{EC (mS/m at 25° C) x 6.5 = TDS (mg/L)} \qquad [3]$$

3.6 Data analysis methods

To analyse the temporal isotopic variability in river flows, the data on the hydrological regime were grouped into seasons: dry and wet season. The data were

grouped spatially according to the valley's prominent land-based practices, as Upper, Middle, and Lower physiographic valley regions.

3.6.1 Tracing River Recharge with Stable Isotopes

Statistical analysis was performed using IBM® SPSS® Statistics 20 to determine the maximum, minimum, and arithmetic mean of the chemical and isotopic composition of water samples collected. The isotopic variation observed between different seasons was dependent on local meteorological controls. In this study, three volume-weighted variables, namely $\delta^{18}O$, $\delta^{2}H$, and d-excess values, were examined to explore the nature of their relationship with meteorological parameters such as temperature (T), relative humidity (RH), and precipitation amount (mm/day). A Shapiro-Wilk normality test (Shapiro and Wilk, 1965) was conducted on the extracted data, indicating that it followed a normal distribution (p-value > 0.001). Therefore, a Pearson's parametric correlation test was employed to assess the linear relationship between the two variables.

Table 7: Strength of Pearson's correlation classified by Evans, (1996).

Pearson's Correlation Coefficient (+or-)	Interpretation
0.00-0.10	Very Weak, negligible correlation
0.10-0.39	Weak correlation
0.40-0.59	Moderate Correlation
0.60-0.79	Strong Correlation
0.80-1.00	Very Strong correlation

Analysing Meteoric Water Lines and GNIP Data for hydrological insight.

Using Microsoft Excel2010™, the relationship between the isotope compositions ($\delta^{2}H$ and $\delta^{18}O$) of the main stream and its end-member sources was analysed to gain insights into the processes affecting water isotopic composition from precipitation to surface water. The isotopic results were plotted on a bivariate plot ($\delta^{18}O$ - $\delta^{2}H$ biplot) with reference to global and local meteoric water lines (GMWL and LMWL). The GMWL, established by Craig (1961) with the equation $\delta^{2}H=8*\delta^{18}O+10$, served as a global reference line based on global-scale

precipitation data. LMWLs, derived from localized precipitation data, were also analysed using trendline analysis. The LMWL was defined by annual precipitation collected within the GNIP (Global Network of Isotopes in Precipitation). Relevant GNIP data for the Cape Town region, obtained from the IAEA website and the WISER portal, were used. Rainfall data from the UCT rainfall station (105 m.a.s.l) between 1995 and 2008 were gathered. However, the one-year observation period for rainfall introduced uncertainty into determining the Local Meteoric Water Line (LMWL) due to its limited duration. To address this, the study incorporated the LMWL using the Reduced Major Axis Method (RMA) based on a twelve-year long-term GNIP monitoring database from the UCT rainfall station located 70 km away. Although the monitoring periods did not overlap, the station's similar climatological and lithological conditions provided fundamental information about typical precipitation variability in the region. The LMWL, constructed using GNIP data, aids in understanding processes influencing variable stable isotopic composition during rainfall and recharge events.

Spatiotemporal variations in isotopic composition of valley waters

To analyse the spatiotemporal variation in the stable isotopic composition (unit: parts per thousand) of the main stream and its contributing end-members, samples were categorized based on flow conditions and land-based activities. The average $\delta^{18}O$ and $\delta^{2}H$ values of the river, groundwater, and precipitation were graphically represented using dual-isotope biplots and bar graphs. According to Harris et al. (2010), the volume-weighted averages (V.W.A) of rainfall provided a comprehensive understanding of recharge significance. Unlike the conventional arithmetic mean, this approach considered the isotopic composition of all precipitation within a specific year or sampling duration. Thus, the mean weighted averages of the isotopic composition of rainwater and precipitation d-excess were visually presented alongside the average daily rainfall (mm) volume and daily temperature. The volume-weighted averages for rainfall were calculated using Equation 4.

$$\boldsymbol{\delta}_{\mathbf{WA}} = \frac{\sum(\boldsymbol{Pi\delta i})}{\sum \boldsymbol{Pi}} \qquad \textbf{[4]}$$

Where δi represents the measured $\delta^{18}O$ and $\delta^{2}H$ isotopic composition during the analysed precipitation event, and Pi represents the volume of rainfall during the event period (Gautam et al., 2017).

3.6.2 Hydrochemical Analysis

A bar graph was generated to depict the seasonal averages of pH and EC along the stream network, facilitating the analysis of variations in river samples. Statistical analyses, including Pearson's Correlation, Hierarchical Cluster Analysis, and Principal Component Analysis (PCA) in IBM® SPSS® Statistics 20, were conducted. A PCA/FA analysis was conducted on the dataset containing 13 variables to evaluate important seasonal parameters and sources impacting the quality of river water. PCA, a method that reduces the number of variables in a large dataset while retaining the most significant information, analysed general characteristics of river water and its controlling factors at a seasonal scale.

Multivariate statistical techniques were applied to the correlation matrix of the river hydrochemical dataset to identify major land use sources controlling the chemistry in the Berg River network. Using the PCA method with Varimax Rotation and Kaiser Normalization, two factors were extracted based on principal eigenvalues greater than 1.

To establish the statistical relationship among river hydrochemical ions, TDS, pH, temperature (T), and river elevation, and to identify the sources of dissolved substances, Pearson's correlation coefficient (r) and a correlation matrix generated in SPSS software were used. The HACA unsupervised pattern recognition interface was employed to group river dataset objects with similar associations. Selected river parameters included TDS, Ca^{2+}, Mg^{2+}, Na^{+}, K^{+}, HCO_3^{-}, SO_4^{2-}, Cl^{-}, NO_3^{-}, SiO_2 and pH. The method generated a dendrogram using Ward's method, based on standardized data and the squared Euclidean distance approach, facilitating the visual interpretation of clustering and complementing the reduction in dataset dimensionality.

The Piper trilinear plot was generated in the Geochemist's Workbench-Community Edition™ software to characterize the interaction and hydrochemical evolution in the valley among surface, groundwater, and rainfall systems during the dry and wet

seasons. The plot has two lower triangles, where the percentage milliequivalent (meq/l) defined; of the major ionic species are distributed. The controlling dynamics influencing the dissolved ionic species of the rivers in the valley were quantitatively analysed and interpreted using the Gibbs plot. Hence, a Gibbs Schematic plot was generated in Microsoft Excel 2010(Microsoft Corp., Redmond, WA, USA) incorporating TDS vs $Na^+/ (Na^+ + Ca^{2+})$ or $Cl^-/(Cl^-+HCO_3^-)$.

The origin of dominant river ions in the basin and the relationship between dissolved ions were further delineated using the solute ion-ratio method and bivariate plots of Na^+ vs Cl^-, $Ca^{2+} + Mg^{2+}$ vs HCO_3^-, and the level of ion exchange between Ca^{2+}, Mg^{2+} and Na^+ as a contributory factor to the hydrochemistry of the river was assessed $(Ca^{2+} + Mg^{2+}) - (HCO_3^- + SO_4^{2-})$ vs $Na^+ + K^+ - Cl^-$. The origin source of weathering products controlling the river ion concentrations delineated by Multivariate Statistical Analysis, was assessed by the standard ion-ratio method using the molar ratios of major ions with emphasis on carbonates (Ca^{2+} Mg^{2+}vs HCO_3^-), silicates, and evaporate (Na^+ vs Cl^-) weathering.

3.6.3 Estimating Berg River Flow Contributions with Isotope Mass Balance.

A two-component mixing model was used to derive the quantitative relationship between the Berg River and its end-member sources, with the assumption that only two sources contributed to streamflow generation; precipitation (surface runoff) and baseflow (groundwater). The entirety of each source's contribution was expressed as a fraction (f) equal to 1 (Equation 5). To estimate the dry and wet season contribution of groundwater and rainfall to the streamflow, a two-component end-member model was used for the upper, middle, and lower reaches, which extend around 30 km from the Berg River Dam outlet to the discharge outlet in Northern Paarl. The isotopic mass balance linear equations using the $\delta^{18}O$ tracer defined the two-component end-member model and fractional proportional estimates.

$$X_p + X_{gw} = 1 \qquad [5]$$

$$\delta_s = X_p . \delta_p + X_{gw} . \delta_{gw} \qquad [6]$$

$$X_p = (\delta_s - \delta_{gw})/(\delta_p - \delta_{gw}) * 100 \qquad [7]$$

$$X_{gw} = (\delta_s - \delta_p)/(\delta_{gw} - \delta_p) * 100 \qquad [8]$$

The fraction of precipitation (Xp) and groundwater (Xgw) in the stream mixture (δs) were estimated using the two-component end-member model. δs, δp, and δgw denote the isotopic tracer values for the stream water, precipitation (Source B), and groundwater (Source A), respectively, expressed in parts per thousand (‰). Xp and Xgw are expressed as percentage values.

Given the small size of the Franschhoek-Paarl basin, it was assumed that there was no spatial variability in precipitation inputs and isotopic values. The precipitation end-member contribution component was defined using the precipitation weighted average values and estimated using Equation (7), while the groundwater end-member was estimated using Equation (8) by incorporating bi-weekly groundwater datasets. The recharge fractions (%) of precipitation and groundwater contributing to river flow at a seasonal scale were tabulated and presented in a bar graph. A time-series plot was also created to show the river $\delta^{18}O$ response to seasonal rainfall-runoff events within the hydrological year, displaying the temporal evolution and correlation with the varying quantity of collected rainfall(mm) per seasonal condition and subsequent streamflow (Q, m^3/sec). This aimed to observe the response of direct recharge and the endurance of baseflow conditions in sustaining flow at a seasonal scale in response to the estimated contributing fraction.

3.7 Quality Assurance

To ensure the accuracy of the hydrochemical results of the water samples used in the study, the quality of the chemical data for each sample was evaluated using the Charge Balance Error equation (Equation 9) (Hounslow, 1995). The Cation-Anion balance check was used to determine the percentage variance between the total positive and negative charges, as defined by Murray & Wade, (1996). The Cation-Anion balance of all the samples expressed in meq/l was required to fall within the established limit range of ±5% to be considered acceptable for use. Six samples were found to be outside this range and were therefore not included in the study. The cation-anion balance of all samples is tabulated in Appendix A and B.

$$\mathbf{CBE} = \frac{\boldsymbol{\Sigma cations - \Sigma anions}}{\boldsymbol{\Sigma cations + \Sigma anion}} \times \mathbf{100} \qquad \mathbf{[9]}$$

3.8 Ethical consideration

Prior consent was obtained from the Berg River Dam management and the City of Cape Town, as well as from the residents and farmers within the catchment, before conducting field work at various sampling sites to obtain data. The collected data is subject to oversight by DWS and COCT before publication, as agreed upon to sample streams and their end-member sources in the Berg River Catchment.

3.9 Limitations

Due to the inaccessibility of certain DWS boreholes and gauging systems on private property, some proposed sampling events were affected. Furthermore, the outbreak of COVID-19 caused delays in the sampling process. Additionally, due to limitations in cost, time, and equipment, the interflow component was not included in the mixing rate analysis for the Berg River.

CHAPTER 4: Seasonal Mechanisms and Recharge Sources of the Berg River Isotopic Signature

4.1 Introduction

The following chapter presents the main findings of stable isotopic analysis ($\delta^{18}O$ and $\delta^{2}H$) conducted on precipitation, surface water, and groundwater in the catchment area. Different water bodies have distinct isotopic signatures, helping identify their sources and trace their flow paths in the watershed. As a result, varying hydrological events during the dry and wet seasons produced different isotopic responses. Analysing the Berg River and its sources individually revealed their origin, hydraulic connections, isotopic mixing, and modification processes along various flow paths relative to the LMWL. The river's 30 km flow path was divided into three physiographic zone components to assess how hydrological processes and land activities affected the river's isotopic compositions and end-members.

4.2 Results of stable isotope analysis

This study aimed to explore the relationship between the isotopic compositions ($\delta^{2}H$ and $\delta^{18}O$) of various water sources and understand their contribution to streamflow. The evolving hydrological relationship between the different water entities relative to the meteoric water lines, represented as reference lines, was demonstrated using dry season (Figure 13) and wet season (Figure 14) dual-isotope plots for all collected water samples. These plots compared the isotopic compositions of the Berg River, its sources, and the LMWL (Equation 10) and GMWL (Equation 11).

*** LMWL (Harris et al., 2010): $\delta^{2}H=6.41* \delta^{18}O+8.66$ ($R^2=0.88$)** **[10]**

*** GMWL (Craig, 1961): $\delta^{2}H=8* \delta^{18}O+10$ ($R^2=1$)** **[11]**

In Figure 13, the river data is generally positioned slightly above the LMWL. This indicates that precipitation is the primary source of recharge for both the river and groundwater. The clustering of groundwater samples suggests mixing between different groundwater sources with varying water compositions. The proximity of groundwater samples to the river samples, while being distant from the Volume Weighted Averages (V.W.A) of precipitation, suggests that the river receives significant contributions from groundwater during the dry season. Clear seasonal variation in the isotopic compositions of precipitation is demonstrated (Figure 13), with a higher level of enrichment during warmer, drier periods with infrequent rainfall. Due to low flow conditions in the dry season, some river samples deviate from the LMWL. Similarly, groundwater samples, like the river samples, show an enrichment in heavy isotopes, indicating possible evaporative effects.

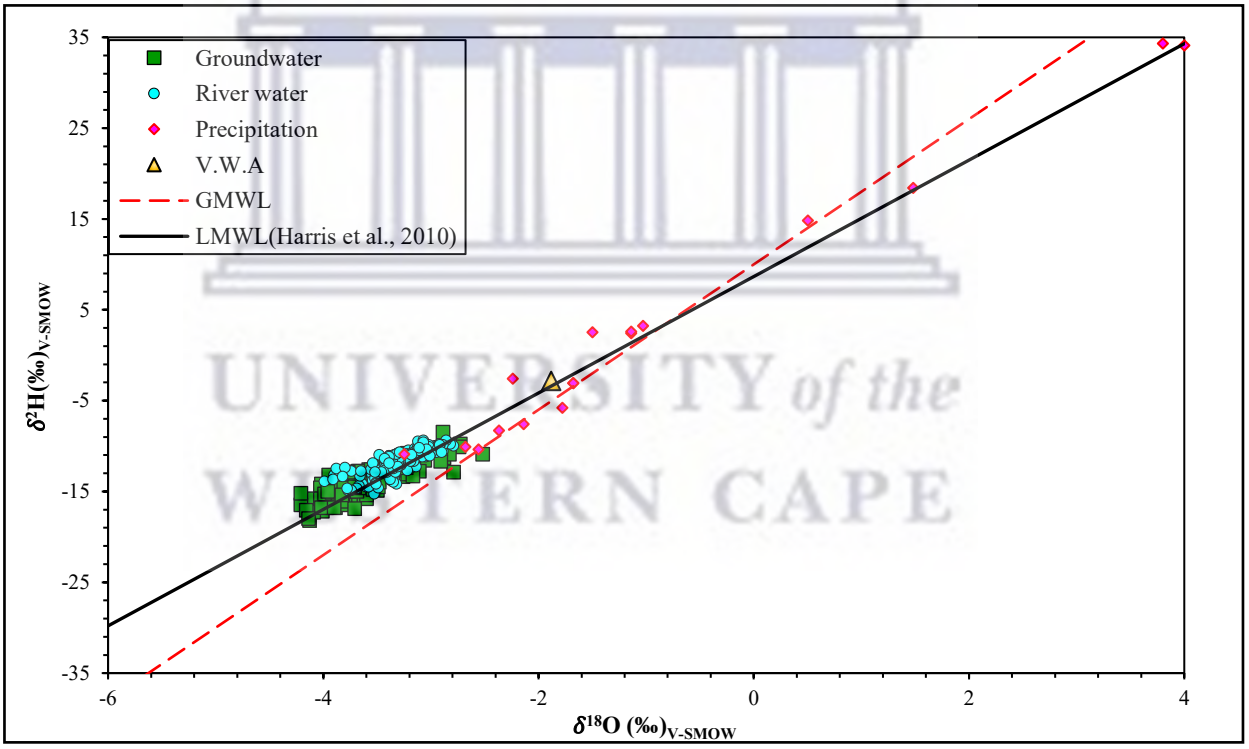

Figure 13: Dual-isotope comparison of the dry seasons δ^2H and $\delta^{18}O$ compositions in three Franschhoek-Paarl valley water bodies, relative to LMWL and GMWL

The results presented in Figure 14 show that the groundwater and surface water samples form a flattened elliptical shape that aligns with or near the LMWL and GMWL. This indicates that both systems were primarily recharged by meteoric

waters and suggests a strong correlation between the isotopic compositions among the water sources. During cold periods with higher rainfall, a more depleted isotopic composition is observed. Water samples located below the GMWL suggest the possibility of open-system enrichment through evaporative processes within the water system. The groundwater samples show a higher level of enrichment in $\delta^{18}O$, indicating the occurrence of evaporative processes. In contrast, the river water samples align closely with the V.W.A of rainfall and demonstrate an enriched $\delta^{2}H$ composition. This suggests that rapid precipitation events are likely responsible for recharging the river system. In Figure 14, the precipitation samples cluster along the LMWL, indicating the presence of local precipitation recharge during the wet season, which leads to a depletion in $\delta^{18}O$.

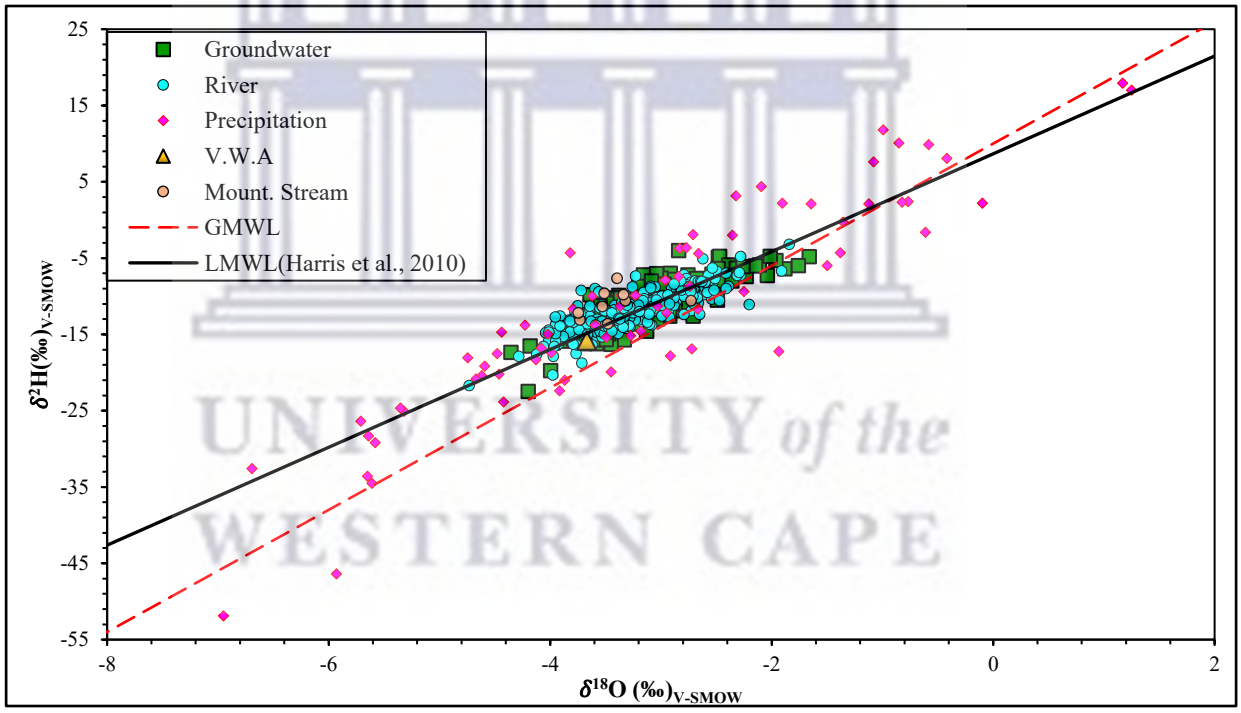

Figure 14: Dual-isotope comparison of the wet seasons $\delta^{2}H$ and $\delta^{18}O$ compositions in the Franschhoek-Paarl valley water bodies, relative to LMWL and GMWL

Multiple groundwater samples deviate from the LMWL and instead align with the Local Evaporation Line (LEL), indicating potential secondary evaporative enrichment. This can happen when recharging waters undergo evaporation before replenishing the aquifer. In Figure 14, some groundwater samples lie below the GMWL, suggesting evaporation before subsurface recharge or the possibility of

receiving recharge from a distant source. However, some groundwater samples cluster above the GMWL but near the LMWL, suggesting a potential occurrence of evaporative conditions at a reduced rate while still receiving recharge from local precipitation.

The study used isotopic samples from rivers and groundwater, categorized by seasonal variations. Two-stage least squares regression analysis was conducted to assess seasonal variability, producing seasonal River Water Lines (RWL) and Groundwater Lines (GWL) shown in Figure 15. Stream water reveals a mean enrichment during the dry season but maintains consistent slopes during both dry (4.62) and wet seasons (4.85), indicating predominantly evaporated water entering the river system from longer flow paths. The RWL slope and intercept consistently remain lower than those of the LMWL and GMWL in both seasons, indicating that the rate of evaporation remains relatively consistent in varying seasons. However, the dry season's RWL slope is slightly smaller, suggesting groundwater may significantly contribute to river flow compared to precipitation and upstream dam inflow.

During the dry season, the GWL is smaller than the RWL, despite having a more depleted isotopic composition, as shown by the seasonal mean. The RWL serves as the proxy for the Local Evaporation Line (LEL) in all collected river water samples. In contrast, in the wet season, the GWL slope is larger than the RWL, indicating multiple flow paths for precipitation entering the river, leading to increased residence time and evaporation in the Berg River. The GWL slope is smaller than both the LMWL and GMWL in both seasons (dry season: 4.57, wet season: 5.21), indicating that evaporation affects water before it reaches the saturated zone. The intercept values (dry season: 2.51, wet season: 5.24), significantly lower than 10, support evaporation presence in groundwater during both seasons. Groundwater positioning near or on the GMWL suggests influence from precipitation and evaporation during infiltration and is evident by the wet seasonal mean enrichment. The study notes seasonal isotopic variations in both groundwater and river water, indicating alignment across seasons.

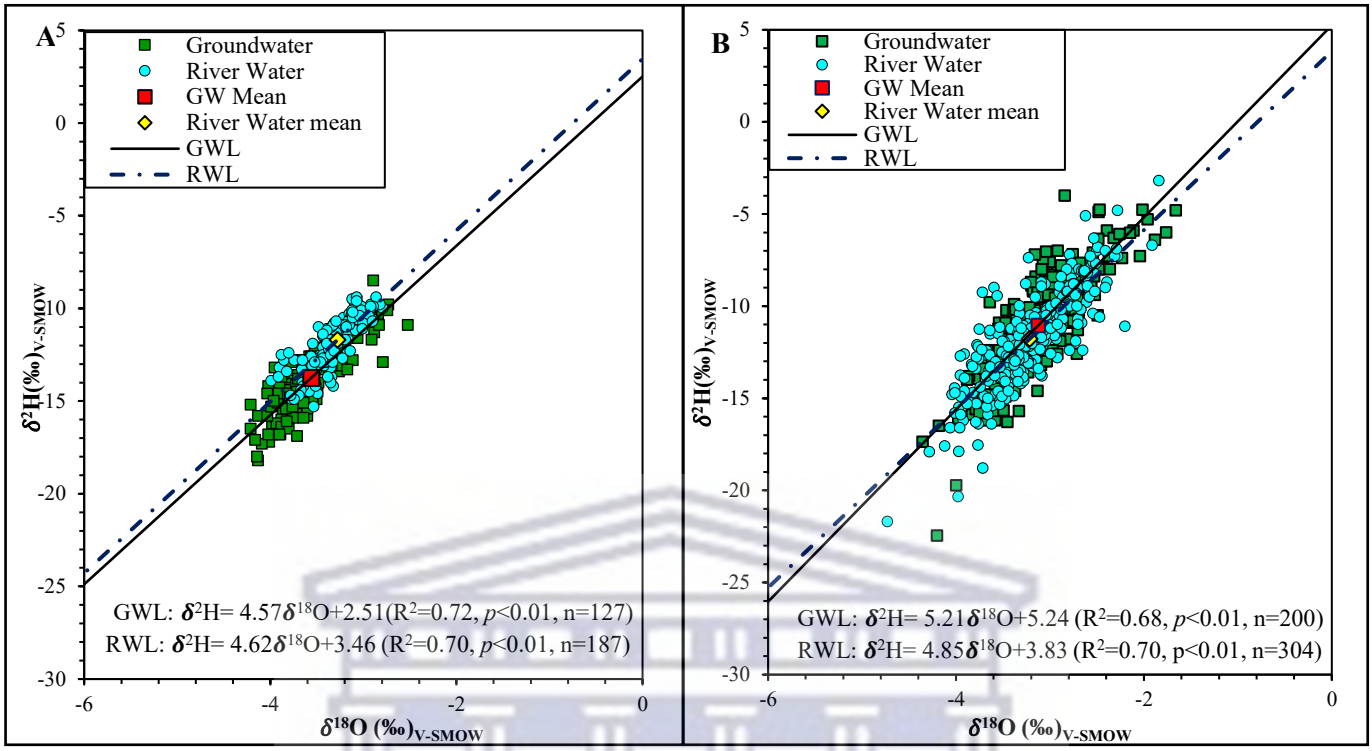

Figure 15: Dual plot of RWL and GWL with seasonal means in the Dry (A) and Wet (B) Seasons.

Appendix A provides the complete dataset, while Table 8 summarizes the δ^2H and $\delta^{18}O$ values' statistical range for various water entities. In the dry season, river water's mean values show no significant seasonal deviation, unlike the wet season. However, during the wet season, there's a wider isotopic range. The mean isotopic composition of river water resembles groundwater and exhibits similar seasonal variation (Table 8 and Figure 11), suggesting consistent inflow from groundwater sources. In contrast, the groundwater's average isotopic signature during the wet season ($\delta^{18}O$: -3.12±0.47‰) resembles local precipitation ($\delta^{18}O$: -3.11±1.76‰), indicating active subsurface replenishment due to increased rainfall. While river water isotopic distribution remains relatively stable, groundwater samples show greater deviation, implying variability in sources and circulation pathways of groundwater across depths and locations.

During dry seasons, river water isotopes in Table 8 are slightly more enriched than groundwater, while in wet seasons, groundwater shows a slight enrichment. River water isotopic compositions are more depleted in $\delta^{18}O$ compared to precipitation in the catchment area, indicating that the river primarily consists of rainfall from the surrounding upstream mountains with minor contribution from the Franschhoek-

Paarl valley. In the wet season, river water isotopic composition becomes more depleted, resembling precipitation. This suggests that the isotopic composition of precipitation is influenced by seasonal conditions, which in turn affects the seasonal recharge of the river flow in the valley.

The d-excess value suggests that both river and groundwater in both dry and wet seasons closely align with the d-excess (10‰) of global atmospheric precipitation. However, they deviate from the precipitation line, indicating some evaporative fractionation during the season. This effect is less pronounced in the wet season, as the systems plot closer to the LMWL, suggesting recharge from atmospheric water sources.

Table 8: Seasonal summary of stable isotopes in Franschhoek-Paarl valley's river water, groundwater, and precipitation (2020-2021).

WATER RESOURCE		DRY SEASON			WET SEASON		
		$\delta^{18}O$ (‰)	**$\delta^{2}H$ (‰)**	**d-excess (‰)**	**$\delta^{18}O$ (‰)**	**$\delta^{2}H$ (‰)**	**d-excess (‰)**
RIVER WATER	**Min**	-3.43	-15.30	12.32	-4.73	-21.70	6.51
	Max	-2.79	-9.40	18.54	-1.84	-3.20	20.49
	Mean	-3.28(±0.25)	-11.69(±1.37)	14.52(±1.12)	-3.22(±0.44)	-11.75(±2.56)	14.03(±1.99)
GROUNDWATER	**Min**	-4.21	-18.20	9.26	-4.36	-22.46	8.08
	Max	-2.52	-8.50	18.48	-1.66	-4.00	19.32
	Mean	-3.56(±0.33)	-13.74(±1.88)	14.73(±1.60)	-3.12(±0.47)	-11.04(±2.98)	13.95(±2.16)
PRECIPITATION	**Min**	-3.25	-10.90	2.10	-6.95	-51.90	-1.74
	Max	4.00	34.30	15.32	1.25	17.92	26.26
	Mean	-0.91(±2.14)	2.96(±14.34)	10.22(±3.52)	-3.11(±1.76)	-11.27(±13.64)	13.61(±5.58)

**(± Standard deviation)*

Precipitation Isotopic Composition Characterization

Table 9 provides statistical information on the isotopic composition of precipitation in the valley during the dry and wet seasons. In the dry season (November to March), precipitation shows a wide range of isotopic enrichment, with $\delta^{18}O$ values from -3.25‰ to 4.00‰ (V-SMOW) and $\delta^{2}H$ values from -10.40‰ to 34.3‰ (V-SMOW). The weighted mean values for $\delta^{18}O$ and $\delta^{2}H$ are -1.86‰ and -2.73‰, respectively. In contrast, the wet season displays a more depleted isotopic

composition, with $\delta^{18}O$ values from -6.95‰ to 1.25‰ (V-SMOW) and $\delta^{2}H$ values from -51.90‰ to 17.92‰ (V-SMOW). The weighted mean values for $\delta^{18}O$ and $\delta^{2}H$ during the wet season are -3.52‰ and -15.71‰, respectively. Overall, the wet season exhibits a more depleted isotopic composition compared to the dry season.

In the valley during the dry season, d-excess values range from 2.10‰ to 15.32‰ (n=17), with an arithmetic mean of 10.22‰. Conversely, in the wet season, d-excess values range from -1.74‰ to 26.26‰, with an arithmetic mean of 13.61‰. It is important to note that the rainfall stations in the valley received limited to no precipitation during the dry season, resulting in variable isotopic ratios among the stations due to the ongoing influence of evaporation.

Table 9: Summary of seasonal precipitation isotopic compositions at three rainfall stations

Rainfall station	Elevation	Season	Precipitation Amount	V.W.A (‰)			Max (‰)			Min (‰)		
	(m.a.s.l)		(mm)	$\delta^{18}O$	$\delta^{2}H$	*d*-excess	$\delta^{18}O$	$\delta^{2}H$	*d*-excess	$\delta^{18}O$	$\delta^{2}H$	*d*-excess
RF1	179	Dry (*n=10*)	70.2	-1.60	-0.54	12.29	4.00	34.3	15.32	-3.25	-10.90	2.10
		Wet (*n=30*)	588.9	-3.68	-15.92	13.53	1.25	17.92	26.26	-6.95	-51.90	3.26
BG47-RF#1	175	Dry (*n=4*)	102	-2.55	-2.55	17.88	-2.14	-7.60	11.34	-2.68	-10.40	9.52
		Wet (*n=27*)	400	-3.54	-15.00	13.33	-0.10	9.89	20.98	-6.69	-32.57	-1.74
UWC-RF#1	113	Dry (*n=3*)	35.7	-1.49	1.81	13.74	-1.03	3.20	14.50	-1.78	-5.80	8.44
		Wet (*n=14*)	377	-3.79	-16.49	13.90	-1.38	2.20	18.94	-5.93	-46.40	1.04

Most seasonal precipitation samples in Figure 16 are positioned above the GMWL and the seasonal V.W.A., indicating limited influence from sub-cloud processes on the isotopic composition during both seasons. The wet season displays a more depleted isotopic composition compared to the dry season. Each rainfall station displays a unique pattern between the seasons, highlighting distinct isotopic variations under different climatic conditions.

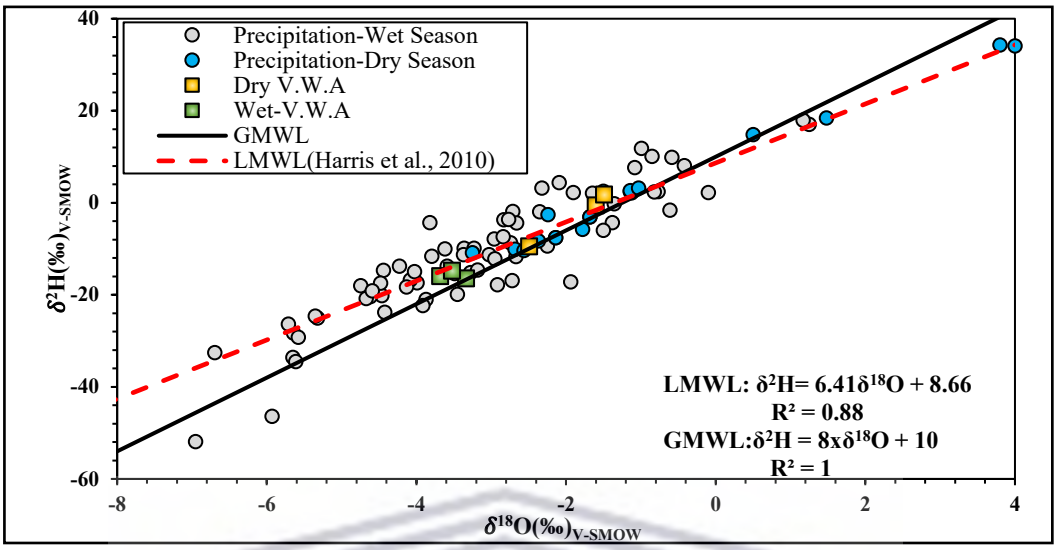

Figure 16: Correlation between seasonal precipitation isotopes and GMWL and LMWL.

The influence of meteorological factors on Precipitation isotopes

Table 10 displays correlations between meteorological controls in the basin and seasonal precipitation values of $\delta^{18}O$, $\delta^{2}H$, and d-excess at three rainfall stations. In the dry season, moderate correlations exist between air temperature (T) and both $\delta^{18}O$ (r=0.56) and δ2H (r=0.55), while d-excess values show no significant influence. Relative humidity correlates with d-excess values (r=0.48) but not with $\delta^{18}O$ and $\delta^{2}H$. Precipitation amounts have a strong inverse relationship with $\delta^{18}O$ and $\delta^{2}H$ and a strong positive correlation with d-excess. In contrast, in the wet season, air temperature weakly influences d-excess values, while its impact on $\delta^{18}O$ and $\delta^{2}H$ lacks significance. Relative humidity has no relationship with any variable($p>0.05$), while precipitation amount (PA) has a strong to moderate influence on the variables throughout the season. To address inconclusive results with non-significant p-values (>0.05), establishing a long-term rainfall isotope database is crucial. Such a database would offer valuable insights into meteorological factors' influence on rainfall isotopic composition in the valley. The analysis reveals that the seasonal variation in precipitation $\delta^{18}O$ compositions can be attributed to variations in precipitation amount (PA), highlighting its significant role in shaping the isotopic composition of rainfall.

Table 10: A summary of seasonal Pearson's correlation coefficients and significance levels for the linear relationship between weighted $\delta^{18}O$ (‰), $\delta^{2}H$ (‰), and D-excess (‰) with T, RH, and PA

Governing meteorological controls	Dry Season						Wet Season					
	$\delta^{18}O$‰		$\delta^{2}H$‰		D-excess‰		$\delta^{18}O$‰		$\delta^{2}H$‰		D-excess‰	
	r	*p*	r	*p*	r	*p*	r	*p*	r	*p*	r	*p*
Air temperature (T, °C)	0.56	**<0.05****	0.55	**<0.05****	-0.39	0.12	0.21	0.68	0.06	0.64	-0.29	**<0.05****
Relative humidity (RH, %)	-0.31	0.23	0.29	0.26	0.48	**<0.05****	-0.20	0.11	-0.21	0.09	0.09	0.47
Precipitation Amount (PA, mm)	-0.89	**<0.01****	-0.71	**<0.01****	0.75	**<0.01****	-0.88	**<0.01****	-0.78	**<0.01****	0.58	**<0.01****

*** Significant at 0.05 (2-tailed test).**

Seasonal variations in precipitation compositions (Figure 17) illustrates an enriched composition during warmer, drier periods with infrequent rainfall and a more depleted composition during colder, wetter periods with larger rainout events. Enriched $\delta^{18}O$ precipitation is generally observed with lower precipitation amounts, while depleted signature coincides with higher precipitation amounts, indicating an "amount effect" during both dry and wet seasons. Enriched $\delta^{2}H$ and $\delta^{18}O$ values occur in December and January in the dry season, while relatively depleted values are recorded in May and August during the wet season. Table 10 data supports the "amount effect," showing an inverse relationship between precipitation amount and isotopic values in both seasons. Decreased precipitation amounts during the dry season led to gradual isotopic enrichment and decreased d-excess values, while increased precipitation amounts during the wet season result in gradual isotopic depletion and increased d-excess values. Figure 17 highlights seasonal differences in precipitation d-excess values, with lower values in the dry season and higher values in the wet season. These observations suggest that the isotopic composition of valley precipitation is influenced by seasonal precipitation dynamics and additional moisture sources, such as increased surficial water bodies, fynbos, and agricultural-dominated terrains.

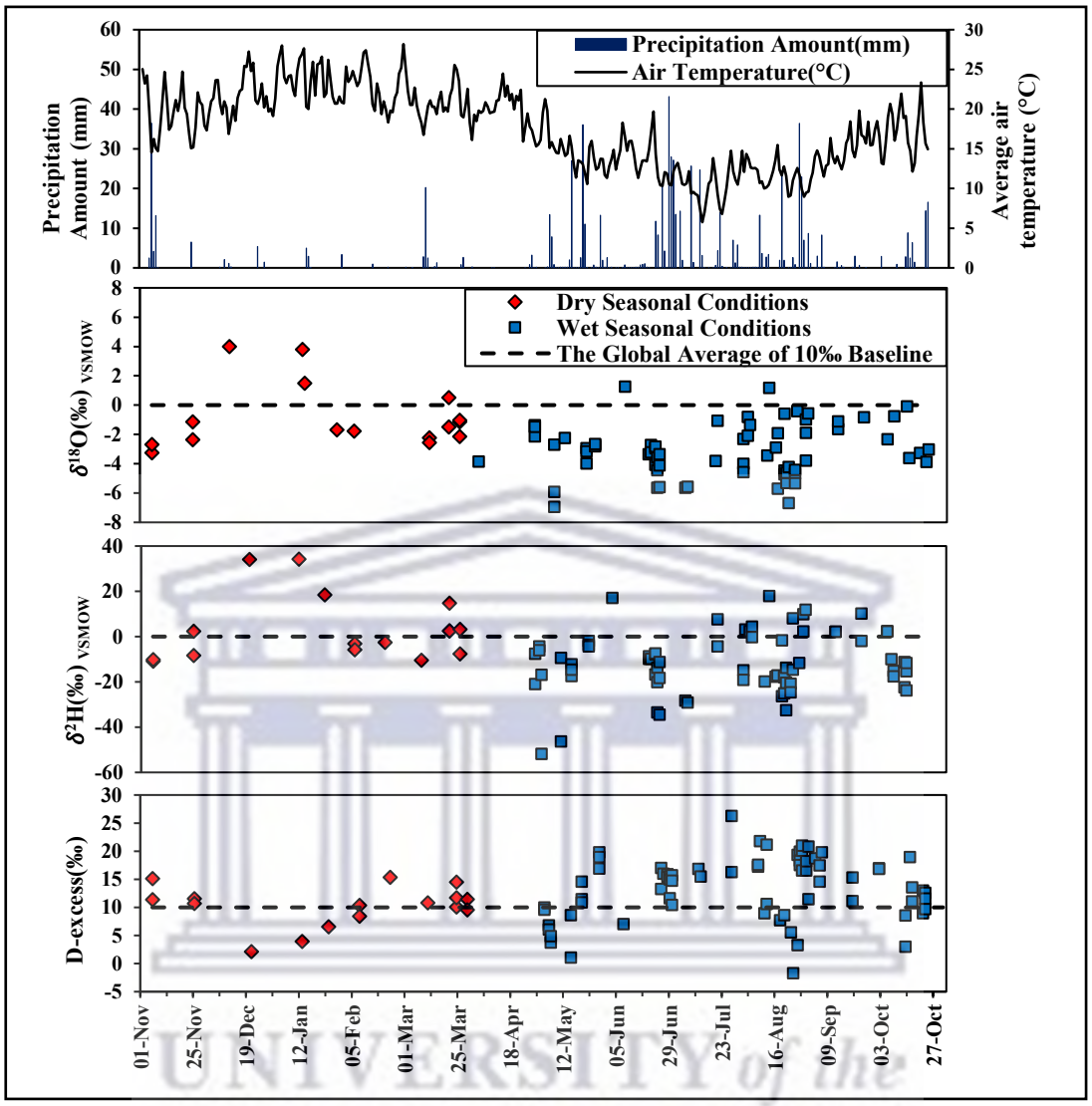

Figure 17: Temporal valley precipitation variations of $\delta^{18}O$, $\delta^{2}H$, and D-excess (‰) in relation to precipitation amount during the dry and wet seasons.

Stream Water Characterization

Table 11 provides a statistical summary of the $\delta^{18}O$, $\delta^{2}H$, and d-excess data for river samples in the catchment area. Under dry-low flow conditions (n=137), the mean $\delta^{18}O$ and $\delta^{2}H$ values are -3.28‰ and -11.69‰, respectively, with ranges of -3.99‰ to -2.79‰ for $\delta^{18}O$ and -15.30‰ to -9.40‰ for $\delta^{2}H$. During the wet-high flow conditions (n=232), mean $\delta^{18}O$ and $\delta^{2}H$ values are -3.22‰ and -11.75‰, respectively, with ranges of -4.73‰ to -1.84‰ for $\delta^{18}O$ and -21.70‰ to -3.20‰ for $\delta^{2}H$. In the dry seasons, $\delta^{18}O$ compositions appear slightly depleted and

consistent along the main stream, reflecting decreased precipitation amounts (Figure 17). In contrast, the wet seasons show increased river flow associated with greater variation and depletion in isotopic values.

Most river data collected exhibit a narrow range, with more variability during wet seasons. This suggests that the isotopic distribution along the main stream and tributaries is more depleted during dry seasons and more enriched during wet seasons. River isotopic compositions characterized by physiographic zones, with the upper region showing the most depleted signature in both seasons, and the middle, lower, and upper regions following this pattern during dry and wet seasons, respectively. The Franschhoek and Wemmershoek Rivers, draining into the upper region, contribute to its more depleted isotopic signature.

Table 11: Statistical summary of seasonal isotopic values in stream network across three physiographic zones in the Franschhoek-Paarl valley basin.

REGION		DRY SEASON			WET SEASON		
		$\delta^{18}O$ (‰)	$\delta^{2}H$ (‰)	*d*-excess (‰)	$\delta^{18}O$ (‰)	$\delta^{2}H$ (‰)	*d*-excess (‰)
Upper	**Min**	-3.99	-15.30	12.32	-4.28	-20.34	6.51
	Max	-2.79	-9.40	18.02	-1.91	-4.80	19.74
	Average	-3.27(±0.25)	-11.85(±1.54)	14.30(±1.01)	-3.24(±0.44)	-12.03(±2.63)	13.92(±2.05)
Middle	**Min**	-3.91	-14.20	13.12	-4.73	-21.70	10.28
	Max	-2.89	-9.40	18.54	-1.84	-3.20	20.49
	Average	-3.31(±0.24)	-11.60(±1.13)	14.84(±1.19)	-3.20(±0.44)	-11.33(±2.27)	14.26(±1.90)
Lower	**Min**	-3.43	-12.30	12.50	-4.01	-18.79	10.92
	Max	-2.90	-9.60	16.04	-2.52	-5.10	17.37
	Average	-3.14(±0.19)	-10.85(±0.86)	14.24(±1.07)	-3.16(±0.50)	-11.82(±3.59)	13.48(±1.76)

**Standard Deviation (± SD)*

During the dry season, $\delta^{18}O$ and $\delta^{2}H$ spatial river compositions (Figure 18) remain relatively stable in the upper and middle reaches, with a slight enrichment towards the lower reach. The Franschhoek and Wemmershoek Rivers (G1H003, FRANS1, G1H080, and WEM1) flow into the Berg River, impacting its isotopic composition depending on successive tributary inflow. The Dwars River and the Berg River show similar compositions in the dry season, but the tributary's influence diminishes in the wet season. Marginal spatial differences between dry and wet seasons suggest variations in evaporation and water inflow. Below the Berg River

Dam, river points (G1H077 and BGR1) display homogeneous enriched signatures with a reduced d-excess composition. Along the main stream, isotopic fluctuations are minimal, except at the Wemmershoek River confluence (BGR6). The lower reach in Figure 18 shows higher isotopic variation in the wet season, possibly due to increased flow.

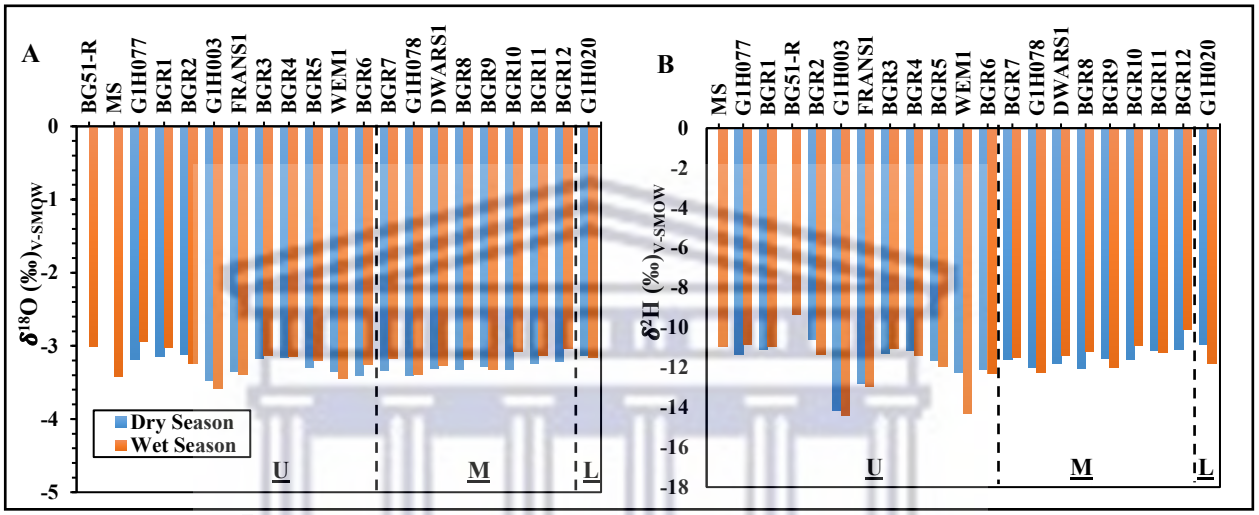

Figure 18: Average River seasonal isotopic variations of A) $\delta^{18}O$ and B) $\delta^{2}H$ in the upper (U), middle (M) and lower (L) reaches.

During the dry season, the upper reach shows relatively depleted $\delta^{18}O$ (-3.99‰) and $\delta^{2}H$ (-15.3‰) compositions, while both upper and lower reaches show slight enrichment in the wet season, likely from rapid precipitation recharge. The Berg River's $\delta^{18}O$ and $\delta^{2}H$ compositions vary significantly across seasons, with more fluctuations in the wet season. In Figure 19, the tributaries show depleted isotopic signatures relative to the main river, consistent with the observations in Figure 18, reflecting similar climatic and catchment influences. The river isotopic signatures in dry and wet seasons are similar to those of the groundwater, as indicated by their distribution along the groundwater regression line. However, it is evident that the wet season $\delta^{2}H$ and $\delta^{18}O$ compositions plot closer to the LMWL compared to the dry season.

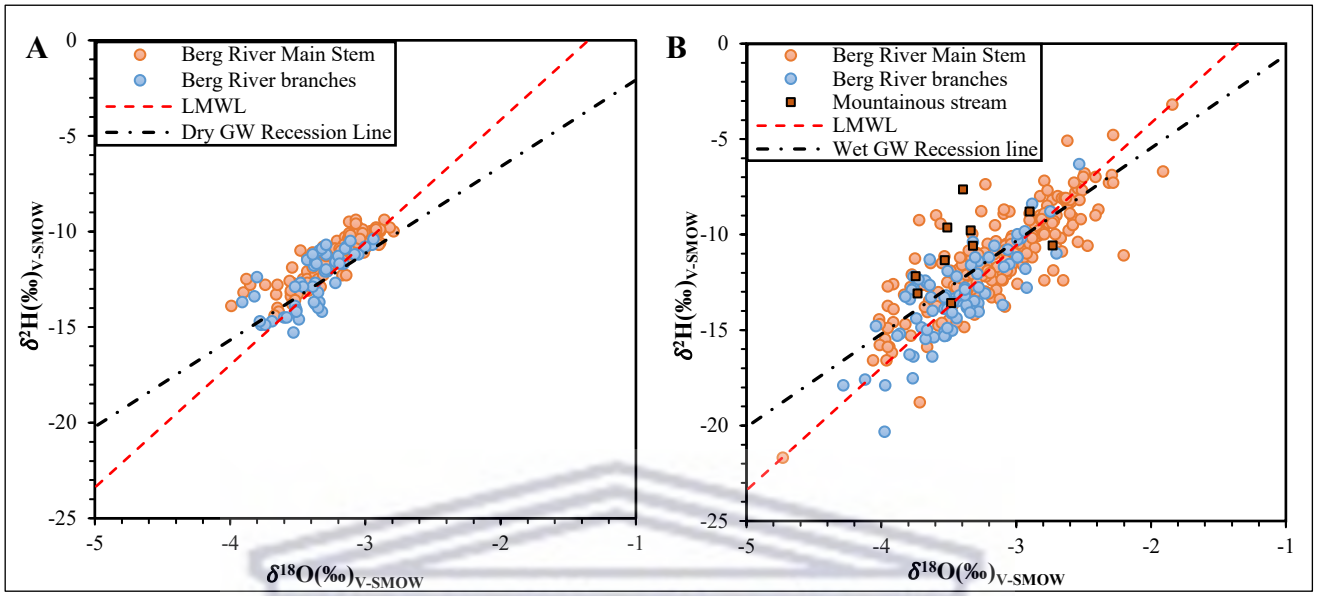

Figure 19: River dual-isotope plot showing the relationship between δ^2H and $\delta^{18}O$ during the A) dry and B) wet seasons

To assess the relationship between altitude and δ^2H, δ^2H was chosen due to its sensitivity to environmental changes and linear relationship with $\delta^{18}O$. Figure 20 shows the negative correlation between river isotopic composition and altitude during each seasonal condition. Samples from the dam outlet were excluded due to potential evaporation effects. A weak linear relationship between δ^2H and river altitude is observed in the mountainous region, suggesting limited reliance on precipitation, especially at lower altitudes below 150m.a.s.l. Equations 12 and 13 describe this relationship during the dry and wet seasons. Seasonal analysis reveals minimal fluctuations in isotopic composition along the river flow path, indicating high spatial consistency, likely due to the gentle topography of the Berg River, with a maximum elevation of 220m. Thus, the influence of altitude on the river's isotopic composition is considered negligible.

$$\delta^2H\ (‰) = -0.014E\text{-}9.613 \quad (r = -0.51,\ p<0.05) \qquad [12]$$

$$\delta^2H\ (‰) = -0.018E\text{-}9.170 \quad (r = -0.48,\ p<0.05) \qquad [13]$$

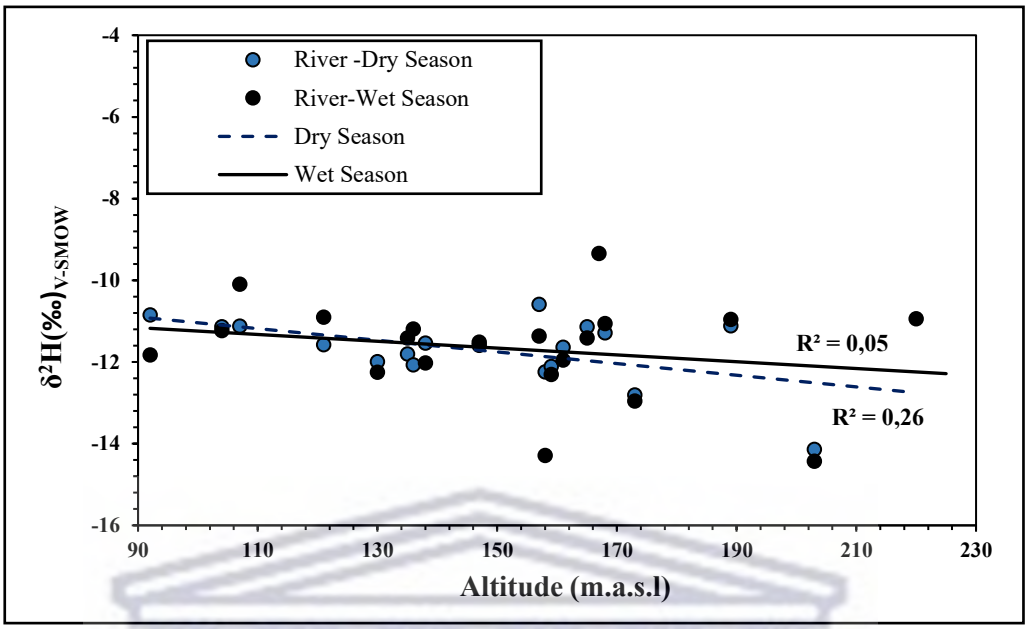

Figure 20: The correlation between δ^2H (‰) and varying riverbed elevation.

Groundwater Characterization

Table 12 provides statistical summaries of 327 groundwater samples collected from 14 stations across the upper, middle, and lower valley regions. Samples were taken at various depths: shallow (<30mbgl) and deep (>30mbgl). In the dry season, $\delta^{18}O$ values ranged from -4.21‰ to -2.52‰, with an average of -3.55‰, while δ^2H values ranged from -18.20‰ to -8.50‰, with an average of -13.69‰. In the wet season, $\delta^{18}O$ values ranged from -4.36‰ to -1.66‰, with an average of -3.12‰, and δ^2H values ranged from -22.46‰ to -4.00‰, with an average of -11.00‰. Groundwater exhibited higher seasonal variation compared to river sources, with slightly enriched average values during the wet season: $\delta^{18}O$ increased by 0.43‰ and δ^2H by 2.69‰ compared to the dry season.

Table 12: Seasonal groundwater statistical summary in the valley regions

REGION		DRY SEASON			WET SEASON		
		$\delta^{18}O$ (‰)	$\delta^{2}H$ (‰)	*d*-excess (‰)	$\delta^{18}O$ (‰)	$\delta^{2}H$ (‰)	*d*-excess (‰)
Upper	Min	-4.21	-18.20	12.78	-4.36	-22.46	9.08
	Max	-2.89	-8.50	18.40	-2.23	-4.00	19.32
	Average	-3.69(±0.29)	-14.07(±1.99)	15.38(±1.31)	-3.25(±0.40)	-11.40(±3.00)	14.56(±2.01)
Middle	Min	-4.21	-18.00	9.26	-4.18	-16.50	8.08
	Max	-2.52	-9.80	18.48	-1.66	-4.78	17.15
	Average	-3.41(±0.46)	-13.41(±2.09)	13.83(±1.96)	-2.84(±0.60)	-9.91(±2.97)	12.85(±2.20)
Lower	Min	-3.71	-14.80	11.58	-3.63	-16.30	10.76
	Max	-2.91	-11.70	15.76	-2.26	-6.10	17.25
	Average	-3.14(±0.20)	-10.85(±1.04)	14.09(±1.11)	-3.01(±0.34)	-10.97(±2.53)	13.12(±1.81)

**Standard Deviation (± SD)*

Table 13 compares deep (>30mbgl) and shallow groundwater (<30mbgl) isotopes during both seasonal conditions. The deep groundwater showed a marginal isotopic depletion compared to shallow groundwater. The shallow groundwater showed consistent isotopic signatures, suggesting a single recharge source, while deep groundwater indicated contributions from multiple recharge sources.

Table 13: Seasonal isotopic comparison (‰) of deep (>30mbgl) and shallow (<30mbgl) groundwater.

BOREHOLE DEPTH		DRY		WET	
		$\delta^{18}O$ (‰)	$\delta^{2}H$ (‰)	$\delta^{18}O$ (‰)	$\delta^{2}H$ (‰)
>30MBGL	Min	-4.21	-18.20	-4.36	-22.46
	Max	-2.52	-9.80	-1.66	-4.77
	Average	-3.59 (±0.39)	-13.92(±1.84)	-3.15(±0.52)	-11.19(±3.16)
<30MBGL	Min	-3.95	-16.90	-3.86	-16.20
	Max	-2.89	-8.50	-2.23	-4.00
	Average	-3.47(±0.29)	-13.14(±2.04)	-3.06(±0.35)	-10.56(±2.47)

**Standard Deviation (± SD)*

In Figure 21, groundwater isotopic compositions vary between dry and wet seasons. Dry season groundwater is depleted, while wet season groundwater is enriched due to evaporation. These differences are seen across regions and depths, including deep boreholes (>30mbgl), represented by textured bars. This suggests the occurrence of different recharge and mixing processes. Deep groundwater in the upper region is relatively more depleted compared to the middle to lower areas. Samples from

recreational areas (PGE1 and BRRBH) have enriched isotopes, likely due to human influences. The upper region is less impacted by human activities. These findings show spatial and depth-related differences in groundwater

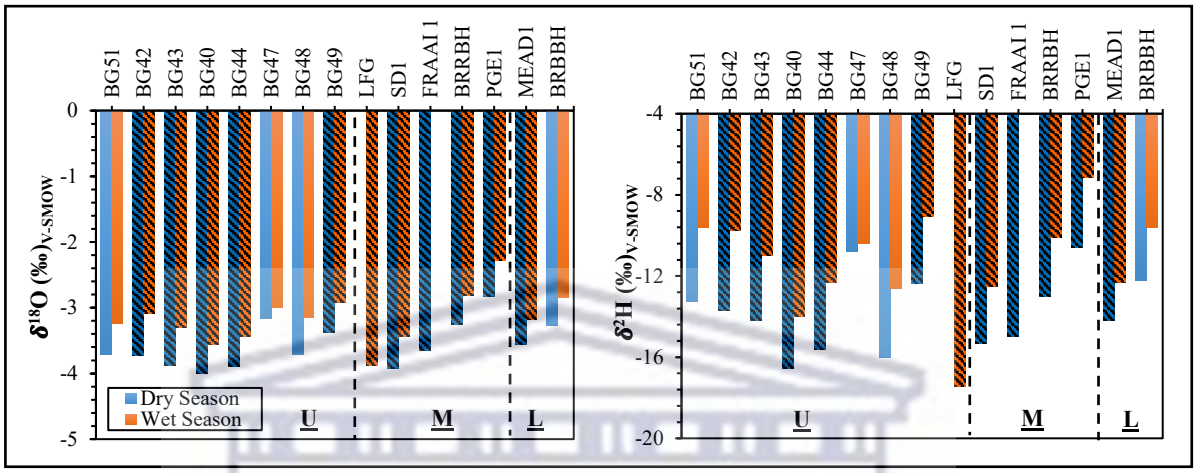

Figure 21: Spatial groundwater isotopic distribution by physiographic zones.

The influence of evaporation on river and groundwater isotopes

The study investigated the influence of evaporation on river and groundwater isotopic composition using d-excess values. Most groundwater samples show low d-excess values (≤10‰), indicating minimal evaporation impact. However, some sites in the middle to lower valley regions show signs of evaporation. Precipitation has higher d-excess values (12.23‰ in dry season, 12.37‰ in wet season) compared to the global average. River water exhibits a wider range of d-excess values than groundwater, ranging from 12.50‰ to 18.54‰ in dry season and 6.51‰ to 20.49‰ in wet season. Groundwater d-excess values range from 9.26‰ to 18.48‰ in dry season and 8.08‰ to 19.32‰ in wet season.

Figure 21 shows a moderate correlation between river water and groundwater d-excess values with $\delta^{18}O$. A decrease in d-excess values aligns with $\delta^{18}O$ enrichment, especially noticeable in the wet season. Approximately 2% of groundwater samples in the dry season and 3% in the wet season fall below the global threshold of 10‰ (indicated by the red line in Figure 22). In comparison, approximately 2% of wet season river samples exhibit d-excess values below the threshold.

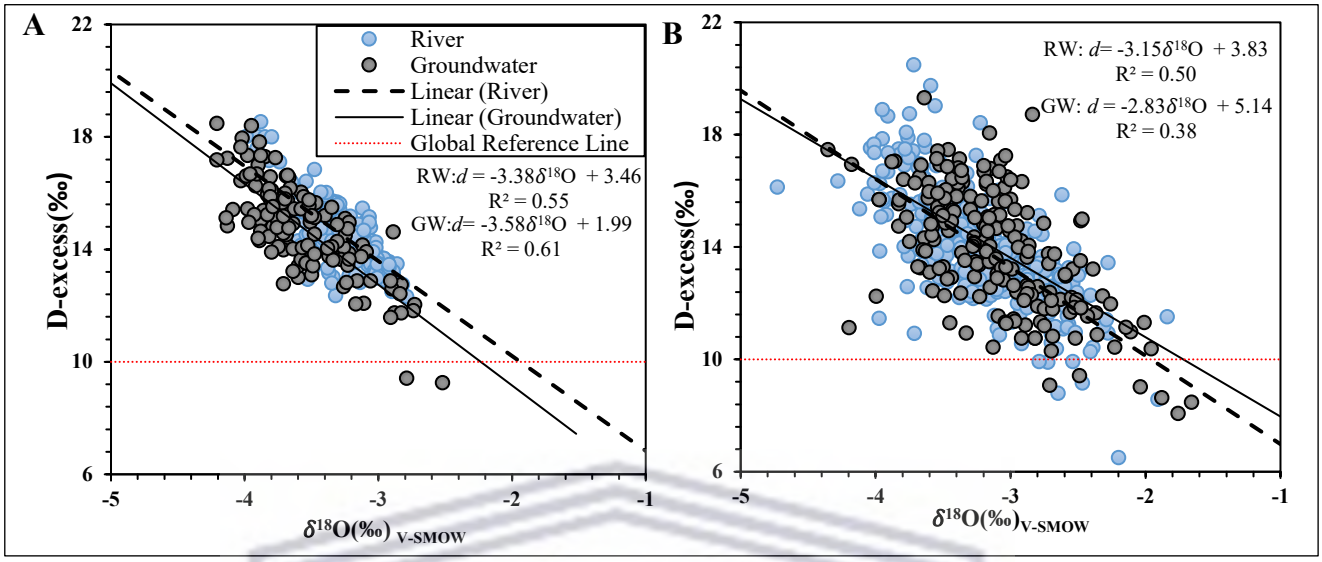

Figure 22: The relation between d-excess and $\delta^{18}O$ for groundwater and river water in the Franschhoek-Paarl valley during the A) dry and B) wet seasons

4.3 Discussion: Tracing River recharge through seasonal stable isotopic signatures

Precipitation-river relation

The Global Meteoric Water Line (GMWL) showed a higher slope and intercept compared to the Local Meteoric Water Line (LMWL), indicating the impact of increased temperatures and low humidity during the dry season. These conditions led to the evaporation of falling precipitation (Harris et al., 2010; Li et al., 2014). The catchment's precipitation was suggestive of similar rainfall patterns to that of the Cape Town region, as it plotted on and was adjacent to the Cape Town LMWL.

In the dry season, rainfall isotopes (Figure 13) became more enriched and deviated from the LMWL due to decreased precipitation, higher temperatures, and increased evaporation (Friedman, 1962). Conversely, the wet season showed isotopic signatures along the LMWL, indicating higher rainfall and less evaporation (Dansgaard, 1964). Some seasonal precipitation samples deviated from the LMWL, similarly observed in Punjab, India, where additional moisture sources and the "reservoir effect" influenced isotopic variation (Krishan et al., 2021). Additionally, deviation from the GMWL during the wet season suggested evaporative processes altering the isotopic composition after surface contact, resulting in a different composition compared to the original moisture (Yao et al., 2018). During the dry season, rainfall isotopic signatures are enriched, typical of a Mediterranean climate (Diamond, 2014; Halenyane, 2017). This variation is attributed to the seasonal rain-out effect, influenced by moisture sources, trajectory processes, evaporative variability, and local climatic conditions in the warm, semi-arid region.

The nature and evolution of isotopic signatures in precipitation depended on the condensation temperature in clouds and surrounding air temperature (Friedman et al., 1964). During the dry season, higher air temperatures moderately enriched precipitation isotopic signatures (Table 10). However, in the wet season, $\delta^{2}H$ and $\delta^{18}O$ showed no correlation with local air temperature, suggesting other factors related to moisture sources may have obscured the 'temperature effect.' The weak relationship between rainfall isotopes and temperature aligns with expectations for

low latitude areas (Rozanski et al., 1993; Harris et al., 2010). Large-scale moisture sources, as observed in China (Tao et al., 2021), can influence air temperature. In the wet season, valley precipitation d-excess showed a negative correlation with air temperature ($p<0.05$), similar to findings in the Hemuqiao watershed of China by Gou et al. (2022). Increased air temperatures in these cases led to decreased relative humidity and elevated sub-cloud evaporation, enriching the $\delta^{18}O$ composition relative to precipitation d-excess composition (Wu et al., 2014; Guan et al., 2013), particularly evident during the dry season with lighter precipitation.

The modification of precipitation d-excess values suggested the influence of evaporative moisture from inland water or ground surfaces, along with secondary evaporation (Deng et al., 2016; Jiang et al., 2018). Primary meteorological factors, such as relative humidity (RH, %) and precipitation amount (PA, mm), are suggested to control the sub-cloud evaporation effect (Guan et al., 2013). Artificial impoundments, with larger surface areas than flowing rivers, expose stored water to increased evaporation, altering the microclimate and potentially affecting temperature and moisture concentrations (Ahmed et al., 2011). As discussed in section 2.2, precipitation isotopic compositions tended to decrease with increasing altitude, particularly in high-elevation areas where the decrease was more pronounced, typically per 100 meters. However, the study's selected rainfall sites, situated in lower elevated regions, posed challenges in assessing the altitude effect within the catchment.

During dry seasons, rivers integrate the isotopic composition of previous rainfall events, assuming that the catchment is surrounded by mountainous terrains (Gat, 2010). In this study, river samples on and adjacent to the LMWL indicated potential recharge from the Franschhoek-Drakenstein mountains. The clustering river pattern suggested shared water sources among the main river and tributaries, reflecting a well-mixed recharge composition of local rainfall and groundwater. The river, groundwater, and rainfall association indicated frequent interaction among these systems, partially due to the influence of evaporative precipitation that recharged the system and induced possible isotopic exchange.

In the catchment, rainfall runoff into streams varied due to topography, land surfaces, and drainage networks, showing minimal seasonal changes in isotopic patterns of surface water bodies. This homogenized pattern resulted from local precipitation trends influenced by the "amount effect" and modified evaporation, driven by climatic patterns. In the dry season, evaporative enrichment was prominent due to reduced precipitation, leading to insignificant influence of precipitation-induced isotopic compositions on river signatures. Alternatively, in the wet season with increased rainfall, a portion of the isotopic composition closely resembled the river isotopic signatures.

The river closely followed the LMWL, indicating significant recharge from precipitation, with deviations suggesting evaporation influence. Meteorological parameters and hydrological modifications altered the precipitation isotopic composition before entering the river system, such as evaporation at the soil surface and during surface runoff, resulting in differences between river water and precipitation isotopic compositions. These findings highlighted the role of direct runoff in shaping isotopic variation along the stream network and modifying precipitation's original isotopic composition.

Groundwater to river relation

During the recession period, groundwater discharge dominated river flows, influenced by the geological framework and water storage capacity (Bloomfield et al., 2009; Klaus & McDonnell, 2013). The valley's fracture network led to similarities between river and subsurface water isotopic signatures, indicating groundwater dominance. However, groundwater isotopic variations (Figure 20) suggested mixing and isotopic exchange processes in the deep unsaturated zone over a long residence time (Asoka et al., 2017). This indicated multiple sources contributing to the larger isotopic variation in groundwater compared to river water, including indirect recharge, anthropogenic drawdown, irrigation return flow, and groundwater-surface water interaction. Despite mixing processes at deeper depths, the isotopic variations of recharge water were not fully homogenized relative to the river waters.

Diamond (2014) highlighted the influence of subsurface sources on river isotopic patterns, creating a blend of water sources along the river's course. This mixing dampened distinct isotopic compositions from specific subsurface sources, resulting in an invariable isotopic pattern in river flow. Groundwater showed minimal seasonal isotopic variation compared to river sources. In the wet season, there was a slight enrichment in average δ^2H and $\delta^{18}O$ values compared to the dry season. The complex flow path, characterized by fractured networks, led to a longer residence time and the emergence of seeps or springs contributing to river systems. Le Maitre and Colvin (2008) and Diamond (2014) observed a mixture of water sources from various groundwater discharges, influencing the isotopic variability of the stream in response to precipitation. in isotopic signatures between groundwater and rainfall suggested distant groundwater flow from previously recharged areas.

In semi-arid regions, surface water bodies undergo increased evaporation and fractionation due to solar radiation and high temperatures, resulting in enriched isotopic signatures (Zhu et al., 2016). Contrary to expectations, downstream distribution of river isotopic data in the valley showed gradual isotopic changes, implying the dominance of a single recharge source and a continuous contribution of recharge flow to the river. The slope of the seasonal RWL remained consistent during both dry (-4.62) and wet (-4.85) seasons, indicating that seasonal changes did not significantly affect the degree of evaporation in the stream water (Simpson & Herczeg, 1991).

In the dry season, reduced precipitation and flow led to heavier isotopic compositions in the stream due to evaporation from open water sources, and replenished by sub-surface water bodies under baseflow conditions. In contrast, the wet season, characterized by increased rainfall and flow velocity, showed enriched isotopic compositions. While overall seasonal variation in the river's isotopic patterns was marginal, the Franschhoek and Wemmershoek Rivers, originating from higher altitudes and with shorter flow paths, displayed depleted isotopic compositions compared to the Berg River, resulting in less enrichment in the tributaries under both seasonal conditions.

Groundwater and dams may have extended a regulatory effect on rainfall runoff into streams, suggesting minimal to homogeneous seasonal changes in the river's isotopic composition. Chen et al. (2020), Li et al. (2016) and Li et al. (2019) found similar results in China, noting that rivers downstream from dams experienced reduced isotopic variability seasonally. The Berg River and Wemmershoek Dams limit downstream flow, increasing residence time and evaporation, which made stored river water isotopically homogeneous. The seasonal degree of evaporation in the stream network marginally varied and was more affected compared to shallow and deep groundwater, as indicated by Winter et al. (1998). Generally, in semi-arid regions during low flow conditions, residual surface waters undergo significant isotopic enrichment (> +3‰) due to increased evaporation (Gonfiantini, 1986), further amplified by dams. This enrichment may drive the recycling of river water, resulting in additional isotopic enrichment (Zhou et al., 2021).

River samples that deviated from the LMWL, suggests increased evaporative fractionation due to slow flow rates. Conversely, the weak correlation between river altitude and isotopes suggested either a shared recharge area or dampening of the altitude effect by hydrological parameters (Wassenaar et al., 2009; Bershaw et al., 2012). The marginal variation might also be due to significant mixing in fractured conduits, with tributaries having more depleted isotopic compositions compared to the mainstream under both seasonal conditions. Yeh et al. (2014) studied a mountainous catchment in Taiwan and found that tributaries in mountainous areas primarily consisted of interflow before merging with the main river. In the lower reach of the river (Figure 17), near an industrial outlet, significant fluctuations in isotopic signatures were observed, likely influenced by external water sources and upstream mixing. The relatively consistent $\delta^{18}O$ variation in the river and groundwater in comparison to precipitation suggested mixing with stored water from the dam and surrounding groundwater during flow through the catchment.

The d-excess varied along the Berg River, with higher values downstream compared to upstream. This variation suggested differences in moisture sources and the influence of the two dams, which increased evaporation and isotopic enrichment, modifying the d-excess value. Traditionally, d-excess is associated with climatic parameters, with warmer seasons typically experiencing stronger

evaporation processes (Gat et al., 1994). Despite depleted river $\delta^{18}O$ signatures, d-excess values increased during the dry season, suggesting that factors other than evaporation contributed to river d-excess modification (Guo et al., 2017).

The d-excess and $\delta^{18}O$ relationship in wet seasonal groundwater and river water samples suggested that d-excess values decreased relative to the enrichment in $\delta^{18}O$, indicating pre-recharge evaporation in the water sources (Gupta & Deshpande, 2005). Approximately, 4.67% of groundwater samples showed reduced d-excess values, indicating hydrological changes during their time in the vadose or saturated zone. Mixing processes such as rainfall recharge, river interaction, irrigation return flow, or dam release altered the isotopic composition. Groundwater samples with d-excess values above 10‰ indicated minimal evaporation during recharge. Seasonal variations in river water d-excess indicated the influence of precipitation on the dominant sources contributing to streamflow (Jung et al., 2020).

4.4 Summary

Assessing changes in rainfall isotopes helped understand how seasons affected river recharge. Rainwater that was absorbed by plants, seeped into soil, or flowed into rivers influenced the river's isotopic signature. Seasonal variations in isotopic signatures indicated increased rainfall events during the wet season and more enriched rainfall during the dry season. Dry season air temperatures moderately enriched precipitation isotopic signatures, while factors related to moisture sources generating precipitation obscured the 'temperature effect' during the wet season. Evaporation and climatic conditions played a role in the rain-out effect, causing variations in precipitation isotopic signatures. The catchment's geological framework influenced water storage and flow, with groundwater discharge dominating rivers. The river and groundwater showed distinct isotopic variations, with the river showing a homogenized isotopic pattern due to the discharge and mixing of various subsurface sources. Human activities, such as dam construction and irrigation, also impacted the water's isotopic compositions. Analysis of d-excess values indicated recharge from various moisture sources with minimal evaporation. Groundwater and the Berg River showed stable isotopic patterns, reflecting consistent environmental conditions.

CHAPTER 5: Hydrochemical Characterization and Process Detection in River Hydrochemistry

5.1 Introduction

This chapter presents the hydrochemical analysis of river water samples and recharge sources in the Berg River's upper, middle, and lower regions. The chapter aimed to determine the river's ion sources, flow path, and natural and anthropogenic processes influencing the river's seasonal variation by using hydrochemical and statistical techniques. Methods like Piper and Gibbs diagrams were used to characterize the hydrochemistry and understand evolutionary mechanisms controlling the river chemistry. The ion-ratio method was used to delineate water-rock interactions, while Pearson's correlation and factor analysis identified similar physicochemical attributes and processes affecting streamflow quality.

5.2 Results

5.2.1 Statistical physicochemical analysis of the valley's water resources.

Table 14 summarises the physicochemical parameters of surface water, groundwater, and precipitation collected during the 2020-2021 sampling campaign. The data from Appendix A and B are used to categorise the samples (n) into upper, middle, and lower physiographic valley zones.

Temperature

The river water temperature in Table 14 varies seasonally from 10.40°C to 28.40°C, with a mean value of 17.94°C±4.55°C. During the dry season, with high air temperatures and low flow conditions, the river water temperature was highest, while it was lowest during the wet season. The upper reach had the highest river temperature (28.40°C) during the dry season, while the middle reach had the lowest (10.40°C) during the wet season. Groundwater temperatures ranged from 10.20°C to 25.40°C, with less variation than surface water. Precipitation in the valley had a larger temperature variation, ranging from 6.70°C to 25.30°C.

pH

The pH values range from slightly acidic to alkaline. River water shows an acidic pH range between 4.25 to 8.38 (Figure 22), with a mean value of 6.88±0.70, while groundwater sources show a range of 2.69 to 8.33, with a mean value of 5.96±1.04. Precipitation ranges from 4.75 to 8.79, with a mean value of 6.94±0.71. The pH variation in river water was insignificant at a seasonal scale.

EC

EC is an indicator of water ion composition and, in this study, the river EC concentrations ranges from 16.00 µS/cm to 362.00 µS/cm, with a mean value of 78.82 µS/cm±30.61. The Franschhoek River, a tributary of the Berg River in the upper reach, and BGR5 of the Berg River shows the highest EC levels in the dry and wet seasons, as shown in Figure 22. The surface water's EC levels shows a marginal fluctuation between the seasons, mostly during the wet season. Groundwater's EC values ranged between 34.40µS/cm to 867.00µS/, with a mean value of 219.73 µS/cm±175.49µS/cm. As indicated in Table 14, seasonal precipitation shows the lowest ionic concentration.

Table 14: Summary of Physicochemical and Hydrochemical Data from Berg River Stream Network and Recharge Sources.

Sampling region	Water type	Parameter	EC (μS/cm)	TDS (mg/L)	pH	T (°C)	Ca^{2+} (mg/L)	Mg^{2+} (mg/L)	Na^{+} (mg/L)	K^{+} (mg/L)	HCO_3^{-} (mg/L)	SO_4^{2-} (mg/L)	Cl^{-} (mg/L)	SiO_2 (mg/L)	NO_3- (mg/L)
Upper reach	River	Min	16.00	10.40	4.25	11.20	0.30	0.17	2.03	BDL	0.00	BDL	5.61	0.03	BDL
		Max	362.00	235.30	8.31	28.40	17.63	5.55	36.44	5.54	92.72	14.13	43.92	9.44	10.64
		Mean(±SD)	77.74	46.37	6.80	23.29	4.54	1.65	6.67	0.62	15.70	2.23	12.71	2.48	1.23
	Groundwater	Min	48.50	31.53	3.02	13.30	BDL	0.03	3.68	BDL	0.00	BDL	6.74	0.74	BDL
		Max	202.10	131.37	7.32	22.80	14.70	7.12	32.49	3.02	90.28	26.08	79.40	11.53	10.88
		Mean(±SD)	110.36	71.73	5.31	18.47	4.42	2.51	9.43	0.43	17.67	3.92	14.75	4.75	2.40
Middle Reach	River	Min	36.70	23.86	5.56	10.40	0.14	0.59	3.25	BDL	1.22	BDL	6.74	0.59	BDL
		Max	163.80	106.47	8.38	28.10	13.04	4.15	89.13	3.27	90.28	26.08	79.40	7.32	10.88
		Mean(±SD)	84.00	54.41	7.01	18.08	5.45	1.93	8.05	1.12	17.67	3.92	14.75	2.59	2.40
	Groundwater	Min	34.40	22.36	2.69	10.20	3.00	1.68	8.47	BDL	0.00	BDL	10.17	0.84	BDL
		Max	867.00	563.55	8.20	23.60	21.14	26.84	102.02	39.00	140.30	35.17	218.71	16.70	9.82
		Mean(±SD)	359.21	233.49	6.78	18.72	12.09	7.66	43.61	1.50	75.04	10.89	62.18	9.84	2.08
Lower Reach	River	Min	45.00	29.25	6.03	12.20	1.34	0.91	4.34	0.10	3.66	1.46	8.81	0.16	0.31
		Max	153.20	99.58	8.03	27.40	12.26	3.94	14.09	2.64	44.48	8.74	25.28	3.73	4.30
		Mean(±SD)	85.90	55.84	7.28	19.97	5.80	2.21	7.97	1.28	19.28	4.16	14.95	2.04	2.14
	Groundwater	Min	310.00	186.00	3.86	15.50	4.97	3.21	33.87	0.34	34.16	2.34	60.41	2.43	BDL
		Max	580.00	348.00	8.33	25.40	31.74	9.19	96.96	2.98	169.58	42.33	101.77	17.86	5.98
		Mean(±SD)	450.60	270.36	6.58	21.14	19.74	6.47	54.14	1.77	93.32	12.04	74.98	7.67	0.24
Precipitation		Min	3.00	1.95	4.75	6.70	0.27	0.09	0.24	BDL	1.22	BDL	0.83	BDL	BDL
		Max	253.00	164.45	8.79	25.30	8.77	2.29	13.14	4.82	30.50	10.38	26.11	0.26	54.99
		Mean(±SD)	38.38	24.94	6.94	14.97	4.65	1.19	1.95	0.58	16.32	2.55	4.49	0.94	3.38

*****BDL represents Below Detection Limit*

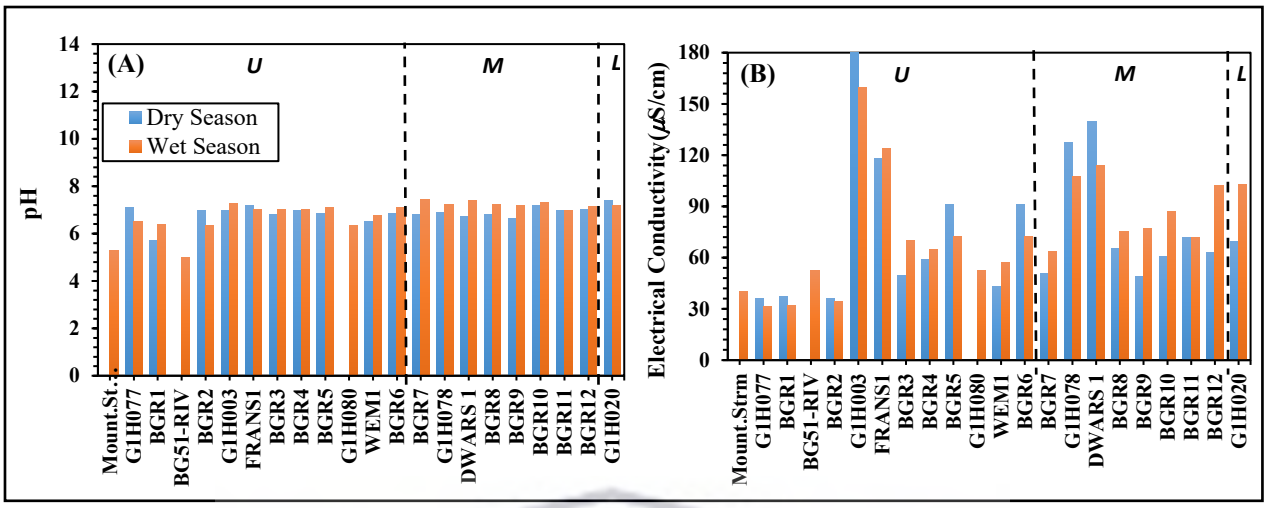

Figure 23: Seasonal averages of (A) pH and (B) electrical conductivity (EC) in the upper (U), middle (M), and lower (L) reaches of the Berg River.

5.2.2 Dominant water types

Precipitation and groundwater discharge are leading end-member components contributing to the Berg River's baseflow. Figures 24 and 25 depict the solute signatures of river water, groundwater, and rainfall hydrochemistry using Piper diagrams. In Figure 24A, a proportion of the 187 samples of the Berg, Wemmershoek, Dwars, and Franschhoek Rivers of the upper region, during the dry season, shows three hydrochemical facies of Na-Cl water type (71%), with a reduced concentration of Ca^{2+}, Mg^{2+}, and HCO_3; and evolves to a mixing water type Ca-Mg-Cl (28%) and Ca-Na-HCO_3(1%). Figure 24B of the wet season reveal three hydrochemical facies with an input of Ca^{2+}, Mg^{2+}, and Cl^-, with minor input of HCO_3^- and Na^+. The mixed Ca-Mg-Cl water type (68%) dominates the streamflow, where Ca^{2+} and Mg^{2+} are in excess of Na^+ and K^+; however, Ca-HCO3 (17%) water type and Na-Cl (15%) water type is less dominant. The mountainous stream derivative of the wet seasonal conditions shows a similar chemical composition to the rainfall distributed of a Ca-HCO3 water type in Figure 25B, where some samples evolve by the contribution of Cl^- reflecting a mixed Ca-HCO_3-Cl water type, and suggesting a fresh recharge of meteoric origin. The seasonal evolution of water types in the river reveals that the chemical composition is influenced by varying factors.

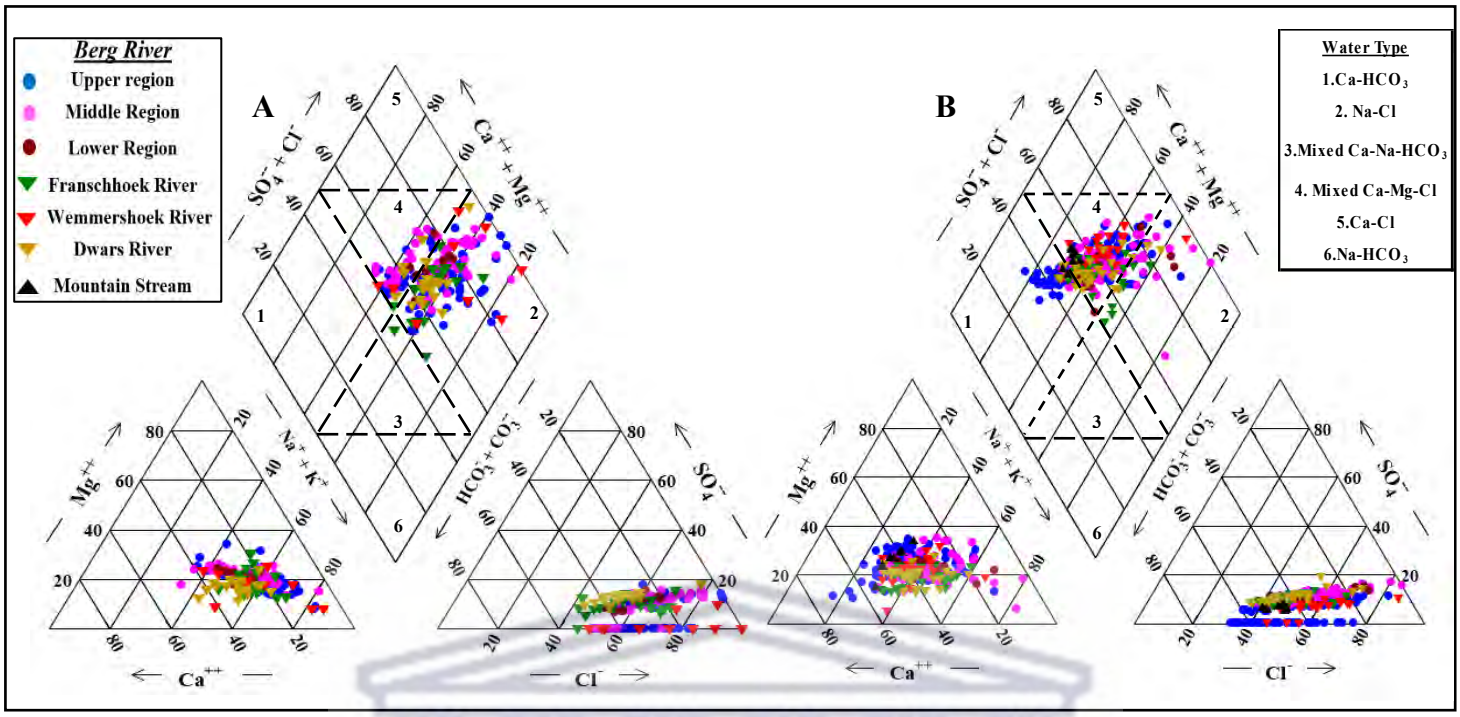

Figure 24: Piper diagram depicting the facies evolution during the A) dry and B) wet seasons in the Berg River and its tributaries.

In Figure 25A, the Piper plot reveals five types of groundwater (GW) facies showed by the 122 samples of the dry season: Na-Cl water type (59%), with a reduced ion concentration of Ca^{2+} and Mg^{2+}, mixed Ca-Mg-Cl (23%), Ca-HCO3 (8%), Ca-Na-HCO_3 (8%), and Na-HCO_3 (2%). The average concentration of Na^+ during the dry season is higher in groundwater than in river water, at 26.82 mg/L compared to 22.99 mg/L, respectively. The dominant anion in groundwater during the dry season is Cl, with an average concentration of 44.01 mg/L. In contrast, during the wet season, the dominant anion in river water is HCO_3^-, with an average concentration of 42.92 mg/L. As groundwater migrates from the mountainous areas, samples evolve into a mixed Ca-Mg-Cl groundwater type, with slightly higher concentrations of Ca^{2+} and Mg^{2+} compared to Na^+ and K^+. The concentration of strong acids (SO_4^{2-} and Cl^-) significantly exceeds that of weak acids (HCO_3^- and CO_3^{2-}) in this groundwater type.

The hydrochemistry of both streamflow and groundwater shows overlapping characteristics during different seasonal conditions, indicating that they undergo to similar geogenic and anthropogenic processes. Figure 24B shows that during the wet season, the valley's groundwater shows four hydrochemical facies: Ca-Mg-Cl (41%), Na-Cl water type (35%), Ca-HCO_3 (18%), and Ca-Na-HCO_3 (6%).

Similarly, both river and groundwater samples demonstrate an increase in Ca^{2+} in a small group of samples that form a Ca-Mg-Cl water type. Furthermore, there is an enrichment in HCO_3- in relation to Cl- reduction, causing samples to plot in quadrant 1, which displays a Ca-HCO_3 water type.

In relation to the wet and dry seasonal groundwater and surface water, the hydrochemistry of rainfall in Figure 25 is characterized by three facies that transition from a Ca-HCO3 (38% and 87%) with reduced Cl^- and SO_4^{2-}, mixed Ca-Mg-Cl (25 % and 8%), and Na-Cl (25 % and 5%). However, during the dry season, one precipitation sample shows a Ca-Cl water type.

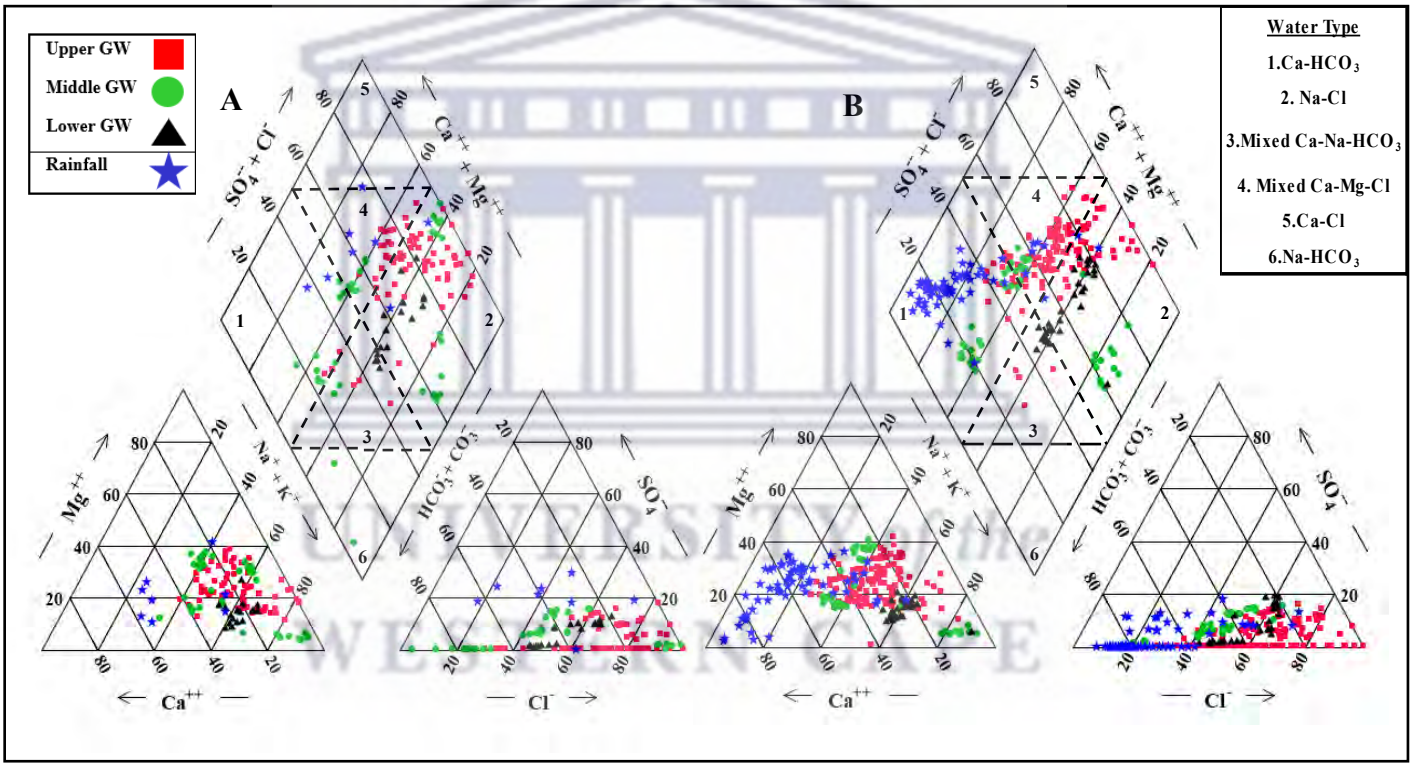

Figure 25: Piper diagram depicting the valley's groundwater and rainfall facies evolution during the A) dry and B) wet seasons.

5.2.3 Gibbs Diagram

In Figure 26, the legend includes symbols representing river components (B.R. - Berg River, W.R. - Wemmershoek River, F.R. - Franschhoek River, D.R. - Dwars River) and seasonal sampling conditions (D.S. - Dry Season, W.S. - Wet Season). The Gibbs diagrams provide insights into the dominant mechanisms governing the composition of river solutes along the flow path. Na^+, Cl^-, and HCO_3^- are the most

abundant ions in the river samples regardless of season or location. Particularly, Na^+ and Cl^- strongly influence the river's EC, serving as key indicators for assessing ion sources and understanding processes that modify the river's ion composition.

River water TDS values ranges from 10 to 300 mg/L. During the dry season, the $Na^+/(Na^+ + Ca^{2+})$ molar ratio is less than 0.5 in only 2% of the samples, while during the wet season, this ratio falls below 0.5 in 39.42% of the samples. These findings suggest that during the dry season, most river samples have a high $Na^+/(Na^+ + Ca^{2+})$ ratio with moderate TDS, indicating a dominant influence of rocks and strong correlation between river hydrochemical composition and local geology. These findings are supported by consistent patterns observed in Figure 26A and results from the Piper Trilinear Diagram in Figure 24. Additionally, a subgroup of river samples falls within the transition zone between rock-water interaction and precipitation, indicating a mixing regulation mechanism influenced by both rock-forming minerals and precipitation recharge.

During the dry season, 41% of river samples have a $Cl^-/(Cl^- + HCO3^-)$ ratio <0.5, while in the wet season, this ratio increases to 75% of samples. Figure 26 illustrates that rock-water interactions primarily govern the Berg River and its tributaries' hydrochemistry in both seasons. This implies a significant influence of rock-forming minerals on solute composition in the streamflow. Most samples from the Wemmershoek, Franschhoek, and Dwars Rivers exhibit low $Na^+/ (Na^+ + Ca^{2+})$ ratios and moderate TDS values, highlighting a dominant rock influence. However, some Berg River samples in the upper region during the dry season and middle region during the wet season show diluted TDS concentrations and increased $Na^+/(Na^+ + Ca^{2+})$ ratios, suggesting atmospheric precipitation dominance in shaping the river's chemical composition.

Most samples align with the typical pattern on the Gibbs plot, but some are on the outskirts of the characteristic boomerang shape, suggesting a marginal influence of anthropogenic activities on solute concentrations in the river. Most samples align with the typical pattern on the Gibbs plot, suggesting that cations and anions primarily come from atmospheric precipitation, rock weathering, and soil dissolution. Some Berg River samples in the upper dry season and middle wet

season show lower TDS concentrations, indicating a shift towards precipitation dominance.

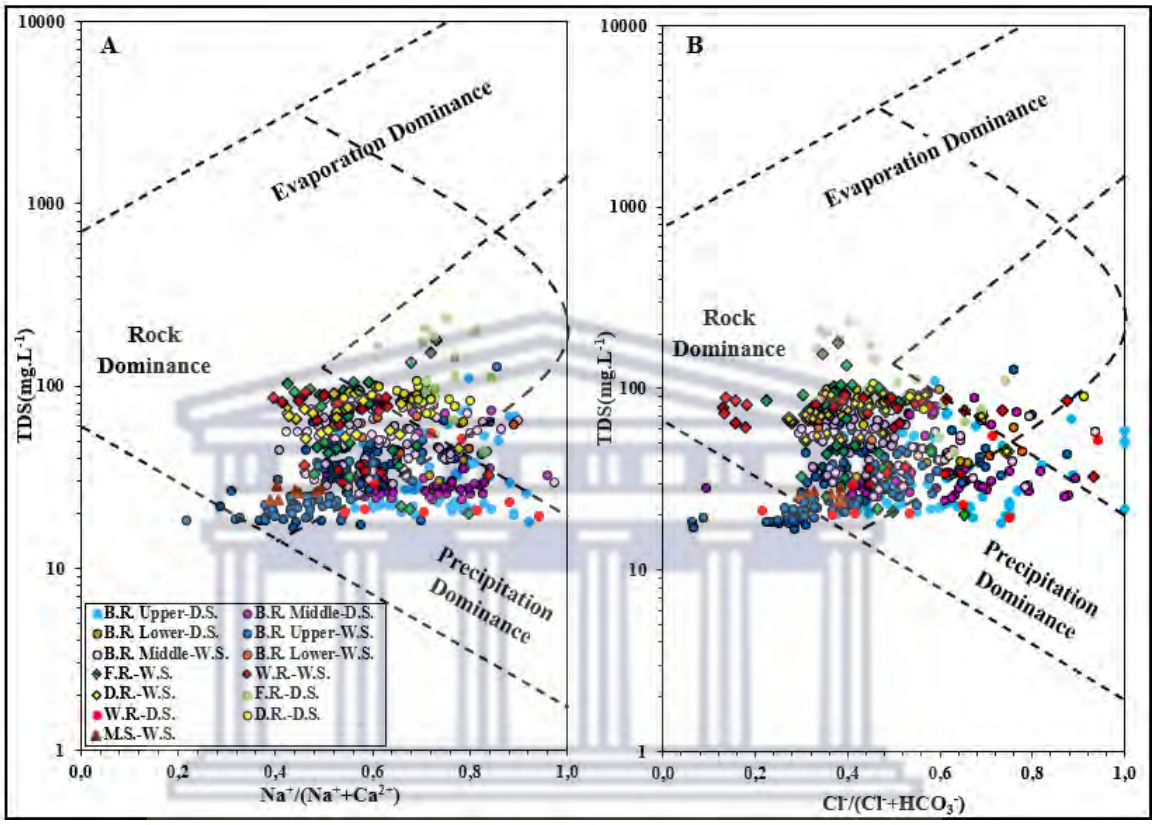

Figure 26: Gibbs diagram of river samples collected during A) dry and B) wet seasons, showing cation and anion ratios

5.2.4 Determining the origin of ions by the ion-ratio method

Figure 27's bivariate plots reveal the source origin of primary ions in the river basin and their relationships. In the dry season, Na^+ and Cl^- dominate as cation and anion solutes, respectively. The wet season sees an increase in Ca^{2+}, Mg^{2+}, and HCO_3^- concentrations, indicating seasonal variations in the dominant ions and changing river water composition.

A) Chemical weathering

Chemical weathering plays a significant role in the presence of major river ions, and their molar ratios are used to assess the extent of weathering in the river. The bivariate plot in Figure 27A reveals that a Na^+ vs. Cl^- ratio of 1 indicates silicate weathering or cation exchange. However, most of the seasonal river samples fall below the 1:1 trend line, where a marginal subgroup of river samples (8% during the dry season and 2% during the wet season) show Na^+ concentrations above the 1:1 stoichiometric ratio line, indicating a Na/Cl ratio greater than 1. This implies other Na^+-bearing salts dissolution or ion exchange influencing the river's Na^+ composition.

Elevated levels of Na^+ and Cl^- in natural water samples often indicate rock salt dissolution. However, in Figure 27A only one sample from each season had a Na^+/Cl^- ratio approximately equal to 1 and aligns on the 1:1 trendline, suggesting a marginal dominance of river Na^+ and Cl^- relative to silicate weathering, although both weathering processes were relatively low. Overall, 95% of river samples deviate below the 1:1 line, indicating chloride ion mobility is more dominant than sodium ions. This may be attributed to anthropogenic practices or naturally by the second form of ionic exchange.

Figure 27B shows the molar ratios of alkaline earth elements $(Ca^{2+}+ Mg^{2+})/HCO_3^-$. Approximately 81% of river samples have a molar ratio >0.5, aligning above the 2:1 trendline. This suggests that the river is supplied by an excess of alkaline earth's $Ca^{2+}+ Mg^{2+}$ contrary to HCO_3^-, revealing that $Ca^{2+}+ Mg^{2+}$ along the river network originates from additional sources with carbonate weathering being negligible. In contrast, approximately 19% of the river samples fall below the 2:1 line, indicating a significant excess of HCO_3^- over Ca^{2+} and Mg^{2+}, with a subsequent decline in Ca^{2+} and Mg^{2+}.

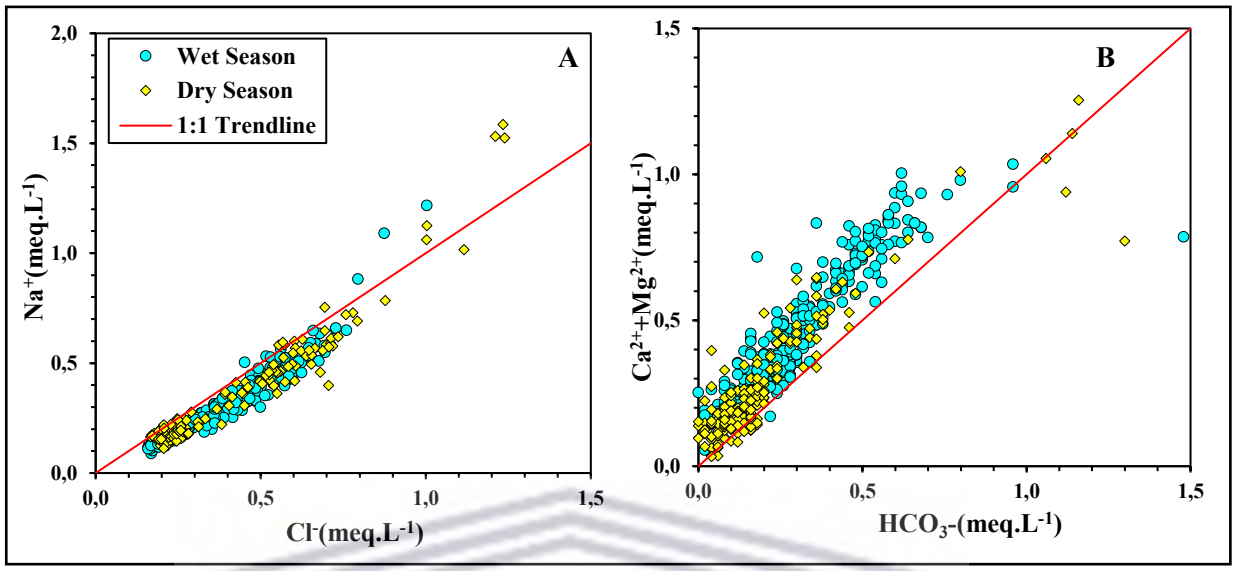

Figure 27: Biplots of normalized molar ratios of surface water in the Franschhoek-Paarl valley basin A) Na^+ vs. Cl^- B) $Ca^{2+}+Mg^{2+}$ vs. HCO_3^-.

B) Ion exchange

The occurrence of ion exchange in the river water was assessed using the bivariate plot in Figure 27. Among the total river samples, 3% show Na^+ enrichment in the Berg River waters, indicating the occurrence of cation exchange. The cation exchange ratio of $(Ca^{2+} + Mg^{2+})$ -$(HCO_3^- + SO_4^{2-})$ (meq. L^{-1}) versus $(Na^+ + K^+ - Cl^-)$ (meq. L^{-1}), as depicted in Figure 27, shows that the majority of river samples do not align along the y = -x line. Instead, they cluster to the zero margin of the x-axis. While some river water samples do show ion exchange behaviour by aligning along the trendline, the slope of the best-fit line is close to -1, indicating a moderate negative relationship (y = -0.81x + 0.03). This reveals that ion exchange is a marginal contributor governing the streamflow solutes.

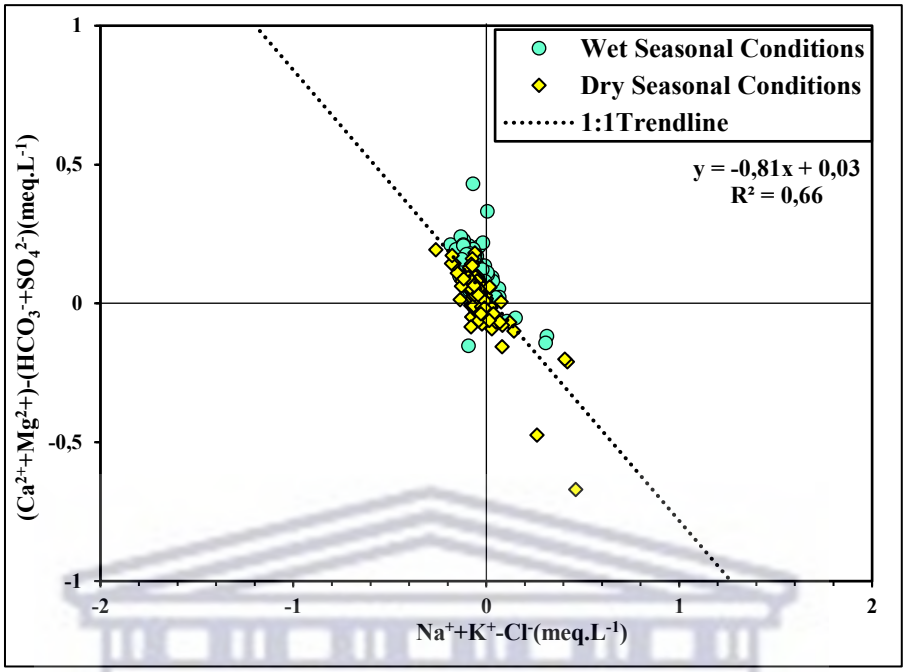

Figure 28: Biplot of surface water normalized molar ratios in the Franschhoek-Paarl valley.

5.2.5 River physicochemical correlation analysis

Table 15 displays the correlation matrix based on the significance of the level of 0.01 that illustrates various factors affecting the hydrochemical processes and relation between ions along the Berg River's flow path.

Cl^-, a prevalent soluble salt in the river, shows a positive correlation with Na^+(0.94), Ca^{2+} (0.64), Mg^{2+}(0.73), TDS (0.81), HCO_3^- (0.72), NO_3^- (0.64), SO_4^{2-} (0.92) and K^+ (0.78), implying they come from similar sources. This suggests the leaching of secondary salts, weathering of rock minerals, contamination through anthropogenic practices and reverse ion exchange. The strong positive correlation between Cl^- and Na^+ suggests that the river is recharged by rich NaCl water.

The use of fertilisers for agricultural practices in the valley is reflected by the strong positive correlation between SO_4^{2-} with Mg^{2+} (0.72) and K^+(0.80). NO_3^- has a positive moderate correlation with Mg^{2+}(0.61), Na^+ (0.60), HCO_3^- (0.61), K^+(0.72), Cl^-(0.64) and SO_4^{2-}(0.67), suggesting that river ions originate from similar sources signifying a significant agricultural input in the river. Ca^{2+} shows a strong positive correlation between, Mg^{2+}, and HCO_3^-, and a moderate correlation ($p<0.01$, $r=0.52$)

with Na^+ suggesting possible Ca/Na ion exchange. A positive, moderate, and statistically significant correlation ($r<0.67$) exists between SiO_2 and Ca^{2+}, K^+, HCO_3-, and SO_4^{2-}, suggesting a weathering signature of silicate minerals. The correlation between water temperature (T) and other parameters is negative and negligible, suggesting that temperature has an insignificant over the accumulation of river ions in the area. The analysis indicates a weak and negative correlation between elevation and the studied parameters, implying that elevation does not play a significant role in the accumulation and evolution of river ions. The correlation analysis indicates that various factors contribute to the hydrochemical evolution of river ions and may serve as potential sources for their presence.

Table 15: Pearson's correlation matrix of major river ions, 2020-2021 sampling.

	Ca^{2+}	Mg^{2+}	Na^+	K^+	HCO_3^-	SO_4^{2-}	Cl	SIO_2	NO_3^-	TDS	T	pH	Elevation
Ca^{2+}	1												
Mg^{2+}	0.78**	1											
Na^+	0.52**	0.61**	1										
K^+	0.68*	0.74*	0.66**	1									
HCO_3-	**0.88****	0.82**	0.71**	0.72**	1								
SO_4^{2-}	0.65**	0.72**	0.85**	0.80**	0.68**	1							
Cl^-	0.64**	0.73**	**0.94****	0.78**	0.72**	0.92**	1						
SIO_2	0.44**	0.50**	0.62**	0.59**	0.48**	0.67**	0.69**	1					
NO_3-	0.55**	0.61**	0.60**	0.72**	0.61**	0.67**	0.64**	0.48**	1				
TDS	0.63**	0.71**	0.69**	0.83**	0.67**	0.77**	0.81**	0.64**	0.66**	1			
T	-0.42**	-0.38**	-0.04	-0.11*	-0.31**	-0.16**	-0.11*	0.04	-0.08	-0.08	1		
pH	0.13**	0.18**	0.13**	0.24**	0.12**	0.24**	0.16**	0.18**	0.22**	0.20**	-0.08	1	
Elevation	-0.02	-0.09*	-0.04	-0.20**	0.04	-0.23**	-0.07	0.09*	-0.20**	-0.06	0.03	-0.34**	1

***Note Correlation is significant at **0.01 and *0.05 level, T=Temperature*

5.2.6 Hierarchical cluster analysis

The dendrogram displayed in Figure 29 consists of two clusters that classify the river sampling locations based on major cations, anions, and physical parameters. It depicts the relationship between the physicochemical attributes of the river water along the flow path during the sampling campaign.

Cluster A includes river samples from the middle to the lower region, affected by agricultural, industrial, and urban activities. Notable samples within this cluster include BGR10 to BGR12, G1H020, and tributaries G1H078 and Dwars 1. Among these, is the upper Franschhoek River (Frans 1 and G1H003), located at higher elevation, exhibits higher solute concentrations due to influences from the Langrug informal settlement and agricultural activities. This separation of the Franschhoek River indicates similar hydrochemical and environmental conditions as the river in the lower valley region. Samples within each reach tend to cluster together, suggesting variations in hydrochemical characteristics along specific river reaches.

Cluster B includes G1H077 (Berg River Dam outlet), BGR1 to BGR9, Mount Stream, and the Wemmershoek River, along with G1H080 (Wemmershoek Dam outlet) and Wem1, situated in the upper and middle regions. The first subgroup in Cluster B, located near the Berg River Dam, includes G1H077, BGR1, BGR2, Mount Stream (MS), and BG51-Riv, is evident of more pristine conditions with lower EC values and reduced mineralization due to reduced point and non-point source pollution influence.

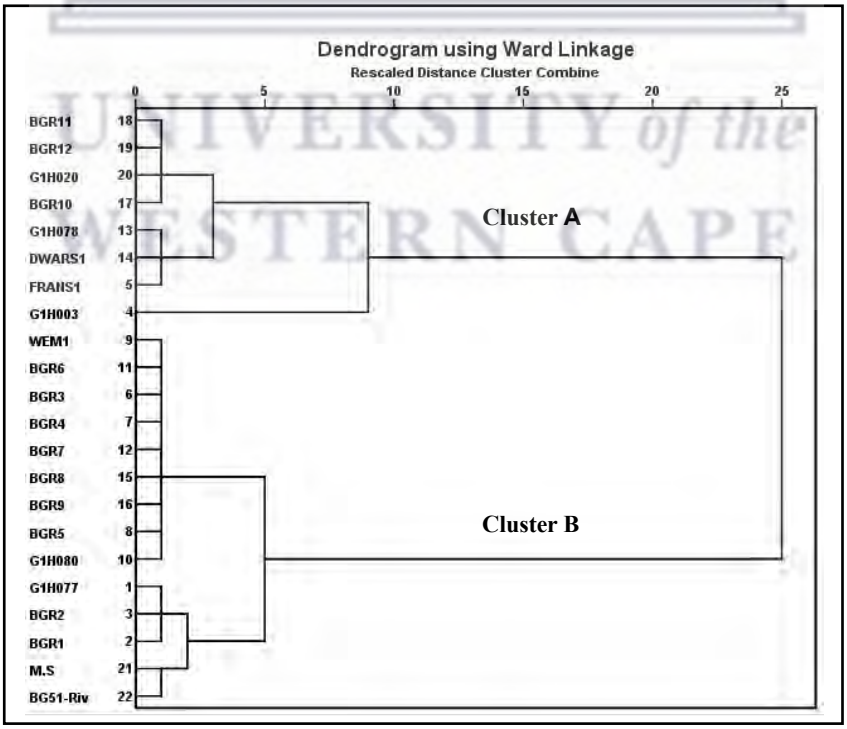

Figure 29: Dendrogram of the river physiochemical variations in the Franschhoek-Paarl valley.

5.2.7 Factor analysis

The multivariate statistical techniques, utilizing the correlation matrix, provide insights into the dominant land use sources controlling the river chemistry along the Berg River network. The results of Factor Analysis (FA) (Table 16) reveal the factors that influenced the chemical variability of water quality in the Berg River.

During the dry season, two factors accounted for 74.74% of the total variation in the river hydrochemical dataset. Factor 1 explained 65.94% of the variance and showed strong loadings (≥0.75) for Cl^-, SO_4^2, Na^+, TDS, K^+, SiO_2, NO_3^-, Ca^{2+}, HCO_3^- and Mg^{2+}, indicating a connection to rock weathering and water salinity. Factor 2 showed a strong correlation with water temperature and a moderate correlation with pH, suggesting the influence of evaporation, geogenic attributes, as well as non-point source pollution from agricultural activities and industrial effluents.

In the wet season, three factors explained 71.11% of the total variation. Factor 1 alone accounted for 53.99% of the variance and displayed strong correlations with Cl^-, SO_4^{2-}, Na^+, and moderate correlations with TDS, K^+, SiO_2, NO_3^-, HCO_3^- and Mg^{2+}. Factor 2 showed a moderate correlation between loadings of Ca^{2+}, HCO_3^- and Mg^{2+}, and a moderate correlation between TDS, K^+, NO_3^- and pH with Factor 3. These results suggest additional contributors to the variability in river quality, likely influenced by the movement of groundwater into the river. The seasonal analysis of Eigenvalues, factor loadings, and hydrochemical parameters indicates that Berg River's hydrochemistry is primarily influenced by hydrological variations and human activities, rather than geochemical processes.

Table 16: Seasonal PCA loadings for physiochemical parameters in Franschhoek-Paarl valley rivers

PARAMETERS	PRINCIPAL FACTOR COMPONENTS DRY SEASON		PRINCIPAL FACTOR COMPONENTS WET SEASON		
	PCA 1	PCA2	PCA 1	PCA2	PCA3
Cl^-	**0.953**	-0.127	**0.922**	0.217	0.179
SO_4^{2-}	**0.900**	-0.134	**0.854**	0.250	0.307
Na^+	**0.962**	-0.063	**0.924**	0.105	0.012
TDS	**0.970**	-0.042	0.540	0.345	0.600
K^+	**0.941**	-0.012	0.505	0.419	0.606
SiO_2	**0.793**	-0.010	0.738	0.001	0.177
NO_3-	**0.800**	0.039	0.552	0.190	0.500
Ph	0.110	0.715	0.109	-0.095	0.722
PO_4^{2-}	0.179	-0.238	0.005	0.030	0.435
WATER TEMPERATURE	0.018	**0.793**	0.093	**-0.830**	0.100
Ca^{2+}	**0.901**	-0.057	0.478	0.664	0.256
HCO_3-	**0.908**	0.058	0.626	0.643	0.130
Mg^{2+}	**0.926**	-0.031	0.521	0.616	0.355
TOTAL EIGENVALUE	9.23	1.23	7.56	1.30	1.10
% OF VARIANCE	65.94	8.80	53.99	9.27	7.85
% OF CUMULATIVE VARIANCE	65.94	74.74	53.99	63.26	71.11

**Bold values represent strong (≥0.75) and positive factor loadings*

5.3 Discussion: Evolutionary transport processes and mechanisms influencing the river solute composition

River solutes are influenced by geological and climatic mechanisms, including rock weathering, atmospheric precipitation, evaporation-crystallization, and human activities (Gao et al., 2009; Han et al., 2018). The geological layers in a catchment area release ions with positive or negative charges, influencing the Electrical Conductivity (EC) of water (Olson, 2012). Water mineralization, as indicated by EC, rises as water interacts with mineral-rich rocks, resulting in the dissolution of minerals and increased salt content (Song et al., 2006).

It was common for stream temperature to vary in space and time due to factors like source temperature, transport time to the stream, and variations in hydrological flow and air temperature (Angelier, 2003). Altitude, river vegetation, and channel width have also been found to influence stream temperature (Gregory et al., 1991). Water pH is crucial for determining water's chemical and biological nature, influenced by factors such as rainfall, climate, land cover, geological material, and hydrological properties (Bartram & Balance, 1996). Acidic streams have been observed in domains subjected to considerable humic acids (Lancaster & Allan, 1995). The Western Cape region's rivers and groundwater have reduced pH and an acidic nature due to the limited buffering capacity of TMG sandy soils and rich quartz sandstone aquifers, against the release of organic humic acid from indigenous fynbos vegetation (Struyf et al., 2012). Consequently, pH values increased spatially along the river flow path but revealed negligible temporal variation (Figure 23A).

The flow rate of water crucially affects river solute mineralization. Rapid flow restricts rock-water interaction, lowering mineral dissolution and EC levels. The surface and subsurface waters in the catchment were all below the background concentration range of TMG waters (<100mS/m ≡ <1000µS/cm), as reported by previous studies (Struyf et al., 2012; Duah, 2010; Madlala, 2015). However, groundwater in the middle to lower regions of the catchment showed elevated seasonal EC levels due to possible lithological changes and increased residence time compared to the river and precipitation. In contrast, groundwater in the upper region showed reduced EC levels and marginal ion concentrations, attributed to the

dominant inert quartz geology and lack of human influence, similar to the river in this region. The low salt concentrations of TMG waters in the elevated terrains were linked to the inert geological systems and precipitation of reduced ionic compositions that flushed out the salts in the system (Smart & Tredoux, 2002). During the dry season, the solute concentrations of the river in the upper region decreased (Figure 23B), indicating a dilution and mixing effect caused by the inflow of low ionic groundwater into the stream, along with increased dam release of recently stored water.

The Berg River and its tributaries form interconnected water bodies that channel watershed entities downstream. Multivariate statistical analysis revealed spatial variations in river solutes along the stream network, possibly influenced by land-based activities, suggesting diverse recharge processes at a basin scale. Consequently, the EC increased downstream from the Berg River dam, particularly in the middle to lower discharging region, possibly due to increased saline irrigation return flows and increased water abstraction. During the dry season, the Franschhoek and Dwars rivers showed the highest seasonal EC variations relative to the main stream, likely due to reduced flow and increased human activities. River samples clustered based on physicochemical association, reflecting varying levels of mineralization and human influence as the river flowed toward the outlet in Northern Paarl.

The Franschhoek River exhibited distinct hydrochemical characteristics, particularly elevated Total Dissolved Solids (TDS) concentrations that exceeded the global average TDS mean of 120 mg/L, in comparison to the other rivers in the catchment (Meybeck, 2003). Previous studies have observed extreme anthropogenic pollution in the Franschhoek River due to agricultural activities along the flow path and inflow from the contaminated Stiebeuel River, influenced by the lack of sanitation services in the Langrug informal settlement (Jackson et al., 2013; Madlala, 2015). Consequently, the tributary in the upper region displayed differences from other sites but showed closer similarities to river samples in the middle to lower valley region. The Franschhoek River during the dry season showed a loading of HCO_3^- irrespective of the absence of carbonate geological

material in the basin and the ion concentration may be influenced by discharged effluent from the contaminated Stiebeuel River or irrigation return flow.

In the dry season, the Berg River's EC decreased from the upper to lower stream reaches. However, heavy rains at the beginning of the wet season caused an increase in the river's EC, likely due to seasonal fluctuations in runoff. This increase may derive from accumulated salts precipitated during the dry season in the surface-weathering zone, combined with persistent evapotranspiration and low precipitation volumes, subsequently mobilized by the river during the wet season. Runoff from land-based activities like agriculture and industry may have contributed to the high salt accumulation in the Berg River during the wet season. Despite increased rainfall during the wet season, there was negligible dilution of river solutes, possibly because runoff was diverted into upper region dams, limiting the peak inflow of fresh recharge.

The correlation analysis revealed strong relationships among specific ions across the stream network, indicating similar sources of origin and transport mechanisms despite varying flow regimes and land-based activities. Nitrate (NO_3^-) and potassium (K^+) concentrations contributed less than 5% of the total anion concentrations, with relatively low K^+ concentrations in the main stream, suggesting minimal impact of agricultural runoff and wastewater effluents on the Berg River. Clark and Ractliffe (2007) reported similar reduced concentrations of K^+ ions in the Berg River, which are biologically active ions. Asare-Donkor et al. (2018) concluded that this reduction could be attributed to the affinity of the ions to be immobilized by sediment containing clay minerals, contributing to the formation of secondary minerals. A positive correlation was observed between K^+ and SO_4^{2-}, potentially attributed to the presence of K_2SO_4, a key potash fertilizer used in agriculture (Shuai et al., 2021). Plants absorbing K^+ could potentially lead to reduced K^+ concentration in river water. Increased flow during the wet season slightly enriched K^+ ions in the river, suggestive of the rapid leaching of ions from the topsoil horizons due to intensified storm and flow events (Godsey et al., 2009; Scholl et al., 2015).

The river solute behaviour under varying seasonal conditions revealed a similar seasonal variance. During the dry season, the river flow was dominated by Na-Cl and a mixed Ca-Mg-Cl water type, with reduced concentrations of Ca^{2+}, Mg^{2+} and HCO_3^-, emulating groundwater observations. Rainfall during both seasons had a dominant Ca-HCO_3 water type, which suggests that the water quality was more pristine. However, the wet season, the surface and groundwater entities revealed enrichment in Ca^{2+} and HCO_3^- ions. Water types along the flow path transitioned from Ca-HCO_3 to mixed Ca-Mg-Cl and Na-Cl. The prevalence of Ca-HCO_3 water type in the upper river network suggested the presence of fresh recharge water unaffected by water-rock interaction. Similar seasonal water types between surface and groundwater samples suggested groundwater processes likely controlled river solutes, governed by similar hydrological processes. The stream water represented a combination of rainfall and groundwater, indicating recharge from both precipitation and groundwater.

The river exhibited an abundance of alkaline earth elements (Ca^{2+}+ Mg^{2+}) compared to HCO_3^-, which suggested that additional sources of Ca^{2+}+ Mg^{2+} were balanced by Cl^- and SO_4^{2-} (Li et al., 2016). High molar ratios (>0.5) were observed in approximately 81% of river samples, and due to the valley being dominated by the TMG sandstone and inert quartz, the contribution of river Ca^{2+} and Mg^{2+} by carbonate dissolution was negligible. As a result, the primary source of these river ions possibly originated naturally through the geochemical process of reverse ion exchange, by the interaction of water and silicate minerals or runoff of agricultural fertilizers (Lakshmanan et al., 2003). According to Madlala (2015), river HCO_3^- may also be generated through the input of wastewater discharge and the use of limestone-based fertilizer concentrated in HCO_3^-. In a non-carbonate terrain, the formation of bicarbonate ions can occur organically through the mixing of precipitation and carbon dioxide within the soil or atmosphere, involving photosynthetic fixation in the root or soil zone (Singh et al., 2013).

The Gibbs and ion-ratio analyses of ion sources in the Berg River network revealed that solutes primarily derived from partial silicate weathering, indicating groundwater-river interaction. The analysis indicated precipitation resulted in marginal dilution of river solutes and decreased TDS values, influenced by a mixed

regulation mechanism involving both rainfall and water-rock interactions. Additionally, anthropogenic factors acted as a secondary influence on the ion compositions. The presence of Na^+ and Cl^- in both the river and groundwater indicated the chemical characteristics of the TMG formation, likely resulted from mature groundwater recharge and marine aerosol dissolution due to the basin's proximity to the sea. Reduced rainfall during the dry season, coupled with climatic processes such as reduced recharge and increased evaporation, could lead to higher concentrations of dissolved Na^+ in groundwater as less water was available to dilute the products of weathering (DeSimone et al., 2014). The strong positive correlation between Na^+ and Cl^- and the seasonal positive loading of Na^+, Cl^-, and SO_4^{2-} suggested a common source, potentially marine aerosols or salinization processes from geogenic and anthropogenic sources (De Clercq et al., 2009). This constant presence of Na^+ and Cl^- indicated that the river was consistently recharged with water rich in Na-Cl.

Na^+ enrichment in the river could be influenced by other sources, including ion exchange processes where Ca^{2+} is adsorbed onto clay minerals, resulting in the release of sodium ions, weathering of Na^+-dominated silicates, and anthropogenic practices (Meybeck, 1987; Cartwright and Weaver, 2005). Overall, during the dry and wet seasons, 9% and 2% of river samples, respectively, were distributed on the 1:1 trendline line; this indicated that the primary origin of Na^+ and Cl^- by rock-weathering, with a marginal influence of silicate weathering. Generally, 95% of the total river samples were distributed below the 1:1 line, indicating that the mobility of Cl^- was more prominent relative to Na^+. The excess Cl^- over Na^+ in the river could be attributed by various sources: Cl^- dissolution from marine aerosols and atmospheric dust in precipitation, silicate mineral weathering, anthropogenic inputs, and reverse ion exchange where Na^+ is replaced by Ca^{2+} (Singh et al., 2004; Al-Shaibani, 2008). Reverse ion exchange, highlighted in Figure 28, was a prominent seasonal form of ion-exchange process, suggesting that cation exchange was a marginal factor in controlling streamflow solutes.

The Franschhoek-Paarl valley, located approximately 60 km from the ocean, received significant Cl^- contributions through precipitation. However, the concentration of Cl^- in rainfall decreased with distance, resulting in a marginal

contribution (Chen et al., 2002). In the middle and lower valley regions dominated by agriculture, higher concentrations of Cl^- were observed, where a strong positive with HCO_3^- (0.72) and K^+(0.78) and moderate correlation with NO_3^- (0.64) was indicative of a possible anthropogenic signature (Eldaw et al., 2021). This could be attributed to the possible introduction of unnatural sources of Cl^- to the river such as irrigation return flow from farms, or the accumulation of organic matter through vegetable decomposition or animal manure. Similar observations of unnatural sources contributing to river Cl^- were noted in the semi-arid Cobras River sub-basin of North-eastern Brazil, where local farmers generated and distributed cattle fodder, leading to an increase in organic matter and identification of Cl^- as a source of river Cl^- (Lima et al., 2017).

5.4 Summary

In summary, the study found that the surface and subsurface movement of water, greatly influenced ion distribution in the Berg River watershed. Various factors, including rainfall patterns, water-rock interactions, and human activities, mobilized these ions, while human activities and land changes disrupted the natural balance of water flow and quality. The Berg River and its tributaries revealed varied solute distributions shaped by local activities. Electrical Conductivity (EC) increased downstream due to factors like increased irrigation runoff and water abstraction. During the dry season, Na^+ and Cl^- dominated both river and groundwater, while in the wet season Cl^- and HCO_3^- became the primary anions, and Na^+ and Ca^{2+} became the primary cations. The evolution of river ions was influenced by the mixing of varying water sources of varying salinities along the flow path governed by a mixed mechanism of rock and precipitation dominance, with anthropogenic activities as a secondary influence. The hydrochemical analysis provided valuable insights into the migration and evolution of river solutes in the Franschhoek-Paarl valley, highlighting heterogeneous hydrochemistry. The composition of river solutes was governed by different factors dependent on the source of recharge, climate, and the influence of anthropogenic and natural processes in the catchment area. Consequently, the rapid dissolution of solutes, influenced by both natural and human factors, threatens the river system's quality, emphasizing the need to manage excessive fertilization practices.

CHAPTER 6: Determining the seasonal river recharge two-end-member contribution, using $\delta^{18}O$ isotopic tracer

6.1 Introduction

This chapter presents the primary results of the study that investigated the end-member sources contributing to runoff in the Berg River at different temporal and spatial scales. The study utilized $\delta^{18}O$ as a tracer, which is an ideal constituent of the water molecule, as it is inert to water-rock interactions, has a unique fingerprint, and is linearly associated with $\delta^{2}H$. The total runoff contributions in the Franschhoek-Paarl valley were derived from two main sources: viz. precipitation and groundwater. To estimate the fractional contribution of these sources, a two-component isotope mass balance model was adopted.

6.2 Results derived by isotope mass balance mixing model.

Equations 6 and 7 define the average seasonal estimates (%) of precipitation and groundwater contributions to the total runoff in the Berg River stream network within the three different physiographic domains in the valley basin. The average values of the end-members, which are groundwater and precipitation during dry and wet seasonal conditions, are presented in Table 17 and illustrated in Figure 30. These values are utilized in the mixing model to determine the fractional contribution of each end-member source that affects the Berg River flow.

In Figure 30, the contribution of groundwater and precipitation varies spatially across the 30 km reach. The average estimates of groundwater and precipitation contribution to the Berg River flows during the dry season are 77.0% and 23.0% in the upper region below the Berg River Dam, 98.0% and 2.0% in the middle zone, and 83.0% and 17.0% in the urbanized lower region, respectively. Conversely, during the wet season, the contribution of groundwater and precipitation generates an estimate of 87.0% and 13.0% in the upper region, 47.0% and 53.0% in the middle region, and 70.0% and 30.0% in the lower region, respectively.

Table 17: Seasonal fractional contribution of groundwater and precipitation to the Berg River

Physiographic region	Component 1 δRain (‰)	Component 2 δGW (‰)	Mixture δRW (‰)	Mixing fraction f Rain (‰)	Mixing fraction f GW (‰)
Dry Seasonal Conditions					
Upper	-1.86	-3.68	-3.27	0.23	0.77
Middle	-1.86	-3.33	-3.31	0.02	0.98
Lower	-1.86	-3.40	-3.14	0.17	0.83
Wet Seasonal Conditions					
Upper	-3.51	-3.21	-3.25	0.13	0.87
Middle	-3.51	-2.84	-3.20	0.53	0.47
Lower	-3.51	-3.01	-3.16	0.30	0.70

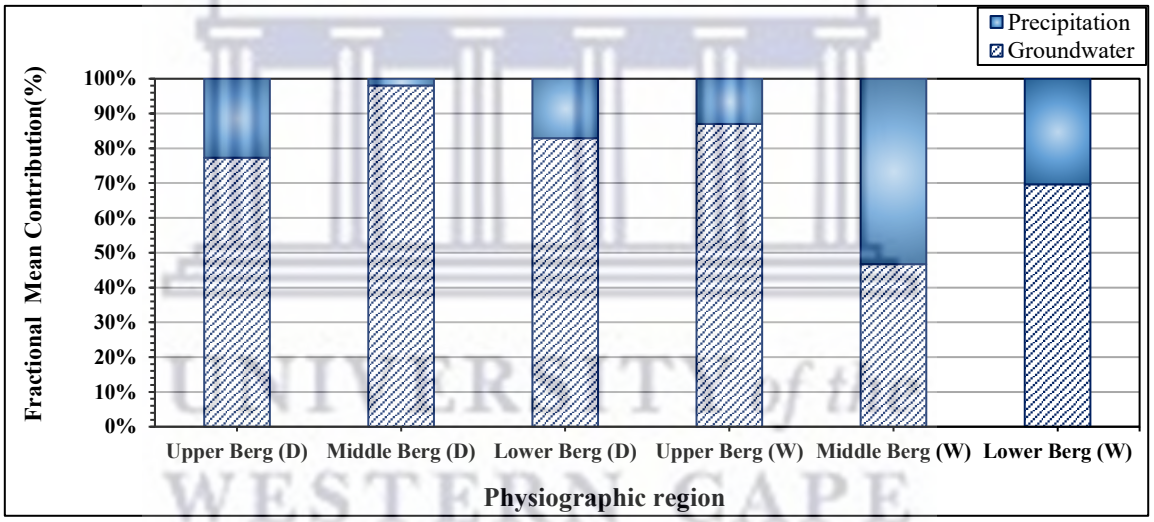

Figure 30: Fractional precipitation and groundwater contributions to the river

The results show that during the dry season, the primary source of recharge in the three physiographic domains is groundwater, with precipitation contributing a smaller percentage. However, in the wet season, the contribution of precipitation to the stream increases, even in the upper region where the contribution of precipitation is reduced. The use of the $\delta^{18}O$ tracer revealed that different rainfall patterns lead to varying levels of precipitation contribution to the stream. The proportionate contribution of precipitation increases during the wet season, and this relationship between rainfall amount and streamflow is explored in Figure 30 at the Berg River outlet hydrological station, G1H020, in the lower region. These findings

indicate that the response of the stream to rainfall is influenced by both the amount of rainfall and land cover entities.

Figure 31 illustrates the correlation between the daily average discharge (Q, m^3/sec) of the Berg River at the hydrological station G1H020 and the average event-based rainfall (mm/day) obtained from the Vinpro, Dwars, and La Motte meteorological stations. The dry season (November to March) is characterized by low flow (Q, m^3/sec) conditions and reduced rainfall distribution, leading to negligible streamflow variation. Conversely, the wet season is marked by larger and more rapid rainfall events, resulting in a gradual increase in rainfall amount (mm/day) and discharged flow. This trend is exemplified in June, when the discharge flow reached its peak at 339.97 m^3/sec, accompanied by a rise in the rainfall amount (mm). The annual correlation between the discharging flow at the Northern Paarl outlet and the valley's precipitation amount is weakly significant, with a correlation coefficient of 0.36 ($p<0.01$), suggesting that the natural streamflow has a dampening and delayed response to local precipitation.

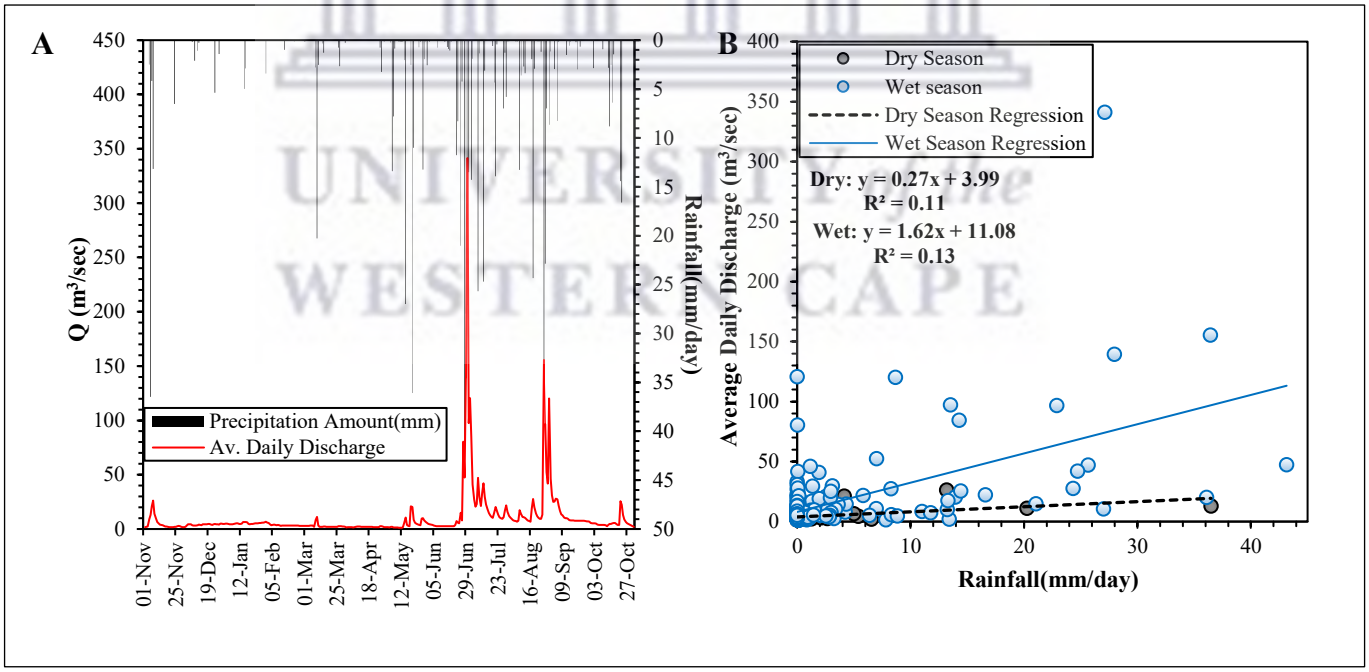

Figure 31: A) Streamflow discharge (Q, m^3/sec) and precipitation distribution from 2020-2021 in Northern Paarl. B) Seasonal correlation between precipitation and streamflow.

6.3 Discussion: Seasonal response of the Berg River to runoff components

Recharge plays a significant role in facilitating the interaction, migration, and chemical modifications of water among different water bodies (Shang et al., 2019). The variation in streamflow reflected the difference in runoff generated from precipitation and groundwater components in the catchment.

During the dry season, groundwater was found to be the major contributor to the upper (≈77%), middle (≈98%), and lower (≈82%) physiographic zones of the Berg River network. The total rainfall during this season was 207.9 mm, accounting for approximately 16% of the total flow. However, in the wet season, rapid events generated 597.14 mm of rainfall, contributing to approximately 31% of the total wet season flow, with dependence, on meteorological parameters and land use activities, which increased the runoff production. The temporal variability of the river isotopic signatures showed a stronger resemblance to the dry and wet season groundwater, indicating that the river was mainly recharged by groundwater flow paths.

It was revealed that groundwater was the dominant source of recharge to the Berg River in both the dry and wet seasons, despite an increase in the streamflow's responsiveness to precipitation during periods of higher rainfall. It was theoretically anticipated that groundwater would be the dominant source of recharge to the Berg River during the dry season, established by the hydraulic surface-groundwater connection and the permeable-fractured nature of the TMG lithology. In support, Madlala (2015) observed in the Upper Berg River Catchment, incorporating base flow separation techniques at three hydrological stations (G1H003-Franschhoek River, G1H077-Dam outlet, and G1H076-Dam inlet), that the mean BFI value between the 2012 to 2014 study period ranged between 7% to 8%. This indicated that the discharge from the subsurface dominated the streamflow throughout that period.

In the upper valley region dominated by the Berg and Wemmershoek dams, during the dry season, the groundwater contribution was relatively less compared to the

contribution during the wet seasonal conditions. Mohammed and Scholz (2016) studied the extent of the reservoir effect on the Lower Zab River flow, a tributary of the Tigris River in northeast Iraq, during the pre- and post-damming periods. Similarly, to the observation of the dry seasonal groundwater contribution to the Berg River, they observed a decrease in groundwater contribution during the post-damming period, which was attributed to the dam releasing water during dry seasonal conditions, and conversely reducing the baseflow index (BFI).

Mountainous terrains have been recognized as crucial sources of freshwater for lowland plains, functioning as "water towers" (Viviroli & Weingartner, 2008). This study, therefore, anticipated that in the upper region of the wet season, precipitation would dominate streamflow due to the recharge of mainstream and tributary headwaters originating in the Franschhoek and Drakenstein mountains and that the increased rainfall intensity in the mountain range typically increased the distribution of surface runoff, owing to the sharp incline. Studies by Chen et al. (2018) and Tao et al. (2021) similarly observed that surface runoff was more prominent in elevated inclined terrains, where high-intensity impact and minimal friction facilitated flow generation in the Loess Plateau, China. However, during high runoff events of the wet seasonal conditions in the Franschhoek-Paarl valley, surface water from the highlands drained into impoundments along the floodplain, increasing the lag time of direct recharge to the river downstream from the dam. This caused the Berg River in the upper region to become more reliant on groundwater during the wet season, indicating a disconnection between the headwater stream and the river below the dam. The dam release of water caused fluctuations in the river stage at hourly to seasonal scales, governing the movement of water and solute ions between the river and aquifer units (Harvey & Gooseff, 2015). This was supported by Madlala's (2015) assessment of baseflow contribution at the inlet and outlet stations of the Berg River Dam, which showed that the river disconnection by diversion and artificial storage of upstream river flow resulted in pressure on the major end-member components that generate streamflow. As river disconnection reduced flow below the dam, storage and constant water release increased the contribution of water originating from the subsurface.

The reduced precipitation contribution to the river of the upper region during the wet season might have been dampened by the presence of the Berg River and Wemmershoek dams, which prompted the downstream river to respond to heavy rainfall and runoff in a controlled manner while also promoting baseflow conditions. However, water released from the dams has a regulatory effect on downstream river flow, leading to a mixing effect that reduces the isotopic signature of rainfall in the river. This increased streamflow can also result in channel incision, enhancing connectivity with shallow bedrock groundwater aquifers. As a result, a distinct reservoir effect on groundwater contribution was observed during both the dry and wet seasons.

During the dry season, the Berg River was a critical water source for farms, vineyards, and recreational services dominant in the middle to lower valley regions required to sustain irrigation demands. This demand for water may have placed pressure on the river system and led to an increase in groundwater contribution as illustrated in Figure 30 to support the perennial flow of the main stream, as compared to the low inflow from tributaries. Hence, the abundance of crop cover in the region improved the soil structure and increased the root networks. As a result, the local precipitation recharge may have been intercepted by vegetation, infiltrated and stored in soil pores, or even within the prominent subsurface fracture network. This could have led to a higher proportion of groundwater discharging into the river. This delayed and dampened the response of the river to precipitation of the dry season, possibly causing isotope exchange along its flow path before reaching the river.

During the wet season, the groundwater contribution to the Berg River decreased in the middle to lower physiographic regions of the valley. This decrease may have been caused by active interflow, which was detected by the J2000iso model developed by Watson et al. (2022). The model revealed that surface runoff and interflow were prominent processes during the wet season, accounting for 30% to 36% of the total yearly stimulated flows in the catchment. These processes may have dampened the groundwater component in the stream. This increased surface runoff may have contributed to the rise in precipitation contribution and subsequent tributary inflow into the Berg River.

The influence of meteorological factors on streamflow during the wet and dry seasons was examined by analysing the correlation between precipitation amount and river discharge at the G1H020 outlet of the Berg River. This analysis allowed for assessing the river's dependency on precipitation input. Dawood et al. (2017) utilized a statistical methodology to analyse the variation and trend in rainfall in the Hindu Kush region and found a direct effect of rainfall trend on the discharging trend of the Swat River. Figure 31 showed a direct relationship between river water discharge (Q) and rainfall amount, as expected as high flow conditions in Western Cape rivers are typically associated with heavier rainfall events influenced by cold front systems.

The weak correlation ($r=0.36$, $p<0.01$) between annual flow and precipitation amount suggested that the Berg River's hydrological seasonal regime was marginally influenced by the temporal distribution of rainfall. This suggested that precipitation accounted for approximately 36% of the observed variability in annual streamflow and had marginal influence on the seasonal streamflow dynamics. Decreased rainfall events caused by climate variability would directly affect the groundwater and overall runoff necessary to sustain the river flow, which was crucial for supporting economic and ecological activities in the catchment. The wet season's linear regression slope was larger than the dry season's slope, indicating greater responsiveness of runoff during wet conditions to seasonal rainfall variations.

The study revealed that the groundwater responded rapidly to direct runoff within a short time frame, suggestive of a direct preferential pathway and a prominent hydrological connection between rainfall-impacted surfaces and the groundwater beneath. Consequently, precipitation recharge had a delayed effect on effectively recharging the river. The results indicated that subsurface flow paths and groundwater storage played a pivotal role in the seasonal hydrology of the Berg River in the Franschhoek-Paarl valley. The isotope mass balance analysis highlighted the influence of factors such as rainfall intensity, flow paths, and land cover on the stream's response to rainfall events and subsequent runoff changes.

During the wet season, the runoff generated from rainfall was more pronounced, and an increase in rainfall amount led to an increase in streamflow. However, reduced precipitation resulted in delayed recharge, and over-abstraction or pollution of groundwater sources that would indirectly impact the river resource. Reducing the quantity of water could lead to a depletion in quality, emphasizing the importance of sustainable groundwater resource management to maintain the health and functionality of the river ecosystem.

6.4 Summary

The results showed that groundwater was the primary source of discharge in both seasons, although there was an increase in the streamflow's responsiveness to precipitation during periods of higher rainfall. Land-based activities regulated the distribution and flow of runoff into the river system, while diversion and artificial storage of upstream river flow caused river disconnection and pressure on the major end-member components that generated streamflow. The study also found that the dams controlled downstream river flow and caused a mixing effect that reduced rainfall isotopic signature in the river below. However, uncertainties existed in estimating the contribution of groundwater and precipitation to streamflow, and the binary mixing model used was limited to average seasonal climatic conditions in a baseline period. The study concluded that groundwater was the primary component of runoff, and the seasonal rainfall distribution influenced changes in runoff in the Berg River.

CHAPTER 7: Conclusions and Recommendations

7.1 Conclusions

This study applied a quantitative research approach to characterize the streamflow regime of the Berg River in the Franschhoek-Paarl valley during the dry and wet seasons. The study employed three methods, including a mass balance model, stable isotopic analysis, and hydrochemical analysis, to achieve its objectives.

The **first objective** was to characterize the seasonal mechanisms regulating the isotopic composition of the river, groundwater and precipitation resources of the catchment area, using stable isotope techniques. The results showed that during both dry and wet seasons, the mixing of river water and groundwater was prevalent, with groundwater discharge dominating the streamflow during dry conditions. The isotopic signature of various water sources played a crucial role in identifying patterns of hydrological processes, including interactions between water sources, mixing, and recharge and discharge sources.

The statistical analysis of δ^2H and $\delta^{18}O$ isotopic compositions in precipitation showed that the valley's rainfall underwent isotopic enrichment during the dry season and depletion during the wet season. The river water showed a more depleted isotopic signature relative to the rainfall, indicating recharge from rainfall generated in the upper Franschhoek mountainous area and groundwater sources. However, the weak linear relationship between δ^2H and the altitude of the river water suggested that the river flow was marginally dependent on direct recharge from the valley's rainfall and more dependent on rainfall originating in the mountainous area of higher elevation, with groundwater discharge having a more prominent recharging influence.

The research question answered in the section was “what dominant processes are controlling the river stable isotopic composition in the valley?” The dominant processes controlling the river stable isotopic composition in the valley were isotopic exchange and modifications between varying water sources, which were affected by sub-cloud and moisture recycling from soil and open surface water sources governed by meteorological parameters. Overall, the groundwater and the

Berg River Dam, along with the Wemmershoek dam, maintained the homogenized isotopic nature of the river. Understanding the isotopic nature of the Berg River's sources of recharge, their mechanisms, and seasonal changes is crucial for managing and sustaining the river source for present and future needs in the valley basin.

The **second objective** of the study was to characterize the seasonal behaviour and sources of solutes in the Berg River network using hydrochemical techniques. Through multivariate statistical analysis, the river was divided into two distinct clusters along its flow path defined by the major cations, anions, and physical parameters. This revelation showed that the hydrochemical characteristics of the Franschhoek River in the upper region and Dwars River in the middle region, with increased loadings of Cl^- and HCO_3^-, had a distinct relation to the mainstream in the lower region of the valley. This indicated that the river solutes behaved differently at a spatial scale along the stream network. The analysis using PCA, Piper diagram, Gibbs diagram, and bivariate plots revealed a prevalent Na-Cl water type during the dry season, influenced by rock-water interactions. In the wet season, there was an increase in Ca^{2+} and HCO_3^-, indicating the dominance of Ca-HCO_3 and Ca-Mg-Cl water types. The absence of carbonate rocks in the valley suggested that the increase in ion concentrations resulted from natural geochemical processes such as reverse ion exchange and biogeochemical activities involving carbonic acid generation, in addition to runoff from anthropogenic sources.

The research question answered in the section was "how did hydrochemical processes control runoff ionic compositions during dry and wet seasonal conditions?" The Total Dissolved Solids (TDS) concentration in the Berg River remained relatively stable over time, with variations in discharge being more significant than variations in ion concentration between seasons. The composition of river solutes was influenced by factors such as recharge source, climate, and anthropogenic and natural processes in the catchment area. River ion concentrations were primarily regulated by a mixed mechanism of rock and precipitation dominance, with anthropogenic activities as a secondary influence. The dilution effect resulting from increased rainfall of low TDS concentration during the wet seasonal conditions was marginal in the river system, suggesting that the geological

characteristics of the catchment, leaching of salts, and runoff from land practices, masked the dilution signature of the precipitation component in the river.

The **third objective** of the study aimed to determine the relative contribution of the dominant sources recharging the Berg River during baseflow and wet seasonal conditions. To achieve this, the study employed an isotope mass balance mixing model that utilized the mean seasonal $\delta^{18}O$ isotopic values of surface runoff (precipitation) and baseflow (groundwater) resources. The model estimated the proportionate contribution of each source to the Berg River at a seasonal scale. Groundwater accounted for 77.0%, 98.0%, and 83.0% of the runoff in the respective regions. In the wet season, precipitation contributed to 13.0% in the upper region, 53.0% in the middle region, and 30.0% in the lower region, while groundwater accounted for 87.0%, 47.0%, and 70.0% of the runoff in those regions. The study found that during the dry season, groundwater was the dominant source of river replenishment, while precipitation contributed very little to surface runoff. However, during the wet season, an increase in rainfall led to an increase in surface runoff recharging the river, with precipitation contributing more to runoff compared to the dry season.

The research question answered in the section was "how did the contribution of groundwater and precipitation sources influence the runoff hydrology in the basin?" Groundwater was the dominant source of river replenishment during the dry season, while rainfall recharge increased surface runoff during the wet season. Groundwater discharge was revealed as an important seasonal component maintaining the constant flow of the river, while meteorological and land-based practices such as impoundments, storm water drains, vegetation, and irrigation return flow, spatiotemporally dampened the precipitation contributing signature in the river.

7.2 Recommendations

The seasonal connection between groundwater and surface water in the Franschhoek-Paarl valley increases the vulnerability of surface water bodies in the basin to changes in groundwater quantity and quality. Consequently, ineffective management of groundwater sources and rising climate variability could negatively affect the quantity and quality of water needed to maintain the flow of the Berg River.

Given the limitation of a one-year hydrological dataset, the ability to fully assess long-term hydrological processes in the basin using isotopic methods, it is recommended to expand the monitoring network within the valley basin. This can be achieved by increasing sampling frequency and exploring other water sources, particularly focusing on the interflow component, to gain deeper insights into subsurface flow paths that contribute to streamflow generation. Additionally, investigating intra-rainfall runoff events can offer significant insights into valley hydrological processes. Future studies should aim to include interflow to assess overall mixing rates of the river's three components (groundwater, rainfall, and interflow). Despite the potential benefits, interflow was excluded from this study due to constraints related to cost and time.

It would be useful to investigate the fractional contributions of different ion sources (i.e., anthropogenic input, atmospheric input, and rock weathering) to the river solutes, as this was not the focus of this study. This would provide a better understanding of the factors that influence the solute concentration in river sources and help with managing and controlling sources that contaminate the river.

References

Adams, K. M. (2011). *The inorganic pollution of the Franschhoek River: Sources and Solutions* (MSc. Thesis, University of the Western Cape, Cape Town, South Africa). Retrieved from: UWCscholar- ETD Repository.

Adar E.M., Dody, A., Geyh, M.A., Yair, A., Yakirevich, A., & Issar, A.S. (1998). Distribution of stable isotopes in arid storms I. Relation between the distribution of isotopic composition in rainfall and in the consequent runoff. *Hydrogeology Journal*, *6*(1), 50–65.

Adomako, D., Osae, S., Akiti, T. T., Faye, S., & Maloszewski, P. (2011). Geochemical and isotopic studies of groundwater conditions in the Densu River Basin of Ghana. *Environmental Earth Sciences*, *62*(5), 1071–1084.

Aggarwal, P.K., Romatschke, U., Araguas-Araguas, L., Belachew, D., Longstaffe, F.J., Berg, P., Schumacher, C., & Funk, A. (2016). Proportions of convective and stratiform precipitation revealed in water isotope ratios. *Nature Geoscience* ,*9*(8), 624–629.

Ahmed, K., Das, M., Islam, M.M., Akter, M.S., Islam, S. & Al-Mansur, M.A. (2011). Physico-Chemical Properties of Tannery and Textile Effluents and Surface Water of River Buriganga and Karnatoli, Bangladesh. *World Applied Sciences Journal*, *12*(2), 152-159.

Ala-aho P., Soulsby C., Pokrovsky O.S., Kirpotin S.N., Karlsson J., Serikova S., Vorobyev S.N., Manasypov, R.M., Loiko S. &Tetzlaff D. (2018). Using stable isotopes to assess surface water dynamics and hydrological connectivity in a high-latitude wetland and permafrost influenced landscape*, Journal of Hydrology*, *556*, 279-293.

Al-Shaibani, A.M. (2008). Hydrogeology and Hydrochemistry of a shallow Alluvial Aquifer, Western Saudi Arabia. *Hydrogeology Journal*, *16*(1), 155-165.

Angelier, E. (2003). *Ecology of streams and Rivers*. Science Publishers, Inc., Enfield.

Asare-Donkor, N.K., Ofosu, J. O., & Adimado, A. A. (2018). Hydrochemical characteristics of surface water and ecological risk assessment of sediments from settlements within the Birim River basin in Ghana. *Environmental Systems Research*, *7*(1), 1–17.

Asoka, A., Gleeson, T., Wada, Y., & Mishra, V. (2017). Relative contribution of monsoon precipitation and pumping to changes in groundwater storage in India. *Nature Geoscience*, *10*(2), 109–117.

Aza-Gnandji, C.D.R., Xu, Y., Raitt, L., & Levy, J. (2013). Salinity of irrigation water in the Philippi farming area of the Cape Flats, Cape Town, South Africa. *Water SA*, *39*(2).

Bartram, J., & Balance, R. (1996). Water Quality Monitoring: A Practical Guide to the Design and Implementation of Fresh Water Quality Studies and Monitoring Programmes, *United Nations Environment Programme; World Health Organization*. Chapman & Hall, London, 400.

Baskaran, S., Ransley, T., Brodie, R.S., & Baker, P. (2009*).* Investigating groundwater-river interactions using environmental tracers. *Australian Journal of Earth Sciences*, *56*(1), 13-19.

Belcher, T., Grobler, D., & Barrow, S. (2015*). Freshwater assessment for the proposed Boschendal Hydroelectric scheme* (Report No. P274). Blue Science. Retrieved from: http://www.cesnet.co.za/pubdocs/Boschendal%20hydroelectric%20scheme%20AJ0812_140/Appendix%20G%20_%20Freshwater%20Specialist%20Report.pdf

Bershaw, J., Penny, S.M., & Garzione, C.N. (2012). Stable isotopes of modern water across the Himalaya and eastern Tibetan Plateau: Implications for estimates of paleoelevation and paleoclimate. *Journal of Geophysical Research: Atmospheres*,*117*(D2).

Bhagat, H., Ghosh, P., & Kumar, D. (2021). Estimation of seasonal base flow contribution to a tropical river using stable isotope analysis. *Journal of Hydrology*, *601*,126661.

Birkel, C., Soulsby, C., & Tetzlaff, D. (2011). Modelling catchment-scale water storage dynamics: reconciling dynamic storage with tracer-inferred passive storage. *Hydrological Processes*, *25*(25), 3924–3936.

Bosman, A., & Basson, G. R., & Bosman, D.E., (2016). Hydraulic model study of the blowback behaviour of the bottom outlet of the Berg River Dam, South Africa. *Journal of the South African Institution of Civil Engineering*, *58*(1), 43-52.

Botai, C.M., Botai, J.O., & Adeola, A.M. (2018). Spatial distribution of temporal precipitation contrasts in South Africa. *South African Journal of Science, 114*(7-8), 70–78.

Botha, J.F., Verwey, J.P., van der Voort, I., Vivier, J.J., Buys, J., Colliston, W.P., & Loock, J.C., (1998). *Karoo Aquifers: Their Geology, Geometry and Physical Properties* (Report no 487/1/98). WRC. Retrieved from https://www.wrc.org.za/wp-content/uploads/mdocs/487-1-98.pdf

Bowen, G.J., Cai, Z., Fiorella, R.P., & Putman, A.L. (2019). Isotopes in the Water Cycle: Regional- to Global-Scale Patterns and Applications. *Annual Review of Earth and Planetary Sciences*, *47*(1), 453–479.

Bhatt, D., & Mall, R.K. (2015). Surface Water Resources, Climate Change and Simulation Modeling. *Aquatic Procedia*, *4*, 730–738.

Birkel, C., & Soulsby, C. (2015). Advancing tracer-aided rainfall-runoff modelling: a review of progress, problems and unrealised potential. *Hydrological Processes*, *29*(25), 5227–5240.

Bloomfield, J.P., Allen, D.J., & Griffiths, K.J. (2009). Examining geological controls on baseflow index (BFI) using regression analysis: An illustration from the Thames Basin, UK. *Journal of Hydrology*, *373*(1-2), 164–176.

Brunner, P., Simmons, C. T., Cook, P. G., & Therrien, R. (2010). Modeling Surface Water-Groundwater Interaction with MODFLOW: Some Considerations. *Ground Water*, *48*(2), 174–180.

Bunn, S.E., & Arthington, A.H. (2002). Basic principles and ecological consequences of altered flow regimes for aquatic biodiversity. *Environmental Management,30*(4), 492–507.

Cartwright, I., & Weaver, T.R. (2005). Hydrogeochemistry of the Goulburn Valley Region of the Murray Basin, Australia: implications for flow paths and resource vulnerability. *Hydrogeology Journal*, *13*(5-6), 752-770.

CapeNature. (2013). 2013/2014 Western Cape Landcover product [vector geospatial dataset] 2013. Retrieved from the SANBI Biodiversity GIS website: http://bgis.sanbi.org/SpatialDataset/Detail/610 [Accessed on 15 March 2020]

Chen, K., Meng, Y., Liu, G., Xia, C., Zhou, J., & Li, H. (2020). Identifying hydrological conditions of the Pihe River catchment in the Chengdu Plain based on spatio-temporal distribution of 2H and 18O. *Journal of Radioanalytical and Nuclear Chemistry*, *324*(3), 1125–1140.

Chen, J., Wang, F., Xia, X., & Zhang, L. (2002). Major Element chemistry of the Changjiang (Yangtze River). *Chemical Geology*, *187*(3-4), 231-255.

Chen Z., Nie Z.., Zhang G.., Wan L., & Shen J. (2006). Environmental isotopic study on the recharge and residence time of groundwater in the Heihe River Basin, northwestern China. *Hydrogeology Journal*, *14*(8),1635-1651.

Chen, H., Zhang, X., Abla, M., Lü, D., Yan, R., Ren, Q., Ren, Z., Yang, Y., Zhao, W., Lin, P., Liu, B., & Yang, X. (2018). Effects of vegetation and rainfall types on surface runoff and soil erosion on steep slopes on the Loess Plateau, China. *Catena*, *170*, 141–149.

Chen, F., Zhang, M., Argiriou, A.A., Wang, S., Ma, Q., Zhou, X., Wu, X., & Chen, J. (2021). Modeling Insights into Precipitation Deuterium Excess as an Indicator of Raindrop Evaporation in Lanzhou, China. *Water,13*(2), 193.

Chiverton, A., Hannaford, J., Holman, I., Corstanje, R., Prudhomme, C., Bloomfield, J., & Hess, T.M. (2014). Which catchment characteristics control the temporal dependence structure of daily river flows? *Hydrological Processes*, *29*(6), 1353–1369.

Clark, B.M., & Ractliffe, S.G. (Eds.). (2007). *Berg River Baseline Monitoring Programme Final Report* – Volume 5: Synthesis. No. P WMA 19/G10/00/ 2107. Pretoria, South Africa: Department of Water Affairs & Forestry (DAFF). Report No. P WMA 19/G10/00/ 2107 Retrieved from: http://www.fewlbnexus.uct.ac.za/sites/default/files/image_tool/images/91/DWAF%20VOLUME5_Synthesis_Berg%20River%20Baseline%20Monitoring%20Programme.pdf

Clow, D.W., & Mast, M. A. (2010). Mechanisms for chemostatic behavior in catchments: Implications for CO2 consumption by mineral weathering. *Chemical Geology*, *269*(1-2), 40–51.

Colvin, C., Riemann, K., Brown, C., Le Maitre, D., Mlisa, A., Blake, D., Aston, T., Maherry, A., & Engelbrecht, J., Pemberton, C., Magoba, R., Soltau, L., & Prinsloo, E. (2009). *Ecological and environmental impacts of large-scale groundwater development in the Table Mountain group (TMG) aquifer system* (Report no 1327/1/08). WRC. Retrieved from https://www.wrc.org.za/wp-content/uploads/mdocs/1327-1-081.pdf

Congjian, S., Weihong, L., Yaning, C., Xingong, L., & Yuhui, Y. (2015). Isotopic and hydrochemical composition of runoff in the Urumqi River, Tianshan Mountains, China. *Environmental Earth Sciences*, *74*(2), 1521–1537.

Coplen, T.B., & Wassenaar, L.I. (2015). LIMS for Lasers 2015 for achieving long-term accuracy and precision of δ^2H, $\delta^{17}O$, and$\delta^{18}O$ of waters using laser absorption spectrometry. *Rapid Communications in Mass Spectrometry*, *29*(22), 2122–2130.

Cosgrove, W.J., & Loucks, D.P. (2015). Water management: Current and future challenges and research directions. *Water Resources Research*,*51*(6), 4823-4839.

Clark, I. D., &Fritz, P. (1997). *Environmental Isotopes in Hydrogeology* (1st ed.). Boca Raton, Florida: Crc Press.

Craig, H. (1961). Isotope variations in Meteoric Waters. *Science*, *133*(3465),1702-1703.

Cullis, J.D.S., & Horn, A., Rossouw, N., Fisher-Jeffes, L., Kunneke, M.M., & Hoffman, W. (2019). Urbanisation, climate change and its impact on water quality and economic risks in a water-scarce and rapidly urbanising catchment: case study of the Berg River Catchment. *H2Open Journal*, *2*(1), 146–167.

Dansgaard, W. (1964). Stable isotopes in precipitation. *Tellus*, *16*(4), 436–468.

Darling, W.G, Bath, A.H, & Talbot, J.C. (2003). The O and H stable isotope composition of freshwaters in the British Isles.2. Surface waters and Groundwater. *Hydrology and Earth System Sciences*, *7*(2), 183-195.

Dawood, M., Mahmood, S., Rahman, G., & Rahman, A (2017). *Impact of Rainfall Fluctuation on River Discharge In Hindu Kush Region, Pakistan*. 10, 246-259.

De Clercq, W., Ellis, F., Fey, M., van Meirvenne, M., Engelbrecht, H.& de Smet, G. (2006). *Research on Berg River Management: Summary of Water Quality Information System and Soil Quality Studies*. Cape Town, South Africa: Water Research Commission. Report No 951/3/06. Available from https://www.wrc.org.za/wp-content/uploads/mdocs/951-3-06.pdf

De Clercq, W.P., Fey, M., & Jovanovic, N. (2009). *An overview of the salinization problem in the Berg River catchment (South Africa)*. Available from https://www.witpress.com/Secure/elibrary/papers/RAV09/RAV09033FU1.pdf

De Clercq, W., Jovanovic, N., & Fey, M. (2010). *Land use impacts on salinity in Berg River water Research on Berg River water management Report to the Water Research Commission*. Retrieved from https://www.wrc.org.za/wp-content/uploads/mdocs/1503-1-10%20Agricultural%20Water%20Management1.pdf

Degu, A.M., Hossain, F., Niyogi, D., Pielke, R., Shepherd, J.M., Voisin, N., & Chronis, T. (2011). The influence of large dams on surrounding climate and precipitation patterns. *Geophysical Research Letters*, 38(4).

Deng, H., Yang, S., Lian, E., Li, C., Yang, C., & Wei, H. (2016). Three Gorges Dam alters the Changjiang (Yangtze) river water cycle in the dry seasons: Evidence from H-O isotopes. *Science of the Total Environment*, *562*, 89–97.

Department of Water Affairs and Forestry (DAFF). (1996). *South African Water Quality Guidelines. Volume 4: Agricultural use: irrigation., s.l.* Pretoria, South Africa: Department of Water Affairs and Forestry (DAFF). Retrieved from: https://www.dws.gov.za/iwqs/wq_guide/edited/Pol_saWQguideFRESHIrrigationvol4.pdf

Department of Water Affairs and Forestry (DAFF). (2015). *Irrigation Strategy for South Africa*. Pretoria, South Africa: Department of Water Affairs and Forestry (DAFF). Available fromhttps://www.dws.gov.za/iwqs/wq_guide/edited/Pol_saWQguideFRESHIrrigationvol4.pdf

Dinçer, T., Payne, B.R., Florkowski T., Martinec, J., & Tongiorgi, E. (1970). Snowmelt runoff from measurements of tritium and oxygen-18. *Water Resources Research*, *6*(1), 110-124.

DWS. (2016). *National Groundwater Strategy*, Pretoria, South Africa: DWS. Retrieved from: https://www.dws.gov.za/Groundwater/Documents/NGS_Draft-Final_04012017.pdf

DWAF. (1996). *South African Water Quality Guidelines- Volume 1(2) Domestic Use*, Pretoria, South Africa: Department of Water Affairs and Forestry. Retrieved from https://www.dws.gov.za/Groundwater/documents/Pol_saWQguideFRESHDomesticusevol1.pdf

DeSimone, L. A., McMahon, P. B., & Rosen, M. R. (2014). Water Quality in Principal Aquifers of the United States, 1991-2010. In *U.S. Geological Survey Circular 1360.*

Diamond, R. (2014). *Stable isotope hydrology of the Table Mountain Group* (PhD. Thesis, University of Cape Town, Cape Town, South Africa). Retrieved from OpenUCT.

Duah AA. (2010). *Sustainable utilisation of Table Mountain group aquifers* (MSc. Thesis, University of the Western Cape, Cape Town South Africa). Retrieved from UWCScholar-ETD Repository.

Dube, K., Nhamo, G., & Chikodzi, D. (2022). Climate change-induced droughts and tourism: Impacts and responses of Western Cape province, South Africa. *Journal of Outdoor Recreation and Tourism*, *39*,100319.

Durowoju, O.S., Butler, M., Ekosse, G.-I. E., & Odiyo, J. O. (2019). Hydrochemical Processes and Isotopic Study of Geothermal Springs within Soutpansberg, Limpopo Province, South Africa. *Applied Sciences*, *9*(8), 1688

Eldaw, E., Huang, T., Mohamed, A. K., & Mahama, Y. (2021). Classification of groundwater suitability for irrigation purposes using a comprehensive approach based on the AHP and GIS techniques in North Kurdufan Province, Sudan. *Applied Water Science*, *11*(7).

Evans, J.D. (1996). *Straightforward Statistics for the Behavioural Sciences.* Pacific Grove, Brooks/Cole Publishing Co, Ca.

Fan, Y., Chen, Y., He, Q., Li, W., & Wang, Y. (2016). Isotope characterization of river waters and water source identification in an inland river, central Asia. *Water*, *8*(7), 286.

Fell, J. (2018). *An analysis of surface water from an informal settlement, Langrug, Franschhoek: down a slippery slope* (MSc. Thesis, University of Cape Town, Cape Town, South Africa). Retrieved from OpenUCT

Fetter, Jr., C.W. (2000). *Applied Hydrogeology* (4th ed.). Upper Saddle River, New Jersey: Prentice-Hall. Retrieved from https://arjzaidi.files.wordpress.com/2015/09/unimasr-com_e7ce669a880a8c4c70b4214641f93a02.pdf

Fey, M., V., & De Clercq, W., P. (2004). *Dryland Salinity impacts on Western Cape Rivers, Research on Berg River water management Report to the Water Research Commission*, Report No. 1342/1/04: Pretoria, South Africa. Retrieved from https://www.wrc.org.za/wp-content/uploads/mdocs/1342-1-041.pdf

Fidal, J., & Kjeldsen, T. R. (2020). Accounting for soil moisture in rainfall-runoff modelling of urban areas. *Journal of Hydrology*, *589*, 125122

Foks, S.S., Raffensperger, J.P., Penn, C.A., & Driscoll, J.M. (2019). Estimation of baseflow by Optimal Hydrograph Separation for the Conterminous United States and implications for national – extent hydrologic models. *Water*,*11*(8),1629.

Freeze, R.A., & Cherry, J.A. (1979). *Groundwate*r. Englewood Cliffs, New Jersey: Prentice –Hall, Inc.

Freshwater Research Unit. (2008). Environmental flow assessments for Rivers: Manual for the building block methodology (updated edition, Report No TT 354/08). In J.M., King, R.E., Tharme. & M.S., De Villiers (Eds.). Pretoria: Water Research Commission. Retrieved from http://www.wrc.org.za/wp-content/uploads/mdocs/TT%20354-CONSERVATION.pdf [Accessed 04 Feb 2020].

Friedman, I., Machta, L., & Soller, R. (1962). Water-vapor exchange between a water droplet and its environment. *Journal of Geophysical. Research, 67*(7), 2761-2766.

Fritz, K. M., Schofield, K. A., Alexander, L. C., McManus, M. G., Golden, H. E., Lane, C. R., Kepner, W. G., LeDuc, S. D., DeMeester, J. E., & Pollard, A. I. (2018). Physical and Chemical connectivity of streams and riparian wetlands to downstream waters: A synthesis. *JAWRA Journal of American Water Resources Association*, *54*(2), 323-345.

Gao, Q., Tao, Z., Huang, X., Nan, L., Yu, K., & Wang, Z. (2009). Chemical weathering and CO2 consumption in the Xijiang River basin, South China. *Geomorphology*, *106*(3-4), 324–332.

Gao, M., Chen, X., Wang, J., Soulsby, C., & Cheng, Q. (2021). Climate and landscape controls on spatio-temporal patterns of stream water stable isotopes in a large glacierized mountain basin on the Tibetan Plateau. *Science of the Total Environment*, *771*, 144799.

Gat, J., Mook, W., & Meijer, H. (2001). Environmental Isotopes in the Hydrological Cycle– Principles and Applications. In Mook, W.G. (Ed.) *Documents in Hydrology,2*(39). Retrieved from https://www.hydrology.nl/images/docs/ihp/Mook_II.pdf

Gat, J.R. (2010). *Isotope Hydrology: A Study of the Water Cycle – Series on Environmental Science and Management* (Vol.6). London: Imperial College Press. Retrieved from https://books-library.net/files/books-library.online-01311223Ls8W4.pdf

Gat, J. R., Bowser, C. J., & Kendall, C. (1994). The contribution of evaporation from the Great Lakes to the continental atmosphere: estimate based on stable isotope data. *Geophysical Research Letters*, *21*(7), 557–560.

Gautam, M. K., Lee, K.-S., Bong, Y.-S., Song, B.-Y., & Ryu, J.-S. (2017). Oxygen and hydrogen isotopic characterization of rainfall and throughfall in four South Korean cool temperate forests. *Hydrological Sciences Journal*, *62*(12), 2025–2034.

Geological Survey, 1984. 3318 Cape Town Geological Series 1:250000. Geological Survey. Geological-Survey. Retrieved from https://maps.geoscience.org.za/portal/home/item.html?id=cd4d3eac038c4cda9b8aa2aa885b8eea [Accessed: 12 May 2020].

Gonfiantini, R. (1986). Environmental isotopes in lake studies. In P. Fritz and J.C. Fontes (Eds.), *Handbook of Environmental Isotope Geochemistry, Vol. 2*. The Terrestrial Environment (pp. 113–186). Amsterdam: Elsevier.

Gibson, J. J., Price, J. S., Aravena, R., Fitzgerald, D. F., & Maloney, D. (2000). Runoff generation in a hypermaritime bog-forest upland. *Hydrological Processes*, *14*(15), 2711–2730.

Gibson, J. J., Aggarwal, P., Hogan, J., Kendall, C., Martinelli, L. A., Stichler, W., Rank, D., Goni, I., Choudhry, M., Gat, J., Bhattacharya, S., Sugimoto, A., Fekete, B., Pietroniro, A., Maurer, T., Panarello, H., Stone, D., Seyler, P., Maurice-Bourgoin, L., & Herczeg, A. (2002). Isotope studies in large river basins: A new global research focus. *Eos, Transactions American Geophysical Union*, *83*(52), 613.

Gibson, J. J., Yi, Y., & Birks, S. J. (2016). Isotope-based partitioning of streamflow in the oil sands region, northern Alberta: Towards a monitoring strategy for assessing flow sources and water quality controls. *Journal of Hydrology: Regional Studies*, *5*, 131–148.

Godsey, S. E., Kirchner, J. W., & Clow, D. W. (2009). Concentration-discharge relationships reflect chemostatic characteristics of US catchments. *Hydrological Processes*, *23*(13), 1844–1864.

Gou, J., Qu, S., Shi, P., Li, D., Chen, X., Wang, Y., Shan, S., & Si, W. (2018). Application of Stable Isotope Tracer to Study Runoff Generation during Different Types of Rainfall Events. *Water*, *10*(5), 538.

Gou, J., Qu, S., Guan, H., Shi, P., Su, Z., Lin, Z., Liu, J., & Zhu, J. (2022). Relationship between precipitation isotopic compositions and synoptic atmospheric circulation patterns in the lower reach of the Yangtze River. *Journal of Hydrology*, *605*, 127289.

Gregory, S. V., Swanson, F. J., McKee, W. A., & Cummins, K. W. (1991). An Ecosystem Perspective of Riparian Zones. *BioScience*, *41*(8), 540–551.

Guan, H., Zhang, X., Skrzypek, G., Sun, Z., & Xu, X. (2013). Deuterium excess variations of rainfall events in a coastal area of South Australia and its relationship with synoptic weather systems and atmospheric moisture sources. *Journal of Geophysical Research: Atmospheres*, *118*(2), 1123–1138.

Guo, X., Tian, L., Wang, L., Yu, W., & Qu, D. (2017). River recharge sources and the partitioning of catchment evapotranspiration fluxes as revealed by stable isotope signals in a typical high-elevation arid catchment. *Journal of Hydrology*, *549*, 616–630.

Gupta, S.K., & Deshpande, R. D. (2005). Groundwater isotopic investigations in India: What has been learned? *Current Science (Bangalore)*, *89*(5), 825–835.

Halenyane, K. (2017). *Investigating recharge rates in the Table Mountain Springs using oxygen and hydrogen isotopes*, *Master's Thesis*. Cape Town, South Africa: University of Cape Town.

Halder, J., Terzer, S., Wassenaar, L. I., Araguás-Araguás, L. J., & Aggarwal, P. K. (2015). The Global Network of Isotopes in Rivers (GNIR): integration of water isotopes in watershed observation and river research. *Hydrology and Earth System Sciences*, *19*(8), 3419–3431.

Han, T., Li, Y., Qin, J., Li, X., Yang, Q., & He, X. (2018). Hydrochemical Changes and Influencing Factors in the Dongkemadi Region, Tanggula Range, China. *Water*, *10*(12), 1856.

Harris, C., Burgers, C., Miller, J., & Rawoot, F. (2010). O-And H-Isotope record of Cape Town Rainfall from 1996-2008, and its application to recharge studies of Table Mountain Groundwater, South Africa. *South African Journal of Geology*, 113(1), 33-56.

Huang, J., Zhan, J., Yan, H., Wu, F., & Deng, X. (2013). Evaluation of the Impacts of Land Use on Water Quality: A Case Study in The Chaohu Lake Basin. *The Scientific World Journal*, *2013*, 1–7.

Hounslow, A.W. (1995). *Water Quality Data: Analysis and Interpretation* (1st ed.). Boca Raton, Florida: CRC Press.

Huziy, O., & Sushama, L. (2016). Impact of lake–river connectivity and interflow on the Canadian RCM simulated regional climate and hydrology for Northeast Canada. *Climate Dynamics*, *48*(3-4), 709–725.

Hughes, D.A (2010). Unsaturated zone fracture flow contributions to streamflow: evidence for the process in South Africa and its importance. *Hydrological Processes*, *24*(6), 767–774.

IAEA/GNIP. *Precipitation Sampling Guide*. Vienna, Austria: International Atomic Energy Agency. (2014). Retrieved from: http://wwwnaweb.iaea.org/napc/ih/documents/other/gnip_manual_v2.02_en_hq.pdf [Accessed 5 March 2020].

IAEA/WMO. (2021). *The Global Network of Isotopes in Precipitation*, [Data file]. The GNIP Database. Retrieved from: https://nucleus.iaea.org/wiser. [Accessed: 12 May 2021].

Jackson, V. A., Paulse, A. N., Odendaal, J. P., & Khan, W. (2013). Identification of Point Sources of Metal Pollution in the Berg River, Western Cape, South Africa. *Water, Air, & Soil Pollution*, *224*(3).

Jankowski, J., Acworth, R., I, & Shekarforoush, S. (1998). Reverse ion-exchange in deeply weathered porphyritic dacite fractured aquifer system, Yass, New South Wales, Austria. In. Arehart G., & Hulston J (Eds.), *Proceedings of 9th international symposium on water–rock interaction*,243–246.

Jasechko, S. (2019). Global Isotope Hydrogeology—Review. *Reviews of Geophysics*, *57*(3), 835–965.

Jiang, R., Bao, Y., Shui, Y., Wang, Y., Hu, M., Cheng, Y., Cai, A., Du, P., & Ye, Z. (2018). Spatio-Temporal Variations of the Stable H-O Isotopes and Characterization of Mixing Processes between the Mainstream and Tributary of the Three Gorges Reservoir. *Water*, *10*(5), 563.

Jiang, Y., Gui, H., Yu, H., Wang, M., Fang, H., Wang, C., Chen, C., Zhang, Y., & Huang, Y. (2020). Hydrochemical Characteristics and Water Quality Evaluation of Rivers in Different Regions of Cities: A Case Study of Suzhou City in Northern Anhui Province, China. *Water*, *12*(4), 950.

Jódar, J., Custodio, E., Liotta, M., Lambán, L. J., Herrera, C., Martos-Rosillo, S., Sapriza, G., & Rigo, T. (2016). Correlation of the seasonal isotopic amplitude of precipitation with annual evaporation and altitude in alpine regions. *Science of the Total Environment*, *550*, 27–37.

Jung, H., Koh, D.C., Kim, Y.S., Jeen, S-W., & Lee, J. (2020). Stable isotopes of water and nitrate for the identification of groundwater flowpaths: A review, *Water*,*12* (1), 138.

Jung, Y.-Y., Koh, D.-C., Shin, W.-J., Kwon, H.-I., Oh, Y.-H., & Lee, K.-S. (2021). Assessing seasonal variations in water sources of streamflow in a temperate mesoscale catchment with granitic bedrocks using hydrochemistry and stable isotopes. *Journal of Hydrology: Regional Studies*, *38*, 100940.

Kendall, C., & Coplen, T. B. (2001). Distribution of oxygen-18 and deuterium in river waters across the United States. *Hydrological Processes*, *15*(7), 1363–1393.

Kendall, C. & Caldwell, E. (1998). Chapter 2-Fundamentals of Isotope Geochemistry. In C. Kendall. & J.J. McDonnell (Eds.), *Isotope tracers in catchment hydrology* (pp.51-86). Amsterdam: Elsevier Science B.V. Retrieved from https://www.semanticscholar.org/paper/Fundamentals-of-Isotope-Geochemistry-Kendall-Caldwell/9d130536a43d5de07a1aaefebcee0bfd45b984bf

Khatri, N., & Tyagi, S. (2014). Influences of natural and anthropogenic factors on surface and groundwater quality in rural and urban areas. *Frontiers in Life Science*, *8*(1), 23–39.

Klaus, J., & McDonnell, J. J. (2013). Hydrograph separation using stable isotopes: Review and evaluation. *Journal of Hydrology*, *505*, 47–64.

Kondolf, G. M., Boulton, A. J., O'Daniel, S., Poole, G. C., Rahel, F. J., Stanley, E. H., Wohl, E., Bång, A., Carlstrom, J., Cristoni, C., Huber, H., Koljonen, S., Louhi, P., & Nakamura, K. (2006). Process-Based Ecological River Restoration: Visualizing Three-Dimensional Connectivity and Dynamic Vectors to Recover Lost Linkages. *Ecology and Society*, *11*(2).

Krishan, G., Kumar, B., Sudarsan, N., Rao, M. S., Ghosh, N. C., Taloor, A. K., Bhattacharya, P., Singh, S., Kumar, C. P., Sharma, A., Jain, S. K., Sidhu, B. S., Kumar, S., & Vasisht, R. (2021). Isotopes (δ18O, δD and 3H) variations in groundwater with emphasis on salinization in the state of Punjab, India. *Science of the Total Environment*, *789*, 148051.

Kumar, A., Sanyal, P., & Agrawal, S. (2019). Spatial distribution of $\delta^{18}O$ values of water in the Ganga River basin: Insight into the hydrological processes. *Journal of Hydrology*, *571*, 225–234.

Lagura, C. F., & Urbino, G.A. (2011). Liquid water isotope analyser (LWIA) equipment and method validation and its application to hydrology. Philippines: Integrated Chemists of the Philippines.

Lakhraj-Govender, R., & Grab, S. W. (2019). Rainfall and river flow trends for the Western Cape Province, South Africa. *South African Journal of Science*, *115*(9/10).

Lakshmanan, E., Kannan, R., & Senthil Kumar, M. (2003). Major ion chemistry and identification of hydrogeochemical processes of ground water in a part of Kancheepuram district, Tamil Nadu, India. *Environmental Geosciences*, *10*(4), 157–166.

Lambs, L., Gurumurthy, G. P., & Balakrishna, K. (2011). Tracing the sources of water using stable isotopes: first results along the Mangalore-Udupi region, south-west coast of India. *Rapid Communications in Mass Spectrometry*, *25*(19), 2769–2776.

Lancaster, J., & Allan, J.D. (1995). Stream ecology: Structure and Function of running waters. *Journal of ecology*, *83*(4),735.

Le Maitre, D. C., & Colvin, C. A. (2008). Assessment of the contribution of groundwater discharges to rivers using monthly flow statistics and flow seasonality. *Water SA*, *34*(5), 549.

Levy, J., & Xu, Y. (2011). Review: Groundwater management and groundwater/surface-water interaction in the context of South African water policy. *Hydrogeology Journal*, *20*(2), 205–226.

Li, S.-L., Yue, F.-J., Liu, C.-Q., Ding, H., Zhao, Z.-Q., & Li, X. (2014). The O and H isotope characteristics of water from major rivers in China. *Chinese Journal of Geochemistry*, *34*(1), 28–37.

Li, C., Yang, S., Lian, E., Yang, C., Deng, K., & Liu, Z. (2016). Damming effect on the Changjiang (Yangtze River) river water cycle based on stable hydrogen and oxygen isotopic records. *Journal of Geochemical Exploration*, *165*, 125–133.

Li, Z., Lin, X., Xiang, W., Chen, X., & Huang, T. (2017). Stable isotope tracing of headwater sources in a river on China's Loess Plateau. *Hydrological Sciences Journal*, *62*(13), 2150–2159.

Li, Z., Coles, A. E., & Xiao, J. (2019). Groundwater and streamflow sources in China's Loess Plateau on catchment scale. *Catena, 181*, 104075.

Li, J., Wang, W., Wang, D., Li, J., & Dong, J. (2020). Hydrochemical and Stable Isotope Characteristics of Lake Water and Groundwater in the Beiluhe Basin, Qinghai–Tibet Plateau. *Water*, *12*(8), 2269.

Li, L., Stewart, B., Zhi, W., Sadayappan, K., Ramesh, S., Kerins, D., Sterle, G., Harpold, A., & Perdrial, J. (2022). Climate Controls on River Chemistry. *Earth's Future*, *10*(6).

Lintern, A., Webb, J. A., Ryu, D., Liu, S., Bende-Michl, U., Waters, D., Leahy, P., Wilson, P., & Western, A. W. (2017). Key factors influencing differences in stream water quality across space. *Wiley Interdisciplinary Reviews: Water*, *5*(1), e1260.

Liu, C.-W., Lin, K.-H., & Kuo, Y.-M. (2003). Application of factor analysis in the assessment of groundwater quality in a blackfoot disease area in Taiwan. *Science of the Total Environment*, *313*(1-3), 77–89.

Liu, Z., Tian, L., Yao, T., & Yu, W. (2008). Seasonal deuterium excess in Nagqu precipitation: influence of moisture transport and recycling in the middle of Tibetan Plateau. *Environmental Geology*, *55*(7), 1501–1506.

Liu, F., Hunsaker, C., & Bales, R. C. (2013). Controls of streamflow generation in small catchments across the snow-rain transition in the Southern Sierra Nevada, California. *Hydrological Processes*, *27*(14), 1959–1972.

Liu, Y., Yamanaka, T., Zhou, X., Tian, F., & Ma, W. (2014). Combined use of tracer approach and numerical simulation to estimate groundwater recharge in an alluvial aquifer system: A case study of Nasunogahara area, central Japan. *Journal of Hydrology*, *519*, 833–847.

Liu, Q., Tian, L. D., Wang, J. L., Wen, R., Weng, Y. B., Shen, Y. P., Vladislav, M., & Kanaev, E. (2015). A study of longitudinal and altitudinal variations in surface water stable isotopes in West Pamir, Tajikistan. *Atmospheric Research*, *153*, 10–18.

Liu, J., Gao, Z., Wang, M., Li, Y., Yu, C., Shi, M., Zhang, H., & Ma, Y. (2019). Hydrochemical and isotopic characteristics of surface water in the Lhasa River basin. *Arabian Journal of Geosciences*, *12*(16).

Machavaram, M. V., Whittemore, D. O., Conrad, M. E., & Miller, N. L. (2006). Precipitation induced streamflow: An event-based chemical and isotopic study of a small stream in the Great Plains region of the USA. *Journal of Hydrology*, *330*(3-4), 470–480.

Madlala, T.E. (2015). *Determination of groundwater-surface water interaction, upper Berg River catchment, South Africa* (MSc. Thesis, University of the Western Cape, Cape Town, South Africa). Retrieved from: UWCscholar-ETD Repository

Meybeck, M. (1987). Global chemical weathering of surficial rocks estimated from river dissolved loads. *American Journal of Science*, *287*(5), 401–428.

Meybeck, M. (2003). Global Occurrence of Major Elements in Rivers. *Treatise on Geochemistry*, *5*, 605.

McFarlane, D., George, R. P., Barrett-Lennard, E. G., & Mat Gilfedder. (2016). Salinity in Dryland Agricultural Systems: Challenges and Opportunities. *Springer EBooks*, 521–547.

McGuire, K. J., McDonnell, J. J., Weiler, M., Kendall, C., McGlynn, B. L., Welker, J. M., & Seibert, J. (2005). The role of topography on catchment-scale water residence time. *Water Resources Research*, *41*(5).

McGuire, K. J., & McDonnell, J. J. (2006). A review and evaluation of catchment transit time modeling. *Journal of Hydrology*, *330*(3-4), 543–563.

Miller, O. L., Miller, M. P., Longley, P. C., Alder, J. R., Bearup, L. A., Pruitt, T., Jones, D. K., Putman, A. L., Rumsey, C. A., & McKinney, T. (2021). How Will Baseflow Respond to Climate Change in the Upper Colorado River Basin? *Geophysical Research Letters*, *48*(22).

Miller, M. P., Susong, D. D., Shope, C. L., Heilweil, V. M., & Stolp, B. J. (2014). Continuous estimation of baseflow in snowmelt-dominated streams and rivers in the Upper Colorado River Basin: A chemical hydrograph separation approach. *Water Resources Research*, *50*(8), 6986–6999.

Milner, V. S., Yarnell, S. M., & Peek, R. A. (2019). The ecological importance of unregulated tributaries to macroinvertebrate diversity and community composition in a regulated river. *Hydrobiologia*, *829*(1), 291–305.

Milliman J.D., & Farnsworth, K.L. (2011). *River Discharge to the Coastal Ocean: A Global synthesis*, pp. 142-144.Cambridge, Cambridge University Press. Retrieved from: http://assets.cambridge.org/97805218/79873/frontmatter/9780521879873_frontmatter.pdf

Mitchell, M. G. E., Bennett, E. M., & Gonzalez, A. (2013). Linking Landscape Connectivity and Ecosystem Service Provision: Current Knowledge and Research Gaps. *Ecosystems*, *16*(5), 894–908.

Modie, L. T., Kenabatho, P. K., Stephens, M., & Mosekiemang, T. (2022). Investigating groundwater and surface water interactions using stable isotopes and hydrochemistry in the Notwane River Catchment, South East Botswana. *Journal of Hydrology: Regional Studies*, *40*, 101014.

Mohammed, R., & Scholz, M. (2016). Impact of climate variability and streamflow alteration on groundwater contribution to the base flow of the Lower Zab River (Iran and Iraq). *Environmental Earth Sciences*, *75*(21).

Mokua, R. A., Glenday, J., Nel, J., & Butler, M. (2020). Combined use of stable isotopes and hydrochemical characteristics to determine streamflow sources in the Jonkershoek catchment, South Africa. *Isotopes in Environmental and Health Studies*, *56*(3), 238–259.

Mul, M. L., Mutiibwa, R. K., Uhlenbrook, S., & Savenije, H. H. G. (2008). Hydrograph separation using hydrochemical tracers in the Makanya catchment, Tanzania. *Physics and Chemistry of the Earth, Parts A/B/C*, *33*(1-2), 151–156.

Munyaneza, O., Wenninger, J., & Uhlenbrook, S. (2012). Identification of runoff generation processes using hydrometric and tracer methods in a meso-scale catchment in Rwanda. *Hydrology and Earth System Sciences*, *16*(7), 1991–2004.

Murray, K., & Wade, P. (1996). Checking anion-cation charge balance of water quality analyses: Limitations of the traditional method for non-potable waters. *Water SA,22*(1), 27–32.

Naicker, S., & Demlie, M. (2013). Environmental isotopic and hydrochemical characteristics of groundwater from the Sandspruit Catchment, Berg River Basin, South Africa. *Water Science and Technology*, *69*(3), 601–611.

Nilsson, C., & Renöfält, B. M. (2008). Linking Flow Regime and Water Quality in Rivers: a Challenge to Adaptive Catchment Management. *Ecology and Society*, *13*(2).

O' Keeffe, J. (1986). *Ecological research on South African rivers-a preliminary synthesis*. National Scientific Programmes Unit: CSIR., Report No.121. Retrieved from http://hdl.handle.net/10204/2359.

Olson, J.R. (2012). *The Influence of Geology and Other Environmental Factors on Stream Water Chemistry and Benthic Invertebrate Assemblages* (PhD Thesis, Utah State University, Utah). Retrieved from: All Graduate Theses and Dissertations (1327).

Ogrinc, N., Kocman, D., Miljević, N., Vreča, P., Vrzel, J., & Povinec, P. (2018). Distribution of H and O stable isotopes in the surface waters of the Sava River, the major tributary of the Danube River. *Journal of Hydrology*, *565*, 365–373.

Peng, H., Mayer, B., Harris, S., & Krouse, H. R. (2007). The influence of below-cloud secondary effects on the stable isotope composition of hydrogen and oxygen in precipitation at Calgary, Alberta, Canada. *Tellus B: Chemical and Physical Meteorology*, *59*(4), 698-704.

Peng, T.-R., Wang, C.-H., Huang, C.-C., Fei, L.-Y., Chen, C.-T. A., & Hwong, J.-L. (2010). Stable isotopic characteristic of Taiwan's precipitation: A case study of western Pacific monsoon region. *Earth and Planetary Science Letters*, *289*(3-4), 357–366.

Peng, T.-R., Liu, K.-K., Wang, C.-H., & Chuang, K.-H. (2011). A water isotope approach to assessing moisture recycling in the island-based precipitation of Taiwan: A case study in the western Pacific. *Water Resources Research*, *47*(8).

Pietersen, K., & Parsons, R. (2002). *A synthesis of the hydrogeology of the Table Mountain Group: formation of a research strategy*. Water Research Commission. Retrieved from https://www.wrc.org.za/wp-content/uploads/mdocs/TT-158-01.pdf

Pinder, G. F., & Jones, J. F. (1969). Determination of the ground-water component of peak discharge from the chemistry of total runoff. *Water Resources Research*, *5*(2), 438–445.

Piper, A. M. (1944). A graphic procedure in the geochemical interpretation of water-analyses. *Transactions, American Geophysical Union*, *25*(6), 914-928.

Poage, M.A. and Chamberlain, C.P. (2001). Empirical relationships between elevation and the stable isotope composition of precipitation and surface waters: considerations for studies of paleoelevation change. *American Journal of Science*, *301*(1), 1–15.

Postel, S. L. (1998). Water for Food Production: Will There Be Enough in 2025? *BioScience*, *48*(8), 629–637.

Price, K. (2011). Effects of watershed topography, soils, land use, and climate on baseflow hydrology in humid regions: A review. *Progress in Physical Geography*, *35*(4), 465–492.

Ractliffe, S. G. (2009). The hydrological characteristics of the Berg River. *Transactions of the Royal Society of South Africa*, *64*(2), 96–118.

Trenberth, K.E., Jones, P.D., Ambenje, P., Bojariu, R., Easterling, D., Klein Tank, A., Parker, D., Rahimzadeh, F., Renwick, J.A., Rusticucci, M., Soden, B. and Zhai, P. (2007) Observations: Surface and Atmospheric Climate Change. In: Solomon, S., Qin, D., Manning, M., Chen, Z., Marquis, M., Averyt, K.B., Tignor, M. and Miller, H.L., (Eds.), *Climate Change 2007: The Physical Science Basis. Contribution of Working Group I to the Fourth Assessment Report of the Intergovernmental Panel on Climate Change*, Cambridge University Press, Cambridge, UK and New York, USA.

Rossouw, N. (2008). *Berg River Dam: Designed with Rivers in Mind*. The water wheel, July/August.Water Research Commission. Retrieved from

https://www.wrc.org.za/wpcontent/uploads/mdocs/WaterWheel_2008_04_12%20Berg%20p%2033-37.pdf

Rozanski, K., Araguás-Araguás, L., & Gonfiantini, R. (1993). Isotopic Patterns in Modern Global Precipitation. *Climate Change in Continental Isotopic Records*, 1–36. Retrieved from https://www.researchgate.net/profile/Roberto_Gonfiantini/publication/257359208_Isotopic_patterns_in_Global_Precipitation/links/02e7e53c68ce1ca0e7000000/Isotopic-patterns-in-Global-Precipitation.pdf

Saifullah, M., Li, Z., Li, Q., Hashim, S., & Zaman, M. (2015). Quantifying the Hydrological Response to Water Conservation Measures and Climatic Variability in the Yihe River Basin, China. *Outlook on Agriculture*, *44*(4), 273–282

Scheepers, R., & Armstrong, R. A. (2002). New U/Pb SHRIMP zircon ages of the Cape Granite Suite; implications for the magmatic evolution of the Saldania Belt. *South African Journal of Geology*, *105*(3), 241–256.

Scholl, M. A., Shanley, J. B., Murphy, S. F., Willenbring, J. K., Occhi, M., & González, G. (2015). Stable-isotope and solute-chemistry approaches to flow characterization in a forested tropical watershed, Luquillo Mountains, Puerto Rico. *Applied Geochemistry*, *63*, 484–497.

Sferratore, A., Garnier, J., Billen, G., Conley, D. J., & Pinault, S. (2006). Diffuse and Point Sources of Silica in the Seine River Watershed. *Environmental Science & Technology*, *40*(21), 6630–6635.

Shamsuddin, M. K. N., Sulaiman, W. N. A., Ramli, M. F., Mohd Kusin, F., & Samuding, K. (2018). Assessments of seasonal groundwater recharge and discharge using environmental stable isotopes at Lower Muda River Basin, Malaysia. *Applied Water Science*, *8*(120).

Shang, X., Jiang, X., Jia, R., & Wei, C. (2019). Land Use and Climate Change Effects on Surface Runoff Variations in the Upper Heihe River Basin. *Water*, *11*(2), 344.

Shanley, J. B., McDowell, W. H., & Stallard, R. F. (2011). Long-term patterns and short-term dynamics of stream solutes and suspended sediment in a rapidly weathering tropical watershed. *Water Resources Research*, *47*(7).

Shao, G., Zhang, D., Guan, Y., Sadat, M. A., & Huang, F. (2020). Application of Different Separation Methods to Investigate the Baseflow Characteristics of a Semi-Arid Sandy Area, Northwestern China. *Water*, *12*(2), 434.

Shapiro, & Wilk, M. B. (1965). An Analysis of Variance Test for Normality (Complete Samples). *Biometrika*, *52*(3/4), 591-611. Available at: http://www.bios.unc.edu/~mhudgens/bios/662/2008fall/Backup/wilkshapiro1965.pdf

Sharma, D. A., Rishi, M. S., & Keesari, T. (2016). Evaluation of groundwater quality and suitability for irrigation and drinking purposes in southwest Punjab, India using hydrochemical approach. *Applied Water Science*, *7*(6), 3137–3150.

Shi, M., Wang, S., Argiriou, A. A., Zhang, M., Guo, R., Jiao, R., Kong, J., Zhang, Y., Qiu, X., & Zhou, S. (2019). Stable Isotope Composition in Surface Water in the Upper Yellow River in Northwest China. *Water*, *11*(5), 967.

Shi, D., Tan, H., Chen, X., Rao, W., & Basang, R. (2021). Uncovering the mechanisms of seasonal river–groundwater circulation using isotopes and water chemistry in the middle reaches of the Yarlungzangbo River, Tibet. *Journal of Hydrology*, *603*, 127010.

Siebert, S., Burke, J., Faures, J. M., Frenken, K., Hoogeveen, J., Döll, P., & Portmann, F. T. (2010). Groundwater use for irrigation – a global inventory. *Hydrology and Earth System Sciences*, *14*(10), 1863–1880.

Silva, P. S., Campos, J. E. G., Cunha, L. S., Mancini, L. H., Silva, P. S., Campos, J. E. G., Cunha, L. S., & Mancini, L. H. (2018). Relationships of stable isotopes, water-rock interaction and salinization in fractured aquifers, Petrolina region, Pernambuco State, Brazil. *REM - International Engineering Journal*, *71*(1), 19–25.

Simpson, H. J., & Herczeg, A. L. (1991). Salinity and evaporation in the River Murray Basin, Australia. *Journal of Hydrology*, *124*(1-2), 1–27.

Singh, K. P., Malik, A., Mohan, D., & Sinha, S. (2004). Multivariate statistical techniques for the evaluation of spatial and temporal variations in water quality of Gomti River (India)—a case study. *Water Research*, *38*(18), 3980–3992.

Singh, A. K., Raj, B., Tiwari, A. K., & Mahato, M. K. (2013). Evaluation of hydrogeochemical processes and groundwater quality in the Jhansi district of Bundelkhand region, India. *Environmental Earth Sciences*, *70*(3), 1225–1247.

Singh, A.K., & Kumar, S.R. (2015). Quality assessment of groundwater for drinking and irrigation use in semi-urban area of Tripura, India, *Ecology, Environment and Conservation*, *21*(1), 97-108.

Singh, N. K., Emanuel, R. E., & McGlynn, B. L. (2016). Variability in isotopic composition of base flow in two headwater streams of the southern Appalachians. *Water Resources Research*, *52*(6), 4264–4279.

Smakhtin, V.U. (2001). Estimating continuous monthly baseflow time series and their possible applications in the context of the ecological reserve, *Water SA*, *27*(2), 213-217.

Smart, M. and Tredoux, G. (2002). Groundwater Quality and Fitness for Use. In: Pietersen & Parsons (Eds.). *A Synthesis of the Hydrogeology of the Table Mountain Group-formation of a Research Strategy*, Pretoria, Water Research Commission, Report no TT 158/01.

Song, X., Liu, X., Xia, J., Yu, J., & Tang, C. (2006). A study of interaction between surface water and groundwater using environmental isotope in Huaisha River basin. *Science in China Series D: Earth Sciences*, *49*(12), 1299–1310.

Stewart, M., Cimino, J., & Ross, M. (2007). Calibration of Base Flow Separation Methods with Streamflow Conductivity. *Ground Water*, *45*(1), 17–27.

Struyf, E., Bal, K., Backx, H., Vrebos, D., Casteleyn, A., De Deckere, E., Schoelynck, J., Brendonck, L., Raitt, L., & Meire, P. (2012). Nitrogen, phosphorus and silicon in riparian ecosystems along the Berg River (South Africa): The effect of increasing human land use. *Water SA*, *38*(4).

Sun, C., Li, X., Chen, Y., Li, W., Stotler, R. L., & Zhang, Y. (2016). Spatial and temporal characteristics of stable isotopes in the Tarim River Basin. *Isotopes in Environmental and Health Studies*, *52*(3), 281–297.

Tao, Z., Li, M., Si, B., & Pratt, D. (2021). Rainfall intensity affects runoff responses in a semi-arid catchment. *Hydrological Processes*, *35*(4).

Trinh, D. A., Luu, M. T. N., & Le, Q. T. P. (2017). Use of stable isotopes to understand run-off generation processes in the Red River Delta. *Hydrological Processes*, *31*(22), 3827–3843.

Tazioli, Cervi, Doveri, Mussi, Deiana, & Ronchetti. (2019). Estimating the Isotopic Altitude Gradient for Hydrogeological Studies in Mountainous Areas: Are the Low-Yield Springs Suitable? Insights from the Northern Apennines of Italy. *Water*, *11*(9), 1764.

Theron, J. N. (1984). *The geology of Cape Town and environs.* Explanation of sheets 3318 CD and DC, and 3418 AB, AD, and BA: 1–77. Pretoria: Geological Survey of South Africa.

Theron, J. N., Gresse, P. G., Siegfried, H. P. & Rogers, J. 1992. *The geology of the Cape Town area*: 1–140. Pretoria: Geological Survey of South Africa.

Torres, M. A., West, A. J., & Clark, K. E. (2015). Geomorphic regime modulates hydrologic control of chemical weathering in the Andes–Amazon. *Geochimica et Cosmochimica Acta*, *166*, 105–128.

Tweed, S., Leblanc, M., Cartwright, I., Bass, A., Travi, Y., Marc, V., Bach, T.N., Duc, N.D., Massuel, S., & Kumar, U.S. (2020). Stable Isotopes of Water in Hydrogeology, In: Maurice, P. A. (Eds.). *Encyclopaedia* of Water: Science, Technology and Society, 1-10. Wiley, Hoboken, NJ.

Uhlenbrook, S., & Hoeg, S. (2003). Quantifying uncertainties in tracer-based hydrograph separations: a case study for two-, three- and five-component hydrograph separations in a mountainous catchment. *Hydrological Processes*, *17*(2), 431–453.

UNEP-WCMC, IUCN, & NGS (2018). Protected Planet Report 2018. *UNEP-WCMC, IUCN and NGS: Cambridge UK; Gland, Switzerland; and Washington, D.C., USA.* Available from *https://livereport.protectedplanet.net/pdf/Protected_Planet_Report_2018.pdf*

Vaughn, B. H., & Fountain, A. G. (2005). Stable isotopes and electrical conductivity as keys to understanding water pathways and storage in South Cascade Glacier, Washington, USA. *Annals of Glaciology*, *40*, 107–112.

Viviroli, D., & Weingartner, R. (2008). "Water Towers"—A Global View of the Hydrological Importance of Mountains. In: Wiegandt, E. (Eds.). *Mountains: Sources of Water, Sources of Knowledge. Advances in Global Change Research,* vol. 31., Springer, Dordrecht.

Walling, D. E., & Fang, D. (2003). Recent trends in the suspended sediment loads of the world's rivers. *Global and Planetary Change*, *39*(1-2), 111–126.

Wang, G., Zhang, J., He, R., Liu, C., Ma, T., Bao, Z., & Liu, Y. (2016). Runoff sensitivity to climate change for hydro-climatically different catchments in China. *Stochastic Environmental Research and Risk Assessment*, *31*(4), 1011–1021.

Wang, B., Zhang, H., Liang, X., Li, X., & Wang, F. (2019). Cumulative effects of cascade dams on river water cycle: Evidence from hydrogen and oxygen isotopes. *Journal of Hydrology*, *568*, 604–610.

Wang, W., Chen, Y., Wang, W., Xia, Z., Li, X., & Kayumba., P. M. (2021). Hydrochemical characteristics and evolution of groundwater in the dried-up river oasis of the Tarim Basin, Central Asia. *Journal of Arid Land,* 13, 977–994.

Wassenaar, L. I., Van Wilgenburg, S. L., Larson, K., & Hobson, K. A. (2009). A groundwater isoscape (δD, δ18O) for Mexico. *Journal of Geochemical Exploration*, *102*(3), 123–136.

Weaver, J., Cavé, L., & Talma, A. (2007). *Groundwater sampling (2nd), A comprehensive guide for sampling methods,* Pretoria: Water Research Commission: Report no TT 307/07.

Winter T.C, Harvey J.W, Franke O.L & Alley W.M. (1998). *Groundwater and surface water: a single resource*, North Dakota: U.S Geological Survey, Circular no 1139.

Winter, T. C. (2007). The Role of Ground Water in Generating Streamflow in Headwater Areas and in Maintaining Base Flow1, [Online]. *JAWRA Journal of the American Water Resources Association*, *43*(1), 15–25. Available from https://core.ac.uk/download/pdf/17270152.pdf [Accessed 03 June 2020].

Winter, K. (2016). Interim Measures Towards Sustainable Drainage in the Informal Settlements of South Africa. In Charlesworth, S. and Booth, C. (Eds.*). Sustainable Surface Water Management: A Handbook for SuDS*, 328-344 pp., John Wiley & Sons.

Woo, M.-K., & Thorne, R. (2003). Streamflow in the Mackenzie Basin, Canada. *Arctic*, *56*(4), 328–340.

Water Research Commission (WRC). (2012). *Water Resources of South Africa Study 2012(WR2012)* [Vector geospatial dataset]. Available from http://waterresourceswr2012.co.za/ [Accessed on 20 March 2020].

Watson, A., Vystavna, Y., Kralisch, S., Helmschrot, J., van Rooyen, J., & Miller, J. (2023). Towards the development of an isotope-enabled rainfall-runoff model: Improving the ability to capture hydrological and anthropogenic change. *Hydrological Processes*.

Wu, H., Zhang, X., Xiaoyan, L., Li, G., & Huang, Y. (2014). Seasonal variations of deuterium and oxygen-18 isotopes and their response to moisture source for precipitation events in the subtropical monsoon region. *Hydrological Processes*, *29*(1), 90–102.

Wu, W. (2016). Hydrochemistry of inland rivers in the north Tibetan Plateau: Constraints and weathering rate estimation. *Science of the Total Environment*, *541*, 468–482.

Xiao, J., Zhang, F., & Jin, Z. (2016). Spatial characteristics and controlling factors of chemical weathering of loess in the dry season in the middle Loess Plateau, China. *Hydrological Processes*, *30*(25), 4855–4869.

Xiao, D., Brantley, S. L., & Li, L. (2021). Vertical Connectivity Regulates Water Transit Time and Chemical Weathering at the Hillslope Scale. *Water Resources Research*, *57*(8).

Yang, K., Han, G., Song, C., & Zhang, P. (2019). Stable H-O Isotopic Composition and Water Quality Assessment of Surface Water and Groundwater: A Case Study in the Dabie

Mountains, Central China. *International Journal of Environmental Research and Public Health*, *16*(21), 4076.

Yang, Z., Zhou, Y., Wenninger, J., Uhlenbrook, S., & Wan, L. (2015). Simulation of Groundwater-Surface Water Interactions under Different Land Use Scenarios in the Bulang Catchment, Northwest China. *Water*, *7*(11), 5959–5985.

Yang, W., Xiao, C., Zhang, Z., Li, M., & Liang, X. (2021). Impact of reservoirs on baseflow recession analysis: a case study of the Chaersen Reservoir in Northeast China. *Hydrological Sciences Journal*, *66*(6), 951–960.

Yao, T., Zhang, X., Guan, H., Zhou, H., Hua, M., & Wang, X. (2018). Climatic and environmental controls on stable isotopes in atmospheric water vapor near the surface observed in Changsha, China. *Atmospheric Environment*, *189*, 252–263.

Yeh, H.-F., Lin, H.-I., Lee, C.-H., Hsu, K.-C., & Wu, C.-S. (2014). Identifying Seasonal Groundwater Recharge Using Environmental Stable Isotopes. *Water*, *6*(10), 2849–2861.

Zhang, R., Li, Q., Chow, T. L., Li, S., & Danielescu, S. (2012). Baseflow separation in a small watershed in New Brunswick, Canada, using a recursive digital filter calibrated with the conductivity mass balance method. *Hydrological Processes*, *27*(18), 2659–2665.

Zhou, J., Wu, J., Liu, S., Zeng, G., Qin, J., Wang, X., & Zhao, Q. (2015). Hydrograph Separation in the Headwaters of the Shule River Basin: Combining Water Chemistry and Stable Isotopes. *Advances in Meteorology*, *2015*, 1–10.

Zhou, M., Xia, J., Lu, J., Deng, S., & Lin, F. (2017). Morphological adjustments in a meandering reach of the middle Yangtze River caused by severe human activities. *Geomorphology*, *285*, 325–332.

Zhou, J., Liu, G., Meng, Y., Xia, C., Chen, K., & Chen, Y. (2021). Using stable isotopes as tracer to investigate hydrological condition and estimate water residence time in a plain region, Chengdu, China. *Scientific Reports*, *11*(1),2812.

Zhu, G., Li, J., Shi, P., He, Y., Cai, A., Tong, H., Liu, Y., & Yang, L. (2016). Relationship between sub-cloud secondary evaporation and stable isotope in precipitation in different regions of China. *Environmental Earth Sciences*, *75*(10).

Appendix

A. River Water and Groundwater data sheet

- Ion values are in mg/L

Date	Sample ID	Data Source	EC	TDS	pH	Temp	Ca^{2+}	Mg^{2+}	Na^{+}	K^{+}	HCO_3^{-}	SO_4^{2-}	Cl^{-}	CB	NO_3^{-}	PO_4^{2-}	SiO_2	$\delta^{18}O$	$\delta^{2}H$	Water Type
03-Nov-20	G1H003	River	165,00	107,25	6,38	23,50	7,70	3,00	16,77	2,16	26,84	9,34	27,62	0,10	4,18	0,00	8,58	-3,60	-14,50	Na-Cl
25-Nov-20	G1H003	River	172,00	111,80	7,18	18,60	5,63	3,68	16,56	2,20	21,96	8,03	26,87	2,85	0,90	0,00	8,87	-3,53	-15,30	Na-Cl
08-Dec-20	G1H003	River	170,80	111,02	6,99	20,30	3,40	1,61	15,89	2,51	9,76	8,32	28,10	-3,13	1,21	0,00	8,30	-3,77	-14,90	Na-Cl
22-Dec-20	G1H003	River	320,00	208,00	7,17	26,30	12,91	3,59	25,86	5,54	68,32	14,13	35,58	-4,58	9,70	0,00	9,44	-3,49	-14,60	Na-Cl
13-Jan-21	G1H003	River	254,90	165,69	6,99	26,70	17,63	4,56	24,41	3,29	70,76	9,37	35,53	0,93	4,83	0,00	3,60	-3,58	-14,50	Ca-Mg-Cl
25-Jan-21	G1H003	River	265,00	172,25	7,68	25,30	11,10	5,55	23,35	2,78	48,80	8,59	39,57	0,06	7,65	0,00	7,40	-3,34	-13,70	Na-Cl
08-Feb-21	G1H003	River	362,00	235,30	6,14	24,20	13,30	4,76	35,04	5,34	64,66	9,90	43,92	4,03	6,33	0,00	7,36	-3,37	-13,80	Na-Cl
22-Feb-21	G1H003	River	290,00	188,50	7,27	21,50	14,55	5,04	35,19	3,43	69,54	9,70	42,93	3,88	10,53	0,41	6,90	-3,35	-13,20	Na-Cl
08-Mar-21	G1H003	River	308,90	200,79	6,67	20,30	9,44	3,65	36,44	4,46	79,30	6,84	43,75	-4,00	7,51	0,12	4,98	-3,32	-14,20	Na-Cl
24-Mar-21	G1H003	River	221,10	143,72	6,98	22,50	6,08	4,97	18,03	2,10	36,60	8,35	31,08	-3,14	10,64	0,00	4,96	-3,37	-12,70	Na-Cl
07-Apr-21	G1H003	River	206,30	134,10	7,62	21,30	10,81	2,97	20,29	2,54	42,70	6,58	28,17	2,99	8,56	0,34	4,58	-3,50	-13,60	Na-Cl
19-Apr-21	G1H003	River	273,00	177,45	7,48	19,30	11,77	5,45	27,98	3,97	58,56	9,32	35,55	4,38	9,42	0,00	5,71	-3,28	-13,60	Na-Cl
03-May-21	G1H003	River	236,00	153,40	7,69	18,20	11,14	4,88	25,06	3,63	58,56	6,76	31,00	4,03	8,25	0,00	6,70	-2,93	-11,80	Na-Cl
17-May-21	G1H003	River	122,90	79,89	7,03	13,50	8,78	2,33	11,05	1,76	34,16	4,07	18,74	-0,76	1,39	0,00	5,63	-4,12	-17,60	Ca-Mg-Cl
31-May-21	G1H003	River	105,00	68,25	7,44	14,60	9,91	2,77	10,69	1,44	30,50	4,01	20,03	3,20	1,54	0,10	3,23	-3,43	-13,50	Ca-Mg-Cl
14-Jun-21	G1H003	River	144,50	93,93	7,02	14,40	12,27	2,89	12,82	1,67	35,38	4,75	22,98	4,43	2,32	0,00	5,54	-3,61	-15,40	Ca-Mg-Cl
29-Jun-21	G1H003	River	118,30	76,90	7,03	12,90	11,19	3,67	9,03	1,92	35,38	5,00	17,74	4,74	2,76	0,22	1,40	-3,97	-17,90	Ca-Mg-Cl
12-Jul-21	G1H003	River	142,20	92,43	6,39	12,50	15,70	2,40	10,54	1,74	48,80	6,78	21,18	-1,83	2,22	0,00	3,10	-3,86	-15,20	Ca-HCO3
26-Jul-21	G1H003	River	161,90	105,24	7,29	14,80	10,95	3,54	12,61	1,45	35,38	8,15	24,63	-0,75	2,17	0,00	5,55	-3,31	-13,50	Ca-Mg-Cl
10-Aug-21	G1H003	River	157,40	102,31	7,23	14,30	16,07	2,46	10,52	1,36	37,82	6,93	22,13	3,75	1,81	0,00	4,45	-3,66	-12,53	Ca-Mg-Cl
23-Aug-21	G1H003	River	147,00	95,55	6,06	15,40	14,91	2,28	11,55	1,68	37,82	6,59	22,08	3,40	1,70	0,00	3,45	-3,45	-13,35	Ca-Mg-Cl
06-Sep-21	G1H003	River	129,60	84,24	6,88	13,40	8,22	2,39	10,96	1,43	18,30	6,10	19,01	2,88	2,02	0,00	4,43	-3,76	-12,83	Ca-Mg-Cl
20-Sep-21	G1H003	River	160,00	104,00	7,39	12,70	10,77	4,23	13,63	1,98	36,60	7,22	23,08	4,37	2,07	0,00	6,56	-3,62	-14,00	Ca-Mg-Cl
13-Oct-21	G1H003	River	154,40	100,36	6,64	19,20	7,08	2,86	15,06	1,85	29,28	8,08	25,76	-3,13	2,21	0,00	5,53	-3,77	-17,54	Na-Cl
27-Oct-21	G1H003	River	138,40	89,96	7,62	20,40	14,38	2,31	12,40	1,57	39,04	6,25	22,22	3,14	1,77	0,00	4,38	-3,48	-14,14	Ca-Mg-Cl
03-Nov-20	Frans 1	River	130,00	84,50	7,89	22,00	6,71	2,44	13,05	3,01	24,40	6,31	23,52	-0,62	2,07	0,12	6,35	-3,52	-13,90	Na-Cl
25-Nov-20	Frans 1	River	127,70	83,01	7,30	18,40	4,53	1,82	11,13	0,74	13,42	4,89	20,67	-1,44	0,90	0,00	6,63	-3,35	-14,00	Na-Cl
08-Dec-20	Frans 1	River	142,50	92,63	6,96	21,90	6,72	2,25	14,26	1,95	23,18	7,14	26,04	-2,97	1,21	0,13	7,20	-3,69	-14,70	Na-Cl
22-Dec-20	Frans 1	River	150,90	98,09	7,19	25,60	5,94	2,18	13,99	1,85	28,06	5,14	22,20	-2,65	3,48	0,00	6,07	-3,39	-12,90	Na-Cl
13-Jan-21	Frans 1	River	132,00	85,80	7,43	25,00	1,96	1,23	5,05	0,21	14,64	0,00	7,30	-2,52	0,60	0,00	1,67	-3,22	-12,70	Ca-Mg-Cl
25-Jan-21	Frans 1	River	100,00	65,00	7,53	28,40	2,28	2,28	7,06	0,36	8,54	2,34	15,98	-1,73	0,43	0,00	2,77	-3,22	-11,60	Na-Cl
08-Feb-21	Frans 1	River	82,90	53,89	6,20	26,50	3,59	1,50	8,98	0,67	10,98	2,79	16,34	0,79	0,89	nd	3,06	-3,29	-11,20	Na-Cl
22-Feb-21	Frans 1	River	67,80	44,07	7,75	24,30	1,72	1,45	7,95	0,49	8,54	1,85	14,68	-2,52	0,14	0,00	2,78	-3,20	-11,30	Na-Cl
08-Mar-21	Frans 1	River	119,50	77,68	6,89	22,70	4,06	1,81	12,81	0,80	10,98	3,90	24,39	-1,09	0,10	0,00	2,76	-3,38	-13,70	Na-Cl
24-Mar-21	Frans 1	River	128,40	83,46	6,74	23,20	5,30	2,33	11,38	1,16	18,30	4,57	23,15	-3,33	2,04	0,00	4,46	-3,28	-12,10	Na-Cl
07-Apr-21	Frans 1	River	30,90	20,09	7,17	21,10	3,35	2,62	12,21	0,93	12,20	4,97	22,58	-0,62	3,31	0,00	4,79	-3,33	-14,00	Na-Cl
19-Apr-21	Frans 1	River	32,30	21,00	7,12	19,20	7,66	2,55	14,61	1,50	24,40	4,13	24,10	4,13	2,22	0,21	4,01	-3,23	-13,10	Na-Cl
03-May-21	Frans 1	River	33,50	21,78	7,28	18,00	8,44	2,23	14,91	1,37	26,84	4,32	23,37	4,01	3,54	0,00	7,12	-3,42	-13,20	Na-Cl
17-May-21	Frans 1	River	72,30	47,00	7,10	13,80	6,09	2,21	11,68	1,95	15,86	3,44	21,80	4,87	1,38	0,00	3,38	-3,32	-10,40	Na-Cl
31-May-21	Frans 1	River	49,20	31,98	7,32	13,90	8,63	2,58	9,39	1,20	26,84	3,20	17,39	4,08	1,26	0,00	2,95	-2,92	-12,80	Ca-Mg-Cl
14-Jun-21	Frans 1	River	68,70	44,66	7,07	12,60	6,18	2,23	10,08	0,92	14,64	3,63	20,25	3,67	1,83	0,15	3,52	-3,06	-10,80	Ca-Mg-Cl
29-Jun-21	Frans 1	River	39,10	25,42	6,67	12,70	9,79	2,40	7,53	1,66	28,06	3,89	15,48	3,85	2,03	0,65	1,85	-3,76	-16,40	Ca-Mg-Cl
12-Jul-21	Frans 1	River	50,30	32,70	7,14	11,70	12,52	3,73	9,98	1,59	46,36	6,03	19,91	-1,43	2,21	0,00	1,48	-3,52	-13,20	Ca-HCO3
26-Jul-21	Frans 1	River	70,40	45,76	7,86	14,00	14,95	2,59	12,27	1,81	37,82	6,95	22,92	4,35	2,39	0,00	4,37	-3,38	-12,80	Ca-Mg-Cl
10-Aug-21	Frans 1	River	68,50	44,53	6,90	14,20	8,93	3,08	9,14	0,69	23,18	6,05	20,29	1,66	1,88	0,00	2,92	-3,67	-12,42	Ca-Mg-Cl
23-Aug-21	Frans 1	River	69,40	45,11	6,24	14,70	10,93	3,21	10,84	1,36	32,94	6,07	21,06	2,14	1,95		2,98	-3,36	-13,83	Ca-Mg-Cl
06-Sep-21	Frans 1	River	56,20	36,53	7,47	13,70	5,71	2,79	9,57	1,14	19,52	5,26	17,67	1,73	1,94	0,00	3,65	-3,77	-12,91	Ca-Mg-Cl
20-Sep-21	Frans 1	River	75,10	48,82	6,48	16,60	10,63	3,29	11,64	1,41	34,16	5,87	20,52	3,19	1,95	0,00	4,19	-3,70	-14,88	Ca-Mg-Cl
13-Oct-21	Frans 1	River	66,60	43,29	6,16	18,50	14,24	2,73	13,08	1,71	41,48	6,47	22,89	2,93	1,92	0,12	7,46	-3,29	-12,08	Ca-Mg-Cl
27-Oct-21	Frans 1	River	74,60	48,49	7,40	21,10	11,18	2,98	10,15	0,98	29,28	5,40	20,75	3,77	1,87	0,00	5,77	-3,05	-11,56	Ca-Mg-Cl
03-Nov-20	Wem 1	River	85,00	55,25	6,40	27,00	4,03	1,78	9,64	0,71	8,54	3,07	21,37	-1,39	4,24	0,00	1,65	-3,74	-14,90	Na-Cl
25-Nov-20	Wem 1	River	79,50	51,68	6,96	18,20	2,39	1,28	8,33	0,28	1,22	2,96	19,47	-3,02	1,53	0,00	1,66	-3,78	-14,70	Na-Cl
08-Dec-20	Wem 1	River	29,70	19,31	6,95	19,10	0,30	0,23	4,68	0,15	2,44	BD	7,33	-1,17	0,23	nd	1,67	-3,48	-12,70	Na-Cl
22-Dec-20	Wem 1	River	35,30	22,95	7,30	22,40	0,52	0,50	3,73	0,13	3,66	BD	6,79	-3,91	1,11	nd	1,65	-3,30	-12,10	Na-Cl
13-Jan-21	Wem 1	River	31,60	20,54	7,04	22,30	0,92	0,88	3,91	0,12	8,54	BD	6,07	-3,13	0,93	nd	1,64	-3,29	-12,00	Na-Cl
25-Jan-21	Wem 1	River	45,00	29,25	6,82	22,70	2,33	0,94	3,55	0,03	9,76	BD	6,74	-0,23	0,32	0,00	1,56	-3,38	-11,80	Ca-Mg-Cl
08-Feb-21	Wem 1	River	31,20	20,28	5,45	22,70	3,13	1,17	3,63	0,10	12,20	BD	7,11	1,56	0,31	0,15	1,49	-3,43	-11,50	Ca-Mg-Cl
22-Feb-21	Wem 1	River	31,40	20,41	5,48	21,70	1,56	0,62	3,53	0,21	6,10	BD	7,03	-1,81	0,31	0,00	1,45	-2,95	-10,70	Na-Cl
08-Mar-21	Wem 1	River	32,60	21,19	5,54	21,50	0,36	0,17	3,40	0,09	0,00	BD	7,28	-5,95	0,41	BD	1,32	-3,14	-10,80	Na-Cl
24-Mar-21	Wem 1	River	32,70	21,26	7,35	20,70	1,86	0,23	2,56	0,05	1,22	BD	7,32	-0,39	0,39	0,00	1,41	-3,05	-11,20	Na-Cl
07-Apr-21	Wem 1	River	127,30	82,75	7,74	21,00	4,12	0,21	3,24	0,10	6,10	1,61	7,34	3,61	0,39	0,14	1,67	-2,96	-10,20	Ca-Mg-Cl
19-Apr-21	Wem 1	River	141,70	92,11	7,30	19,60	3,55	1,05	3,01	0,06	10,98	BD	7,13	1,89	0,35	0,00	1,35	-3,10	-13,70	Ca-Mg-Cl
03-May-21	Wem 1	River	137,00	89,05	7,11	19,80	3,45	0,97	3,31	0,14	9,76	BD	7,50	3,70	0,39	0,00	1,78	-2,70	-11,00	Ca-Mg-Cl
17-May-21	Wem 1	River	132,70	86,26	6,41	14,40	4,32	2,03	7,01	0,28	12,20	2,34	15,38	0,89	0,87	0,00	1,66	-3,53	-15,10	Ca-Mg-Cl
31-May-21	Wem 1	River	115,40	75,01	6,38	15,20	4,35	1,63	5,79	0,15	7,32	2,01	13,77	4,92	0,74	0,00	2,97	-3,62	-16,40	Ca-Mg-Cl
14-Jun-21	Wem 1	River	133,30	86,65	6,43	14,80	3,43	2,66	7,09	0,16	9,76	2,56	15,48	3,90	1,11	0,16	1,86	-3,52	-15,30	Ca-Mg-Cl
29-Jun-21	Wem 1	River	125,90	81,84	6,88	12,40	5,72	1,18	4,01	0,02	18,30	BD	9,03	0,29	0,18	0,00	1,02	-3,74	-14,40	Ca-HCO3
12-Jul-21	Wem 1	River	123,50	80,28	6,61	11,70	5,21	1,92	5,46	0,41	19,52	1,95	11,51	-1,42	0,58	0,00	1,49	-3,88	-15,30	Ca-Mg-Cl
26-Jul-21	Wem 1	River	56,30	36,60	6,82	12,80	8,03	1,66	6,55	0,26	19,52	2,75	15,71	0,53	1,54	0,00	2,98	-3,79	-16,30	Ca-Mg-Cl
10-Aug-21	Wem 1	River	53,30	34,65	6,85	12,90	6,22	2,16	6,69	0,32	15,86	2,60	14,98	3,32	1,44	0,00	1,45	-3,47	-13,57	Ca-Mg-Cl
23-Aug-21	Wem 1	River	51,90	33,74	5,25	13,50	4,25	2,09	6,61	0,31	9,76	2,69	15,25	2,51	1,64	0,00	2,89	-3,67	-15,48	Ca-Mg-Cl
06-Sep-21	Wem 1	River	45,80	29,77	6,46	12,20	4,88	1,65	5,47	0,22	14,64	2,16	11,84	0,32	1,21	0,00	2,17	-3,44	-14,39	Ca-Mg-Cl
20-Sep-21	Wem 1	River	56,50	36,73	7,52	14,10	5,86	2,08	7,45	0,46	14,64	2,73	16,27	2,77	1,96	BD	2,63	-3,47	-15,04	Ca-Mg-Cl
13-Oct-21	Wem 1	River	50,00	32,50	6,50	16,70	1,60	1,16	7,60	0,60	1,22	2,72	17,17	-3,68	1,98	BD	3,16	-3,53	-15,33	Na-Cl
27-Oct-21	Wem 1	River	52,10	33,87	7,43	19,30	5,33	1,98	6,90	0,56	9,76	2,75	17,67	1,90	2,57	BD	4,06	-3,28	-12,78	Ca-Mg-Cl
26-Jul-21	G1H080	River	131,10	85,22	6,60	12,80	3,79	2,25	5,82	0,14	13,42	2,16	12,84	0,31	0,22	BD	2,74	-3,66	-15,00	Ca-Mg-Cl
10-Aug-21	G1H080	River	131,50	85,48	6,26	14,00	6,52	2,24	4,29	0,00	18,30	1,90	11,68	1,97	0,16	BD	2,58	-3,64	-12,66	Ca-Mg-Cl
23-Aug-21	G1H080	River	136,50	88,73	6,52	14,20	5,00	1,65	4,96	0,02	12,20	1,93	11,95	2,06	0,14	BD	4,13	-3,28	-14,05	Ca-Mg-Cl
06-Sep-21	G1H080	River	119,80	77,87	7,12	12,70	3,16	1,26	5,23	0,18	9,76	1,76	10,10	1,23	0,13	BD	2,43	-4,28	-17,91	Ca-Mg-Cl
20-Sep-21	G1H080	River	94,40	61,36	6,28	14,00	5,26	1,03	5,90	0,11	12,20	1,89	12,27	1,77	0,18	BD	3,00	-3,98	-20,34	Ca-Mg-Cl
13-Oct-21	G1H080	River	113,30	73,65	5,28	16,60	3,93	2,01	6,03	0,15	15,86	1,87	12,69	-2,29	0,13	BD	3,18	-3,37	-13,69	Ca-Mg-Cl
27-Oct-21	G1H080	River	99,10	64,42	6,48	19,60	5,80	1,66	5,23	0,23	12,20	1,74	12,80	4,90	0,16	BD	3,55	-3,53	-13,90	Ca-Mg-Cl
29-Jun-21	Mount Stream	River	44,20	28,73	4,90	15,20	5,10	1,58	4,16	0,00	20,74	BD	8,64	-1,57	2,52	0,16	0,40	-3,32	-10,60	Ca-HCO3
12-Jul-21	Mount Stream	River	39,70	25,81	5,01	13,90	5,06	1,84	3,85	0,13	18,30	1,72	8,34	0,34	1,23	BD	0,55	-3,73	-13,10	Ca-HCO3
26-Jul-21	Mount Stream	River	41,60	27,04	5,48	16,30	4,23	1,89	3,89	0,10	15,86	1,68	9,04	-1,12	1,23	BD	0,97	-3,48	-13,60	Ca-Mg-Cl
10-Aug-21	Mount Stream	River	40,40	26,26	5,37	16,00	4,95	1,43	3,35	0,00	13,42	1,65	8,45	1,75	1,08	BD	2,22	-3,39	-7,64	Ca-Mg-Cl
23-Aug-21	Mount Stream	River	43,80	28,47	4,81	16,40	5,80	0,94	3,62	0,09	14,64	1,65	8,78	0,38	1,32	BD	1,22	-2,73	-10,58	Ca-Mg-Cl
06-Sep-21	Mount Stream	River	36,50	23,73	5,10	14,60	4,20	1,56	3,37	0,08	12,20	1,66	7,57	4,09	1,11	nd	1,65	-3,74	-12,19	Ca-Mg-Cl
20-Sep-21	Mount Stream	River	39,50	25,68	5,38	15,20	4,17	1,88	4,03	0,04	17,08	1,36	8,34	-0,42	0,89	BD	1,56	-3,51	-9,64	Ca-HCO3
13-Oct-21	Mount Stream	River	41,80	27,17	5,43	19,80	5,55	1,57	3,76	0,04	14,64	1,24	9,27	3,99	0,92	BD	2,36	-3,34	-9,79	Ca-Mg-Cl
27-Oct-21	Mount Stream	River	36,50	23,73	6,06	19,70	3,35	2,07	3,84	0,30	13,42	1,26	8,77	1,83	0,87	BD	1,77	-3,53	-11,35	Ca-Mg-Cl
17-May-21	BG-51	River	54,20	35,23	4,86	12,50	3,74	1,47	5,48	0,08	8,54	1,75	12,35	2,14	0,19	BD	2,69	-2,28	-7,30	Ca-Mg-Cl
31-May-21	BG-51	River	55,20	35,88	5,10	15,90	3,60	1,13	5,92	0,03	7,32	BD	13,06	4,19	0,19	BD	1,62	-2,66	-10,90	Ca-Mg-Cl
14-Jun-21	BG-51	River	55,20	35,88	4,80	12,80	5,25	1,88	5,08	0,03	13,42	BD	13,24	3,66	0,00	BD	2,32	-3,05	-8,80	Ca-Mg-Cl
29-Jun-21	BG-51	River	51,50	33,48	5,00	13,30	4,37	2,05	5,05	0,03	20,74	BD	11,21	-3,87	0,69	BD	1,04	-3,40	-11,60	Ca-HCO3
12-Jul-21	BG-51	River	58,40	37,96	4,84	11,20	5,93	1,55	5,82	0,25	14,64	BD	13,94	3,80	0,18	BD	1,38	-2,79	-7,20	Ca-Mg-Cl
26-Jul-21	BG-51	River	58,30	37,90	5,18	12,40	4,03	2,38	5,92	0,13	14,64	BD	14,03	1,68	0,09	BD	2,00	-3,09	-8,70	Ca-Mg-Cl
10-Aug-21	BG-51	River	52,00	33,80	5,30	13,00	4,34	1,37	5,18	0,04	10,98	BD	12,14	3,08	0,06	BD	1,17	-3,23	-7,38	Ca-Mg-Cl
23-Aug-21	BG-51	River	54,30	35,30	4,64	13,50	3,54	1,45	5,39	0,02	8,54	BD	12,59	3,47	BD	BD	1,86	-2,90	-9,26	Ca-Mg-Cl
06-Sep-21	BG-51	River	44,60	28,99	4,89	13,80	3,37	1,49	4,51	0,06	10,98	BD	9,89	3,16	BD	BD	2,22	-3,29	-12,52	Ca-Mg-Cl
20-Sep-21	BG-51	River	50,50	32,83	4,70	15,20	3,69	1,18	5,44	0,05	13,42	BD	11,69	-2,84	BD	nd	1,41	-3,16	-9,52	Ca-Mg-Cl
13-Oct-21	BG-51	River	49,00	31,85	5,12	18,00	3,37	1,12	5,17	0,11	8,54	BD	11,71	1,81	BD	BD	2,05	-2,77	-7,69	Ca-Mg-Cl
27-Oct-21	BG-51	River	44,00	28,60	5,52	18,60	3,07	2,12	4,90	0,17	12,20	BD	11,33	2,35	BD	nd	1,78	-3,41	-11,22	Ca-Mg-Cl
03-Nov-20	G1H077	River	41,80	27,17	6,20	24,00	1,69	0,71	3,47	0,16	6,10	BD	6,65	0,68	0,15	nd	1,53	-3,34	-12,40	Na-Cl
25-Nov-20	G1H077	River	36,50	23,73	6,69	18,90	1,13	0,43	3,18	0,00	2,44	BD	7,36	-3,70	0,13	0,13	1,57	-3,17	-12,30	Na-Cl
08-Dec-20	G1H077	River	27,80	18,07	6,84	20,30	0,35	0,22	3,94	0,16	2,44	BD	6,65	-3,74	0,15	nd	1,49	-3,46	-12,50	Na-Cl
22-Dec-20	G1H077	River	33,30	21,65	7,31	23,60	0,98	0,61	3,47	0,07	4,88	BD	6,76	-3,53	0,24	0,00	1,64	-3,34	-12,10	Na-Cl
13-Jan-21	G1H077	River	31,60	20,54	6,90	23,90	1,20	0,93	3,78	0,10	7,32	BD	5,89	2,94	0,94	nd	1,35	-3,25	-11,60	Na-Cl
25-Jan-21	G1H077	River	85,00	55,25	8,31	27,60	2,96	1,42	3,14	0,24	10,98	BD	7,09	3,49	0,30	nd	1,76	-3,24	-11,00	Ca-Mg-Cl
08-Feb-21	G1H077	River	33,20	21,58	6,75	24,00	2,56	1,14	3,71	0,14	10,98	BD	7,16	0,59	0,28	nd	1,45	-3,19	-10,70	Ca-Mg-Cl
22-Feb-21	G1H077	River	34,40	22,36	7,62	21,80	2,50	1,14	3,80	0,20	12,20	BD	7,45	-2,71	0,30	nd	1,71	-2,98	-10,70	Ca-Mg-Cl
08-Mar-21	G1H077	River	34,80	22,62	6,81	21,30	1,09	0,58	3,50	0,18	2,44	BD	7,35	2,24	0,35	BD	1,49	-2,99	-10,20	Na-Cl
24-Mar-21	G1H077	River	34,50	22,43	7,45	22,40	1,67	0,70	2,83	0,06	3,66	BD	7,23	0,23	0,36	BD	1,38	-2,95	-10,20	Ca-Mg-Cl
07-Apr-21	G1H077	River	38,80	25,22	7,36	21,80	2,72	0,77	3,50	0,17	7,32	1,66	7,69	-2,18	0,42	BD	1,67	-2,70	-9,00	Ca-Mg-Cl
19-Apr-21	G1H077	River	33,70	21,91	7,22	22,30	3,22	1,24	3,42	0,14	10,98	BD	7,18	4,01	0,31	BD	1,45	-3,03	-11,60	Ca-Mg-Cl
03-May-21	G1H077	River	36,80	23,92	7,35	18,30	3,00	1,08	3,56	0,19	9,76	BD	7,53	3,31	0,35	BD	1,59	-2,73	-8,20	Ca-Mg-Cl
17-May-21	G1H077	River	36,30	23,60	7,04	18,40	4,32	1,04	3,13	0,16	15,86	BD	7,03	-1,85	0,34	BD	1,00	-2,39	-8,70	Ca-HCO3
31-May-21	G1H077	River	34,00	22,10	6,61	16,30	3,84	1,19	2,98	0,07	13,42	BD	6,72	1,41	0,37	BD	1,09	-2,56	-7,80	Ca-HCO3
14-Jun-21	G1H077	River	31,50	20,48	6,54	16,10	4,71	1,47	2,95	0,16	18,30	BD	6,62	0,12	0,36	BD	0,35	-2,61	-8,40	Ca-HCO3

Date	Sample ID	Data Source	EC	TDS	pH	Temp	Ca^{2+}	Mg^{2+}	Na^{+}	K^{+}	HCO_3^{-}	SO_4^{2-}	Cl^{-}	CB	NO_3^{-}	PO_4^{2-}	SiO_2	$\delta^{18}O$	$\delta^{2}H$	Water Type
29-Jun-21	G1H077	River	32,50	21,13	6,59	14,30	4,95	1,20	2,98	0,13	15,86	BD	6,76	3,00	0,39	BD	0,63	-2,57	-9,30	Ca-HCO3
12-Jul-21	G1H077	River	28,60	18,59	7,00	13,20	5,78	1,53	2,53	0,16	19,52	BD	6,18	3,36	0,41	BD	0,43	-3,66	-15,90	Ca-HCO3
26-Jul-21	G1H077	River	28,00	18,20	5,83	15,20	4,64	1,75	2,50	0,18	18,30	BD	6,12	1,72	0,42	BD	0,81	-3,07	-12,10	Ca-HCO3
10-Aug-21	G1H077	River	28,20	18,33	6,06	14,30	7,38	0,69	2,03	0,01	19,52	BD	5,97	2,53	0,40	BD	1,00	-2,82	-9,00	Ca-HCO3
23-Aug-21	G1H077	River	33,70	21,91	5,31	15,30	6,27	0,75	2,35	0,16	17,08	BD	6,10	3,07	0,39	BD	1,41	-2,20	-11,10	Ca-HCO3
06-Sep-21	G1H077	River	27,50	17,88	5,90	13,70	3,90	1,02	2,68	0,41	13,42	BD	6,00	2,04	0,41	BD	0,99	-3,28	-12,98	Ca-HCO3
20-Sep-21	G1H077	River	28,30	18,40	5,82	15,20	3,86	1,78	3,05	0,16	17,08	1,17	5,75	0,99	0,39	BD	0,84	-3,65	-12,72	Ca-HCO3
13-Oct-21	G1H077	River	29,70	19,31	5,32	17,10	3,83	1,09	2,74	0,29	12,20	1,17	5,84	2,30	0,38	BD	1,19	-3,50	-14,48	Ca-HCO3
27-Oct-21	G1H077	River	26,50	17,23	7,62	20,40	3,77	1,63	2,67	0,43	15,86	1,14	5,63	0,73	0,38	BD	1,51	-3,36	-11,74	Ca-HCO3
25-Nov-20	BGR1	River	30,10	19,57	5,52	18,60	1,44	0,43	3,18	0,00	3,66	BD	7,45	-4,75	0,12	0,12	1,57	-3,14	-12,30	Na-Cl
08-Dec-20	BGR1	River	30,20	19,63	6,98	22,30	0,50	0,43	3,86	0,17	2,44	BD	7,04	-1,24	0,14	nd	1,68	-3,35	-11,80	Na-Cl
22-Dec-20	BGR1	River	34,70	22,56	5,79	23,20	0,74	0,49	3,54	0,09	3,66	BD	6,45	-1,75	1,10	nd	1,91	-3,27	-11,70	Na-Cl
13-Jan-21	BGR1	River	31,30	20,35	4,25	25,60	1,88	1,55	3,51	0,13	10,98	BD	6,67	1,20	0,25	nd	1,80	-3,31	-12,20	Ca-Mg-Cl
25-Jan-21	BGR1	River	75,00	48,75	6,93	27,50	2,14	0,93	2,86	0,11	6,10	BD	6,96	2,31	0,29	0,00	1,68	-3,19	-10,90	Ca-Mg-Cl
08-Feb-21	BGR1	River	33,00	21,45	4,90	23,40	2,81	1,09	3,51	0,11	9,76	BD	7,09	3,48	0,27	nd	1,28	-3,21	-10,50	Ca-Mg-Cl
22-Feb-21	BGR1	River	34,20	22,23	5,57	19,90	2,24	1,07	3,84	0,17	7,32	BD	7,41	0,31	0,30	nd	1,85	-2,92	-10,30	Ca-Mg-Cl
08-Mar-21	BGR1	River	34,10	22,17	4,89	18,20	1,03	0,55	3,42	0,14	4,88	BD	7,28	0,73	0,34	BD	1,13	-2,96	-10,00	Na-Cl
24-Mar-21	BGR1	River	33,80	21,97	6,62	23,20	1,48	0,47	3,10	0,07	3,66	BD	7,23	-2,99	0,34	BD	0,94	-3,00	-10,30	Na-Cl
07-Apr-21	BGR1	River	35,40	23,01	6,32	21,40	3,16	0,79	2,80	0,06	6,10	1,62	7,49	0,18	0,41	BD	1,20	-2,59	-8,30	Ca-Mg-Cl
19-Apr-21	BGR1	River	33,70	21,91	6,94	20,20	3,42	1,31	3,32	0,08	12,20	BD	7,15	2,78	0,31	BD	1,30	-3,15	-12,50	Ca-Mg-Cl
03-May-21	BGR1	River	36,00	23,40	6,88	18,70	3,29	1,17	3,42	0,24	10,98	BD	7,47	3,04	0,36	BD	1,71	-2,54	-7,60	Ca-Mg-Cl
17-May-21	BGR1	River	34,10	22,17	5,66	17,60	5,22	0,88	3,06	0,11	14,64	BD	7,15	2,98	0,34	BD	0,03	-1,91	-6,70	Ca-Mg-Cl
31-May-21	BGR1	River	32,00	20,80	7,18	16,80	4,08	0,61	3,01	0,07	10,98	BD	7,08	0,84	0,37	BD	1,00	-2,77	-8,50	Ca-HCO3
14-Jun-21	BGR1	River	32,30	21,00	6,10	15,60	4,35	1,65	3,13	0,15	17,08	BD	6,74	2,36	0,36	BD	0,29	-2,62	-8,40	Ca-HCO3
29-Jun-21	BGR1	River	29,10	18,92	6,10	14,10	4,98	1,27	2,97	0,08	17,08	BD	6,20	3,08	0,39	BD	0,59	-3,05	-10,80	Ca-HCO3
12-Jul-21	BGR1	River	29,90	19,44	6,30	12,30	4,59	1,01	2,79	0,27	13,42	BD	6,52	4,38	0,40	BD	0,64	-3,94	-15,90	Ca-HCO3
26-Jul-21	BGR1	River	28,80	18,72	6,12	14,00	4,21	1,81	2,79	0,20	17,08	BD	6,30	2,91	0,48	BD	0,99	-3,10	-12,10	Ca-HCO3
10-Aug-21	BGR1	River	28,30	18,40	6,78	14,70	5,26	1,16	3,18	0,04	20,74	BD	6,02	-1,26	0,38	BD	0,93	-3,12	-10,58	Ca-HCO3
23-Aug-21	BGR1	River	46,90	30,49	5,00	16,00	4,20	1,20	2,73	0,12	13,42	BD	6,07	4,71	0,38	BD	1,30	-2,72	-11,89	Ca-HCO3
06-Sep-21	BGR1	River	28,00	18,20	6,50	14,00	3,12	1,46	2,76	0,29	15,86	BD	5,91	-2,81	0,40	BD	0,81	-3,66	-14,07	Ca-HCO3
20-Sep-21	BGR1	River	29,50	19,18	6,29	14,10	3,71	1,59	3,03	0,26	14,64	1,19	5,97	2,38	0,39	BD	0,94	-3,69	-12,65	Ca-HCO3
13-Oct-21	BGR1	River	32,90	21,39	6,28	17,50	4,51	1,04	2,65	0,28	13,42	1,16	5,98	2,36	0,37	BD	1,10	-3,33	-13,78	Ca-HCO3
27-Oct-21	BGR1	River	25,90	16,84	7,19	17,90	3,98	1,51	2,52	0,58	14,64	1,15	5,84	2,07	0,39	BD	1,06	-3,10	-10,62	Ca-HCO3
03-Nov-20	BGR2	River	45,00	29,25	7,80	21,50	2,16	0,74	4,69	0,17	8,54	BD	8,03	1,47	0,30	nd	1,50	-3,32	-11,60	Na-Cl
25-Nov-20	BGR2	River	33,50	21,78	7,27	23,40	1,10	0,50	3,51	0,00	0,00	1,58	7,98	-1,86	0,11	nd	1,58	-3,20	-11,60	Na-Cl
08-Dec-20	BGR2	River	30,50	19,83	6,86	22,50	0,53	0,45	4,14	0,10	2,44	BD	7,45	-0,93	0,13	nd	1,66	-3,43	-12,10	Na-Cl
22-Dec-20	BGR2	River	45,10	29,32	7,15	24,80	0,51	0,46	3,71	0,00	3,66	BD	6,61	-4,73	0,58	nd	1,50	-3,13	-10,40	Na-Cl
13-Jan-21	BGR2	River	31,90	20,74	6,41	27,80	1,10	0,83	3,97	0,08	9,76	BD	6,00	-4,94	0,73	nd	1,42	-3,16	-10,90	Na-Cl
25-Jan-21	BGR2	River	35,00	22,75	7,55	27,10	2,81	1,11	3,03	0,02	10,98	BD	7,36	-3,15	0,17	0,00	1,82	-3,05	-10,10	Ca-Mg-Cl
08-Feb-21	BGR2	River	35,10	22,82	7,14	27,20	2,66	1,23	3,85	0,16	9,76	BD	7,65	3,87	0,18	nd	1,58	-3,12	-10,10	Ca-Mg-Cl
22-Feb-21	BGR2	River	35,90	23,34	6,60	24,40	2,72	1,19	4,12	0,16	8,54	BD	8,04	1,31	0,17	nd	1,87	-2,93	-9,90	Ca-Mg-Cl
08-Mar-21	BGR2	River	35,70	23,21	6,30	23,20	1,37	0,67	3,65	0,11	7,32	BD	7,82	-2,64	0,21	BD	1,42	-2,92	-9,80	Na-Cl
24-Mar-21	BGR2	River	36,00	23,40	6,74	23,20	1,70	0,77	3,04	0,04	4,88	1,61	7,77	-1,88	0,26	nd	1,50	-2,86	-9,40	Ca-Mg-Cl
07-Apr-21	BGR2	River	40,30	26,20	7,20	24,00	2,95	0,84	3,39	0,17	6,10	1,71	8,55	-1,08	0,26	BD	2,18	-2,51	-7,70	Ca-Mg-Cl
19-Apr-21	BGR2	River	35,10	22,82	7,45	19,20	3,19	1,35	3,35	0,08	10,98	BD	7,62	2,81	0,21	BD	1,40	-2,77	-9,40	Ca-Mg-Cl
03-May-21	BGR2	River	37,90	24,64	7,55	20,00	3,58	1,17	3,61	0,13	10,98	BD	8,08	3,24	0,22	BD	1,90	-2,64	-8,20	Ca-Mg-Cl
17-May-21	BGR2	River	37,80	24,57	6,66	15,90	4,03	1,30	3,46	0,06	14,64	BD	7,13	2,12	0,32	BD	1,23	-2,47	-10,60	Ca-HCO3
31-May-21	BGR2	River	32,20	20,93	6,56	15,40	3,78	0,88	3,18	0,17	10,98	BD	7,11	3,01	0,41	nd	1,57	-2,95	-11,60	Ca-Mg-Cl
14-Jun-21	BGR2	River	33,20	21,58	6,73	14,30	4,30	1,80	3,42	0,05	18,30	BD	7,20	0,96	0,32	BD	0,41	-2,49	-6,80	Ca-HCO3
29-Jun-21	BGR2	River	28,90	18,79	5,30	12,70	5,43	0,94	2,54	0,10	17,08	BD	5,61	2,60	0,86	BD	0,42	-3,82	-14,70	Ca-HCO3
12-Jul-21	BGR2	River	30,50	19,83	6,22	11,30	4,27	1,24	3,00	0,27	14,64	BD	6,46	3,44	0,69	BD	0,76	-4,06	-16,60	Ca-HCO3
26-Jul-21	BGR2	River	36,90	23,99	5,77	14,30	4,04	1,64	3,58	0,30	14,64	BD	8,18	3,03	0,68	BD	1,59	-3,91	-14,60	Ca-Mg-Cl
10-Aug-21	BGR2	River	32,70	21,26	5,97	14,30	4,73	0,69	2,92	0,14	12,20	BD	7,10	2,81	0,44	BD	1,38	-3,59	-9,00	Ca-Mg-Cl
23-Aug-21	BGR2	River	41,10	26,72	5,85	15,80	6,40	0,59	2,70	0,17	15,86	BD	6,78	4,13	0,33	BD	1,68	-3,08	-13,79	Ca-HCO3
06-Sep-21	BGR2	River	28,20	18,33	5,69	14,10	2,68	1,41	2,87	0,19	14,64	BD	5,93	-3,60	0,43	BD	1,14	-3,91	-12,61	Ca-HCO3
20-Sep-21	BGR2	River	34,80	22,62	6,23	15,30	4,24	1,41	3,48	0,22	14,64	1,11	7,16	2,01	0,39	BD	1,54	-3,56	-9,44	Ca-HCO3
13-Oct-21	BGR2	River	38,10	24,77	5,39	17,80	5,36	1,25	3,83	0,24	17,08	1,25	8,12	0,73	0,19	BD	2,24	-3,29	-12,00	Ca-HCO3
27-Oct-21	BGR2	River	29,00	18,85	6,49	19,70	3,85	1,48	3,06	0,26	17,08	0,98	6,69	-3,79	0,24	nd	1,96	-3,46	-13,39	Ca-HCO3
03-Nov-20	BGR3	River	55,00	35,75	8,10	23,00	2,91	1,57	6,70	0,64	12,20	2,55	13,00	-3,12	0,88	0,00	5,07	-3,34	-12,20	Na-Cl
25-Nov-20	BGR3	River	51,10	33,22	7,12	20,30	1,34	0,56	4,55	0,00	7,32	2,01	9,68	-3,84	0,23	0,13	4,22	-3,42	-13,10	Na-Cl
08-Dec-20	BGR3	River	105,10	68,32	6,88	21,90	1,32	1,33	9,69	1,11	2,44	4,81	18,70	-3,30	0,78	nd	5,91	-3,65	-14,00	Na-Cl
22-Dec-20	BGR3	River	45,00	29,25	7,15	24,70	1,77	0,65	4,67	0,26	10,98	BD	7,05	-3,71	0,79	nd	2,54	-3,31	-12,00	Na-Cl
13-Jan-21	BGR3	River	34,20	22,23	5,88	27,80	1,14	0,82	4,14	0,12	9,76	BD	6,29	-4,64	0,80	nd	1,63	-3,24	-11,00	Na-Cl
25-Jan-21	BGR3	River	45,00	29,25	7,05	27,40	2,45	1,06	4,22	0,08	10,98	BD	8,57	-3,29	0,22	0,00	1,94	-3,04	-10,30	Ca-Mg-Cl
08-Feb-21	BGR3	River	42,30	27,50	6,20	27,10	2,70	1,09	4,32	0,21	9,76	BD	8,35	2,74	0,23	nd	1,32	-2,89	-10,00	Ca-Mg-Cl
22-Feb-21	BGR3	River	39,80	25,87	6,60	24,70	2,70	1,25	4,44	0,27	9,76	BD	8,61	4,08	0,16	nd	2,01	-3,06	-9,70	Ca-Mg-Cl
08-Mar-21	BGR3	River	37,30	24,25	6,21	23,10	1,41	0,64	3,83	0,16	4,88	BD	8,07	-2,38	0,21	nd	1,60	-2,90	-10,00	Na-Cl
24-Mar-21	BGR3	River	41,80	27,17	6,74	25,10	1,64	0,72	3,52	0,10	2,44	1,69	8,07	-1,06	0,34	BD	1,65	-2,89	-10,60	Na-Cl
07-Apr-21	BGR3	River	51,20	33,28	7,25	24,00	2,36	1,13	4,41	0,26	3,66	2,02	10,04	3,02	0,60	BD	2,39	-2,28	-4,80	Ca-Mg-Cl
19-Apr-21	BGR3	River	41,30	26,85	7,24	19,70	2,93	1,20	4,09	0,17	9,76	BD	8,60	2,98	0,34	BD	2,02	-2,94	-11,20	Ca-Mg-Cl
03-May-21	BGR3	River	58,50	38,03	7,31	19,80	4,37	1,29	6,28	0,51	13,42	1,85	11,32	2,75	0,93	BD	2,45	-2,31	-7,30	Ca-Mg-Cl
17-May-21	BGR3	River	63,60	41,34	6,99	15,40	3,61	1,57	5,03	0,25	10,98	1,58	10,13	3,49	0,55	BD	2,77	-2,79	-12,40	Ca-Mg-Cl
31-May-21	BGR3	River	73,60	47,84	6,78	14,50	7,65	2,11	8,04	0,79	23,18	2,72	14,95	3,74	1,07	nd	2,66	-3,03	-10,10	Ca-Mg-Cl
14-Jun-21	BGR3	River	48,40	31,46	6,73	14,30	4,36	1,97	4,54	0,14	15,86	1,65	9,52	1,56	0,59	BD	1,25	-2,69	-8,00	Ca-Mg-Cl
29-Jun-21	BGR3	River	90,70	58,96	7,07	12,60	7,70	1,99	7,10	1,23	20,74	3,50	14,37	4,13	1,85	BD	1,26	-3,97	-15,50	Ca-Mg-Cl
12-Jul-21	BGR3	River	57,00	37,05	7,26	12,90	4,90	1,95	4,87	0,80	19,52	2,71	10,37	-2,40	0,98	BD	0,79	-3,18	-13,30	Ca-Mg-Cl
26-Jul-21	BGR3	River	97,90	63,64	6,96	12,50	9,21	2,62	7,54	0,82	25,62	4,36	15,86	3,31	1,54	BD	3,28	-2,96	-10,80	Ca-Mg-Cl
10-Aug-21	BGR3	River	68,10	44,27	6,77	13,30	4,57	2,55	4,72	0,19	20,74	2,31	9,28	-0,15	0,73	BD	2,09	-3,07	-10,95	Ca-HCO3
23-Aug-21	BGR3	River	79,60	51,74	6,90	12,50	5,98	1,97	5,83	0,58	17,08	3,15	12,35	2,48	1,05	BD	2,57	-3,63	-11,51	Ca-Mg-Cl
06-Sep-21	BGR3	River	64,90	42,19	6,49	13,30	1,43	1,60	5,92	0,75	4,88	2,89	10,73	4,01	1,11	BD	1,68	-3,60	-13,14	Na-Cl
20-Sep-21	BGR3	River	97,70	63,51	8,07	14,00	1,98	2,79	9,43	0,94	15,86	4,44	16,92	-4,19	1,52	BD	2,70	-3,95	-13,75	Na-Cl
13-Oct-21	BGR3	River	102,20	66,43	6,03	16,10	10,10	2,83	10,17	1,01	31,72	5,04	18,85	2,08	1,58	BD	4,17	-3,15	-10,36	Ca-Mg-Cl
27-Oct-21	BGR3	River	53,00	34,45	7,59	19,90	4,32	1,98	4,16	0,47	14,64	2,03	9,39	2,10	0,65	BD	1,80	-3,34	-12,74	Ca-Mg-Cl
03-Nov-20	BGR4	River	85,00	55,25	8,00	21,00	3,91	1,61	8,72	0,97	13,42	3,61	15,99	-2,37	1,21	nd	3,42	-3,54	-12,70	Na-Cl
25-Nov-20	BGR4	River	77,00	50,05	7,13	19,20	1,18	0,98	7,07	nd	0,00	3,10	14,31	-3,12	0,52	0,00	4,42	-3,50	-12,90	Na-Cl
08-Dec-20	BGR4	River	112,80	73,32	7,11	22,40	3,52	1,90	11,20	1,52	13,42	5,73	21,47	-4,85	0,94	nd	6,41	-3,64	-14,20	Na-Cl
22-Dec-20	BGR4	River	56,90	36,99	7,04	24,70	1,48	0,77	5,63	0,41	4,88	1,92	9,50	0,59	0,96	nd	2,42	-3,09	-9,70	Na-Cl
13-Jan-21	BGR4	River	35,70	23,21	6,83	27,90	1,30	0,85	4,20	0,10	8,54	BD	6,68	-1,25	1,72	nd	1,67	-3,30	-11,80	Na-Cl
25-Jan-21	BGR4	River	54,00	35,10	6,91	26,70	2,65	1,19	4,01	0,11	9,76	BD	8,92	-0,59	0,23	0,00	1,86	-2,93	-9,90	Ca-Mg-Cl
08-Feb-21	BGR4	River	43,20	28,08	6,86	27,10	2,77	1,23	4,74	0,22	10,98	BD	9,05	1,76	0,28	nd	1,79	-2,91	-10,00	Ca-Mg-Cl
22-Feb-21	BGR4	River	39,20	25,48	7,41	24,70	2,76	1,19	4,45	0,29	9,76	BD	8,70	3,74	0,16	nd	1,59	-2,96	-10,00	Ca-Mg-Cl
08-Mar-21	BGR4	River	39,20	25,48	6,21	23,10	0,39	0,20	3,92	0,20	3,66	BD	8,20	-4,64	0,20	BD	1,28	-2,79	-10,00	Na-Cl
24-Mar-21	BGR4	River	49,00	31,85	6,42	24,80	1,52	0,86	4,77	0,28	6,10	1,94	9,66	-1,59	0,50	BD	2,47	-2,93	-10,20	Na-Cl
07-Apr-21	BGR4	River	57,00	37,05	7,20	23,70	3,07	1,30	5,20	0,25	4,88	2,30	11,38	4,63	0,87	BD	2,84	-3,01	-10,90	Ca-Mg-Cl
19-Apr-21	BGR4	River	47,90	31,14	7,26	19,70	3,35	1,26	4,66	0,16	8,54	1,56	9,77	3,20	0,48	BD	2,01	-2,72	-9,30	Ca-Mg-Cl
03-May-21	BGR4	River	58,00	37,70	7,23	19,90	4,15	1,51	5,91	0,32	8,54	1,79	11,01	4,25	0,85	BD	2,50	-2,61	-9,80	Ca-Mg-Cl
17-May-21	BGR4	River	62,50	40,63	6,46	15,40	2,06	1,49	5,61	0,31	7,32	1,73	10,76	1,96	0,60	BD	1,75	-2,65	-12,40	Na-Cl
31-May-21	BGR4	River	70,20	45,63	6,83	14,40	6,33	1,92	6,86	0,61	18,30	2,31	13,05	4,77	0,88	BD	2,45	-3,06	-11,60	Ca-Mg-Cl
14-Jun-21	BGR4	River	56,20	36,53	6,70	14,20	4,20	1,95	5,43	0,23	17,08	1,89	10,89	-1,20	0,74	BD	2,15	-2,50	-7,00	Ca-Mg-Cl
29-Jun-21	BGR4	River	90,20	58,63	7,14	12,60	4,07	1,61	7,04	1,25	8,54	3,50	14,36	4,31	1,84	BD	1,40	-4,01	-15,80	Ca-Mg-Cl
12-Jul-21	BGR4	River	56,30	36,60	6,93	13,00	4,31	1,76	4,52	1,31	17,08	2,61	10,05	-2,30	0,89	BD	1,48	-2,70	-10,70	Ca-Mg-Cl
26-Jul-21	BGR4	River	75,00	48,75	7,06	12,80	6,21	2,13	5,93	0,50	21,96	3,48	13,19	-3,11	1,24	BD	3,32	-3,09	-10,90	Ca-Mg-Cl
10-Aug-21	BGR4	River	56,30	36,60	7,03	13,70	4,55	2,78	4,81	0,17	19,52	2,37	9,50	2,48	0,75	BD	1,39	-3,26	-8,79	Ca-HCO3
23-Aug-21	BGR4	River	68,60	44,59	6,53	12,90	4,49	2,31	5,90	0,54	15,86	3,03	12,00	1,71	1,04	BD	3,47	-3,34	-11,47	Ca-Mg-Cl
06-Sep-21	BGR4	River	56,50	36,73	6,79	13,10	4,90	1,71	4,70	0,36	14,64	2,53	9,63	3,01	0,91	BD	2,43	-3,29	-10,99	Ca-Mg-Cl
20-Sep-21	BGR4	River	101,70	66,11	7,98	13,50	8,73	2,74	9,13	0,97	26,84	4,35	16,71	3,89	1,49	BD	3,26	-3,83	-13,16	Ca-Mg-Cl
13-Oct-21	BGR4	River	68,50	44,53	6,29	15,80	3,81	1,86	6,45	0,64	10,98	2,88	12,29	4,34	0,89	BD	4,42	-3,38	-14,86	Ca-Mg-Cl
27-Oct-21	BGR4	River	45,90	29,84	7,62	19,10	4,70	1,64	4,36	0,53	17,08	1,95	9,17	-0,62	0,62	BD	2,76	-3,64	-13,48	Ca-HCO3
03-Nov-20	BGR5	River	170,00	110,50	6,50	25,00	5,08	2,04	17,32	2,49	17,08	10,07	24,60	2,23	0,87	0,10	2,58	-3,90	-13,20	Na-Cl
25-Nov-20	BGR5	River	110,20	71,63	7,09	18,70	3,40	1,35	10,43	2,55	12,20	4,73	19,44	-2,85	0,41	0,00	2,57	-3,55	-13,20	Na-Cl
08-Dec-20	BGR5	River	58,30	37,90	7,22	20,50	1,34	0,94	5,21	0,50	2,44	2,67	11,14	-3,32	0,29	0,00	2,59	-3,53	-12,90	Na-Cl
22-Dec-20	BGR5	River	58,80	38,22	7,44	24,00	1,52	0,79	5,63	0,47	4,88	1,90	9,51	1,25	1,16	nd	2,54	-3,34	-11,90	Na-Cl
13-Jan-21	BGR5	River	49,30	32,05	7,01	25,10	1,79	0,90	5,69	0,49	10,98	1,91	8,75	-4,89	0,57	0,00	1,78	-3,37	-12,70	Na-Cl
25-Jan-21	BGR5	River	75,00	48,75	6,64	24,50	2,67	1,24	5,10	0,41	8,54	2,22	13,54	-4,14	0,28	0,22	2,63	-3,01	-10,40	Ca-Mg-Cl
08-Feb-21	BGR5	River	86,70	56,36	6,33	22,30	4,12	1,70	8,29	1,09	14,64	3,81	15,83	-2,11	0,30	0,56	2,71	-3,31	-10,80	Na-Cl
22-Feb-21	BGR5	River	82,20	53,43	6,90	18,90	1,94	1,05	8,22	1,16	9,76	3,05	13,89	-3,81	0,26	0,48	2,46	-2,82	-9,80	Na-Cl
08-Mar-21	BGR5	River	104,50	67,93	6,81	19,20	1,48	1,06	9,50	1,41	7,32	4,58	16,09	-4,62	0,32	0,49	1,94	-2,99	-10,80	Na-Cl
24-Mar-21	BGR5	River	113,40	73,71	6,76	23,60	2,46	2,04	8,40	1,06	10,98	4,71	15,71	-2,71	0,52	0,45	2,92	-3,15	-10,70	Na-Cl
07-Apr-21	BGR5	River	195,20	126,88	7,09	21,30	2,95	1,54	14,92	2,31	8,54	8,01	26,94	-4,13	1,62	1,40	2,74	-3,07	-10,50	Na-Cl

Date	Sample ID	Data Source	EC	TDS	pH	Temp	Ca^{2+}	Mg^{2+}	Na^{+}	K^{+}	HCO_3^{-}	SO_4^{2-}	Cl^{-}	CB	NO_3^{-}	PO_4^{2-}	SiO_2	$\delta^{18}O$	$\delta^{2}H$	Water Type
19-Apr-21	BGR5	River	61,70	40,11	7,22	22,30	1,94	1,12	5,90	0,51	7,32	2,02	11,08	-1,77	0,39	0,11	2,11	-2,53	-8,20	Na-Cl
03-May-21	BGR5	River	98,90	64,29	7,13	18,50	3,96	2,28	10,26	1,39	15,86	3,36	16,66	4,04	1,26	0,45	2,46	-3,14	-11,70	Na-Cl
17-May-21	BGR5	River	64,20	41,73	6,80	14,40	4,26	1,59	5,61	0,43	12,20	2,05	11,29	3,20	0,64	BD	2,77	-2,54	-10,40	Ca-Mg-Cl
31-May-21	BGR5	River	46,70	30,36	6,91	15,10	2,57	1,25	5,17	0,34	6,10	1,95	11,20	0,86	0,71	BD	2,10	-3,05	-11,00	Na-Cl
14-Jun-21	BGR5	River	71,00	46,15	7,26	14,40	6,14	2,00	6,46	0,57	17,08	2,40	13,50	3,80	0,77	0,11	1,62	-2,90	-10,20	Ca-Mg-Cl
29-Jun-21	BGR5	River	77,10	50,12	7,26	13,20	3,18	2,04	6,50	1,01	15,86	3,02	12,62	-3,30	1,53	BD	1,11	-3,92	-16,20	Na-Cl
12-Jul-21	BGR5	River	49,90	32,44	6,98	13,50	4,00	2,23	4,46	0,37	17,08	2,33	9,12	0,04	0,77	BD	0,84	-2,98	-10,50	Ca-Mg-Cl
26-Jul-21	BGR5	River	70,90	46,09	7,30	12,20	6,31	2,06	6,00	0,69	21,96	3,60	12,57	-1,71	1,07	BD	3,06	-3,37	-13,00	Ca-Mg-Cl
10-Aug-21	BGR5	River	58,70	38,16	7,21	14,20	5,11	2,50	4,59	0,25	17,08	2,67	9,93	4,03	0,67	BD	0,90	-3,58	-14,77	Ca-Mg-Cl
23-Aug-21	BGR5	River	56,70	36,86	6,57	12,70	4,35	1,31	4,74	0,48	9,76	2,47	10,55	3,31	0,76	BD	2,00	-3,28	-11,33	Ca-Mg-Cl
06-Sep-21	BGR5	River	53,30	34,65	7,35	12,30	4,14	1,25	4,39	0,46	10,98	2,42	9,36	1,81	0,85	BD	1,65	-3,68	-13,80	Ca-Mg-Cl
20-Sep-21	BGR5	River	59,70	38,81	7,41	13,50	4,75	1,73	5,36	0,49	15,86	2,44	10,23	2,09	0,75	BD	1,32	-3,22	-11,59	Ca-Mg-Cl
13-Oct-21	BGR5	River	74,70	48,56	6,57	16,30	5,55	1,95	7,66	1,00	17,08	3,53	14,00	3,10	1,09	BD	2,69	-3,15	-12,91	Ca-Mg-Cl
27-Oct-21	BGR5	River	45,60	29,64	7,65	18,20	4,31	1,37	3,89	0,48	10,98	1,78	8,69	4,78	0,57	BD	1,89	-3,58	-13,15	Ca-Mg-Cl
03-Nov-20	BGR6	River	95,00	61,75	6,48	27,00	4,55	1,68	12,57	1,40	10,98	5,73	22,95	0,07	3,19	0,00	1,75	-3,99	-13,90	Na-Cl
25-Nov-20	BGR6	River	88,40	57,46	6,99	18,70	1,55	0,92	9,14	0,60	0,00	3,52	19,12	-3,95	1,33	nd	1,82	-3,67	-14,40	Na-Cl
08-Dec-20	BGR6	River	32,40	21,06	7,36	19,50	0,72	0,61	3,76	0,10	6,10	BD	7,45	-3,38	0,24	0,00	1,72	-3,53	-12,80	Na-Cl
22-Dec-20	BGR6	River	49,20	31,98	7,71	23,20	0,80	0,53	4,03	0,17	7,32	BD	7,36	-4,56	0,41	nd	1,72	-3,47	-12,70	Na-Cl
13-Jan-21	BGR6	River	32,40	21,06	6,98	22,50	0,96	1,22	3,89	0,12	8,54	BD	6,17	0,99	0,69	nd	1,59	-3,35	-11,90	Na-Cl
25-Jan-21	BGR6	River	50,00	32,50	6,40	22,50	2,62	1,20	3,82	0,14	9,76	BD	8,48	0,02	0,37	0,00	1,09	-3,37	-11,80	Ca-Mg-Cl
08-Feb-21	BGR6	River	41,80	27,17	6,80	23,10	2,28	1,06	4,27	0,30	8,54	BD	8,61	1,46	0,36	0,10	1,63	-3,12	-11,20	Na-Cl
22-Feb-21	BGR6	River	45,20	29,38	6,87	21,60	2,21	0,96	4,55	0,32	7,32	BD	8,52	4,63	0,36	0,12	1,65	-3,40	-11,80	Na-Cl
08-Mar-21	BGR6	River	46,30	30,10	6,47	21,20	1,53	0,75	4,04	0,39	6,10	1,70	8,25	-3,64	0,48	BD	1,40	-3,06	-10,30	Na-Cl
24-Mar-21	BGR6	River	53,00	34,45	7,10	22,10	2,25	0,97	3,49	0,20	4,88	1,94	8,61	-2,09	0,44	BD	1,99	-3,15	-10,30	Ca-Mg-Cl
07-Apr-21	BGR6	River	66,90	43,49	7,45	21,10	2,85	1,01	4,06	0,41	6,10	2,30	9,72	-1,17	0,57	0,14	1,32	-2,90	-8,90	Ca-Mg-Cl
19-Apr-21	BGR6	River	35,00	22,75	7,56	19,80	3,27	1,33	3,26	0,11	10,98	BD	7,94	1,57	0,37	BD	1,62	-3,10	-12,40	Ca-Mg-Cl
03-May-21	BGR6	River	40,50	26,33	7,13	19,90	4,76	0,92	5,43	0,40	10,98	1,97	10,94	2,78	0,75	0,15	4,31	-3,04	-11,90	Ca-Mg-Cl
17-May-21	BGR6	River	71,40	46,41	6,80	14,40	2,59	1,68	6,81	0,39	6,10	2,38	14,12	2,33	0,88	BD	5,21	-3,18	-12,40	Na-Cl
31-May-21	BGR6	River	60,20	39,13	6,70	15,50	2,93	1,39	6,46	0,32	6,10	2,12	13,45	2,43	0,82	BD	2,45	-3,40	-12,30	Na-Cl
14-Jun-21	BGR6	River	70,40	45,76	6,60	15,20	5,91	1,88	6,80	0,35	14,64	2,71	15,68	1,05	1,17	BD	1,36	-3,20	-13,10	Ca-Mg-Cl
29-Jun-21	BGR6	River	49,50	32,18	7,39	12,90	4,17	1,64	5,13	0,40	17,08	1,94	10,57	-3,50	0,79	BD	0,98	-3,78	-15,30	Ca-Mg-Cl
12-Jul-21	BGR6	River	50,40	32,76	6,94	13,00	4,57	1,87	4,56	0,54	18,30	2,21	9,07	-0,66	0,73	BD	1,23	-3,22	-11,20	Ca-HCO3
26-Jul-21	BGR6	River	72,20	46,93	7,06	12,60	6,68	1,88	7,51	0,54	19,52	2,93	16,20	-0,56	1,61	BD	2,93	-3,55	-11,50	Ca-Mg-Cl
10-Aug-21	BGR6	River	69,10	44,92	7,18	13,40	6,87	3,33	5,82	0,13	21,96	2,60	14,72	2,59	1,45	BD	2,61	-3,22	-12,20	Ca-Mg-Cl
23-Aug-21	BGR6	River	73,70	47,91	4,47	13,40	4,09	2,05	5,61	0,45	10,98	2,72	13,21	1,58	1,31	BD	3,00	-3,36	-12,68	Ca-Mg-Cl
06-Sep-21	BGR6	River	54,20	35,23	7,09	12,10	5,18	1,68	4,81	0,39	15,86	2,38	9,91	2,26	0,92	BD	2,37	-3,31	-14,20	Ca-Mg-Cl
20-Sep-21	BGR6	River	66,50	43,23	7,27	13,50	2,72	2,02	5,95	0,46	10,98	2,59	11,29	1,75	0,97	BD	1,57	-3,07	-11,90	Ca-Mg-Cl
13-Oct-21	BGR6	River	66,90	43,49	6,52	16,60	2,60	1,62	7,53	0,64	2,44	3,04	17,09	1,81	1,90	nd	3,05	-3,23	-12,99	Na-Cl
27-Oct-21	BGR6	River	56,60	36,79	7,39	18,40	5,73	1,93	5,46	0,02	13,42	2,35	12,50	4,69	1,49	BD	2,84	-3,30	-11,59	Ca-Mg-Cl
03-Nov-20	BGR7	River	85,00	55,25	7,09	28,00	4,71	1,72	9,58	1,14	13,42	4,35	17,61	0,93	3,69	0,10	2,10	-3,85	-12,80	Na-Cl
25-Nov-20	BGR7	River	96,50	62,73	6,82	16,80	2,80	1,46	9,34	0,61	7,32	4,29	17,89	-2,30	1,51	0,00	2,01	-3,66	-13,30	Na-Cl
08-Dec-20	BGR7	River	39,50	25,68	6,72	19,90	0,94	0,79	4,25	0,26	1,22	1,83	8,90	-1,00	0,40	0,00	2,19	-3,43	-12,50	Na-Cl
22-Dec-20	BGR7	River	44,10	28,67	7,16	22,90	1,03	0,65	4,51	0,19	3,66	1,59	8,00	-2,03	1,25	nd	1,84	-3,39	-11,80	Na-Cl
13-Jan-21	BGR7	River	36,70	23,86	7,56	23,00	1,25	0,89	4,38	0,15	9,76	BD	6,74	-2,93	1,00	nd	1,48	-3,29	-10,90	Na-Cl
25-Jan-21	BGR7	River	50,00	32,50	6,74	24,50	3,28	1,16	3,25	0,10	12,20	BD	7,65	-1,51	0,39	0,00	1,73	-3,26	-11,00	Ca-Mg-Cl
08-Feb-21	BGR7	River	37,30	24,25	5,69	22,70	2,90	1,35	4,30	0,19	10,98	BD	8,15	4,36	0,45	0,00	1,19	-3,23	-11,20	Ca-Mg-Cl
22-Feb-21	BGR7	River	38,10	24,77	7,14	21,50	3,03	1,22	4,00	0,24	12,20	BD	8,18	0,14	0,66	BD	1,86	-3,23	-11,30	Ca-Mg-Cl
08-Mar-21	BGR7	River	39,10	25,42	6,43	20,90	1,42	0,66	4,07	0,22	1,22	1,73	8,18	3,48	0,90	BD	1,34	-3,00	-10,50	Na-Cl
24-Mar-21	BGR7	River	42,90	27,89	6,88	20,50	1,69	0,93	4,29	0,17	3,66	2,00	8,62	0,95	1,17	BD	1,61	-3,07	-10,60	Na-Cl
07-Apr-21	BGR7	River	45,70	29,71	7,31	20,60	0,14	0,59	4,81	0,34	0,00	2,22	9,15	-5,35	1,86	BD	1,53	-2,66	-8,10	Na-Cl
19-Apr-21	BGR7	River	39,30	25,55	7,23	20,50	3,29	1,30	4,12	0,27	9,76	1,42	8,13	4,36	1,06	BD	1,34	-3,10	-11,00	Ca-Mg-Cl
03-May-21	BGR7	River	51,70	33,61	7,40	19,30	4,19	1,24	5,53	0,60	17,08	1,94	10,25	-3,58	2,38	0,17	1,93	-3,02	-10,50	Ca-Mg-Cl
17-May-21	BGR7	River	73,70	47,91	8,26	14,00	3,79	1,79	6,82	0,91	10,98	2,64	12,89	4,64	1,59	BD	2,63	-2,99	-12,60	Ca-Mg-Cl
31-May-21	BGR7	River	72,90	47,39	7,56	14,20	6,81	1,94	7,19	0,83	19,52	2,80	13,48	4,68	1,37	BD	3,33	-3,01	-11,00	Ca-Mg-Cl
14-Jun-21	BGR7	River	75,60	49,14	7,07	13,50	7,08	1,95	7,14	0,66	19,52	2,88	13,87	4,37	1,96	0,17	1,79	-2,86	-9,50	Ca-Mg-Cl
29-Jun-21	BGR7	River	79,00	51,35	7,45	12,80	6,88	2,24	6,45	1,12	24,40	3,04	12,90	4,60	1,66	BD	1,84	-3,51	-12,50	Ca-HCO3
12-Jul-21	BGR7	River	57,00	37,05	7,43	11,60	5,60	1,76	4,66	1,03	20,74	2,52	10,01	-1,65	0,89	BD	1,58	-3,08	-10,60	Ca-HCO3
26-Jul-21	BGR7	River	68,50	44,53	7,51	12,30	8,35	1,36	5,26	0,50	18,30	3,28	12,37	3,53	1,21	BD	2,18	-3,33	-12,90	Ca-Mg-Cl
10-Aug-21	BGR7	River	52,00	33,80	7,71	11,80	3,06	2,17	4,48	0,15	14,64	2,25	9,11	-1,30	0,72	BD	2,19	-3,27	-11,59	Ca-Mg-Cl
23-Aug-21	BGR7	River	67,50	43,88	6,75	12,80	1,34	2,11	6,30	0,45	7,32	3,09	11,72	1,58	1,08	BD	1,87	-3,25	-12,18	Na-Cl
06-Sep-21	BGR7	River	56,40	36,66	7,12	11,50	4,67	1,93	4,82	0,63	17,08	2,51	9,67	1,03	0,93	BD	2,61	-3,07	-10,82	Ca-Mg-Cl
20-Sep-21	BGR7	River	75,00	48,75	7,42	12,10	4,68	2,07	6,97	0,89	15,86	3,09	12,86	2,99	1,25	BD	1,68	-3,43	-12,95	Ca-Mg-Cl
13-Oct-21	BGR7	River	89,20	57,98	7,22	16,30	1,53	1,15	8,79	0,99	1,22	4,97	17,70	-3,70	1,77	BD	3,98	-3,45	-13,04	Na-Cl
27-Oct-21	BGR7	River	46,90	30,49	8,14	17,80	5,18	1,67	4,23	0,56	15,86	1,93	9,20	2,97	0,81	BD	2,83	-3,57	-13,41	Ca-Mg-Cl
03-Nov-20	G1H078	River	108,40	70,46	7,75	17,10	4,64	1,80	8,45	2,95	21,96	4,17	13,92	-1,01	5,57	0,44	5,30	-3,80	-12,40	Na-Cl
25-Nov-20	G1H078	River	119,30	77,55	7,18	17,90	3,74	1,80	11,34	1,01	14,64	5,34	19,10	-2,04	2,69	0,00	6,38	-3,91	-13,70	Na-Cl
08-Dec-20	G1H078	River	131,10	85,22	6,79	21,50	5,67	1,74	12,09	2,48	18,30	6,62	20,15	0,47	4,00	0,15	6,22	-3,46	-12,90	Na-Cl
22-Dec-20	G1H078	River	152,90	99,39	7,11	23,60	7,18	2,05	13,38	2,86	28,06	7,03	20,25	0,21	8,10	0,13	6,53	-3,51	-14,10	Na-Cl
13-Jan-21	G1H078	River	152,10	98,87	7,30	24,60	10,66	2,98	13,80	3,08	39,04	6,36	21,34	2,91	5,63	0,14	6,85	-3,37	-11,60	Ca-Mg-Cl
25-Jan-21	G1H078	River	125,00	81,25	6,18	23,00	5,17	2,23	10,53	1,71	20,74	5,44	18,63	-1,87	6,08	0,18	5,90	-3,36	-11,70	Na-Cl
08-Feb-21	G1H078	River	97,70	63,51	6,85	21,30	3,02	2,29	9,47	1,59	19,52	3,35	15,05	-1,36	0,14	0,15	3,48	-3,34	-11,00	Na-Cl
22-Feb-21	G1H078	River	127,10	82,62	6,71	17,90	3,89	1,75	13,37	2,16	21,96	6,45	19,63	-3,60	5,22	0,15	3,87	-2,94	-10,40	Na-Cl
08-Mar-21	G1H078	River	129,30	84,05	5,92	18,50	4,95	2,30	13,71	1,66	21,96	6,94	20,11	0,15	5,22	BD	3,59	-3,08	-11,20	Na-Cl
24-Mar-21	G1H078	River	131,70	85,61	7,18	20,00	9,59	1,56	9,53	1,71	25,62	4,78	20,34	-1,31	9,39	0,69	4,57	-3,32	-10,90	Ca-Mg-Cl
07-Apr-21	G1H078	River	136,10	88,47	7,17	18,60	6,72	2,35	11,91	1,38	15,86	9,08	19,63	3,81	10,28	0,21	5,12	-3,09	-11,70	Na-Cl
19-Apr-21	G1H078	River	124,40	80,86	6,78	18,40	6,20	2,88	12,22	2,05	24,40	5,96	18,30	4,15	4,91	0,24	5,52	-3,20	-11,20	Na-Cl
03-May-21	G1H078	River	122,70	79,76	7,03	15,10	7,30	1,79	12,12	2,04	23,18	5,31	18,79	3,34	5,54	0,28	6,06	-3,44	-12,20	Na-Cl
17-May-21	G1H078	River	83,60	54,34	7,06	12,20	6,17	1,88	7,23	0,83	20,74	2,78	12,77	2,55	1,66	0,10	2,87	-3,51	-14,90	Ca-Mg-Cl
31-May-21	G1H078	River	79,80	51,87	7,42	13,30	6,82	2,13	7,12	1,02	20,74	3,39	12,93	4,68	1,80	0,16	2,14	-3,38	-12,90	Ca-Mg-Cl
14-Jun-21	G1H078	River	143,40	93,21	7,00	12,20	11,87	2,92	12,17	2,40	36,60	6,66	19,83	4,58	7,85	0,70	2,05	-3,28	-11,40	Ca-Mg-Cl
29-Jun-21	G1H078	River	79,70	51,81	7,46	12,00	8,30	2,27	5,85	1,32	25,62	3,17	11,51	4,60	2,41	0,28	2,30	-4,04	-14,80	Ca-HCO3
12-Jul-21	G1H078	River	101,40	65,91	7,15	11,00	10,64	2,86	7,08	1,39	37,82	4,26	14,69	-0,59	2,96	0,19	1,43	-3,51	-13,90	Ca-HCO3
26-Jul-21	G1H078	River	109,00	70,85	7,19	11,30	10,27	2,92	8,25	1,15	30,50	4,81	16,00	4,10	3,49	0,09	6,13	-2,88	-8,40	Ca-Mg-Cl
10-Aug-21	G1H078	River	109,60	71,24	7,64	10,40	10,14	3,15	6,66	0,88	32,94	4,10	14,83	1,59	2,71	0,17	2,90	-3,33	-11,61	Ca-HCO3
23-Aug-21	G1H078	River	128,40	83,46	6,72	10,80	6,74	2,34	8,15	1,25	21,96	4,57	15,68	1,00	3,16	0,21	3,84	-3,47	-14,09	Ca-Mg-Cl
06-Sep-21	G1H078	River	69,70	45,31	6,57	12,10	1,77	1,02	5,58	0,55	3,66	2,89	10,71	0,85	1,62	0,09	2,82	-3,82	-13,27	Na-Cl
20-Sep-21	G1H078	River	104,10	67,67	8,16	14,70	9,03	2,57	8,59	1,19	31,72	4,00	14,68	2,37	2,59	BD	3,80	-3,72	-12,36	Ca-HCO3
13-Oct-21	G1H078	River	114,60	74,49	7,38	15,50	10,84	2,66	10,94	1,98	35,38	4,83	17,46	4,62	3,26	0,43	6,71	-3,30	-11,20	Ca-Mg-Cl
27-Oct-21	G1H078	River	108,90	70,79	7,51	16,90	3,57	1,66	7,82	1,28	7,32	4,06	16,26	1,77	3,52	0,19	4,02	-2,93	-9,84	Na-Cl
03-Nov-20	DWARS 1	River	130,00	84,50	6,69	27,50	6,24	2,16	13,08	2,89	23,18	7,01	21,45	0,02	7,89	0,48	5,33	-3,82	-13,40	Na-Cl
25-Nov-20	DWARS 1	River	137,00	89,05	6,45	16,40	6,44	2,35	12,56	1,81	21,96	7,08	21,19	0,10	3,76	0,00	4,91	-3,52	-12,90	Na-Cl
08-Dec-20	DWARS 1	River	129,70	84,31	6,95	20,70	7,02	1,48	12,79	2,23	20,74	7,19	22,05	-1,17	2,41	nd	5,74	-3,16	-11,70	Na-Cl
22-Dec-20	DWARS 1	River	163,80	106,47	6,83	21,70	7,76	2,50	14,90	2,46	29,28	8,39	24,61	-1,67	3,25	nd	4,08	-3,51	-14,20	Na-Cl
13-Jan-21	DWARS 1	River	137,00	89,05	7,78	21,80	9,78	3,00	12,34	2,18	31,72	7,23	23,19	0,11	0,96	nd	4,50	-3,00	-10,80	Ca-Mg-Cl
25-Jan-21	DWARS 1	River	145,00	94,25	6,13	20,50	8,50	2,65	13,29	2,45	21,96	6,77	25,45	2,56	0,04	0,00	3,58	-3,29	-10,70	Ca-Mg-Cl
08-Feb-21	DWARS 1	River	140,40	91,26	7,07	19,80	7,86	3,09	13,20	2,40	21,96	7,26	25,05	2,58	0,00	nd	4,17	-3,39	-11,20	Ca-Mg-Cl
22-Feb-21	DWARS 1	River	138,40	89,96	6,97	18,10	4,94	1,83	9,17	1,78	2,44	7,92	25,00	-3,92	0,13	BD	5,74	-3,15	-10,90	Na-Cl
08-Mar-21	DWARS 1	River	130,10	84,57	5,92	18,90	6,70	2,05	12,85	2,34	23,18	7,73	22,90	-2,83	0,15	BD	3,86	-3,19	-11,70	Na-Cl
24-Mar-21	DWARS 1	River	145,10	94,32	6,52	19,40	9,19	2,19	10,55	1,75	18,30	8,02	24,12	-0,20	0,11	BD	2,23	-3,11	-10,50	Ca-Mg-Cl
07-Apr-21	DWARS 1	River	140,70	91,46	6,95	18,50	10,52	1,86	11,71	1,91	18,30	8,18	24,00	3,73	0,06	BD	3,18	-2,99	-11,20	Ca-Mg-Cl
19-Apr-21	DWARS 1	River	144,20	93,73	6,89	18,20	11,59	2,32	13,32	2,14	26,84	7,42	24,57	4,29	BD	BD	3,02	-2,99	-10,30	Ca-Mg-Cl
03-May-21	DWARS 1	River	153,50	99,78	6,73	16,10	11,77	2,45	15,17	2,98	31,72	7,98	25,81	3,78	1,91	BD	5,01	-3,38	-13,20	Ca-Mg-Cl
17-May-21	DWARS 1	River	87,80	57,07	7,76	12,20	4,77	1,57	7,38	0,99	14,64	3,22	13,28	2,29	2,04	0,12	5,68	-3,34	-14,10	Ca-Mg-Cl
31-May-21	DWARS 1	River	83,40	54,21	7,63	12,80	4,67	2,70	7,79	1,09	18,30	3,72	13,63	3,81	2,55	0,15	3,30	-3,16	-10,60	Ca-Mg-Cl
14-Jun-21	DWARS 1	River	140,70	91,46	7,01	11,70	13,04	2,22	12,04	2,18	35,38	6,85	20,32	4,34	10,88	0,49	3,03	-2,99	-10,00	Ca-Mg-Cl
29-Jun-21	DWARS 1	River	85,10	55,32	8,18	12,80	8,34	2,35	6,71	1,49	25,62	3,54	12,78	4,77	2,87	0,17	0,59	-3,63	-13,30	Ca-Mg-Cl
12-Jul-21	DWARS 1	River	104,90	68,19	7,40	10,90	11,81	2,96	7,36	1,51	40,26	4,82	15,06	0,31	2,97	0,15	1,37	-3,53	-13,30	Ca-HCO3
26-Jul-21	DWARS 1	River	114,00	74,10	7,77	14,10	11,56	2,88	8,61	1,24	31,72	5,53	17,38	4,07	3,74	BD	3,41	-2,99	-11,20	Ca-Mg-Cl
10-Aug-21	DWARS 1	River	116,70	75,86	7,95	13,50	11,95	3,23	7,80	1,04	35,38	5,05	16,54	3,20	3,55	0,14	3,52	-3,64	-11,32	Ca-HCO3
23-Aug-21	DWARS 1	River	116,60	75,79	6,64	13,00	8,29	3,42	8,85	1,47	25,62	5,37	17,18	4,76	4,26	0,17	3,90	-3,76	-12,21	Ca-Mg-Cl
06-Sep-21	DWARS 1	River	87,30	56,75	7,27	11,00	7,55	2,11	6,91	0,88	23,18	3,75	12,80	3,21	2,07	BD	2,24	-3,79	-13,39	Ca-Mg-Cl
20-Sep-21	DWARS 1	River	110,50	71,83	7,71	11,80	9,62	2,63	9,25	1,45	29,28	4,59	16,27	4,68	3,19	BD	3,96	-3,51	-11,92	Ca-Mg-Cl
13-Oct-21	DWARS 1	River	103,70	67,41	7,04	16,30	10,36	2,78	9,20	2,24	34,16	5,08	16,48	3,12	4,68	0,29	3,41	-2,53	-6,32	Ca-Mg-Cl
27-Oct-21	DWARS 1	River	116,80	75,92	7,90	18,70	7,73	2,38	8,10	1,33	19,52	4,96	18,16	1,72	5,64	0,20	4,30	-2,75	-8,81	Ca-Mg-Cl
03-Nov-20	BGR8	River	110,00	71,50	7,20	27,00	4,77	1,77	10,28	0,00	13,42	4,89	18,66	-1,05	4,70	0,14	2,02	-3,74	-12,80	Na-Cl
25-Nov-20	BGR8	River	113,80	73,97	6,52	16,20	2,14	1,07	10,65	0,88	2,44	5,24	19,86	-2,11	2,10	0,00	1,99	-3,55	-13,40	Na-Cl
08-Dec-20	BGR8	River	41,80	27,17	6,87	19,30	1,20	0,87	4,29	0,00	2,44	1,93	9,21	-2,26	0,47	0,00	2,04	-3,37	-12,50	Na-Cl
22-Dec-20	BGR8	River	45,40	29,51	7,08	21,60	0,96	0,66	4,47	0,21	3,66	1,58	7,94	-2,50	1,15	0,00	1,95	-3,50	-13,30	Na-Cl
13-Jan-21	BGR8	River	39,20	25,48	7,02	21,80	1,22	0,74	4,62	0,29	6,10	1,59	7,49	-2,17	0,81	nd	1,81	-3,41	-12,90	Na-Cl

Date	Sample ID	Data Source	EC	TDS	pH	Temp	Ca^{2+}	Mg^{2+}	Na^{+}	K^{+}	HCO_3^{-}	SO_4^{2-}	Cl^{-}	CB	NO_3^{-}	PO_4^{3-}	SiO_2	$\delta^{18}O$	$\delta^{2}H$	Water Type
25-Jan-21	BGR8	River	135,00	87,75	7,03	16,00	4,26	0,95	3,43	0,16	12,20	BD	8,04	2,00	0,50	0,00	1,72	-3,27	-11,90	Ca-Mg-Cl
08-Feb-21	BGR8	River	40,90	26,59	6,67	21,50	2,71	1,35	4,36	0,19	10,98	BD	8,27	3,20	0,46	0,00	1,81	-3,06	-11,00	Ca-Mg-Cl
22-Feb-21	BGR8	River	40,10	26,07	6,34	20,40	3,04	1,28	4,23	0,24	9,76	BD	8,36	-0,93	0,72	BD	1,85	-3,17	-11,10	Ca-Mg-Cl
08-Mar-21	BGR8	River	39,60	25,74	6,17	20,60	1,52	0,86	3,96	0,20	4,88	1,76	8,32	-4,06	0,82	BD	0,80	-3,03	-11,00	Na-Cl
24-Mar-21	BGR8	River	48,00	31,20	7,16	19,80	1,75	0,71	4,03	0,18	3,66	2,17	9,03	-2,18	1,23	BD	1,80	-3,13	-10,80	Na-Cl
07-Apr-21	BGR8	River	44,50	28,93	7,28	19,30	3,25	1,10	3,72	0,24	14,64	2,13	9,12	2,31	1,80	BD	1,92	-2,76	-8,80	Ca-Mg-Cl
19-Apr-21	BGR8	River	44,10	28,67	6,90	18,70	3,84	1,29	3,76	0,16	8,54	1,77	9,23	3,11	1,39	BD	1,52	-2,58	-9,10	Ca-Mg-Cl
03-May-21	BGR8	River	52,60	34,19	6,65	17,70	3,92	1,33	5,21	0,35	17,08	1,94	10,19	-2,41	2,24	0,14	1,93	-2,82	-9,20	Ca-Mg-Cl
17-May-21	BGR8	River	80,50	52,33	7,14	13,10	3,28	1,05	6,59	0,66	7,32	2,91	13,31	-0,29	1,81	BD	1,45	-3,12	-13,40	Na-Cl
31-May-21	BGR8	River	67,70	44,01	7,21	13,60	4,67	2,70	7,79	1,09	9,76	3,72	13,63	-0,58	2,55	BD	2,01	-3,21	-10,50	Ca-Mg-Cl
14-Jun-21	BGR8	River	98,10	63,77	6,91	12,30	13,04	2,22	12,04	2,18	21,96	6,85	20,32	4,40	10,88	0,35	2,10	-2,83	-9,80	Ca-Mg-Cl
29-Jun-21	BGR8	River	86,10	55,97	7,72	11,30	9,74	2,51	6,01	1,08	29,28	3,52	12,61	3,84	2,83	0,18	2,07	-3,95	-15,90	Ca-HCO3
12-Jul-21	BGR8	River	101,00	65,65	7,41	10,60	7,20	2,47	7,00	1,40	26,84	4,69	14,78	-2,81	2,86	0,16	2,37	-3,20	-11,90	Ca-Mg-Cl
26-Jul-21	BGR8	River	102,90	66,89	7,48	12,10	7,14	2,44	7,65	1,08	18,30	4,80	15,86	3,94	2,90	BD	2,59	-2,84	-10,10	Ca-Mg-Cl
10-Aug-21	BGR8	River	61,90	40,24	8,02	13,00	5,58	3,03	7,23	0,61	18,30	4,38	14,81	2,98	2,79	0,10	4,30	-3,33	-11,24	Ca-Mg-Cl
23-Aug-21	BGR8	River	77,70	50,51	6,15	12,80	4,27	1,38	6,29	0,67	12,20	3,15	12,06	0,93	1,18	BD	2,37	-3,43	-11,82	Ca-Mg-Cl
06-Sep-21	BGR8	River	87,60	56,94	7,14	10,70	8,53	2,30	7,22	1,22	30,50	3,70	12,69	1,33	2,03	BD	2,58	-4,01	-14,45	Ca-HCO3
20-Sep-21	BGR8	River	84,30	54,80	7,51	12,00	2,02	1,10	7,15	0,94	7,32	3,27	13,30	-3,34	1,44	BD	2,85	-3,49	-11,91	Na-Cl
13-Oct-21	BGR8	River	92,80	60,32	7,12	16,40	6,31	2,26	9,54	1,86	20,74	4,91	17,26	1,82	2,73	0,10	3,21	-3,09	-8,92	Ca-Mg-Cl
27-Oct-21	BGR8	River	51,60	33,54	7,96	17,60	5,49	1,57	4,15	0,52	17,08	1,97	9,35	0,98	0,83	BD	2,53	-3,09	-10,85	Ca-Mg-Cl
25-Nov-20	BGR9	River	109,50	71,18	7,05	16,30	3,88	1,65	10,50	1,04	6,10	5,06	19,56	3,54	1,91	0,00	1,89	-3,55	-13,10	Na-Cl
08-Dec-20	BGR9	River	42,00	27,30	6,86	19,00	1,20	0,81	4,45	0,31	2,44	1,96	9,34	-2,37	0,48	0,00	1,28	-3,56	-12,60	Na-Cl
22-Dec-20	BGR9	River	44,60	28,99	7,11	21,50	1,11	0,70	4,51	0,19	3,66	1,65	8,20	-1,83	0,78	0,00	1,87	-3,37	-12,20	Na-Cl
13-Jan-21	BGR9	River	37,00	24,05	7,09	21,90	1,68	0,99	4,12	0,22	8,54	1,56	7,66	3,15	0,46	nd	1,50	-3,31	-10,90	Na-Cl
25-Jan-21	BGR9	River	45,00	29,25	6,12	21,50	2,57	1,14	3,74	0,09	4,88	BD	7,87	-1,91	0,49	0,00	1,69	-3,23	-11,20	Ca-Mg-Cl
08-Feb-21	BGR9	River	37,60	24,44	6,64	21,70	2,64	1,25	4,45	0,22	12,20	BD	8,14	0,42	0,45	0,00	1,71	-3,03	-11,10	Ca-Mg-Cl
22-Feb-21	BGR9	River	39,40	25,61	6,64	20,50	2,89	1,24	4,38	0,25	10,98	BD	8,43	2,86	0,72	BD	1,48	-3,23	-10,90	Ca-Mg-Cl
08-Mar-21	BGR9	River	38,10	24,77	5,56	20,60	1,56	0,68	3,80	0,17	4,88	1,69	8,13	-3,29	0,79	0,00	1,60	-3,13	-10,90	Na-Cl
24-Mar-21	BGR9	River	45,10	29,32	7,13	19,90	1,59	0,82	3,62	0,82	3,66	2,10	9,15	-2,59	1,29	0,09	2,40	-3,12	-10,90	Na-Cl
07-Apr-21	BGR9	River	44,60	28,99	7,12	19,40	2,27	0,84	3,89	0,19	2,44	2,12	8,90	3,06	1,77	BD	1,71	-2,99	-10,10	Ca-Mg-Cl
19-Apr-21	BGR9	River	43,00	27,95	6,70	18,70	3,48	1,32	4,09	0,18	9,76	1,52	8,53	3,61	1,42	0,18	1,48	-3,00	-10,20	Ca-Mg-Cl
03-May-21	BGR9	River	53,90	35,04	6,33	17,60	3,54	1,05	5,79	1,10	9,76	2,05	10,46	4,37	2,26	0,14	1,60	-2,29	-6,90	Na-Cl
17-May-21	BGR9	River	82,20	53,43	6,80	13,10	4,52	1,46	7,19	0,80	13,42	3,00	13,40	1,38	1,87	0,09	2,40	-2,90	-10,50	Ca-Mg-Cl
31-May-21	BGR9	River	74,00	48,10	7,21	13,50	4,98	1,65	7,08	0,85	13,42	2,99	13,16	4,44	1,84	BD	2,92	-3,36	-12,90	Ca-Mg-Cl
14-Jun-21	BGR9	River	88,40	57,46	6,99	12,40	2,60	2,53	10,16	1,34	12,20	5,03	17,55	0,92	6,67	0,26	0,76	-2,64	-8,10	Na-Cl
29-Jun-21	BGR9	River	84,90	55,19	7,64	11,50	9,36	2,43	6,94	1,14	28,06	3,52	13,55	4,32	2,67	0,17	1,87	-4,73	-21,70	Ca-HCO3
12-Jul-21	BGR9	River	89,60	58,24	7,52	11,00	3,99	3,51	7,12	1,23	23,18	4,09	13,61	-1,20	2,34	0,10	2,09	-3,95	-14,90	Ca-Mg-Cl
26-Jul-21	BGR9	River	97,40	63,31	7,32	12,00	1,95	2,12	8,21	1,05	13,42	4,24	14,84	-2,33	2,23	BD	2,37	-3,46	-12,70	Na-Cl
10-Aug-21	BGR9	River	85,70	55,71	7,72	12,90	6,41	2,17	5,26	0,34	15,86	3,38	12,31	4,11	1,76	BD	2,83	-2,74	-8,79	Ca-Mg-Cl
23-Aug-21	BGR9	River	82,10	53,37	6,92	13,00	7,30	2,17	6,38	0,59	20,74	3,61	13,20	2,98	1,81	BD	3,91	-3,59	-13,64	Ca-Mg-Cl
06-Sep-21	BGR9	River	85,80	55,77	7,18	10,80	5,78	2,00	6,46	0,72	17,08	3,63	12,48	3,10	1,95	BD	3,22	-3,91	-13,91	Ca-Mg-Cl
20-Sep-21	BGR9	River	101,40	65,91	7,52	12,20	5,58	2,02	7,51	0,87	15,86	3,53	13,77	4,73	1,80	BD	3,53	-3,76	-12,87	Ca-Mg-Cl
13-Oct-21	BGR9	River	95,70	62,21	7,06	16,50	8,54	2,54	9,64	1,87	25,62	4,95	17,46	4,09	2,72	0,11	3,52	-3,24	-10,97	Ca-Mg-Cl
27-Oct-21	BGR9	River	50,80	33,02	7,97	18,80	5,19	2,03	4,21	0,25	14,64	2,12	9,83	4,60	1,20	BD	1,86	-3,37	-12,12	Ca-Mg-Cl
03-Nov-20	BGR10	River	112,50	73,13	7,36	18,30	5,08	2,13	10,62	1,83	17,08	5,55	19,38	-0,25	4,86	BD	1,39	-3,88	-12,50	Na-Cl
25-Nov-20	BGR10	River	125,00	81,25	6,26	17,30	5,12	2,02	12,23	0,78	14,64	6,25	22,59	-1,68	2,69	nd	1,49	-3,43	-12,70	Na-Cl
08-Dec-20	BGR10	River	49,30	32,05	7,38	19,60	0,29	0,64	6,39	0,44	1,22	2,41	10,28	-0,50	0,72	0,00	2,04	-3,65	-12,80	Na-Cl
13-Jan-21	BGR10	River	43,30	28,15	8,38	22,10	1,64	0,98	4,78	0,27	9,76	1,66	7,45	-3,52	0,95	nd	1,29	-3,33	-12,90	Na-Cl
25-Jan-21	BGR10	River	47,00	30,55	5,73	20,00	2,81	1,22	3,64	0,06	10,98	BD	8,38	-1,98	0,44	0,00	1,69	-3,39	-11,10	Ca-Mg-Cl
08-Feb-21	BGR10	River	40,20	26,13	8,29	20,90	2,61	1,28	4,39	0,26	12,20	BD	8,42	-0,51	0,42	0,00	1,65	-3,02	-11,00	Ca-Mg-Cl
22-Feb-21	BGR10	River	40,60	26,39	7,29	19,00	3,00	1,32	4,36	0,21	10,98	BD	8,67	3,31	0,65	BD	1,57	-3,16	-10,70	Ca-Mg-Cl
08-Mar-21	BGR10	River	41,10	26,72	6,26	19,60	1,78	0,62	4,06	0,27	7,32	1,86	8,38	-1,80	0,86	BD	1,31	-3,01	-10,60	Na-Cl
24-Mar-21	BGR10	River	47,70	31,01	7,92	20,30	2,19	1,15	4,33	0,20	4,88	2,19	9,37	0,96	1,41	BD	1,24	-3,02	-9,90	Ca-Mg-Cl
07-Apr-21	BGR10	River	49,50	32,18	7,60	19,40	2,44	1,19	4,61	0,26	4,88	2,43	9,91	2,02	1,88	BD	1,84	-2,81	-10,00	Ca-Mg-Cl
19-Apr-21	BGR10	River	47,40	30,81	7,76	18,90	3,65	1,27	4,91	0,42	10,98	1,71	9,15	3,73	1,70	BD	1,58	-2,79	-9,90	Ca-Mg-Cl
03-May-21	BGR10	River	57,90	37,64	6,70	16,80	3,79	1,28	6,30	0,71	10,98	2,38	11,44	3,03	2,11	BD	2,41	-2,60	-8,90	Ca-Mg-Cl
17-May-21	BGR10	River	83,50	54,28	7,15	13,60	5,88	1,73	7,37	1,35	17,08	3,18	13,74	3,75	1,72	0,11	1,63	-2,86	-10,70	Ca-Mg-Cl
31-May-21	BGR10	River	96,70	62,86	7,79	13,90	8,62	2,47	9,28	2,10	28,06	4,14	16,52	3,73	2,69	0,16	2,41	-2,57	-7,30	Ca-Mg-Cl
14-Jun-21	BGR10	River	114,80	74,62	7,63	12,70	8,45	2,49	10,60	2,20	26,84	4,53	18,60	3,86	4,16	0,30	2,18	-2,79	-8,90	Ca-Mg-Cl
29-Jun-21	BGR10	River	100,40	65,26	6,90	12,30	10,24	3,34	89,13	0,42	90,28	26,08	79,40	4,60	5,62	0,65	7,32	-2,58	-9,50	Na-Cl
12-Jul-21	BGR10	River	92,40	60,06	7,52	11,90	8,70	2,75	6,71	1,56	32,94	4,35	14,18	-1,90	1,90	0,17	1,42	-3,57	-13,70	Ca-HCO3
26-Jul-21	BGR10	River	103,10	67,02	7,14	12,00	9,96	2,67	8,34	1,65	28,06	5,12	16,81	3,77	2,30	BD	2,68	-2,88	-11,20	Ca-Mg-Cl
10-Aug-21	BGR10	River	86,30	56,10	7,56	11,40	8,65	2,81	6,19	0,73	25,62	3,63	13,30	4,38	1,61	0,08	2,40	-2,88	-10,05	Ca-Mg-Cl
23-Aug-21	BGR10	River	103,40	67,21	6,16	13,20	3,58	3,49	8,25	1,46	18,30	4,68	15,91	0,94	2,11	BD	3,17	-3,78	-12,76	Ca-Mg-Cl
06-Sep-21	BGR10	River	77,50	50,38	7,47	11,60	4,48	1,57	6,22	0,91	13,42	3,52	12,20	0,65	1,45	BD	1,32	-3,95	-12,72	Ca-Mg-Cl
20-Sep-21	BGR10	River	111,80	72,67	7,04	13,50	9,74	2,69	9,62	1,62	30,50	4,88	17,59	3,06	2,35	BD	2,21	-3,58	-13,03	Ca-Mg-Cl
13-Oct-21	BGR10	River	121,10	78,72	7,18	17,30	11,55	3,13	12,24	2,48	40,26	6,10	21,55	1,24	3,30	0,11	3,54	-3,55	-14,63	Ca-Mg-Cl
27-Oct-21	BGR10	River	61,80	40,17	7,90	18,10	2,21	1,70	5,77	0,82	7,32	2,55	10,90	4,16	1,42	BD	2,41	-3,04	-10,24	Na-Cl
03-Nov-20	BGR11	River	122,00	79,30	7,04	20,20	5,20	2,43	11,43	2,31	14,64	6,81	21,10	1,92	5,46	0,00	1,97	-3,48	-11,00	Na-Cl
25-Nov-20	BGR11	River	143,50	93,28	7,38	20,90	6,59	1,79	13,41	1,68	18,30	7,68	24,72	-2,44	3,27	nd	1,96	-3,35	-12,50	Na-Cl
08-Dec-20	BGR11	River	54,00	35,10	7,22	21,00	1,57	1,24	5,24	0,60	3,66	2,80	11,05	-0,78	1,05	0,00	1,97	-3,54	-11,90	Na-Cl
22-Dec-20	BGR11	River	54,50	35,43	7,39	24,60	1,52	0,88	5,18	0,44	10,98	2,09	9,15	0,47	0,95	0,00	1,96	-3,27	-11,40	Na-Cl
13-Jan-21	BGR11	River	46,40	30,16	6,73	23,20	1,75	1,01	5,22	0,40	9,76	2,02	8,37	-3,57	1,08	nd	1,85	-3,37	-11,70	Na-Cl
25-Jan-21	BGR11	River	115,00	74,75	7,58	27,20	2,54	1,12	3,35	0,07	6,10	1,46	8,67	-1,23	0,45	0,00	1,72	-3,22	-10,90	Ca-Mg-Cl
08-Feb-21	BGR11	River	45,70	29,71	6,15	24,10	3,08	1,35	4,35	0,26	8,54	1,42	8,89	4,54	0,48	0,00	1,64	-3,11	-10,50	Ca-Mg-Cl
22-Feb-21	BGR11	River	43,00	27,95	6,99	21,50	3,01	1,38	4,49	0,36	9,76	1,53	9,08	2,18	0,76	0,00	1,84	-3,17	-11,50	Ca-Mg-Cl
08-Mar-21	BGR11	River	43,40	28,21	5,80	21,00	1,51	0,80	4,46	0,31	4,88	2,10	8,74	-3,81	1,19	BD	1,35	-2,89	-9,90	Na-Cl
24-Mar-21	BGR11	River	52,80	34,32	7,37	21,80	2,74	1,38	4,08	0,30	8,54	2,62	9,87	-4,14	2,16	BD	1,76	-3,02	-10,10	Ca-Mg-Cl
07-Apr-21	BGR11	River	61,40	39,91	7,13	21,90	1,78	1,19	5,02	0,58	3,66	3,45	11,30	-3,46	3,03	BD	1,86	-2,41	-9,00	Na-Cl
19-Apr-21	BGR11	River	51,20	33,28	7,49	20,40	3,80	1,47	4,74	0,43	10,98	2,10	9,70	2,96	2,21	BD	1,49	-2,76	-9,40	Ca-Mg-Cl
03-May-21	BGR11	River	65,40	42,51	7,23	19,70	3,39	1,52	6,49	1,00	9,76	3,02	12,06	3,41	2,96	BD	1,44	-2,79	-10,00	Na-Cl
17-May-21	BGR11	River	112,20	72,93	6,94	15,50	4,64	1,98	9,55	1,76	8,54	5,18	19,24	3,89	2,70	0,09	2,94	-3,47	-13,70	Na-Cl
31-May-21	BGR11	River	114,00	74,10	7,34	14,70	10,05	3,31	12,39	2,65	31,72	5,76	22,27	4,23	3,41	0,21	2,26	-3,21	-11,90	Ca-Mg-Cl
14-Jun-21	BGR11	River	119,20	77,48	7,59	14,70	9,28	2,98	10,43	2,37	29,28	5,02	19,34	3,92	4,39	0,27	1,11	-2,81	-9,20	Ca-Mg-Cl
29-Jun-21	BGR11	River	118,00	76,70	7,30	12,50	7,85	3,88	12,93	2,53	34,16	4,68	19,87	4,70	2,88	0,20	0,97	-2,67	-10,20	Ca-Mg-Cl
12-Jul-21	BGR11	River	114,70	74,56	7,00	12,70	11,16	2,45	8,15	1,86	34,16	5,30	18,55	-1,38	2,40	0,17	1,07	-3,56	-13,40	Ca-Mg-Cl
26-Jul-21	BGR11	River	129,10	83,92	6,55	12,70	11,66	2,94	9,85	1,99	28,06	6,57	21,14	4,41	3,06	BD	2,84	-2,67	-10,20	Ca-Mg-Cl
10-Aug-21	BGR11	River	103,00	66,95	7,44	11,30	3,11	2,43	7,57	0,94	7,32	4,37	16,22	2,87	1,97	BD	2,83	-3,16	-11,05	Ca-Mg-Cl
23-Aug-21	BGR11	River	118,20	76,83	6,69	13,50	9,75	2,95	9,38	1,84	29,28	5,49	19,05	2,27	2,55	BD	2,76	-3,77	-12,11	Ca-Mg-Cl
06-Sep-21	BGR11	River	93,20	60,58	7,35	13,60	5,01	2,69	7,84	1,24	17,08	4,34	14,68	3,69	1,88	BD	2,52	-3,75	-11,26	Ca-Mg-Cl
20-Sep-21	BGR11	River	123,30	80,15	7,32	15,00	8,64	3,07	10,82	1,78	28,06	5,54	19,45	3,28	2,74	BD	2,97	-3,28	-11,06	Ca-Mg-Cl
13-Oct-21	BGR11	River	126,90	82,49	6,80	18,40	10,50	3,84	13,24	3,27	35,38	7,29	23,75	3,37	4,67	0,10	2,82	-3,28	-13,86	Ca-Mg-Cl
27-Oct-21	BGR11	River	70,10	45,57	7,10	20,60	2,54	1,30	6,08	1,02	7,32	3,14	12,43	-1,19	2,15	BD	2,77	-3,32	-12,09	Na-Cl
03-Nov-20	BGR12	River	111,20	72,28	7,61	18,30	5,12	2,23	10,22	2,23	15,86	6,16	18,29	1,96	4,80	BD	2,12	-3,12	-9,50	Na-Cl
25-Nov-20	BGR12	River	136,40	88,66	6,91	19,70	6,20	2,62	13,58	1,92	12,20	7,91	25,21	3,96	3,28	0,00	2,08	-3,54	-13,80	Na-Cl
08-Dec-20	BGR12	River	53,90	35,04	7,07	21,50	1,12	1,21	5,34	0,55	2,44	2,78	10,96	-0,63	0,99	0,00	2,17	-3,52	-13,60	Na-Cl
22-Dec-20	BGR12	River	54,60	35,49	7,32	24,90	1,50	0,88	5,18	0,37	4,88	2,13	9,24	-0,43	0,91	0,00	1,99	-3,07	-9,40	Na-Cl
13-Jan-21	BGR12	River	45,40	29,51	7,54	26,40	1,74	0,99	5,09	0,53	9,76	1,89	8,06	-2,78	1,13	0,00	1,79	-3,30	-11,70	Na-Cl
25-Jan-21	BGR12	River	48,00	31,20	7,60	28,10	2,64	1,20	4,06	0,28	8,54	1,47	8,67	-0,10	0,44	0,00	1,62	-3,19	-10,90	Ca-Mg-Cl
08-Feb-21	BGR12	River	43,80	28,47	6,45	24,80	3,03	1,34	4,56	0,30	9,76	1,47	9,02	2,46	0,50	0,00	1,46	-3,06	-10,60	Ca-Mg-Cl
22-Feb-21	BGR12	River	43,20	28,08	7,26	22,30	1,75	0,80	4,74	0,38	6,10	1,49	8,83	-1,45	0,74	BD	1,48	-3,29	-11,30	Na-Cl
08-Mar-21	BGR12	River	43,60	28,34	6,31	21,60	1,76	1,10	4,47	0,32	4,88	2,11	8,83	1,07	1,14	BD	1,51	-2,92	-10,00	Na-Cl
24-Mar-21	BGR12	River	53,00	34,45	6,26	22,00	2,75	1,28	4,14	0,24	6,10	2,63	9,97	-0,85	2,09	BD	1,69	-3,12	-10,40	Ca-Mg-Cl
07-Apr-21	BGR12	River	61,80	40,17	7,15	23,20	2,71	1,34	5,25	0,37	7,32	3,49	11,51	-3,43	3,08	BD	0,82	-2,88	-10,20	Ca-Mg-Cl
19-Apr-21	BGR12	River	51,20	33,28	7,05	20,30	3,97	1,42	5,04	0,52	12,20	2,08	9,65	2,98	2,05	0,09	1,80	-2,41	-7,00	Ca-Mg-Cl
03-May-21	BGR12	River	65,30	42,45	7,11	19,60	2,31	1,71	6,55	0,75	7,32	2,95	11,92	3,92	2,85	BD	2,06	-1,84	-3,20	Na-Cl
17-May-21	BGR12	River	108,10	70,27	7,45	15,40	3,09	1,66	9,85	2,09	4,88	5,05	18,75	3,92	2,67	0,11	1,23	-3,34	-13,60	Na-Cl
31-May-21	BGR12	River	115,00	74,75	6,95	14,70	9,99	3,42	12,66	2,74	32,94	5,81	22,56	3,84	3,42	0,18	2,37	-2,82	-8,00	Ca-Mg-Cl
14-Jun-21	BGR12	River	121,40	78,91	7,53	14,40	9,48	2,97	10,88	2,76	30,50	5,10	19,61	4,21	4,41	0,27	1,59	-2,71	-10,00	Ca-Mg-Cl
29-Jun-21	BGR12	River	123,20	80,08	7,16	12,20	11,69	2,86	10,19	2,68	41,48	4,83	20,86	-1,44	2,91	0,22	1,54	-3,21	-11,90	Ca-Mg-Cl
12-Jul-21	BGR12	River	121,30	78,85	7,04	13,70	10,68	3,27	9,61	2,21	39,04	5,56	20,11	-1,79	2,46	0,20	1,67	-3,44	-12,80	Ca-Mg-Cl
26-Jul-21	BGR12	River	130,80	85,02	7,17	12,00	10,77	3,51	10,96	2,42	32,94	6,66	21,19	3,36	3,12	BD	1,99	-2,58	-9,50	Ca-Mg-Cl
10-Aug-21	BGR12	River	104,20	67,73	7,43	11,40	7,58	3,28	7,61	0,95	23,18	4,43	16,39	3,55	1,99	0,09	1,52	-3,35	-10,85	Ca-Mg-Cl
23-Aug-21	BGR12	River	116,30	75,60	6,25	13,30	4,48	4,15	9,48	1,81	19,52	5,53	19,06	2,53	2,59	BD	2,54	-3,53	-11,15	Ca-Mg-Cl
06-Sep-21	BGR12	River	93,90	61,04	7,13	13,60	7,41	2,99	7,90	1,26	26,84	4,36	14,62	2,50	1,92	BD	2,58	-3,72	-9,25	Ca-Mg-Cl
20-Sep-21	BGR12	River	122,70	79,76	7,42	15,80	5,56	2,48	10,62	1,78	15,86	5,57	19,40	3,44	2,76	BD	3,46	-3,33	-9,98	Na-Cl
13-Oct-21	BGR12	River	126,50	82,23	6,78	18,30	8,72	3,50	13,51	3,05	29,28	7,42	23,68	3,20	4,95	0,12	3,61	-3,07	-11,36	Ca-Mg-Cl
27-Oct-21	BGR12	River	72,20	46,93	7,86	21,10	4,50	1,96	4,58	0,44	9,76	3,19	12,50	1,43	2,14	BD	2,37	-3,33	-12,67	Ca-Mg-Cl
03-Nov-20	G1H020	River	118,90	77,29	7,86	19,20	6,18	2,14	10,73	2,01	18,30	6,17	18,93	2,04	3,88	nd	2,21	-3,43	-11,40	Na-Cl

Date	Sample ID	Data Source	EC	TDS	pH	Temp	Ca^{2+}	Mg^{2+}	Na^{+}	K^{+}	HCO_3^{-}	SO_4^{2-}	Cl^{-}	CB	NO_3^{-}	PO_4^{2-}	SiO_2	$\delta^{18}O$	$\delta^{2}H$	Water Type
25-Nov-20	G1H020	River	153,20	99,58	6,89	21,80	6,74	2,51	14,09	2,09	17,08	8,74	25,28	1,46	2,42	0,00	2,17	-3,01	-11,10	Na-Cl
08-Dec-20	G1H020	River	60,50	39,33	6,93	22,30	1,73	1,27	5,70	0,62	6,10	3,07	11,79	-4,40	0,90	0,00	2,59	-3,31	-12,30	Na-Cl
22-Dec-20	G1H020	River	60,30	39,20	7,17	26,30	1,97	1,04	5,52	0,44	7,32	2,36	9,75	-1,03	1,50	0,00	2,07	-3,39	-11,90	Na-Cl
13-Jan-21	G1H020	River	50,00	32,50	7,45	27,40	2,34	1,18	5,58	0,38	12,20	1,99	8,81	-2,41	0,53	nd	2,02	-3,07	-9,60	Na-Cl
25-Jan-21	G1H020	River	45,00	29,25	7,70	26,30	2,58	1,19	4,34	0,10	9,76	1,50	8,98	-3,07	0,39	0,00	1,71	-2,92	-9,90	Ca-Mg-Cl
08-Feb-21	G1H020	River	45,10	29,32	7,47	25,20	3,12	1,39	4,62	0,23	10,98	1,46	9,17	0,86	0,31	0,00	0,16	-3,04	-10,40	Ca-Mg-Cl
22-Feb-21	G1H020	River	51,40	33,41	7,93	22,90	2,54	1,20	4,90	0,30	9,76	1,51	9,18	-0,40	0,44	BD	1,57	-3,18	-11,00	Ca-Mg-Cl
08-Mar-21	G1H020	River	46,50	30,23	7,11	22,70	1,71	0,91	4,48	0,34	4,88	2,19	9,12	-2,59	0,90	BD	1,34	-2,90	-10,70	Na-Cl
24-Mar-21	G1H020	River	61,50	39,98	7,33	23,30	2,88	1,33	4,87	0,47	6,10	2,92	11,05	0,42	1,73	BD	1,44	-3,11	-10,20	Ca-Mg-Cl
07-Apr-21	G1H020	River	65,80	42,77	7,00	23,40	3,19	1,43	5,64	0,45	4,88	3,34	11,82	4,97	2,24	BD	2,00	-2,60	-8,20	Ca-Mg-Cl
19-Apr-21	G1H020	River	56,90	36,99	7,71	20,60	4,13	1,49	5,27	0,44	10,98	2,31	10,42	4,32	1,97	BD	1,31	-2,52	-9,20	Ca-Mg-Cl
03-May-21	G1H020	River	69,40	45,11	7,29	20,30	2,01	0,98	6,98	0,99	3,66	3,07	12,72	2,69	2,54	BD	1,85	-2,73	-9,40	Na-Cl
17-May-21	G1H020	River	94,40	61,36	7,22	15,10	1,34	1,63	8,59	2,06	4,88	4,33	15,41	1,83	1,93	0,12	1,86	-3,44	-14,60	Na-Cl
31-May-21	G1H020	River	110,00	71,50	8,03	15,40	10,68	2,74	11,18	2,01	28,06	5,48	21,60	4,56	3,20	0,14	2,50	-2,62	-5,10	Ca-Mg-Cl
14-Jun-21	G1H020	River	131,00	85,15	6,92	14,00	10,16	3,20	11,84	2,59	36,60	5,48	20,89	1,83	4,30	0,20	1,83	-2,63	-8,10	Ca-Mg-Cl
29-Jun-21	G1H020	River	104,30	67,80	6,82	12,50	6,12	3,13	11,57	2,18	32,94	4,20	16,00	1,98	2,92	0,19	1,20	-3,96	-16,60	Ca-Mg-Cl
12-Jul-21	G1H020	River	126,30	82,10	6,76	12,30	10,66	3,49	9,61	2,33	41,48	5,65	20,49	-2,94	2,60	0,20	1,62	-3,37	-13,00	Ca-Mg-Cl
26-Jul-21	G1H020	River	135,20	87,88	7,12	12,70	12,26	3,94	10,99	2,26	36,60	7,08	21,76	3,93	3,39	BD	3,18	-2,92	-11,00	Ca-Mg-Cl
10-Aug-21	G1H020	River	109,20	70,98	7,51	12,20	9,68	3,52	8,03	0,95	29,28	4,74	16,54	4,60	2,23	BD	2,92	-3,11	-12,35	Ca-Mg-Cl
23-Aug-21	G1H020	River	123,10	80,02	6,03	14,00	10,34	3,41	9,87	1,84	31,72	6,07	19,36	3,25	2,89	BD	3,73	-3,04	-10,51	Ca-Mg-Cl
06-Sep-21	G1H020	River	93,90	61,04	7,45	14,10	8,36	2,90	7,76	1,35	28,06	4,45	14,32	3,59	1,95	BD	2,12	-4,01	-14,71	Ca-Mg-Cl
20-Sep-21	G1H020	River	135,00	87,75	7,40	16,10	11,38	3,35	11,42	1,89	39,04	6,37	20,45	1,45	3,01	BD	2,31	-3,59	-13,77	Ca-Mg-Cl
13-Oct-21	G1H020	River	103,40	67,21	6,83	18,80	7,90	3,55	9,67	2,64	32,94	6,12	16,73	1,52	3,31	BD	2,80	-3,71	-18,79	Ca-Mg-Cl
27-Oct-21	G1H020	River	80,50	52,33	7,62	21,50	5,13	2,27	6,03	1,03	15,86	3,47	13,14	1,99	2,02	BD	2,50	-3,19	-12,03	Ca-Mg-Cl
25-Nov-20	BG42	Groundwater	60,20	39,13	4,33	19,50	1,72	0,78	6,13	nd	0,00	1,88	13,83	-1,47	0,67	nd	6,27	-3,51	-13,10	Na-Cl
08-Dec-20	BG42	Groundwater	46,70	30,36	4,35	**18,70**	**1,48**	**0,91**	**10,53**	**0,01**	**0,00**	**1,90**	**22,93**	**-6,19**	**0,35**	**nd**	**7,40**	**-4,01**	**-17,20**	**N/A**
22-Dec-20	BG42	Groundwater	66,90	43,49	4,60	20,30	BD	0,75	6,46	nd	1,22	BD	12,12	-2,68	1,23	nd	5,15	-3,68	-13,70	Na-Cl
13-Jan-21	BG42	Groundwater	59,20	38,48	3,02	20,20	0,11	1,11	7,05	0,13	4,88	BD	11,66	-0,32	1,41	nd	3,23	-3,81	-13,90	Na-Cl
25-Jan-21	BG42	Groundwater	55,00	35,75	4,96	20,10	3,12	1,55	4,64	0,01	7,32	BD	12,71	0,72	1,10	nd	4,19	-3,58	-12,60	Ca-Mg-Cl
08-Feb-21	BG42	Groundwater	59,30	38,55	3,90	21,90	3,67	1,65	6,07	0,61	9,76	BD	13,74	4,45	1,29	nd	4,03	-3,69	-12,90	Ca-Mg-Cl
22-Feb-21	BG42	Groundwater	58,80	38,22	3,14	22,70	2,98	1,38	6,09	0,10	8,54	BD	12,88	2,49	1,39	nd	3,97	-3,85	-13,50	Na-Cl
08-Mar-21	BG42	Groundwater	57,40	37,31	4,56	18,90	1,82	0,88	6,42	0,06	4,88	BD	12,63	0,89	1,39	nd	3,97	-3,67	-12,80	Na-Cl
03-May-21	BG42	Groundwater	58,90	38,29	4,71	20,90	4,22	1,22	6,05	0,09	13,42	BD	12,80	-0,42	1,23	nd	3,13	-3,27	-11,80	Ca-Mg-Cl
17-May-21	BG42	Groundwater	60,50	39,33	4,31	19,30	2,66	1,40	5,46	0,00	8,54	BD	12,30	-0,17	1,21	nd	3,42	-2,71	-12,60	Ca-Mg-Cl
31-May-21	BG42	Groundwater	65,00	42,25	4,66	20,00	3,70	1,51	6,63	0,03	6,10	1,73	14,97	3,46	0,65	nd	1,82	-3,64	-9,80	Ca-Mg-Cl
14-Jun-21	BG42	Groundwater	65,60	42,64	4,54	19,10	3,64	1,86	6,24	0,00	9,76	1,62	14,01	1,40	0,71	BD	3,86	-3,15	-8,40	Ca-Mg-Cl
29-Jun-21	BG42	Groundwater	72,10	46,87	4,84	17,30	3,65	1,33	6,95	0,17	6,10	2,11	14,39	4,19	2,92	BD	0,74	-2,82	-11,80	Na-Cl
12-Jul-21	BG42	Groundwater	68,40	44,46	4,95	16,90	3,62	2,02	6,97	0,37	14,64	2,17	13,09	0,37	4,53	BD	0,96	-2,48	-4,90	Ca-Mg-Cl
26-Jul-21	BG42	Groundwater	65,70	42,71	4,96	19,80	3,93	2,27	6,05	0,10	13,42	1,91	13,42	0,83	3,19	BD	1,63	-3,30	-10,60	Ca-Mg-Cl
10-Aug-21	BG42	Groundwater	64,40	41,86	5,18	19,70	7,33	2,09	5,01	0,01	23,18	1,61	12,69	-1,04	2,29	BD	2,34	-2,92	-9,16	Ca-Mg-Cl
23-Aug-21	BG42	Groundwater	68,90	44,79	4,15	20,00	5,00	1,59	5,87	0,17	15,86	1,81	12,92	-1,72	2,97	BD	1,03	-3,30	-11,06	Ca-Mg-Cl
06-Sep-21	BG42	Groundwater	64,40	41,86	4,77	16,90	1,76	1,30	6,03	0,29	4,88	2,16	11,05	3,13	4,92	BD	1,15	-3,68	-12,91	Na-Cl
20-Sep-21	BG42	Groundwater	64,90	42,19	4,64	18,60	4,75	1,44	6,37	0,11	12,20	1,38	12,84	3,65	2,24	nd	1,58	-3,36	-10,55	Ca-Mg-Cl
13-Oct-21	BG42	Groundwater	57,20	37,18	4,29	19,30	4,47	1,37	5,58	0,02	8,54	1,34	12,89	4,24	1,92	BD	2,69	-3,05	-8,25	Ca-Mg-Cl
27-Oct-21	BG42	Groundwater	59,60	38,74	5,34	21,60	3,46	1,68	5,87	0,09	8,54	1,28	12,86	3,57	2,05	BD	2,91	-2,47	-4,77	Ca-Mg-Cl
25-Nov-20	BG43	Groundwater	71,80	46,67	5,28	18,20	1,00	0,69	7,11	0,00	1,22	BD	14,89	-2,82	0,35	nd	6,88	-3,63	-13,60	Na-Cl
08-Dec-20	BG43	Groundwater	58,30	37,90	5,30	18,40	1,80	1,03	6,78	0,00	3,66	BD	15,12	-1,77	0,41	nd	6,47	-3,80	-14,30	Na-Cl
22-Dec-20	BG43	Groundwater	69,50	45,18	4,94	18,70	0,00	0,86	7,60	0,00	2,44	BD	13,88	-3,63	0,84	0,00	7,29	-3,83	-14,70	Na-Cl
13-Jan-21	BG43	Groundwater	61,50	39,98	3,83	19,20	0,02	1,22	7,83	0,00	3,66	BD	12,83	2,30	0,94	0,00	6,24	-3,98	-14,50	Na-Cl
25-Jan-21	BG43	Groundwater	60,00	39,00	5,30	20,00	4,24	1,17	4,68	0,00	8,54	BD	14,07	-2,40	0,78	0,00	6,51	-3,82	-14,40	Ca-Mg-Cl
08-Feb-21	BG43	Groundwater	62,20	40,43	3,65	19,20	2,47	1,39	7,12	0,06	7,32	BD	14,36	2,25	0,86	nd	6,32	-4,02	-14,20	Na-Cl
22-Feb-21	BG43	Groundwater	62,10	40,37	3,50	19,00	1,97	1,21	7,26	0,02	4,88	BD	14,25	3,24	0,88	nd	5,78	-4,03	-14,60	Na-Cl
08-Mar-21	BG43	Groundwater	61,60	40,04	4,82	18,90	0,77	0,75	6,90	0,00	0,00	BD	14,09	0,36	0,94	nd	3,84	-3,90	-14,20	Na-Cl
24-Mar-21	BG43	Groundwater	66,50	43,23	4,96	19,20	3,52	1,44	5,80	0,00	4,88	BD	15,56	2,62	0,80	BD	4,26	-3,89	-13,30	Ca-Mg-Cl
07-Apr-21	BG43	Groundwater	60,60	39,39	5,15	20,50	3,66	1,35	5,57	n.d.	7,32	BD	14,08	1,78	0,82	nd	6,27	-3,39	-11,00	Ca-Mg-Cl
19-Apr-21	BG43	Groundwater	60,60	39,39	5,30	19,60	3,15	1,17	7,04	0,08	9,76	BD	14,10	0,34	0,22	BD	9,31	-3,54	-13,20	Na-Cl
03-May-21	BG43	Groundwater	60,30	39,20	5,01	20,60	2,14	0,94	6,85	0,03	4,88	BD	13,85	1,24	0,33	BD	4,70	-3,58	-13,90	Na-Cl
17-May-21	BG43	Groundwater	65,40	42,51	5,60	19,30	3,45	1,13	7,37	0,01	8,54	BD	15,69	0,29	0,52	BD	3,20	-2,88	-9,40	Na-Cl
31-May-21	BG43	Groundwater	55,00	35,75	5,52	17,60	3,15	1,12	6,66	0,01	7,32	BD	14,19	1,82	0,58	nd	2,30	-2,88	-10,40	Na-Cl
14-Jun-21	BG43	Groundwater	58,00	37,70	4,97	17,40	4,88	1,85	5,76	n.d.	15,86	BD	13,70	0,05	0,61	BD	1,35	-3,18	-9,20	Ca-Mg-Cl
29-Jun-21	BG43	Groundwater	57,10	37,12	5,09	16,50	3,11	1,71	6,61	0,22	12,20	BD	13,55	0,58	0,56	BD	2,04	-3,50	-12,40	Ca-Mg-Cl
12-Jul-21	BG43	Groundwater	58,80	38,22	5,50	13,80	4,83	1,51	5,93	0,06	14,64	BD	13,81	-0,39	0,61	BD	3,02	-3,38	-9,90	Ca-Mg-Cl
26-Jul-21	BG43	Groundwater	61,30	39,85	5,28	16,10	3,08	1,93	6,26	0,02	10,98	BD	14,19	0,39	0,71	0,17	4,06	-3,27	-12,00	Ca-Mg-Cl
10-Aug-21	BG43	Groundwater	59,20	38,48	5,52	15,00	6,18	1,89	4,94	n.d.	20,74	BD	13,12	-2,27	0,83	BD	2,70	-3,46	-10,23	Ca-Mg-Cl
23-Aug-21	BG43	Groundwater	61,80	40,17	4,59	16,40	4,06	1,20	6,05	0,05	12,20	BD	13,78	-1,96	0,91	BD	4,05	-3,40	-10,88	Ca-Mg-Cl
06-Sep-21	BG43	Groundwater	63,90	41,54	4,75	17,60	4,74	1,28	6,28	0,02	10,98	BD	14,08	3,22	0,77	nd	3,80	-3,17	-10,30	Ca-Mg-Cl
20-Sep-21	BG43	Groundwater	65,60	42,64	4,65	17,90	3,00	0,99	7,01	0,06	8,54	0,90	14,01	-1,53	0,83	BD	3,79	-3,43	-12,12	Na-Cl
13-Oct-21	BG43	Groundwater	57,30	37,25	4,85	16,60	2,72	1,42	6,45	0,04	4,88	0,90	13,91	4,15	0,77	BD	3,60	-3,61	-13,16	Na-Cl
27-Oct-21	BG43	Groundwater	55,80	36,27	5,94	18,90	3,96	1,24	5,97	0,12	7,32	BD	13,86	4,83	0,83	BD	6,88	-2,92	-7,00	Ca-Mg-Cl
25-Nov-20	BG44	Groundwater	89,10	57,92	6,54	18,20	1,31	0,84	7,92	0,00	13,42	BD	9,32	-0,43	0,00	nd	7,82	-3,68	-15,30	Na-Cl
08-Dec-20	BG44	Groundwater	82,60	53,69	6,10	18,50	1,32	0,97	5,13	0,15	7,32	BD	9,44	-1,76	0,00	nd	6,11	-3,72	-14,10	Na-Cl
22-Dec-20	BG44	Groundwater	103,60	67,34	6,86	18,70	2,00	1,81	8,92	0,14	25,62	BD	8,83	-2,18	0,00	nd	11,53	-3,86	-15,50	Ca-Na-HCO3
13-Jan-21	BG44	Groundwater	91,00	59,15	5,53	18,20	3,44	3,10	8,75	0,11	40,26	BD	8,33	-4,92	0,36	nd	7,93	-3,79	-15,50	Ca-Mg-Cl
25-Jan-21	BG44	Groundwater	80,00	52,00	6,63	18,30	3,64	1,58	6,63	0,21	25,62	BD	8,31	-3,93	0,00	0,00	10,93	-3,98	-16,40	Ca-Mg-Cl
08-Feb-21	BG44	Groundwater	92,60	60,19	4,63	18,40	4,84	2,01	8,97	0,26	34,16	BD	8,43	0,42	0,00	0,00	6,58	-4,13	-15,80	Ca-Mg-Cl
22-Feb-21	BG44	Groundwater	93,60	60,84	5,60	18,10	2,31	2,14	9,82	0,25	28,06	BD	8,47	1,86	BD	nd	9,20	-3,88	-16,00	Ca-Na-HCO3
08-Mar-21	BG44	Groundwater	93,90	61,04	5,76	17,90	1,02	0,86	8,91	0,17	18,30	BD	8,23	-1,79	BD	BD	3,85	-3,93	-16,20	Ca-Na-HCO3
24-Mar-21	BG44	Groundwater	93,90	61,04	6,41	18,30	0,55	0,46	6,23	0,00	6,10	BD	8,41	-0,20	BD	BD	7,65	-4,03	-15,80	Na-Cl
07-Apr-21	BG44	Groundwater	91,60	59,54	6,46	19,50	0,51	1,74	8,03	0,06	17,08	BD	8,32	0,49	BD	BD	5,59	-3,83	-15,90	Ca-Na-HCO3
19-Apr-21	BG44	Groundwater	94,00	61,10	6,80	19,20	3,37	1,58	8,36	0,09	29,28	BD	8,21	-3,45	BD	BD	7,78	-3,77	-15,10	Ca-Na-HCO3
03-May-21	BG44	Groundwater	97,30	63,25	6,57	19,40	1,72	2,13	10,96	0,17	34,16	BD	8,10	-3,02	BD	BD	10,25	-3,44	-14,60	Ca-Na-HCO3
17-May-21	BG44	Groundwater	78,40	50,96	6,16	19,60	5,82	2,08	4,79	0,53	28,06	BD	9,14	-2,45	BD	BD	4,45	-3,12	-9,80	Ca-HCO3
31-May-21	BG44	Groundwater	50,00	32,50	6,15	18,80	3,48	1,85	4,53	0,13	17,08	BD	9,22	-1,33	BD	BD	2,85	-3,83	-15,10	Ca-HCO3
14-Jun-21	BG44	Groundwater	48,50	31,53	4,97	17,40	4,41	1,83	4,17	0,07	20,74	BD	9,11	-3,75	BD	BD	3,43	-3,09	-9,10	Ca-HCO3
29-Jun-21	BG44	Groundwater	68,00	44,20	5,32	15,90	5,01	1,74	3,93	0,03	15,86	BD	9,04	4,61	BD	BD	1,62	-3,15	-10,20	Ca-HCO3
12-Jul-21	BG44	Groundwater	50,70	32,96	6,03	13,60	4,14	1,63	4,34	0,25	17,08	BD	9,46	-1,02	BD	BD	2,30	-3,54	-10,90	Ca-HCO3
26-Jul-21	BG44	Groundwater	63,80	41,47	6,40	16,67	1,34	1,57	4,27	0,23	8,54	BD	9,28	-1,75	BD	BD	3,65	-3,26	-12,60	Ca-HCO3
10-Aug-21	BG44	Groundwater	69,90	45,44	6,78	16,00	4,72	2,40	3,84	0,01	23,18	BD	8,74	-2,11	BD	BD	1,84	-2,88	-7,79	Ca-Mg-Cl
23-Aug-21	BG44	Groundwater	74,30	48,30	6,71	17,00	3,64	1,83	4,31	0,17	15,86	BD	9,61	-0,65	BD	BD	3,39	-3,27	-13,20	Ca-Mg-Cl
06-Sep-21	BG44	Groundwater	98,90	64,29	6,61	17,60	2,50	2,40	9,95	0,12	29,28	BD	8,16	3,25	BD	BD	8,16	-3,97	-16,10	Ca-Na-HCO3
20-Sep-21	BG44	Groundwater	85,20	55,38	6,51	17,90	5,14	2,13	7,30	0,13	25,62	0,95	9,09	3,88	BD	nd	7,31	-3,52	-11,26	Ca-HCO3
13-Oct-21	BG44	Groundwater	62,20	40,43	5,74	15,90	1,43	2,13	4,74	0,16	10,98	BD	10,15	-0,97	BD	BD	3,00	-3,44	-11,05	Ca-Mg-Cl
27-Oct-21	BG44	Groundwater	64,10	41,67	6,79	19,60	5,05	2,43	4,47	0,24	19,52	BD	10,28	3,37	0,05	BD	2,88	-3,49	-11,93	Ca-HCO3
25-Nov-20	BG40	Groundwater	95,80	62,27	5,16	18,30	1,76	1,32	11,20	0,00	2,44	1,98	23,41	-4,10	0,36	nd	5,97	-3,89	-16,80	Na-Cl
08-Dec-20	BG40	Groundwater	88,40	57,46	5,04	19,00	1,10	0,60	5,75	0,08	1,22	BD	12,57	-2,44	0,62	0,00	4,91	-3,66	-13,10	Na-Cl
22-Dec-20	BG40	Groundwater	106,40	69,16	4,85	18,80	0,00	1,50	12,16	0,00	1,22	1,85	22,66	-3,34	0,63	nd	7,03	-4,13	-18,20	Na-Cl
13-Jan-21	BG40	Groundwater	93,40	60,71	3,35	18,60	0,24	2,32	11,88	0,00	4,88	1,83	21,54	-0,42	1,31	nd	6,98	-3,88	-16,40	Na-Cl
25-Jan-21	BG40	Groundwater	85,00	55,25	4,91	18,50	2,24	2,34	11,68	0,02	7,32	BD	23,22	2,35	0,61	0,00	7,28	-4,09	-17,30	Na-Cl
08-Feb-21	BG40	Groundwater	93,30	60,65	3,63	18,50	4,22	2,12	10,53	0,05	6,10	BD	23,72	4,68	0,65	nd	4,19	-4,21	-16,50	Na-Cl
22-Feb-21	BG40	Groundwater	92,80	60,32	3,52	18,50	3,04	1,51	11,56	0,10	7,32	1,36	23,43	-1,78	0,67	BD	5,09	-3,97	-16,80	Na-Cl
08-Mar-21	**BG40**	**Groundwater**	**90,70**	**58,96**	**4,16**	**18,10**	**0,21**	**0,59**	**10,98**	**0,02**	**2,44**	**1,61**	**23,02**	**-14,78**	**0,78**	**BD**	5,00	-4,02	-16,80	**N/A**
24-Mar-21	**BG40**	**Groundwater**	**91,90**	59,74	**4,64**	**18,30**	**1,51**	**1,08**	**7,96**	**nd**	**0,00**	**1,76**	**22,75**	**-14,12**	**0,72**	**BD**	5,61	-4,16	-17,10	**N/A**
07-Apr-21	**BG40**	**Groundwater**	**88,30**	57,40	**4,78**	**19,50**	**1,06**	**0,85**	**9,10**	**nd**	**0,00**	**1,80**	**22,36**	**-12,63**	**0,69**	**BD**	4,86	-3,79	-15,60	**N/A**
19-Apr-21	BG40	Groundwater	90,00	58,50	5,03	20,20	1,55	1,18	11,57	0,16	1,22	BD	23,00	0,95	0,61	0,12	3,83	-3,57	-14,30	Na-Cl
03-May-21	BG40	Groundwater	91,80	59,67	4,64	19,90	2,76	1,21	10,90	0,04	2,44	BD	22,51	2,74	0,66	BD	2,68	-3,64	-14,80	Na-Cl
17-May-21	BG40	Groundwater	91,80	59,67	3,85	18,40	0,87	0,72	10,79	0,34	0,00	BD	22,24	-3,87	1,10	BD	4,48	-3,65	-15,30	Na-Cl
31-May-21	BG40	Groundwater	80,00	52,00	5,07	18,30	6,18	1,60	10,16	0,01	14,64	BD	21,91	1,39	0,82	BD	3,50	-3,37	-14,60	Na-Cl
14-Jun-21	BG40	Groundwater	87,90	57,14	4,78	18,00	2,23	0,77	9,62	0,05	1,22	BD	21,87	-3,47	0,83	BD	4,93	-3,18	-11,10	Na-Cl
29-Jun-21	BG40	Groundwater	87,60	56,94	4,96	16,70	7,46	1,71	10,02	0,02	15,86	BD	21,66	4,28	0,69	BD	2,80	-3,54	-12,90	Ca-Mg-Cl
12-Jul-21	BG40	Groundwater	88,40	57,46	4,95	15,20	3,17	2,65	9,66	0,13	9,76	BD	21,96	1,28	0,83	BD	2,83	-3,46	-13,10	Na-Cl
26-Jul-21	**BG40**	**Groundwater**	**89,40**	58,11	**4,99**	**17,20**	**1,47**	**0,88**	**10,35**	**0,01**	**0,00**	**1,57**	**22,22**	**-5,03**	**0,74**	**BD**	**4,37**	**-3,54**	**-15,60**	**N/A**
10-Aug-21	BG40	Groundwater	92,60	60,19	5,41	18,00	5,88	2,64	8,37	0,00	15,86	BD	21,20	0,95	0,69	BD	3,12	-3,23	-12,51	Ca-Mg-Cl
23-Aug-21	BG40	Groundwater	64,70	42,06	4,90	19,30	2,15	1,41	9,96	0,05	4,88	BD	22,47	-4,07	0,72	BD	6,21	-3,58	-14,25	Na-Cl
06-Sep-21	BG40	Groundwater	96,20	62,53	5,23	18,10	4,74	2,08	11,33	0,06	9,76	1,78	22,53	3,99	0,64	BD	3,36	-3,97	-16,10	Na-Cl
20-Sep-21	BG40	Groundwater	97,40	63,31	4,71	18,10	1,12	1,70	11,01	0,04	2,44	1,55	22,12	-1,55	0,65	BD	3,21	-3,80	-13,95	Na-Cl
13-Oct-21	BG40	Groundwater	82,10	53,37	4,74	16,00	7,37	1,71	10,08	0,00	14,64	1,19	22,00	3,34	0,68	BD	2,57	-3,61	-12,57	Ca-Mg-Cl
27-Oct-21	BG40	Groundwater	84,40	54,86	5,61	16,90	6,40	2,29	7,39	0,11	8,54	1,18	21,84	3,18	0,73	BD	9,50	-3,36	-13,11	Ca-Mg-Cl
25-Nov-20	BG49	Groundwater	176,40	114,66	4,72	18,20	6,16	4,18	16,04	0,71	21,96	9,59	31,75	-3,12	10,58	nd	6,48	-3,56	-12,60	Na-Cl
08-Dec-20	BG49	Groundwater	167,40	108,81	5,56	17,90	4,41	5,19	15,48	1,74	19,52	8,92	30,98	-0,55	8,44	nd	7,32	-3,29	-12,40	Na-Cl

Date	Sample ID	Data Source	EC	TDS	pH	Temp	Ca^{2+}	Mg^{2+}	Na^{+}	K^{+}	HCO_3^{-}	SO_4^{2-}	Cl^{-}	CB	NO_3^{-}	PO_4^{2-}	SiO_2	$\delta^{18}O$	$\delta^{2}H$	Water Type
22-Dec-20	BG49	Groundwater	202,10	131,37	5,15	18,20	2,04	3,71	11,08	3,02	0,00	8,93	31,16	-4,86	11,71	nd	5,84	-3,36	-12,90	Na-Cl
13-Jan-21	BG49	Groundwater	179,10	116,42	3,97	18,20	4,33	7,12	15,04	2,80	30,50	8,51	29,21	0,89	15,37	nd	6,62	-3,22	-11,90	Ca-Mg-Cl
25-Jan-21	BG49	Groundwater	175,00	113,75	5,26	18,10	5,73	5,07	11,65	1,18	18,30	7,39	30,49	-2,91	16,52	nd	5,45	-3,40	-12,00	Ca-Mg-Cl
08-Feb-21	BG49	Groundwater	179,80	116,87	5,00	18,10	5,30	6,17	15,55	1,60	25,62	8,28	31,41	0,39	17,84	nd	6,43	-3,51	-12,90	Na-Cl
22-Feb-21	BG49	Groundwater	181,40	117,91	5,62	18,00	5,11	6,46	17,60	1,77	23,18	8,75	31,47	4,84	18,42	nd	5,45	-3,47	-12,10	Na-Cl
08-Mar-21	BG49	Groundwater	180,80	117,52	5,66	17,90	4,05	6,07	15,76	1,70	20,74	9,33	31,15	0,62	19,41	nd	5,19	-3,26	-12,00	Na-Cl
24-Mar-21	BG49	Groundwater	181,30	117,85	5,05	18,30	6,02	3,68	12,48	1,01	12,20	9,35	30,65	-3,60	20,32	BD	6,39	-3,28	-12,60	Ca-Mg-Cl
07-Apr-21	BG49	Groundwater	177,50	115,38	4,74	18,20	4,62	4,17	13,75	1,27	10,98	9,24	30,31	-0,97	19,11	nd	6,85	-3,25	-12,60	Na-Cl
19-Apr-21	BG49	Groundwater	181,90	118,24	5,03	18,40	8,02	5,63	15,76	1,74	34,16	8,34	30,74	-0,23	17,43	BD	5,54	-3,20	-10,80	Ca-Mg-Cl
03-May-21	BG49	Groundwater	182,30	118,50	5,13	18,50	5,67	5,52	15,89	1,78	23,18	8,69	31,10	1,23	16,97	nd	3,54	-3,53	-13,00	Ca-Mg-Cl
17-May-21	BG49	Groundwater	179,40	116,61	5,02	17,70	4,21	6,07	15,61	1,70	20,74	8,66	30,49	1,85	17,20	BD	3,58	-3,01	-9,50	Na-Cl
31-May-21	BG49	Groundwater	185,00	120,25	5,33	16,70	7,04	6,40	14,77	1,38	25,62	8,56	30,48	3,23	16,80	BD	3,43	-3,00	-8,30	Ca-Mg-Cl
14-Jun-21	BG49	Groundwater	177,50	115,38	3,65	17,50	7,96	4,99	13,47	0,93	23,18	8,78	30,06	0,26	16,65	BD	3,00	-2,39	-5,90	Ca-Mg-Cl
29-Jun-21	BG49	Groundwater	174,80	113,62	5,21	15,50	7,79	6,05	13,68	1,18	25,62	8,72	30,28	1,90	15,89	BD	2,56	-2,37	-7,30	Ca-Mg-Cl
12-Jul-21	BG49	Groundwater	178,80	116,22	6,92	15,30	6,09	6,60	13,57	1,21	21,96	9,32	30,43	1,94	17,68	BD	3,38	-2,56	-8,80	Ca-Mg-Cl
26-Jul-21	BG49	Groundwater	177,60	115,44	5,54	15,30	6,25	6,74	14,77	1,36	26,84	8,99	30,92	1,44	16,19	BD	3,79	-2,32	-6,30	Ca-Mg-Cl
10-Aug-21	BG49	Groundwater	194,20	126,23	5,58	16,10	13,43	6,93	32,49	0,90	19,52	13,79	81,26	-3,99	17,10	BD	3,14	-3,20	-8,89	Na-Cl
23-Aug-21	BG49	Groundwater	191,70	124,61	4,55	17,10	4,89	4,47	15,36	1,27	18,30	6,79	29,00	2,07	17,11	BD	4,16	-3,18	-9,10	Na-Cl
06-Sep-21	BG49	Groundwater	182,90	118,89	5,15	17,70	6,18	6,09	14,85	1,32	18,30	8,82	31,33	4,26	17,39	nd	3,98	-3,03	-7,73	Ca-Mg-Cl
20-Sep-21	BG49	Groundwater	185,00	120,25	5,26	17,70	8,07	5,67	15,22	1,36	25,62	8,59	29,40	4,61	16,70	BD	5,58	-2,76	-7,19	Ca-Mg-Cl
13-Oct-21	BG49	Groundwater	158,90	103,29	5,28	15,80	6,33	5,41	15,41	1,61	18,30	9,47	30,09	4,48	18,05	BD	7,52	-3,24	-11,85	Ca-Mg-Cl
27-Oct-21	BG49	Groundwater	174,00	113,10	6,34	19,70	5,29	3,21	13,52	1,24	4,88	7,48	30,22	2,65	18,26	BD	2,73	-2,86	-8,85	Na-Cl
25-Nov-20	BG51	Groundwater	72,40	47,06	6,26	18,20	0,78	0,82	4,86	0,03	1,22	BD	11,06	-2,04	nd	nd	6,45	-3,58	-13,20	Na-Cl
08-Dec-20	BG51	Groundwater	71,50	46,48	5,99	19,10	1,77	1,09	4,33	0,18	3,66	BD	10,72	1,15	0,00	nd	6,27	-3,70	-13,60	Na-Cl
22-Dec-20	BG51	Groundwater	82,00	53,30	6,05	22,80	0,44	0,75	4,94	0,37	2,44	BD	10,32	-3,69	0,13	nd	6,64	-3,81	-14,70	Na-Cl
13-Jan-21	BG51	Groundwater	72,10	46,87	5,35	19,80	0,44	0,75	4,94	0,37	1,22	BD	10,32	0,89	0,13	nd	5,26	-3,35	-11,30	Na-Cl
25-Jan-21	BG51	Groundwater	60,00	39,00	4,91	18,30	2,57	1,09	4,37	0,09	7,32	BD	10,08	-2,91	0,00	nd	5,37	-3,70	-13,80	Ca-Mg-Cl
08-Feb-21	BG51	Groundwater	70,20	45,63	4,49	20,60	1,82	1,59	5,31	0,20	12,20	BD	10,35	-3,63	0,00	nd	4,83	-3,95	-13,20	Na-Cl
22-Feb-21	BG51	Groundwater	72,60	47,19	5,94	19,50	3,42	1,99	5,11	0,20	13,42	BD	10,52	4,16	BD	nd	3,56	-3,88	-13,70	Ca-Mg-Cl
08-Mar-21	BG51	Groundwater	82,50	53,63	5,31	19,60	0,71	1,61	4,84	0,21	6,10	BD	10,61	-1,96	BD	nd	3,61	-3,68	-12,80	Na-Cl
24-Mar-21	BG51	Groundwater	67,90	44,14	5,70	20,20	1,91	1,35	3,72	0,03	4,88	BD	10,31	-0,20	BD	BD	3,45	-3,77	-12,90	Ca-Mg-Cl
07-Apr-21	BG51	Groundwater	73,10	47,52	6,09	19,90	1,47	0,76	3,68	0,08	1,22	BD	10,05	-0,93	BD	BD	4,60	-3,71	-13,40	Na-Cl
19-Apr-21	BG51	Groundwater	73,90	48,04	6,17	20,30	0,61	0,84	4,63	0,31	2,44	BD	10,23	-3,06	BD	BD	2,74	-3,48	-11,80	Na-Cl
03-May-21	BG51	Groundwater	67,50	43,88	6,10	20,00	4,11	1,66	4,55	0,00	13,42	BD	10,19	3,02	BD	BD	3,02	-3,40	-11,40	Ca-Mg-Cl
17-May-21	BG51	Groundwater	99,40	64,61	6,03	18,90	3,66	1,64	4,37	0,16	12,20	BD	9,98	3,02	0,06	BD	2,89	-3,39	-10,30	Ca-Mg-Cl
31-May-21	BG51	Groundwater	60,00	39,00	6,61	18,40	4,15	1,62	4,52	0,17	14,64	BD	9,99	1,85	BD	BD	2,63	-3,36	-10,40	Ca-Mg-Cl
14-Jun-21	BG51	Groundwater	87,50	56,88	6,46	17,80	7,95	2,37	4,69	0,28	26,84	BD	10,85	3,66	0,05	BD	2,33	-2,99	-10,70	Ca-HCO3
29-Jun-21	BG51	Groundwater	88,30	57,40	6,27	15,80	5,38	1,92	4,50	0,12	18,30	BD	10,88	1,50	0,05	BD	1,55	-3,47	-10,90	Ca-Mg-Cl
12-Jul-21	BG51	Groundwater	80,00	52,00	5,96	13,30	1,48	1,88	5,17	0,41	8,54	BD	10,92	1,70	0,07	BD	1,37	-3,00	-7,60	Na-Cl
26-Jul-21	BG51	Groundwater	89,00	57,85	6,42	16,40	4,22	2,20	5,73	0,36	18,30	BD	11,83	1,29	0,25	BD	2,99	-2,84	-4,00	Ca-Mg-Cl
10-Aug-21	BG51	Groundwater	93,90	61,04	6,39	15,90	1,58	2,70	5,42	0,07	12,20	BD	11,14	2,30	BD	BD	3,10	-3,07	-7,49	Ca-Mg-Cl
23-Aug-21	BG51	Groundwater	62,40	40,56	6,09	16,90	2,76	1,54	5,05	0,24	8,54	BD	11,54	2,60	BD	BD	3,70	-3,04	-8,69	Ca-Mg-Cl
06-Sep-21	BG51	Groundwater	68,40	44,46	5,94	16,50	4,01	1,74	4,93	0,15	15,86	BD	11,04	-0,87	BD	BD	5,83	-3,13	-9,04	Ca-Mg-Cl
20-Sep-21	BG51	Groundwater	75,50	49,08	6,10	16,60	5,08	2,05	5,26	0,18	17,08	0,93	10,53	4,75	BD	nd	2,94	-3,16	-7,20	Ca-Mg-Cl
13-Oct-21	BG51	Groundwater	103,20	67,08	5,98	16,90	2,26	1,70	5,06	0,26	13,42	BD	10,84	-4,64	0,10	BD	3,65	-3,67	-12,40	Ca-Mg-Cl
27-Oct-21	BG51	Groundwater	101,00	65,65	7,11	22,80	4,23	1,62	3,91	0,27	12,20	0,88	11,18	-1,11	0,06	BD	3,35	-2,95	-8,86	Ca-Mg-Cl
25-Nov-20	BG47	Groundwater	116,00	75,40	6,24	17,70	2,53	1,12	10,54	0,00	4,88	1,94	22,14	-4,82	0,00	nd	6,00	-3,12	-10,80	Na-Cl
08-Dec-20	BG47	Groundwater	121,30	78,85	6,39	18,00	3,30	1,38	10,12	0,42	8,54	1,72	21,98	-4,38	0,00	nd	6,22	-3,25	-11,50	Na-Cl
22-Dec-20	BG47	Groundwater	152,30	99,00	6,59	18,40	2,37	1,32	11,38	0,42	7,32	1,91	21,70	-2,59	0,16	nd	5,78	-2,89	-8,50	Na-Cl
13-Jan-21	BG47	Groundwater	157,10	102,12	4,91	18,70	4,08	2,32	10,88	0,37	17,08	BD	21,33	-0,25	0,43	nd	5,44	-3,09	-10,80	Na-Cl
25-Jan-21	BG47	Groundwater	115,00	74,75	6,29	18,20	4,60	3,20	8,24	0,19	15,86	BD	22,20	-1,72	0,00	0,00	5,43	-3,25	-10,90	Ca-Mg-Cl
08-Feb-21	BG47	Groundwater	159,10	103,42	4,51	19,40	6,94	2,28	10,67	0,31	24,40	BD	23,46	-2,67	0,00	nd	5,61	-3,22	-10,80	Ca-Mg-Cl
22-Feb-21	BG47	Groundwater	167,90	109,14	5,24	19,30	5,33	2,12	11,96	0,41	23,18	BD	23,74	-3,87	BD	BD	5,89	-3,23	-11,10	Ca-Mg-Cl
08-Mar-21	BG47	Groundwater	150,20	97,63	4,84	18,90	8,04	1,59	11,62	0,31	25,62	BD	23,39	-1,59	BD	nd	3,12	-3,13	-11,30	Ca-Mg-Cl
24-Mar-21	BG47	Groundwater	174,00	113,10	6,37	19,20	7,18	1,84	8,99	0,25	15,86	BD	23,72	-1,22	BD	nd	4,77	-3,31	-11,60	Ca-Mg-Cl
07-Apr-21	BG47	Groundwater	169,00	109,85	6,42	20,60	6,98	1,83	10,38	0,33	23,18	BD	23,44	-4,10	nd	nd	5,30	-3,34	-13,20	Ca-Mg-Cl
19-Apr-21	BG47	Groundwater	182,40	118,56	6,40	20,50	3,83	2,91	11,76	0,46	20,74	BD	23,96	-3,16	BD	BD	4,66	-3,19	-11,30	Na-Cl
03-May-21	BG47	Groundwater	180,40	117,26	6,49	19,40	7,86	0,03	11,67	0,62	20,74	BD	23,51	-4,41	BD	BD	5,07	-3,16	-11,80	Na-Cl
17-May-21	BG47	Groundwater	169,20	109,98	6,97	19,60	4,13	1,72	11,53	0,60	13,42	BD	23,43	-0,96	0,07	BD	2,95	-2,80	-10,50	Na-Cl
31-May-21	BG47	Groundwater	125,00	81,25	6,56	18,80	4,85	1,76	11,17	0,73	21,96	BD	20,33	-2,30	BD	BD	3,68	-3,08	-9,50	Na-Cl
14-Jun-21	BG47	Groundwater	165,70	107,71	6,46	19,10	10,74	2,32	10,87	0,41	37,82	BD	21,97	-1,18	BD	BD	1,71	-2,72	-8,00	Ca-HCO3
29-Jun-21	BG47	Groundwater	181,30	117,85	6,50	17,80	4,59	4,04	10,00	0,42	21,96	BD	22,29	0,93	BD	BD	1,17	-2,52	-9,40	Ca-Mg-Cl
12-Jul-21	BG47	Groundwater	147,70	96,01	6,39	16,50	12,63	2,32	10,57	1,10	46,36	BD	21,57	-2,20	BD	BD	1,30	-2,71	-9,30	Ca-HCO3
26-Jul-21	BG47	Groundwater	166,50	108,23	6,77	17,90	11,58	2,60	10,70	0,70	41,48	BD	22,27	-1,27	BD	BD	2,97	-2,23	-7,40	Ca-HCO3
10-Aug-21	BG47	Groundwater	199,60	129,74	6,47	18,60	5,06	4,33	10,44	0,52	30,50	BD	23,33	-3,65	BD	BD	2,99	-3,37	-10,20	Ca-Mg-Cl
23-Aug-21	BG47	Groundwater	194,10	126,17	7,20	19,00	9,52	2,28	10,46	0,41	29,28	BD	24,37	-1,73	BD	BD	2,74	-2,80	-9,81	Ca-Mg-Cl
06-Sep-21	BG47	Groundwater	118,20	76,83	5,81	17,50	4,00	1,84	12,23	0,42	10,98	3,41	23,59	-1,29	0,35	BD	3,89	-3,11	-10,20	Na-Cl
20-Sep-21	BG47	Groundwater	116,40	75,66	5,73	17,20	7,91	2,28	11,50	0,29	24,40	3,60	22,63	-1,06	0,30	BD	2,39	-3,27	-11,08	Ca-Mg-Cl
13-Oct-21	BG47	Groundwater	153,20	99,58	6,26	16,90	5,55	3,64	12,11	0,54	29,28	0,00	22,80	-0,27	0,09	BD	3,69	-3,49	-13,02	Ca-Mg-Cl
27-Oct-21	BG47	Groundwater	161,40	104,91	7,32	17,90	7,53	3,97	11,13	0,49	34,16	0,00	22,59	0,07	0,09	BD	3,10	-3,15	-11,19	Ca-Mg-Cl
25-Nov-20	BG48	Groundwater	161,50	104,98	5,43	18,10	4,96	3,49	15,85	0,31	13,42	6,10	35,58	-4,61	3,61	nd	7,86	-3,71	-15,70	Na-Cl
08-Dec-20	BG48	Groundwater	155,20	100,88	5,44	18,30	6,53	3,12	14,87	1,23	15,86	6,06	35,37	-4,65	3,64	nd	8,96	-3,60	-15,80	Na-Cl
22-Dec-20	BG48	Groundwater	189,40	123,11	5,42	19,20	3,56	5,58	16,61	1,30	14,64	6,52	36,46	-0,42	7,29	nd	8,79	-3,50	-14,90	Na-Cl
13-Jan-21	BG48	Groundwater	171,50	111,48	5,27	19,70	4,82	6,77	15,13	1,18	21,96	6,08	33,58	1,76	8,50	nd	9,34	-3,60	-15,40	Ca-Mg-Cl
25-Jan-21	BG48	Groundwater	165,00	107,25	5,47	18,50	8,86	4,12	13,92	1,03	24,40	5,47	36,18	-4,12	8,46	nd	10,28	-3,75	-15,90	Ca-Mg-Cl
08-Feb-21	BG48	Groundwater	176,20	114,53	4,76	19,70	5,89	4,61	16,22	1,16	15,86	6,04	37,14	-0,86	9,59	nd	9,49	-3,80	-16,50	Na-Cl
22-Feb-21	BG48	Groundwater	180,70	117,46	4,75	19,50	5,11	5,09	17,37	1,25	13,42	6,56	38,46	0,68	BD	BD	7,95	-3,82	-16,10	Na-Cl
08-Mar-21	BG48	Groundwater	180,60	117,39	5,05	19,30	3,24	4,62	17,01	1,25	8,54	6,91	37,56	-1,13	12,14	nd	5,51	-3,71	-16,90	Na-Cl
24-Mar-21	BG48	Groundwater	188,50	122,53	5,25	20,60	4,33	5,65	13,41	0,79	7,32	7,41	38,47	-2,83	13,37	nd	5,81	-3,90	-16,80	Ca-Mg-Cl
07-Apr-21	BG48	Groundwater	183,70	119,41	5,43	19,90	4,20	5,85	15,12	0,70	7,32	7,38	37,65	1,14	12,66	nd	7,45	-3,67	-16,10	Ca-Mg-Cl
19-Apr-21	BG48	Groundwater	187,90	122,14	5,41	20,20	4,65	6,33	17,38	1,39	15,86	6,56	38,18	2,34	10,43	nd	5,57	-3,58	-16,20	Na-Cl
03-May-21	BG48	Groundwater	188,40	122,46	5,60	19,60	5,41	5,18	17,10	1,24	7,32	6,86	38,71	2,68	10,01	BD	7,07	-3,33	-15,70	Na-Cl
17-May-21	BG48	Groundwater	189,80	123,37	5,63	19,50	4,46	6,22	16,80	1,21	15,86	7,43	39,47	3,02	9,89	BD	6,05	-3,23	-13,60	Na-Cl
31-May-21	BG48	Groundwater	175,00	113,75	5,36	19,00	12,23	4,39	14,32	0,85	9,76	5,71	31,54	3,46	7,50	BD	4,26	-3,20	-8,70	Ca-Mg-Cl
14-Jun-21	BG48	Groundwater	185,80	120,77	5,83	17,90	5,77	6,51	15,84	1,26	8,54	7,75	37,31	-3,40	10,12	BD	3,37	-3,13	-14,60	Ca-Mg-Cl
29-Jun-21	BG48	Groundwater	161,50	104,98	5,70	17,50	7,97	3,85	12,95	0,65	30,50	7,04	29,60	-0,28	2,23	BD	3,08	-2,82	-11,80	Ca-Mg-Cl
12-Jul-21	BG48	Groundwater	170,20	110,63	7,14	14,30	9,36	5,34	13,30	0,99	26,84	7,99	32,47	-1,68	15,27	BD	2,55	-2,49	-10,50	Ca-Mg-Cl
26-Jul-21	BG48	Groundwater	168,00	109,20	5,38	17,80	8,39	3,93	13,97	1,20	19,52	7,96	33,90	-3,53	11,96	BD	6,83	-2,89	-11,90	Ca-Mg-Cl
10-Aug-21	BG48	Groundwater	163,90	106,54	6,53	19,80	14,29	3,10	8,07	0,30	29,28	BD	13,86	-3,06	0,08	BD	5,94	-3,86	-13,81	Ca-HCO3
23-Aug-21	BG48	Groundwater	151,00	98,15	6,49	18,60	14,70	3,43	9,83	0,39	21,96	0,00	13,18	-3,27	0,21	BD	7,19	-2,95	-11,24	Ca-Mg-Cl
06-Sep-21	BG48	Groundwater	164,20	106,73	5,31	17,40	10,85	3,95	14,32	0,82	62,22	5,74	34,67	-0,90	4,43	BD	4,12	-2,97	-9,40	Ca-Mg-Cl
20-Sep-21	BG48	Groundwater	158,50	103,03	5,76	17,00	8,34	4,26	14,52	1,10	71,98	5,87	31,41	3,57	3,78	BD	4,24	-3,09	-13,20	Ca-HCO3
13-Oct-21	BG48	Groundwater	136,80	88,92	5,39	17,20	9,06	4,44	14,36	0,78	26,84	5,61	33,50	3,56	2,18	BD	5,18	-3,10	-11,75	Ca-Mg-Cl
27-Oct-21	BG48	Groundwater	146,10	94,97	6,52	21,30	11,79	3,14	12,79	0,88	19,52	4,82	30,80	4,26	1,75	nd	5,23	-2,90	-11,00	Ca-Mg-Cl
26-Jul-21	LFG	Groundwater	86,10	55,97	4,85	14,00	7,98	2,06	8,72	0,12	15,86	2,44	20,30	3,63	1,19	BD	3,87	-3,60	-15,70	Ca-Mg-Cl
10-Aug-21	LFG	Groundwater	86,70	56,36	4,61	15,50	8,72	2,62	7,84	0,06	21,96	2,30	19,35	2,00	1,10	BD	7,57	-3,49	-15,67	Ca-Mg-Cl
23-Aug-21	LFG	Groundwater	86,00	55,90	4,87	16,10	7,21	1,81	8,29	0,09	12,20	2,44	20,46	2,59	1,14	BD	3,77	-4,36	-17,37	Ca-Mg-Cl
06-Sep-21	LFG	Groundwater	87,70	57,01	5,01	15,20	7,44	1,93	9,34	0,12	14,64	2,42	20,43	4,06	1,21	BD	4,26	-4,20	-22,46	Ca-Mg-Cl
20-Sep-21	LFG	Groundwater	92,50	60,13	4,75	16,80	2,12	1,24	9,87	0,12	0,00	2,23	20,45	1,38	1,34	BD	5,93	-3,83	-14,92	Na-Cl
13-Oct-21	LFG	Groundwater	79,30	51,55	4,75	19,50	6,40	1,86	9,62	0,12	12,20	2,28	20,82	3,38	1,80	BD	6,73	-4,00	-19,73	Ca-Mg-Cl
27-Oct-21	LFG	Groundwater	84,60	54,99	5,57	21,80	4,16	2,54	8,04	0,09	4,88	2,28	20,41	4,42	1,55	nd	7,02	-3,69	-16,21	Ca-Mg-Cl
03-Nov-20	SD1	Groundwater	120,00	78,00	7,10	20,00	9,81	2,33	12,42	1,85	64,66	BD	10,93	-3,77	BD	0,08	9,52	-4,21	-15,20	Ca-HCO3
25-Nov-20	SD1	Groundwater	136,30	88,60	7,21	19,10	8,69	2,31	12,69	1,11	59,78	BD	10,98	-3,45	0,00	0,00	9,46	-3,99	-15,30	Ca-HCO3
08-Dec-20	SD1	Groundwater	128,20	83,33	6,79	21,10	5,64	2,20	11,90	1,96	45,14	BD	10,94	-0,91	0,00	0,11	10,50	-3,76	-15,00	Ca-Na-HCO3
22-Dec-20	SD1	Groundwater	155,80	101,27	7,32	21,40	11,63	1,68	12,65	39,00	130,54	BD	10,96	-3,86	0,14	0,11	9,59	-4,14	-18,00	Na-HCO3
13-Jan-21	SD1	Groundwater	136,30	88,60	7,25	20,80	15,96	2,23	11,49	1,92	81,74	BD	10,58	-3,44	1,09	0,00	10,15	-3,69	-15,00	Ca-HCO3
25-Jan-21	SD1	Groundwater	125,00	81,25	6,74	20,10	5,21	2,52	9,59	1,21	37,82	BD	10,36	0,22	0,00	0,00	14,24	-3,92	-15,10	Ca-HCO3
08-Feb-21	SD1	Groundwater	73,00	47,45	6,12	19,70	5,79	2,43	12,41	2,02	53,68	BD	10,91	-4,71	0,00	0,00	8,43	-3,91	-14,60	Ca-Na-HCO3
22-Feb-21	SD1	Groundwater	135,00	87,75	6,94	19,80	10,69	2,72	12,60	2,11	58,56	BD	10,90	3,49	BD	0,14	12,08	-3,81	-14,60	Ca-HCO3
08-Mar-21	SD1	Groundwater	136,00	88,40	6,11	19,30	9,92	2,19	12,18	1,99	61,00	BD	10,73	-1,83	BD	BD	6,72	-3,83	-15,40	Ca-HCO3
24-Mar-21	SD1	Groundwater	131,50	85,48	6,98	20,10	8,47	2,56	9,35	1,13	50,02	BD	10,62	-2,31	BD	0,10	9,63	-3,96	-15,00	Ca-HCO3
07-Apr-21	SD1	Groundwater	134,20	87,23	7,16	20,60	10,60	2,17	10,72	1,22	76,86	BD	10,44	-2,79	BD	BD	9,26	-3,75	-15,80	Ca-HCO3
19-Apr-21	SD1	Groundwater	137,70	89,51	6,94	20,50	13,50	2,87	12,43	2,09	75,64	BD	10,49	-3,56	BD	0,20	14,58	-3,59	-13,90	Ca-HCO3
03-May-21	SD1	Groundwater	137,00	89,05	6,85	20,10	13,15	2,79	12,42	2,10	65,88	BD	10,57	-2,59	BD	0,16	6,05	-4,18	-16,50	Ca-HCO3
17-May-21	SD1	Groundwater	142,60	92,69	7,06	17,00	13,04	2,56	11,72	1,63	79,30	BD	10,36	-4,03	BD	0,15	4,23	-3,88	-14,00	Ca-HCO3
31-May-21	SD1	Groundwater	129,80	84,37	7,05	13,50	13,39	2,89	11,71	1,83	79,30	BD	10,40	3,14	nd	0,12	11,78	-3,42	-12,10	Ca-HCO3
14-Jun-21	SD1	Groundwater	131,70	85,61	7,07	12,90	13,74	3,41	10,81	1,31	89,06	BD	10,26	-3,90	BD	0,13	10,86	-3,44	-12,60	Ca-HCO3
29-Jun-21	SD1	Groundwater	130,20	84,63	6,97	13,20	13,86	3,41	10,69	1,14	92,72	BD	10,25	-4,01	BD	0,13	6,83	-2,87	-10,40	Ca-HCO3
12-Jul-21	SD1	Groundwater	34,40	22,36	7,05	10,20	16,33	3,13	11,00	1,77	75,64	BD	10,53	-4,81	BD	0,11	6,47	-3,18	-11,60	Ca-HCO3

Date	Sample ID	Data Source	EC	TDS	pH	Temp	Ca^{2+}	Mg^{2+}	Na^{+}	K^{+}	HCO_3^{-}	SO_4^{2-}	Cl^{-}	CB	NO_3^{-}	PO_4^{2-}	SiO_2	$\delta^{18}O$	$\delta^{2}H$	Water Type
26-Jul-21	SD1	Groundwater	135,80	88,27	6,93	11,30	15,93	3,57	11,43	1,76	87,84	BD	10,57	-3,17	BD	0,09	8,22	-3,11	-11,30	Ca-HCO3
10-Aug-21	SD1	Groundwater	137,30	89,25	7,73	11,20	13,89	3,07	9,47	0,91	74,42	BD	10,17	-4,35	BD	BD	11,57	-3,61	-12,87	Ca-HCO3
23-Aug-21	SD1	Groundwater	135,10	87,82	6,03	12,10	14,53	2,97	11,50	2,44	64,66	1,63	11,86	-3,64	0,06	BD	10,06	-3,18	-10,75	Ca-HCO3
06-Sep-21	SD1	Groundwater	139,80	90,87	7,05	13,70	13,83	2,57	11,65	1,61	73,20	BD	10,62	4,70	BD	0,17	12,69	-3,27	-12,04	Ca-HCO3
20-Sep-21	SD1	Groundwater	143,20	93,08	7,51	16,50	14,11	2,78	12,17	1,92	57,34	0,95	10,70	4,48	BD	BD	12,05	-3,50	-12,89	Ca-HCO3
13-Oct-21	SD1	Groundwater	122,70	79,76	6,75	19,90	14,80	3,20	11,95	1,67	73,20	0,95	10,83	1,29	BD	BD	12,24	-3,55	-11,23	Ca-HCO3
27-Oct-21	SD1	Groundwater	128,20	83,33	7,68	20,70	13,06	3,06	8,91	0,92	57,34	0,95	10,69	2,07	0,05	BD	16,20	-2,94	-9,55	Ca-Mg-HCO3
03-Nov-20	BRRBH	Groundwater	517,00	336,05	7,38	19,60	3,00	2,63	97,25	0,42	119,56	35,17	80,85	-3,81	9,42	0,39	10,25	-2,79	-12,90	Na-Cl
25-Nov-20	BRRBH	Groundwater	516,00	335,40	6,68	19,10	3,29	2,41	98,90	nd	108,58	34,01	81,79	-1,38	4,75	0,39	10,69	-3,26	-13,40	Na-Cl
08-Dec-20	BRRBH	Groundwater	496,00	322,40	6,89	20,50	6,13	2,02	96,63	0,33	122,00	33,82	85,48	-4,40	4,39	0,56	11,27	-3,37	-13,20	Na-Cl
13-Jan-21	BRRBH	Groundwater	532,00	345,80	8,17	21,90	3,19	3,41	93,43	0,34	242,78	he lowest c	6,34	4,08	0,57	0,57	10,01	-3,48	-12,70	Na-HCO3
25-Jan-21	BRRBH	Groundwater	555,00	360,75	6,47	21,50	10,30	2,68	69,67	0,22	63,44	30,24	86,54	-4,32	6,35	6,35	16,04	-3,16	-12,40	Na-Cl
08-Feb-21	BRRBH	Groundwater	528,80	343,72	7,74	22,00	9,52	2,84	94,85	0,38	137,86	31,44	86,01	-4,87	6,62	0,57	11,17	-3,11	-12,80	Na-Cl
22-Feb-21	BRRBH	Groundwater	527,10	342,62	8,20	20,80	6,81	2,54	102,02	0,60	93,94	31,29	86,55	3,83	6,47	0,57	9,65	-3,24	-13,10	Na-Cl
08-Mar-21	BRRBH	Groundwater	517,70	336,51	6,97	20,60	5,83	1,98	96,78	0,29	117,12	29,98	83,46	-2,37	6,52	0,44	10,21	-3,34	-13,10	Na-Cl
24-Mar-21	BRRBH	Groundwater	510,10	331,57	7,14	20,30	10,54	2,26	75,72	0,21	63,44	29,14	82,97	0,30	6,60	0,47	10,47	-3,48	-13,30	Na-Cl
07-Apr-21	BRRBH	Groundwater	502,00	326,30	6,95	19,70	8,50	2,21	84,22	0,14	76,86	28,91	81,38	1,37	5,56	0,35	6,94	-3,50	-14,70	Na-Cl
19-Apr-21	BRRBH	Groundwater	512,00	332,80	7,47	20,10	16,92	6,48	46,52	2,02	54,90	16,99	78,56	-0,24	BD	nd	9,16	-2,98	-12,40	Na-Cl
03-May-21	BRRBH	Groundwater	481,00	312,65	6,58	18,30	5,35	2,95	94,36	0,43	112,24	27,77	76,48	0,54	4,92	0,72	16,70	-2,97	-12,40	Na-Cl
17-May-21	BRRBH	Groundwater	536,10	348,47	7,56	17,60	8,96	2,87	93,63	0,26	117,12	27,00	79,89	0,30	5,13	0,62	9,87	-2,43	-7,90	Na-Cl
31-May-21	BRRBH	Groundwater	484,00	314,60	7,37	16,50	9,27	2,89	92,25	0,38	43,92	26,74	81,42	0,96	6,03	0,60	8,09	-3,02	-9,40	Na-Cl
14-Jun-21	BRRBH	Groundwater	496,00	322,40	7,63	15,60	11,87	2,59	86,31	0,27	98,82	26,51	81,54	-0,06	6,91	0,49	10,40	-2,75	-10,20	Na-Cl
29-Jun-21	BRRBH	Groundwater	474,00	308,10	7,21	15,10	7,94	2,98	8,47	2,34	34,16	4,11	16,13	-1,43	2,57	BD	0,84	-3,49	-12,17	Ca-HCO3
12-Jul-21	BRRBH	Groundwater	489,00	317,85	7,57	14,50	4,70	4,25	89,19	0,29	115,90	27,39	78,21	0,85	5,91	0,54	7,36	-2,04	-7,30	Na-Cl
26-Jul-21	BRRBH	Groundwater	501,00	325,65	7,40	14,50	14,47	3,33	90,94	0,37	111,02	28,28	81,48	0,35	8,16	0,54	9,53	-2,48	-8,00	Na-Cl
10-Aug-21	BRRBH	Groundwater	512,00	332,80	7,09	11,40	13,93	2,52	79,19	0,28	102,48	27,02	81,43	-4,45	7,89	0,38	8,03	-2,59	-7,77	Na-Cl
23-Aug-21	BRRBH	Groundwater	506,00	328,90	6,67	12,80	12,80	2,54	88,08	0,30	112,24	29,05	80,01	0,06	7,11	0,46	11,35	-2,85	-10,45	Na-Cl
06-Sep-21	BRRBH	Groundwater	527,00	342,55	7,62	13,90	10,86	3,50	97,89	0,35	82,96	29,28	87,98	3,30	9,82	0,90	10,79	-2,72	-8,33	Na-Cl
20-Sep-21	BRRBH	Groundwater	536,00	348,40	7,10	15,70	8,89	3,48	97,57	0,34	76,86	28,25	79,51	3,23	9,65	0,30	12,38	-2,63	-8,93	Na-Cl
13-Oct-21	BRRBH	Groundwater	404,40	262,86	7,39	17,90	3,60	2,83	99,28	0,39	87,84	29,89	82,79	4,68	9,39	0,29	7,85	-2,69	-9,73	Na-Cl
27-Oct-21	BRRBH	Groundwater	492,00	319,80	8,20	18,40	5,84	2,92	94,58	0,49	89,06	29,93	83,16	4,83	9,26	0,29	10,14	-3,06	-11,61	Na-Cl
03-Nov-20	PGE1	Groundwater	303,00	196,95	7,20	20,40	16,16	10,87	23,10	1,41	93,94	7,35	41,24	-2,05	1,26	0,00	9,25	-2,52	-10,90	Ca-HCO3
25-Nov-20	PGE1	Groundwater	301,00	195,65	6,98	20,90	14,28	11,48	23,66	0,55	85,40	7,33	41,81	-0,56	0,69	0,12	9,46	-3,06	-11,60	Ca-HCO3
08-Dec-20	PGE1	Groundwater	306,00	198,90	6,15	22,30	14,11	10,35	24,57	1,32	84,18	8,23	48,04	-4,47	0,08	nd	10,80	-2,73	-9,80	Ca-Mg-Cl
22-Dec-20	PGE1	Groundwater	349,00	226,85	6,52	21,70	14,11	12,55	24,87	1,33	91,50	9,00	49,13	-3,72	4,54	nd	8,07	-2,88	-11,30	Ca-Mg-Cl
13-Jan-21	PGE1	Groundwater	281,30	182,85	5,50	20,30	15,71	12,13	21,35	1,05	87,84	8,08	43,36	-1,68	0,88	nd	10,68	-2,74	-10,10	Ca-HCO3
25-Jan-21	PGE1	Groundwater	265,00	172,25	6,20	20,20	10,85	7,53	17,15	0,79	47,58	6,51	41,35	-3,85	0,92	0,00	12,01	-2,83	-9,90	Ca-Mg-Cl
08-Feb-21	PGE1	Groundwater	299,40	194,61	5,90	21,80	12,00	11,89	23,40	1,13	78,08	10,41	44,70	-2,48	0,30	nd	10,16	-2,90	-10,60	Ca-Mg-Cl
22-Feb-21	PGE1	Groundwater	307,30	199,75	2,69	21,40	14,44	11,08	24,46	1,33	63,44	9,86	45,22	4,00	0,35	BD	8,79	-2,84	-10,30	Ca-Mg-Cl
08-Mar-21	PGE1	Groundwater	282,50	183,63	5,98	22,70	10,63	10,75	23,79	1,20	75,64	8,97	44,51	-3,91	0,51	BD	9,08	-2,83	-10,90	Ca-Mg-Cl
24-Mar-21	PGE1	Groundwater	290,90	189,09	6,26	22,00	11,89	7,79	18,85	0,72	51,24	6,66	44,27	-3,61	BD	BD	8,92	-2,91	-10,40	Ca-Mg-Cl
07-Apr-21	PGE1	Groundwater	323,00	209,95	7,13	21,90	21,14	9,38	19,96	0,60	92,72	6,82	43,03	-1,55	BD	BD	7,62	-2,55	-8,20	Ca-HCO3
19-Apr-21	PGE1	Groundwater	284,00	184,60	6,35	21,10	16,57	11,07	23,27	1,15	96,38	8,03	43,72	-1,43	0,54	BD	8,94	-2,88	-10,70	Ca-HCO3
03-May-21	PGE1	Groundwater	365,00	237,25	6,64	21,90	17,13	11,46	23,51	1,18	71,98	6,40	44,35	-0,93	0,21	BD	10,40	-2,70	-11,30	Ca-Mg-Cl
17-May-21	PGE1	Groundwater	296,50	192,73	6,41	17,70	15,30	12,80	22,71	0,93	97,60	6,24	41,99	-1,14	0,78	BD	6,68	-2,11	-5,90	Ca-HCO3
31-May-21	PGE1	Groundwater	250,00	162,50	6,95	14,90	14,63	12,27	22,15	0,72	79,30	8,16	42,77	3,13	0,35	BD	8,48	-2,54	-7,10	Ca-Mg-Cl
14-Jun-21	PGE1	Groundwater	331,00	215,15	6,49	15,90	18,04	13,10	21,98	0,90	81,74	10,92	42,27	-1,04	BD	BD	9,40	-1,66	-4,80	Ca-Mg-Cl
29-Jun-21	PGE1	Groundwater	342,00	222,30	6,43	16,40	17,83	12,32	21,77	0,85	98,82	4,60	43,07	4,78	BD	BD	5,07	-1,88	-6,40	Ca-HCO3
12-Jul-21	PGE1	Groundwater	283,00	183,95	5,98	12,90	11,61	12,10	20,15	0,69	68,32	10,02	43,63	-1,79	0,47	BD	7,55	-1,96	-5,30	Ca-Mg-Cl
26-Jul-21	PGE1	Groundwater	300,00	195,00	6,49	12,00	16,91	13,40	21,63	0,94	82,96	7,30	41,98	-0,77	0,95	BD	10,07	-1,76	-6,00	Ca-HCO3
10-Aug-21	PGE1	Groundwater	300,00	195,00	6,61	13,30	16,72	12,39	20,13	0,53	61,00	8,13	40,45	-1,91	0,09	BD	10,98	-2,51	-7,96	Ca-Mg-Cl
23-Aug-21	PGE1	Groundwater	291,60	189,54	6,26	15,90	14,95	10,23	22,60	1,06	71,98	9,08	44,64	-3,88	BD	nd	10,23	-2,15	-6,02	Ca-Mg-Cl
06-Sep-21	PGE1	Groundwater	289,00	187,85	6,49	14,20	13,27	12,34	22,74	0,74	69,54	8,12	47,35	3,49	0,32	BD	11,80	-2,53	-8,38	Ca-Mg-Cl
20-Sep-21	PGE1	Groundwater	291,00	189,15	6,38	16,50	13,68	11,81	22,59	0,88	67,10	5,59	41,85	3,56	0,09	nd	7,48	-2,48	-6,36	Ca-Mg-Cl
13-Oct-21	PGE1	Groundwater	212,90	138,39	5,92	18,10	13,26	11,88	22,91	1,07	59,78	8,37	42,18	3,09	0,51	BD	11,44	-2,60	-7,76	Ca-Mg-Cl
27-Oct-21	PGE1	Groundwater	272,80	177,32	6,82	21,20	11,66	11,79	22,47	1,17	80,52	7,78	43,12	1,60	0,28	nd	10,50	-2,01	-4,78	Ca-Mg-Cl
25-Nov-20	FRAAI 1	Groundwater	787,00	511,55	6,33	22,60	13,58	20,58	92,46	nd	24,40	BD	218,71	-1,37	nd	0,64	7,50	-3,71	-15,10	Na-Cl
08-Dec-20	FRAAI 1	Groundwater	757,00	492,05	6,20	22,00	13,33	23,47	89,28	1,33	30,50	5,11	216,72	-1,55	0,37	nd	11,49	-3,58	-15,00	Na-Cl
22-Dec-20	FRAAI 1	Groundwater	867,00	563,55	6,52	23,60	13,75	26,84	92,51	1,29	34,16	5,23	215,98	1,39	0,82	nd	9,88	-3,64	-15,90	Na-Cl
13-Jan-21	FRAAI 1	Groundwater	768,00	499,20	6,48	22,40	14,43	26,37	81,99	1,15	18,30	4,78	205,16	2,36	0,68	nd	12,02	-3,64	-14,20	Na-Cl
25-Jan-21	FRAAI 1	Groundwater	710,00	461,50	6,73	22,30	**11,82**	**16,94**	**70,65**	**0,84**	**0,00**	**3,84**	**206,32**	-7,49	0,67	nd	12,43	-3,58	-14,60	**N/A**
08-Feb-21	FRAAI 1	Groundwater	444,70	289,06	5,44	22,20	14,36	22,78	85,15	1,30	12,20	4,29	213,47	0,14	0,69	0,00	5,37	-3,54	-14,80	Na-Cl
22-Feb-21	FRAAI 1	Groundwater	762,00	495,30	7,05	22,50	14,98	25,92	89,69	1,11	18,30	4,51	213,39	3,00	0,82	nd	10,89	-3,64	-15,10	Na-Cl
08-Mar-21	FRAAI 1	Groundwater	768,00	499,20	6,06	22,20	13,11	24,83	87,84	1,18	17,08	4,90	213,09	1,20	0,82	BD	10,89	-3,76	-15,30	Na-Cl
24-Mar-21	FRAAI 1	Groundwater	406,90	264,49	6,52	22,80	16,46	20,36	70,82	0,83	0,00	4,84	215,51	-4,94	0,79	nd	11,72	-3,79	-14,80	Na-Cl
08-Dec-20	MEAD 1	Groundwater	458,00	297,70	7,06	24,50	19,54	5,70	62,68	1,78	145,18	3,36	72,82	-3,30	0,00	nd	7,44	-3,57	-14,50	Ca-Na-HCO3
22-Dec-20	MEAD 1	Groundwater	558,00	362,70	7,10	24,40	26,97	5,14	67,88	1,82	154,94	3,82	76,49	-0,09	3,97	nd	11,70	-3,52	-12,60	Ca-Na-HCO3
13-Jan-21	MEAD 1	Groundwater	479,00	311,35	6,36	23,20	27,15	4,65	61,78	1,29	134,20	2,54	74,06	1,32	0,95	nd	9,89	-3,54	-14,80	Ca-Na-HCO3
25-Jan-21	MEAD 1	Groundwater	450,00	292,50	6,83	23,00	20,94	5,70	56,28	1,60	135,42	3,05	72,82	-4,01	0,00	nd	15,60	-3,53	-14,10	Ca-Na-HCO3
08-Feb-21	MEAD 1	Groundwater	476,50	309,73	6,37	24,30	19,00	7,51	61,55	1,57	140,30	2,34	72,77	-1,36	0,00	nd	10,75	-3,49	-14,50	Ca-Na-HCO3
22-Feb-21	MEAD 1	Groundwater	494,80	321,62	6,30	22,80	26,67	5,74	65,83	2,77	128,10	3,65	75,07	4,92	BD	nd	8,15	-3,48	-14,00	Na-Cl
08-Mar-21	MEAD 1	Groundwater	491,00	319,15	6,20	22,50	21,12	5,30	60,77	1,60	114,68	3,86	73,95	1,56	BD	nd	9,85	-3,67	-14,60	Na-Cl
24-Mar-21	MEAD 1	Groundwater	492,60	320,19	6,95	23,80	20,16	6,16	52,81	1,16	102,48	4,00	74,72	-0,40	BD	nd	5,65	-3,71	-14,50	Na-Cl
07-Apr-21	MEAD 1	Groundwater	491,00	319,15	7,18	23,90	20,43	5,32	55,22	1,29	104,92	3,99	73,14	0,34	BD	nd	6,12	-3,53	-15,00	Na-Cl
19-Apr-21	MEAD 1	Groundwater	502,00	326,30	7,22	22,30	24,52	6,74	63,99	1,80	132,98	3,32	73,02	3,36	BD	BD	9,67	-3,45	-16,30	Ca-Na-HCO3
03-May-21	MEAD 1	Groundwater	500,00	325,00	7,28	22,00	29,27	6,11	65,49	1,87	142,74	3,37	75,01	3,56	BD	BD	10,47	-3,47	-14,90	Ca-Na-HCO3
17-May-21	MEAD 1	Groundwater	489,90	318,44	7,64	18,40	31,74	5,77	63,92	1,87	143,96	3,41	73,96	3,94	BD	BD	17,86	-2,98	-11,20	Ca-Na-HCO3
31-May-21	MEAD 1	Groundwater	465,00	302,25	7,18	19,90	28,50	6,16	60,59	1,90	169,58	3,44	75,17	-3,74	BD	BD	8,70	-3,54	-12,40	Ca-Na-HCO3
14-Jun-21	MEAD 1	Groundwater	495,00	321,75	6,95	18,40	25,65	6,07	58,17	1,62	120,78	3,62	74,09	2,43	BD	BD	11,54	-2,78	-10,90	Na-Cl
29-Jun-21	MEAD 1	Groundwater	483,00	313,95	7,27	17,70	28,25	6,30	61,09	1,47	126,88	3,26	75,30	3,96	BD	BD	6,89	-3,16	-10,23	Na-Cl
12-Jul-21	MEAD 1	Groundwater	497,00	323,05	6,94	15,50	23,69	5,53	56,98	1,14	100,04	3,88	75,45	3,70	BD	BD	7,10	-2,75	-10,80	Na-Cl
26-Jul-21	MEAD 1	Groundwater	500,00	325,00	7,65	17,20	30,68	8,26	59,98	1,46	141,52	4,03	75,11	3,57	BD	BD	4,40	-2,69	-10,70	Ca-Na-HCO3
10-Aug-21	MEAD 1	Groundwater	511,00	332,15	7,25	17,80	22,10	5,47	50,98	1,01	89,06	4,08	73,41	2,44	0,18	nd	6,56	-3,22	-10,08	Na-Cl
23-Aug-21	MEAD 1	Groundwater	492,00	319,80	8,33	17,70	26,40	6,19	61,09	1,70	120,78	4,22	75,89	3,65	BD	BD	10,87	-3,28	-12,22	Na-Cl
06-Sep-21	MEAD 1	Groundwater	513,00	333,45	7,32	19,10	27,56	7,63	61,81	1,43	123,22	4,24	77,43	4,83	BD	nd	12,38	-3,15	-12,64	Na-Cl
20-Sep-21	MEAD 1	Groundwater	519,00	337,35	7,29	19,50	25,92	6,64	60,43	1,52	130,54	4,08	69,85	3,59	BD	BD	9,04	-3,07	-11,31	Ca-Na-HCO3
13-Oct-21	MEAD 1	Groundwater	344,00	223,60	7,23	20,70	26,78	7,39	61,14	1,48	130,54	4,14	70,78	4,74	BD	nd	10,21	-3,63	-15,18	Ca-Na-HCO3
27-Oct-21	MEAD 1	Groundwater	463,00	300,95	7,85	25,40	27,40	6,58	60,55	1,65	132,98	4,03	71,71	3,36	BD	BD	11,16	-3,04	-10,99	Ca-Na-HCO3
03-Nov-20	BRBBH	Groundwater	417,00	271,05	6,59	18,70	10,77	5,54	46,02	2,28	45,14	17,39	71,72	-1,16	0,00	0,00	7,50	-2,91	-11,70	Na-Cl
25-Nov-20	BRBBH	Groundwater	386,00	250,90	6,10	21,30	9,37	5,42	45,45	2,31	46,36	14,57	66,40	0,22	nd	nd	7,57	-3,31	-12,20	Na-Cl
08-Dec-20	BRBBH	Groundwater	354,00	230,10	6,28	21,00	8,10	5,71	41,16	2,17	41,48	12,93	65,42	-1,36	BD	0,00	7,72	-3,35	-12,70	Na-Cl
22-Dec-20	BRBBH	Groundwater	410,00	266,50	6,46	22,30	10,28	5,45	44,97	2,46	59,78	11,47	65,57	-1,46	0,22	0,00	7,67	-3,17	-13,30	Na-Cl
25-Jan-21	BRBBH	Groundwater	310,00	201,50	6,22	20,40	15,94	5,78	33,87	1,95	43,92	12,92	61,39	1,34	0,00	nd	7,00	-3,23	-12,40	Na-Cl
08-Feb-21	BRBBH	Groundwater	377,50	245,38	6,51	20,70	16,70	6,18	39,59	2,35	85,40	14,01	60,41	-4,16	0,00	nd	6,48	-3,50	-12,80	Na-Cl
22-Feb-21	BRBBH	Groundwater	376,70	244,86	5,54	20,90	12,62	6,84	43,93	2,54	68,32	15,17	63,69	-1,01	BD	nd	5,98	-3,22	-12,10	Na-Cl
08-Mar-21	BRBBH	Groundwater	386,80	251,42	5,20	20,30	14,33	5,69	42,46	2,21	63,44	15,71	66,80	-2,60	BD	BD	5,35	-3,38	-13,00	Na-Cl
24-Mar-21	BRBBH	Groundwater	413,60	268,84	5,95	20,90	8,73	9,19	36,23	1,44	34,16	18,19	72,18	-2,95	BD	BD	6,97	-3,52	-12,40	Na-Cl
07-Apr-21	BRBBH	Groundwater	414,00	269,10	6,24	22,90	13,34	6,52	39,56	1,56	43,92	18,53	72,73	-3,17	BD	nd	7,68	-3,10	-11,90	Na-Cl
19-Apr-21	BRBBH	Groundwater	441,00	286,65	6,29	22,00	4,97	3,21	96,96	0,34	108,58	27,14	82,49	0,71	5,98	0,70	6,77	-3,04	-13,00	Na-Cl
03-May-21	BRBBH	Groundwater	448,00	291,20	6,29	22,30	14,80	7,80	51,20	2,98	62,22	12,23	83,34	0,80	BD	BD	5,62	-2,90	-11,10	Na-Cl
17-May-21	BRBBH	Groundwater	435,80	283,27	3,86	21,00	12,99	6,96	50,89	2,85	75,64	11,08	82,82	-4,09	BD	BD	6,40	-2,92	-12,60	Na-Cl
31-May-21	BRBBH	Groundwater	395,00	256,75	6,42	20,50	11,66	7,63	45,63	2,23	61,00	10,44	77,02	-2,08	BD	BD	3,78	-3,17	-10,80	Na-Cl
14-Jun-21	BRBBH	Groundwater	427,00	277,55	6,28	19,60	14,72	7,15	46,01	1,84	73,20	14,60	77,06	-4,34	BD	BD	4,05	-2,36	-8,00	Na-Cl
29-Jun-21	BRBBH	Groundwater	401,00	260,65	6,20	18,60	14,51	6,96	43,58	1,88	56,12	7,44	73,98	1,22	0,06	nd	3,50	-2,70	-9,50	Na-Cl
12-Jul-21	BRBBH	Groundwater	409,00	265,85	6,35	19,10	14,87	8,05	40,23	1,32	52,46	14,23	68,92	1,40	BD	BD	2,97	-2,26	-6,10	Na-Cl
26-Jul-21	BRBBH	Groundwater	507,00	329,55	6,38	20,30	16,27	7,13	55,80	1,45	54,90	31,95	87,86	-2,29	BD	BD	7,03	-2,48	-8,00	Na-Cl
10-Aug-21	BRBBH	Groundwater	476,00	309,40	6,40	19,10	17,31	7,07	41,20	0,99	51,24	24,40	76,97	-3,77	BD	nd	5,03	-3,04	-7,05	Na-Cl
23-Aug-21	BRBBH	Groundwater	466,00	302,90	7,33	19,90	15,86	7,78	45,63	1,36	50,02	27,37	84,17	-4,34	BD	BD	3,62	-2,68	-7,65	Na-Cl
06-Sep-21	BRBBH	Groundwater	580,00	377,00	6,37	19,80	19,55	8,18	60,99	2,10	56,12	42,33	101,77	-3,51	BD	nd	7,10	-2,97	-8,42	Na-Cl
20-Sep-21	BRBBH	Groundwater	560,00	364,00	6,42	20,30	16,30	7,47	54,26	1,93	54,90	33,47	91,34	-4,19	BD	BD	2,43	-3,09	-8,00	Na-Cl
13-Oct-21	BRBBH	Groundwater	359,50	233,68	6,19	19,30	19,08	7,26	54,48	1,85	61,00	37,77	83,64	-2,20	BD	nd	3,82	-3,03	-12,99	Na-Cl
27-Oct-21	BRBBH	Groundwater	487,40	316,81	7,04	20,80	21,47	7,12	53,44	2,25	50,02	36,92	84,22	-0,30	BD	nd	6,34	-2,87	-9,11	Na-Cl

B. Precipitation data sheet

Date	Sample ID	Data Source	EC	TDS	pH	Temp	Ca^{2+}	Mg^{2+}	Na^{+}	K^{+}	HCO_3^{-}	SO_4^{2-}	Cl^{-}	CB	NO_3^{-}	PO_4^{2-}	SiO_2	$\delta^{18}O$	$\delta^{2}H$	Water Type	Rainfall Amount
06-Nov-20	RF1	Rainfall	-	-	-	-	-	-	-	-	-	-	-	-	-	-	-	-3,25	-10,90	-	41,6
25-Nov-20	RF1	Rainfall	38,10	24,77	6,23	18,70	1,16	0,61	2,92	0,16	1,22	2,35	6,70	-3,79	0,43	0,11	0,00	-1,14	2,40	Na-Cl	5,4
08-Dec-20	RF1	Rainfall	-	-	-	-	-	-	-	-	-	-	-	-	-	-	-	-1,68	-3,10	-	3
21-Dec-20	RF1	Rainfall	-	-	-	24,00	-	-	-	-	-	-	-	-	-	-	-	4,00	34,10	-	2,4
13-Jan-21	RF1	Rainfall	-	-	-	24,50	-	-	-	-	-	-	-	-	-	-	-	3,80	34,30	-	6,8
25-Jan-21	RF1	Rainfall	60,00	39,00	6,18		-	-	-	-	-	-	-	-	-	-	-	1,48	18,40	-	2,6
08-Feb-21	RF1	Rainfall	11,00	7,15		19,90	-	-	-	-	-	-	-	-	-	-	-	-1,68	-3,10	-	3,2
11-Mar-21	RF1	Rainfall	10,30	6,70	6,26	19,10	0,27	0,09	0,61	0,05	1,22	BD	1,17	-4,73	0,24	BD	0,07	-2,24	-2,60	Na-Cl	0,7
24-Mar-21	RF1	Rainfall	-	-	-	23,00	-	-	-	-	-	-	-	-	-	-	-	0,50	14,80	-	4
29-Mar-21	RF1	Rainfall	9,80	6,37	6,30	18,20	2,71	0,71	1,17	0,46	3,66	3,51	4,01	1,99	5,88	0,13	0,14	-1,14	2,60	Ca-Cl	0,5
03-May-21	RF1	Rainfall	39,80	25,87	7,17	17,30	-	-	-	-	-	-	-	-	-	-	-	-3,87	-21,00	-	0,2
06-May-21	RF1	Rainfall	17,10	11,12	6,50	15,50	-	-	-	-	-	-	-	-	-	-	-	-6,95	-51,90	-	28,3
12-May-21	RF1	Rainfall	24,50	15,93	6,92	17,50	4,85	0,75	0,24	0,11	15,86	0,00	1,15	4,11	0,71	BD	0,09	-2,25	-9,40	Ca-HCO3	28
27-May-21	RF1	Rainfall	17,10	11,12	6,54	16,10	3,32	0,98	0,51	0,04	13,42	0,00	1,57	1,00	0,51	BD	0,04	-3,99	-17,40	Ca-HCO3	45
31-May-21	RF1	Rainfall	45,00	29,25	7,14	15,00	3,33	1,07	0,74	0,00	13,42	0,00	1,85	2,54	0,31	BD	0,03	-2,71	-1,90	Ca-HCO3	16
08-Jun-21	RF1	Rainfall	108,30	70,40	6,98	12,50	4,43	1,30	2,30	0,11	14,64	BD	5,64	3,89	0,30	BD	0,02	1,25	17,00	Ca-HCO3	1,7
25-Jun-21	RF1	Rainfall	34,10	22,17	7,70	12,20	5,11	1,29	2,37	0,01	18,30	BD	5,55	0,80	0,29	BD	0,02	-3,36	-9,90	Ca-HCO3	45,1
26-Jun-21	RF1	Rainfall	34,60	22,49	7,54	13,80	4,97	1,39	2,56	0,05	17,08	BD	5,98	2,85	0,31	BD	0,02	-3,23	-9,90	Ca-HCO3	8,2
29-Jun-21	RF1	Rainfall	34,20	22,23	7,67	11,10	-	-	-	-	-	-	-	-	-	-	-	-2,96	-7,90	-	36,4
29-Jun-21	RF1	Rainfall	12,09	7,86	7,38	11,50	3,40	1,32	0,80	0,02	15,86	0,00	1,37	2,44	0,55	BD	0,02	-5,65	-33,60	Ca-HCO3	20,8
30-Jun-21	RF1	Rainfall	12,64	8,22	7,72	11,80	3,48	1,21	0,91	0,11	15,86	BD	1,35	2,83	0,55	BD	0,01	-5,61	-34,50	Ca-HCO3	28,9
12-Jul-21	RF1	Rainfall	27,50	17,88	7,62	7,80	4,46	1,46	1,64	0,12	17,08	BD	4,48	1,33	0,17	BD	-0,08	-5,64	-28,30	Ca-HCO3	84,3
13-Jul-21	RF1	Rainfall	26,80	17,42	7,71	8,10	4,85	1,68	2,08	0,10	18,30	BD	5,17	2,95	0,17	BD	0,01	-5,58	-29,20	Ca-HCO3	2,9
27-Jul-21	RF1	Rainfall	49,50	32,18	7,33	9,00	3,43	1,83	5,10	0,15	10,98	2,01	11,09	1,23	0,25	BD	0,05	-3,82	-4,30	Ca-Mg-Cl	24,2
09-Aug-21	RF1	Rainfall	17,34	11,27	8,07	15,50	6,67	0,53	0,70	BD	19,52	BD	2,49	2,08	0,37	BD	0,04	-2,32	3,17	Ca-HCO3	4,7
12-Aug-21	RF1	Rainfall	18,87	12,27	8,09	16,10	6,76	0,51	0,86	0,03	20,74	BD	2,53	0,70	0,36	BD	0,04	-2,09	4,36	Ca-HCO3	7,3
18-Aug-21	RF1	Rainfall	13,00	8,45	8,79	6,80	-	-	-	-	-	-	-	-	-	-	-	-3,45	-19,92	-	31
20-Aug-21	RF1	Rainfall	53,70	34,91	6,50	16,00	4,94	1,39	0,52	0,04	18,30	BD	2,20	2,96	0,69	BD	0,07	1,17	17,92	Ca-HCO3	6
23-Aug-21	RF1	Rainfall	18,10	11,77	6,78	6,70	4,85	1,00	0,55	0,05	17,08	BD	2,23	1,04	0,70	BD	0,06	-2,92	-17,82	Ca-HCO3	7,5
26-Aug-21	RF1	Rainfall	36,40	23,66	-	-	5,00	0,77	0,99	0,12	14,64	2,31	3,21	-2,72	1,36	BD	0,10	-0,61	-1,63	Ca-HCO3	38
27-Aug-21	RF1	Rainfall	36,70	23,86	6,66	12,80	5,96	2,29	1,45	0,08	24,40	BD	3,78	4,20	0,30	BD	0,05	-4,74	-18,05	Ca-HCO3	22,8
28-Aug-21	RF1	Rainfall	37,70	24,51	6,78	12,70	5,75	2,26	1,36	0,11	25,62	BD	3,86	0,59	0,29	BD	0,03	-4,23	-13,78	Ca-HCO3	0,4
31-Aug-21	RF1	Rainfall	36,00	23,40	6,69	12,50	6,72	0,27	1,21	0,12	19,52	BD	3,74	-1,39	0,29	BD	0,03	-4,44	-14,71	Ca-HCO3	6,8
06-Sep-21	RF1	Rainfall	30,00	19,50	7,33	7,40	2,22	1,43	2,17	0,14	10,98	BD	4,61	2,47	0,51	BD	0,08	-0,99	11,81	Ca-HCO3	9,7
20-Sep-21	RF1	Rainfall	50,30	32,70	7,71	13,30	3,54	1,89	2,44	0,47	15,86	1,35	5,06	2,26	0,59	n.d	0,08	-1,64	2,10	Ca-HCO3	7,9
02-Oct-21	RF1	Rainfall	53,60	34,84	7,21	17,00	3,36	1,60	3,85	0,60	12,20	4,37	7,69	-2,62	1,63	BD	0,09	-0,85	10,10	Ca-Mg-Cl	5,8
14-Oct-21	RF1	Rainfall	30,00	19,50	7,30	16,50	4,38	1,55	1,78	0,17	15,86	1,88	4,08	1,58	1,11	BD	0,06	-0,77	2,41	Ca-HCO3	14
17-Oct-21	RF1	Rainfall	52,00	33,80	7,29	17,70	4,46	2,21	13,14	1,80	9,76	6,56	26,11	-0,52	1,56	n.d	0,03	-3,27	-15,17	Na-Cl	25
22-Oct-21	RF1	Rainfall	59,40	38,61	7,04	17,60	4,62	1,81	4,88	0,35	13,42	2,33	11,32	1,09	0,52	BD	0,08	-3,03	-11,31	Ca-Mg-Cl	12,8
23-Oct-21	RF1	Rainfall	49,30	32,05	6,97	18,30	4,69	1,45	4,88	0,31	12,20	2,24	11,24	0,87	0,52	BD	0,09	-3,49	-15,37	Ca-Mg-Cl	19,2
31-Jan-21	UWC-RF#1	Rainfall	30,00	19,50	5,50	20,00	-	-	-	-	-	-	-	-	-	-	-	-1,78	-5,80	-	3,2
10-Mar-21	UWC-RF#1	Rainfall	42,00	27,30	4,77	21,00	4,88	1,54	1,41	2,33	19,52	4,51	3,29	-1,54	36,10	1,60	0,26	-1,50	2,50	Ca-HCO3	30
27-Mar-21	UWC-RF#1	Rainfall	40,30	26,20	5,01	21,50	8,77	1,95	3,27	4,46	29,28	10,38	7,02	-2,25	54,99	1,34	0,13	-1,03	3,20	Ca-HCO3	2,5
05-May-21	UWC Rf-#1	Rainfall	253,00	164,45	6,79	24,00	-	-	-	-	-	-	-	-	-	-	-	-1,38	-4,30	-	13
15-May-21	UWC-RF#1	Rainfall	3,60	2,34	6,96	14,50	7,18	1,87	1,59	1,68	28,06	3,43	2,93	0,84	15,43	2,48	0,00	-5,93	-46,40	Ca-HCO3	32
20-May-21	UWC-RF#1	Rainfall	36,00	23,40	6,45	14,00	4,30	0,85	0,76	0,14	15,86	BD	1,93	1,11	4,72	0,64	-0,01	-2,95	-12,20	Ca-HCO3	33
28-May-21	UWC-RF#1	Rainfall	21,20	13,78	7,01	16,50	4,84	0,96	0,91	0,63	17,08	BD	2,52	3,38	5,65	0,90	0,06	-2,83	-3,70	Ca-HCO3	19
25-Jun-21	UWC-RF#1	Rainfall	26,20	17,03	7,38	11,00	3,78	1,07	0,55	0,01	15,86	BD	0,83	3,02	1,26	0,19	0,02	-2,74	-8,70	Ca-HCO3	20
29-Jun-21	UWC-RF#1	Rainfall	24,80	16,12	7,07	11,80	5,02	1,00	1,33	0,20	18,30	BD	3,22	0,59	2,26	0,21	0,04	-4,08	-16,80	Ca-HCO3	55
29-Jun-21	UWC-RF#1	Rainfall	32,40	21,06	7,06	12,40	6,13	1,15	1,97	0,16	20,74	1,49	4,65	-1,24	3,45	0,36	0,03	-4,46	-20,20	Ca-HCO3	29
30-Jun-21	UWC-RF#1	Rainfall	15,70	10,21	7,49	14,80	4,20	1,51	1,56	0,18	17,08	BD	3,53	3,39	2,59	0,25	0,04	-3,37	-11,30	Ca-HCO3	24
08-Aug-21	UWC-RF#1	Rainfall	80,60	52,39	7,23	12,60	5,32	1,92	1,26	0,65	23,18	2,75	2,18	-0,40	8,58	0,43	0,07	-4,02	-14,96	Ca-HCO3	24
26-Aug-21	UWC-RF#1	Rainfall	53,90	35,04	7,40	19,00	5,12	1,67	0,70	0,65	21,96	BD	2,08	2,54	6,36	0,33	0,03	-4,48	-17,51	Ca-HCO3	40
28-Aug-21	UWC-RF#1	Rainfall	46,00	29,90	7,45	12,50	8,43	0,76	0,64	0,70	26,84	BD	2,10	2,92	6,39	0,33	0,02	-4,62	-20,43	Ca-HCO3	27
30-Aug-21	UWC-RF#1	Rainfall	52,70	34,26	7,43	9,80	8,39	0,70	0,59	0,68	25,62	BD	2,19	3,81	6,40	0,33	0,06	-4,67	-20,82	Ca-HCO3	16
05-Sep-21	UWC-RF#1	Rainfall	46,80	30,42	7,52	13,00	8,39	1,90	1,75	0,57	30,50	1,75	3,85	1,58	8,82	1,07	0,10	-1,90	2,20	Ca-HCO3	17
23-Oct-21	UWC-RF#1	Rainfall	35,40	23,01	-	12,40	6,24	1,91	1,84	1,38	23,18	3,08	4,67	0,66	3,58	0,50	0,26	-2,67	-11,69	Ca-HCO3	28
06-Nov-20	BG00047-RF	Rainfall	-	-	-	-	-	-	-	-	-	-	-	-	-	-	-	-2,68	-10,10	-	40
25-Nov-20	BG00047-RF	Rainfall	-	-	-	-	0,76	1,02	1,81	0,11	3,66	1,73	3,65	1,06	1,39	0,00	0,18	-2,37	-8,30	Ca-Mg-Cl	17
24-Mar-21	BG00047-RF	Rainfall	21,40	13,91	6,94	23,00	2,03	0,24	1,21	0,37	4,88	2,01	2,70	-3,86	4,52	0,38	0,10	-2,56	-10,40	Ca-Mg-Cl	40
29-Mar-21	BG00047-RF	Rainfall	19,70	12,81	6,98	20,20	3,43	0,46	1,65	0,55	7,32	3,56	4,29	-3,39	2,48	BD	0,10	-2,14	-7,60	Ca-Mg-Cl	23,1
05-May-21	BG00047-RF	Rainfall	118,30	76,90	7,24	25,30	-	-	-	-	-	-	-	-	-	-	-	-1,50	-6,00	-	14
06-May-21	BG00047-RF	Rainfall	3,00	1,95	7,22	13,10	3,94	1,27	1,16	0,33	14,64	1,96	3,05	-0,88	1,37	BD	0,09	-2,72	-16,90	Ca-HCO3	8
20-May-21	BG00047-RF	Rainfall	30,00	19,50	7,30	13,50	3,51	0,99	1,06	0,12	13,42	BD	2,59	2,02	0,64	0,10	0,09	-3,18	-14,60	Ca-HCO3	54
28-May-21	BG00047-RF	Rainfall	16,30	10,60	7,12	15,90	3,66	1,12	1,13	0,08	14,64	BD	2,50	2,44	0,78	BD	0,07	-2,66	-4,40	Ca-HCO3	27
29-Jun-21	BG00047-RF	Rainfall	55,30	35,95	6,96	11,60	2,35	1,03	1,55	0,19	13,42	BD	1,31	3,33	2,41	0,66	0,02	-2,84	-7,40	Ca-HCO3	42
29-Jun-21	BG00047-RF	Rainfall	80,90	52,59	6,82	12,00	2,46	1,72	3,10	1,58	13,42	2,95	7,07	-4,48	4,05	3,17	-0,07	-3,59	-13,80	Ca-Mg-Cl	33
30-Jun-21	BG00047-RF	Rainfall	31,10	20,22	6,22	12,90	6,29	1,46	1,47	0,97	23,18	1,69	4,31	-1,32	2,19	1,68	0,03	-4,13	-18,30	Ca-HCO3	28
27-Jul-21	BG00047-RF	Rainfall	65,80	42,77	6,87	14,20	6,17	1,85	4,10	0,44	21,96	1,57	11,21	-4,36	BD	BD	0,04	-1,08	7,60	Ca-HCO3	4
08-Aug-21	BG00047-RF	Rainfall	31,20	20,28	7,23	12,60	6,69	0,97	0,94	0,15	21,96	BD	2,89	1,90	3,00	0,11	0,02	-4,59	-19,17	Ca-HCO3	15
09-Aug-21	BG00047-RF	Rainfall	29,70	19,31	7,09	21,30	2,95	1,26	3,73	0,05	20,74	BD	2,97	-1,14	BD	BD	0,02	-0,82	2,34	Ca-HCO3	3
12-Aug-21	BG00047-RF	Rainfall	31,30	20,35	7,20	12,60	6,25	0,10	0,42	BD	17,08	BD	1,84	0,92	0,77	BD	0,04	-1,36	-0,26	Ca-HCO3	2
24-Aug-21	BG00047-RF	Rainfall	20,40	13,26	7,08	15,30	3,20	0,83	0,70	0,46	13,42	BD	1,70	0,39	BD	BD	0,14	-1,94	-17,22	Ca-HCO3	26
26-Aug-21	BG00047-RF	Rainfall	28,30	18,40	7,10	12,10	6,20	0,12	0,39	0,06	15,86	BD	1,84	3,79	0,77	BD	0,01	-5,71	-26,37	Ca-HCO3	35
27-Aug-21	BG00047-RF	Rainfall	16,55	10,76	7,15	13,30	4,81	0,54	0,69	n.d	14,64	BD	1,89	3,45	0,14	BD	-0,01	-5,32	-25,07	Ca-HCO3	25
28-Aug-21	BG00047-RF	Rainfall	17,10	11,12	-	13,50	-	-	-	-	-	-	-	-	-	-	-	-6,69	-32,57	-	10
30-Aug-21	BG00047-RF	Rainfall	3,47	2,26	-	11,30	-	-	-	-	-	-	-	-	-	-	-	-5,35	-24,64	-	7
31-Aug-21	BG00047-RF	Rainfall	18,07	11,75	7,03	12,70	4,30	0,12	1,31	BD	13,42	BD	1,39	4,09	0,23	BD	-0,02	-0,42	8,06	Ca-HCO3	0,5
03-Sep-21	BG00047-RF	Rainfall	48,00	31,20	7,21	12,23	4,91	0,27	0,50	0,06	13,42	BD	1,86	3,28	0,77	BD	0,07	-3,79	-11,64	Ca-HCO3	5
05-Sep-21	BG00047-RF	Rainfall	40,00	26,00	7,04	12,60	6,40	0,13	1,30	0,14	15,86	BD	3,89	2,63	0,40	BD	0,05	-0,58	9,89	Ca-HCO3	5
20-Sep-21	BG00047-RF	Rainfall	92,50	60,13	4,75	16,80	-	-	-	-	-	-	-	-	-	-	-	-1,12	2,13	-	3
02-Oct-21	BG00047-RF	Rainfall	32,90	21,39	5,56	15,00	-	-	-	-	-	-	-	-	-	-	-	-2,35	-1,99	-	2
14-Oct-21	BG00047-RF	Rainfall	17,90	11,64	5,68	16,90	3,34	0,90	1,80	1,87	12,20	2,14	4,32	0,05	1,21	0,31	0,19	-0,10	2,22	Ca-HCO3	5
16-Oct-21	BG00047-RF	Rainfall	43,40	28,21	6,04	15,40	4,63	1,41	5,47	4,82	18,30	3,09	11,43	1,57	1,22	0,19	0,11	-3,62	-10,03	Na-Cl	8
17-Oct-21	BG00047-RF	Rainfall	29,90	19,44	5,88	14,21	5,19	1,75	8,65	1,49	9,76	3,00	19,97	1,96	0,37	n.d	0,06	-2,77	-3,62	Na-Cl	10
22-Oct-21	BG00047-RF	Rainfall	13,80	8,97	7,14	12,04	5,19	1,18	1,87	1,31	20,74	1,51	4,53	-2,91	2,52	BD	0,10	-3,91	-22,38	Ca-HCO3	12
23-Oct-21	BG00047-RF	Rainfall	68,30	44,40	6,92	16,80	3,09	1,16	1,07	1,04	13,42	BD	2,97	3,10	0,40	BD	0,05	-4,42	-23,84	Ca-HCO3	15

***CB-Charge Balance *n. d-Not Detected *BD-Below detection**